



HAL
open science

Some inversion methods applied to non-destructive testings of steam generator via eddy current probe

Zixian Jiang

► **To cite this version:**

Zixian Jiang. Some inversion methods applied to non-destructive testings of steam generator via eddy current probe. Analysis of PDEs [math.AP]. Ecole Polytechnique X, 2014. English. NNT : . pastel-00943613

HAL Id: pastel-00943613

<https://pastel.hal.science/pastel-00943613>

Submitted on 7 Feb 2014

HAL is a multi-disciplinary open access archive for the deposit and dissemination of scientific research documents, whether they are published or not. The documents may come from teaching and research institutions in France or abroad, or from public or private research centers.

L'archive ouverte pluridisciplinaire **HAL**, est destinée au dépôt et à la diffusion de documents scientifiques de niveau recherche, publiés ou non, émanant des établissements d'enseignement et de recherche français ou étrangers, des laboratoires publics ou privés.

ÉCOLE DOCTORALE DE L'ÉCOLE POLYTECHNIQUE



THÈSE

présentée en vue de l'obtention du titre de

DOCTEUR DE L'ÉCOLE POLYTECHNIQUE

Spécialité : MATHÉMATIQUES APPLIQUÉES

par

Zixian JIANG

Some inversion methods applied to non-destructive testings of steam generator via eddy current probe

Thèse soutenue publiquement le 23 janvier 2014 devant le jury composé de :

Directeur de thèse : Housseem HADDAR - INRIA Saclay
Rapporteurs : Bojan B. GUZINA - University of Minnesota
Sébastien TORDEUX - Université de Pau
Président du jury : Patrick CIARLET - ENSTA ParisTech
Examineurs : Abdellatif ELBADIA - Université de Technologie Compiègne
Alexandre GIRARD - EDF R&D
Armin LECHLEITER - Universität Bremen



Acknowledgments

Mon entière reconnaissance va dans un premier temps à Housseem Haddar qui m'a proposé, il y a presque quatre ans, toujours dans son bureau allongé pour ne pas dire étroit, de commencer un stage de recherche suivi d'un projet de thèse. Son cours en problème inverse m'a initié dans ce domaine étendu. Depuis, il m'a prodigué un encadrement exceptionnel avec son savoir, sa patience et sa bonne humeur qui m'a permis d'élargir et d'approfondir mes connaissances scientifiques et de mener à ce travail. J'apprécie beaucoup son dynamisme et son enthousiasme sous l'apparence de sérénité, dont le contraste rend la motivation plus forte. Je suis extrêmement heureux d'avoir fait mes premiers pas de recherche sous son égide.

Au même titre, je tiens à adresser vivement mes remerciements à Armin Lechleiter qui m'a beaucoup aidé durant la thèse. Comment ne pas me souvenir de son sourire un peu timide sous son abondante chevelure pendant notre première rencontre lors d'une foire aux stages à Chevaleret ? Son incroyable disponibilité et sa rigueur mathématique à l'allemande ont conduit à de nombreuses discussions enrichissantes, que ce soit dans l'antichambre annexe à son ancien bureau au CMAP ou sous le ciel grisâtre de Brême.

Je suis infiniment reconnaissant à Mabrouka El-Guedri et Alexandre Girard, interlocuteurs d'EDF, qui ont lancé ce projet de recherche sur un problème industriel intéressant. Grâce à leur expertise sur le terrain, nous avons pu mieux comprendre le problème réel et bien partir en modélisation et simulation. Les expériences qu'ils ont apportées pendant nos échanges ont beaucoup aidé à valider les méthodes mathématiques et numériques et à interpréter les résultats obtenus. Je les remercie vivement pour leur engagement et leurs suggestions tout au long de ma thèse.

Je tiens à témoigner toute ma reconnaissance à Bojan B. Guzina et Sébastien Tordeux qui me font l'honneur d'être rapporteurs de la thèse. Je suis conscient du temps et du travail qu'ils m'ont consacré à cette occasion et je les remercie pour leur intérêt dont ils ont fait preuve lors de la relecture du manuscrit ainsi que pour la qualité et la pertinence de leurs remarques.

Je suis très heureux que Patrick Ciarlet et Abdellatif Elbadia aient accepté de faire partie de mon jury. Je les remercie en particulier pour l'intérêt qu'ils ont montré pour mon travail.

Je souhaite mentionner l'apport important de Kamel Riahi avec sa compétence en simulation numérique, ce qui permettra d'étendre les méthodes présentées dans la thèse au cas réel 3-D. Je le remercie également pour ses conseils sur la rédaction de ma thèse.

C'est le temps de remercier le personnel du CMAP et de l'équipe DÉFI de l'INRIA Saclay. J'aimerais remercier Antonin Chambolle, directeur du laboratoire mais également enseignant du cours "Problèmes inverses" qui m'a fait découvrir la diversité de sujets dans ce domaine. Mes pensées vont aussi à Valérie Berthou, Wallis Filipi, Jessica Gameiro, Nathalie Hurel, Nasséra Naar, Alexandra Noiret et Sandra Schnakenbourg pour leur prompte et précieuse aide en démarches administratives. Je suis également reconnaissant à Sylvain Ferrand, informaticien du laboratoire, pour sa compétence et sa patience.

Les années passées au sein du CMAP étaient inoubliables grâce àux thésards hors du commun dont j'ai fait la connaissance. Je remercie en particulier Lorenzo Audibert, Nicolas Chaulet, ðihn Liêm Nguyen, Giovanni Migliorati et Tobias Rienmueller de l'équipe DÉFI, ainsi que Gabriel Delgado, Harsha Hutridurga, Mikhail Isaev, Anna Kazeykina, Georgios Michailidis, Laurent Pfeiffer, Matteo Santacesaria et Qu Zheng du CMAP pour leur présence, leur soutien et les moments forts que nous avons vécus ensemble. Je salue mes collègues du bureau Soledad Aronna, Florent Barret, Zhihao Cen, Camille Coron, Khalil Dayri, Sylvie Detournay, Emilie Fabre, Clément Fabre, Thibault Jaisson, Antoine Hocquet, Aymeric Maury, Francisco Silva et Jean-Leopold Vié avec qui j'ai partagé une ambiance amicale et animée du quotidien. Je suis aussi reconnaissant à tous les autres doctorants et permanents du laboratoire pour leur accueil chaleureux.

Ce parcours aurait été bien difficile sans mes amis – Gonghao et sa femme Jinyu, Hélène, Jianqing, Jie, Lili, Lingxuan, Shiguang, Songzhe, Xin, Xue, Qiongyan, Zhiping et tous ceux que j'oublie. Merci à tous pour les moments formidables que nous avons partagés.

J'éprouve ma profonde gratitude à Michel et Yvette, mon parrain et ma marraine, qui depuis sept ans m'accueillent à bras ouverts dans leur famille – un véritable havre de paix durant ces années d'expatriation.

Au moment de conclure, je remercie ma famille et en particulier ma mère à qui je dois tout.

Contents

Introduction	1
I Eddy current inspection with axisymmetric deposits on tubes	7
1 Simulation of eddy current probe	9
1.1 Axisymmetric model	11
1.1.1 Asymptotic behavior for large r	12
1.1.2 Radial cut-off for eddy current simulations	14
1.2 DtN operator and cut-off in the longitudinal direction	16
1.2.1 Analysis of the non-selfadjoint eigenvalue problem	17
1.2.2 Spectral decomposition of the DtN operator	20
1.2.3 On the analysis of spectral error truncation	24
1.3 Numerical test	27
1.3.1 Error of domain cut-off in the radial direction	28
1.3.2 Error introduced by the DtN maps	29
1.4 Appendix: Some properties of the weighted spaces	34
1.4.1 Proof of Lemma 1.1.1	34
1.4.2 Proof of Lemma 1.1.6	36
1.4.3 Proof of Lemma 1.2.1	37
1.5 Appendix: Proof of Proposition 1.1.5	39
1.6 Appendix: Local boundary conditions for radial cut-off	42
1.6.1 Dirichlet boundary condition	42
1.6.2 Robin boundary condition	44
1.7 Appendix: 1-D Calibration	45
2 Identification of lowly-conductive deposits	49
2.1 Modeling of ECT signal for axisymmetric configurations	50
2.2 Shape derivative of the impedance measurements	53
2.2.1 Shape and material derivatives of the solution	53
2.2.2 Shape derivative of the impedance	59
2.2.3 Expression of the impedance shape derivative using the adjoint state	61
2.3 Shape reconstruction of deposits using a gradient method	63
2.3.1 Objective function	63
2.3.2 Regularization of the descent direction	64
2.3.3 Inversion algorithm	65
2.3.4 Numerical tests	65
2.4 On the reconstruction of the deposit conductivity and permeability	72
2.4.1 The cost functional derivative with respect to the conductivity	72
2.4.2 Derivative with respect to the magnetic permeability	73

2.4.3	Numerical tests	74
2.5	On the reconstruction of the shape and physical parameters	76
II Asymptotic models for axisymmetric thin copper layers		79
3	Some asymptotic models for thin and highly conducting deposits	81
3.1	Settings for asymptotic models	82
3.1.1	Rescaled in-layer eddy current model	82
3.1.2	Taylor developments for u_+^δ	83
3.1.3	Transmission conditions between \tilde{u} (or \tilde{w}) and u_\pm^δ	85
3.1.4	Procedure for obtaining approximate transmission conditions $\mathcal{Z}_{m,n}$ between u_\pm^δ	86
3.2	Asymptotic models for deposits with constant thickness	86
3.2.1	Rescaling of the in-layer problem	86
3.2.2	Transmission conditions between \tilde{u} (or \tilde{w}) and u_\pm^δ	88
3.2.3	Computing algorithm for the rescaled in-layer field \tilde{u} (or \tilde{w})	90
3.2.4	Computation of some approximate transmission conditions $\mathcal{Z}_{m,n}$	92
3.2.5	Numerical tests for 1-D models	102
4	Reconstruction of deposit thin layers via asymptotic models	111
4.1	Asymptotic models for deposits with variable layer thickness	112
4.1.1	Formal derivation of approximate transmission conditions $\mathcal{Z}_{1,0}$	112
4.1.2	The asymptotic model of order 0	113
4.1.3	Formal derivation of approximate transmission conditions $\mathcal{Z}_{1,1}$	114
4.1.4	Mixed formulation for the asymptotic model using $\mathcal{Z}_{1,1}$	116
4.1.5	Numerical validation of the 2-D asymptotic models	120
4.1.6	Approximation of the impedance measurements	121
4.1.7	Numerical tests on impedance measurements	123
4.2	Thickness reconstruction via asymptotic model using $\mathcal{Z}_{1,0}$	124
4.2.1	Derivative of the solution with respect to a thickness increment	124
4.2.2	Adjoint state and derivative of the impedance measurements	124
4.2.3	Thickness reconstruction by minimizing a least square cost functional	125
4.3	Thickness reconstruction via asymptotic model using $\mathcal{Z}_{1,1}$	126
4.3.1	Derivative of solution with respect to a thickness increment	126
4.3.2	Adjoint state and derivative of the impedance measurements	127
4.3.3	Thickness reconstruction by minimizing a least square functional	128
4.4	Numerical tests	129
4.4.1	Parameterized thin layers	129
4.4.2	Reconstruction of arbitrary thin layers	130

III	Extension to the 3-D case	133
5	Eddy current tomography using shape optimization	135
5.1	Formulation via vector potentials	136
5.1.1	Problem for vector potential with Coulomb gauge condition	136
5.1.2	Variational formulation of the eddy current problem via vector potentials	138
5.2	Deposit reconstruction via shape optimization	139
5.2.1	Shape and material derivatives of the solution	139
5.2.2	Shape derivative of the impedance measurements	145
5.2.3	Expression of the impedance shape derivative using the adjoint state . . .	148
5.2.4	Shape derivative for a least square cost functional	151
5.2.5	Validation for axisymmetric configurations	152
5.3	Appendices	152
5.3.1	Differential identities	152
5.3.2	Proof of Lemma 5.2.6	152
	Conclusion and perspectives	157
	Bibliography	159

Introduction

Industry context

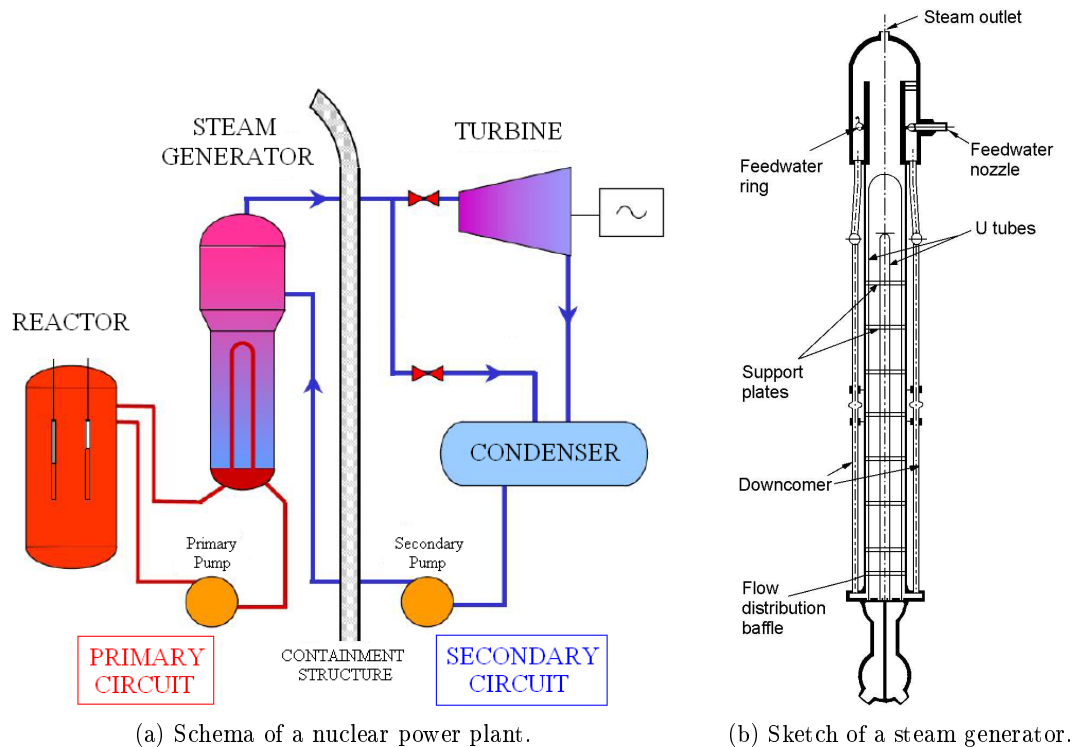
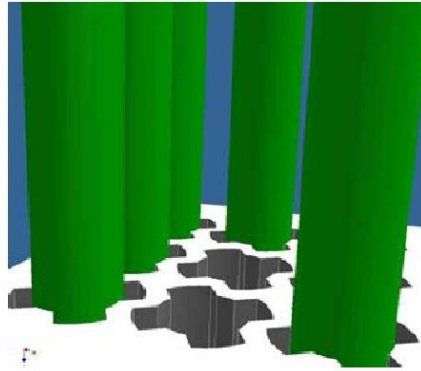
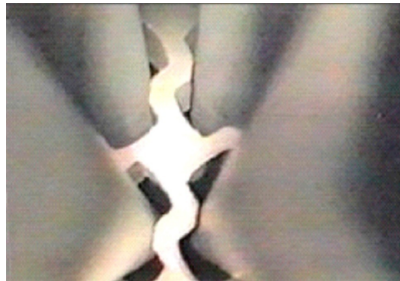


Figure 1

Steam generators (SGs, see Figures 1a, 1b) are critical components in nuclear power plants. Heat produced in a nuclear reactor core is transferred as pressurized water of high temperature via the primary coolant loop into a SG, consisting of tubes in U-shape, and boils coolant water in the secondary circuit on the shell side of the tubes into steam. This steam is then delivered to the turbine generating electrical power. The SG tubes are held by the broached quatrefoil support plates with flow paths between tubes and plates for the coolant circuit (see Figure 2a). Due to the impurity of the coolant water in the secondary circuit, conductive magnetic deposits are observed on the shell side of the U-tubes, usually at the level of the quatrefoil tube support plates (see Figures 2b, 2c) after a long-term exploitation of the SGs. These deposits could, by clogging the flow paths of coolant circuit between the tubes and the support plates, reduce the power productivity and even harm the structure safety. Without disassembling the SG, the lower part of the tubes – which is very long – is inaccessible for normal inspections. Therefore, a non-destructive examination procedure, called eddy current testing (ECT), is widely practiced in industry to detect the presence of defects, such as cracks, flaws, inclusions and deposits [9, 11, 15, 27, 54, 83, 86, 87].



(a) SG tubes and a brached quatrefoil support plate.



(b) Clean SG tube and support plate with flow paths.



(c) Clogged flow paths by deposits.

Figure 2

A brief introduction of the eddy current effect on the site <http://www.ndt-ed.org> reads

Eddy currents are created through a process called electromagnetic induction. When alternating current is applied to the conductor, such as copper wire, a magnetic field develops in and around the conductor. This magnetic field expands as the alternating current rises to maximum and collapses as the current is reduced to zero. If another electrical conductor is brought into the close proximity to this changing magnetic field, current will be induced in this second conductor. Eddy currents are induced electrical currents that flow in a circular path. They get their name from “eddies” that are formed when a liquid or gas flows in a circular path around obstacles when conditions are right.

In the ECT of steam generator, one introduces a probe consisting of two copper wire coils in the tube. Each of these coils is connected to a current generator producing an alternating current and to a voltmeter measuring the voltage change across the coil. One of the coils is excited by its current generator to create a primary electromagnetic field which in turn induces a current flow – the eddy current – in the conductive material nearby, such as the tube and the conducting support plates. Given the deposit-free case as background information, the presence of conducting deposits distorts the eddy current flow and leads to a current change in the two coils, which is measured by the linked voltmeters in terms of impedance. This measurement is

called ECT signal that we use to identify the deposits.

Eddy current model

The study of electromagnetic fields induced by alternative electric currents using mathematical language dates as early as the beginning of the nineteenth century, when Ampère and Faraday carried out their famous experiments on electricity and magnetism. The electromagnetic fields are described by a set of partial differential equations – Maxwell’s equations, named after James Clerk Maxwell who published an early form of these equations describing Ampère’s circuital law and Faraday’s law of induction [57, 58, 59]. In particular, he completed the Ampère’s circuital law by adding a term depicting the displacement currents to describe the capacitive effects. Readers may refer to Jackson [49] for a complete presentation of the classical electromagnetism.

The eddy current approximation of Maxwell’s equations neglects the displacement current. This is based on several assumptions. First of all, the applied alternative electric current, and thus also the electromagnetic fields, are in low frequency regime. Then the conductors should have sufficiently small permittivity with respect to its conductivity such that the displacement current in the conductors are negligible with respect to the eddy currents described by the Faraday’s law. Finally, the conductors should be well separated (see [77]) such that there is no need to use displacement current to describe the capacitive effect which could be caused by small gaps between conductors. There is a rich literature treating the eddy current models. From the engineering point of view, we may refer to the books of Tegopoulos [80] and Mayergoyz [60, Chapter 5] for the analysis and the resolution of the eddy current problem in simple geometrical configurations. A mathematically complete study of the problem can be found in the recent survey of Alonso Rodríguez and Valli [4] which in particular gives a rigorous justification of the eddy current approximation both as the low electric permittivity limit and as the low frequency limit (the works of Costabel et al. [33] and Ammari et al. [6] also treat these cases respectively).

In our problem, we assume that the SG tube is infinitely long and axisymmetric. Since the eddy current probe that we introduced in the tube is axial, which means it cannot detect any angular (or azimuthal) variation, we will consider at the first place an axisymmetric case such that the 3-D eddy current model is reduced to a 2-D problem in cylindrical coordinates. We will formulate the axisymmetric eddy current for a scalar field which is the azimuthal component of the electric field. Then motivated by the fact that the broached quatrefoil support plates (Figure 2a) and the deposits are not axisymmetric, we will extend the model to the 3-D case with a formulation for a vector magnetic potential \mathbf{A} and a scalar electric potential in the conducting components V .

Reconstruction of deposit domain using shape optimization

Based on the eddy current models, we use shape optimization methods for deposit domain reconstruction. A shape optimization problem is a minimization problem of the form

$$\min_{\Omega \in \mathcal{A}} \mathcal{J}(\Omega)$$

where Ω is a domain representing the shape, \mathcal{A} is the class of admissible domains and \mathcal{J} is a shape-dependent cost functional. This kind of problem is first formulated by Hadamard in 1907 [43] and largely developed from the second half of 20th century for optimal shape design in mechanics [73, 38] and for applications in fluid mechanics [61]. Application of shape optimization in electromagnetism is relatively recent. From the engineering approach, some investigations were motivated by electromagnetic device designing [68, 74] or by defect identification [47]. In view of shape optimization for inverse problem, some results concerning the shape derivative based on integral equation approach are discussed (for example, Potthast [72], Costabel and Le Louër [34, 34]). Cagnol and Eller [25] and Hettlich [46] have studied the shape derivative of time-harmonic Maxwell's equations in the (\mathbf{E}, \mathbf{H}) formulation (\mathbf{E} is the electric field and \mathbf{H} the magnetic field). In this thesis, we will discuss shape optimization applied to the eddy current model in the axisymmetric 2-D case for a weighted electric field as well as in the 3-D case for the potentials (\mathbf{A}, V) . We may refer to the books of Zolésio [85], Henrot and Pierre [45] and the course *Conception optimale de structures* of Allaire at Ecole Polytechnique [2] for a general introduction to shape optimization.

In general, the existence of an optimal domain is not ensured unless one assumes some geometrical constraints on the admissible class or considers some special cost functionals. The first results of existence of an optimal domain under geometrical constraints were contributed by Chenaïs [29], Murat and Simon [63, 64] and followed by huge recent developments, for example [5, 26] which treat problems with a homogeneous Neumann condition on the free boundary, and [20, 21, 22, 23, 79] which study the shape optimization problems with a Dirichlet boundary condition on the free boundary. Here we consider shape optimization for inverse problem, the optimal domain is just the target shape to reconstruct, thus exists.

The shape optimization problems can be classified into three main types:

- *Parameterized shape optimization.* One restricts the class of admissible domains to those defined through a function. Thus the shape is characterized by a reduced number of parameters (for example the thickness, the diameter, etc.), which narrows considerably the range of shape variety.
- *Geometrical optimization.* Once an initial domain is given, variations of (a part of) its boundary (free boundary) is possible but its topology cannot be changed.
- *Topological optimization.* Both variations of the boundary and modifications of the topology of the domains are allowed.

Although the last type of shape optimization is the most general, it is also the most difficult in both theoretical and numerical aspects. We may refer to [2] or the book of Bendsoe and Sigmund [12] for this subject. Without being exhaustive, we may cite the results of Guzina – Bonnet [40, 16] and Masmoudi – Pommier – Samet [55, 56] among many others for inverse scattering problems using topological derivative. We may also refer to the work of Dorn – Lesselier [37], Santosa [75] and the references therein for level-set based approaches. In this thesis, we will consider mainly the geometrical optimization from which one easily derive the parameterized shape optimization as its simplified version.

An inverse problem is a framework converting observed measurements into information about an object or system that we are interested in, which is the inverse of the direct problem which

provides measurements from a known object or system. Our problem – reconstruction of deposit shape using eddy current signals – belongs to a big family of inverse problems which is the inverse scattering. Among extensive research on inverse scattering, we may mention the book of Colton and Kress [31] as a reference review on this topic. We may also refer to the book of Kirsch [51] for a general introduction to inverse problems.

A inverse problem is generally ill-posed according to Hadamard’s definition [42] due to its instability. To overcome this difficulty, one should regularize the problem to obtain an approximate solution. The most prevalent regularization method is named after Tikhonov who introduced an additional least-square penalization term to the objective functional [81]. We may refer to Nicolas [65] and Chaulet [28] for examples of inverse scattering problems and for different regularization techniques such as total variation regularization.

In this thesis, the objective is to reconstruct the deposit domain or more precisely its free boundary which is in fact an inner interface of the domain. We will study the transmission conditions on this interface when a shape deformation is applied to the domain, and we will use an H^1 boundary regularization technique to smooth the gradient.

Asymptotic models for thin and highly conducting deposits

There is a another kind of deposits with high conductivity (such as copper) but in the form of thin layers (thickness under $100\mu m$) covering the exterior surface of the SG tubes. This type of deposits does not affect neither the productivity of the electricity power plant nor the structural safety of the steam generator since they do not block the flow paths between the SG tubes and the broached quatrefoil support plates. But by distorting the eddy current signals, their presence can blind the eddy current probes in non-destructive inspections of other kind of problematic defects, such as clogging deposits and cracks of the tube. Therefore, it is crucial to identify and reconstruct them to evaluate their influence in the eddy current testing.

The eddy current model described above for the clogging deposits encounter here a high numerical cost due to the tiny thickness of the thin layer which should be take into account in the discretized computational domain (mesh). To overcome this difficulty, we replace the thin layer with an interface on which appropriate transmission conditions should be set. To determine the effective transmission conditions linking up the solutions at the two sides of the interface, the behavior of in-layer solution is studied using rescaling and asymptotic expansions with respect to a small parameter – the thickness. This is the asymptotic model.

There is a rich literature on approximate boundary (or transmission) conditions for highly conducting materials and on asymptotic models for thin sheets. We may cite the work of Leontovich [52] on the impedance boundary condition and the book of Senior and Volakis [78] on the generalized impedance boundary condition, without using the asymptotic expansions. With asymptotic expansions, Haddar, Joly and Nguyen [44] studied a high order generalized impedance boundary condition for strongly absorbing obstacles with Maxwell’s equations, and Schimdt [76] obtained high order approximate transmission conditions for highly conductive thin sheets. For other related asymptotic models we may cite Tordeux [82] for thin slots, Claeys [30] for thin wires, Delourme [36] for periodic thin rings and Poignard [71] for weakly oscillating thin layers.

In this thesis, we will consider a family of approximate transmission conditions for highly conductive thin layer with different parameters for the rescaling of the conductivity and with different orders in asymptotic expansions with respect to the small parameter characterizing the thickness of layer. Without going into the error analysis, we validate a corresponding family of asymptotic models using these approximate transmission conditions in a simplified configuration and choose the most appropriate asymptotic model which not only ensures sufficient precision but also eases the derivation of inversion in view of further reconstruction of layer thickness.

Outline of the thesis

In Chapter 1 we build the axisymmetric eddy current model in cylindrical coordinates for the azimuthal part of the electric field, given that the meridian part of the electric field is trivial for our problem settings. We proved the existence and uniqueness of the solution in a weighted function space. For numerical tests, we cut off the computational domain with artificial boundaries on which we set some appropriate boundary conditions, in particular the Dirichlet-to-Neumann conditions based on a semi-analytical study of the solution. Numerical simulation of eddy current probe validate this forward model.

Chapter 2 concentrates on inversion algorithm based on the axisymmetric forward model obtained in 1. We define a least square shape-dependent cost functional based on eddy current signals. To minimize this cost functional by descent gradient, we calculate the material and shape derivatives of the solution and introduce an adjoint state to obtain an explicit expression of the gradient on behave of the shape perturbation. This gradient is regularized by a boundary penalizing Laplace-Beltrami operator. Finally we discuss some reconstruction results.

Always in axisymmetric configuration, Chapter 3 studies several asymptotic models for highly conducting thin layer deposits with different approximate transmission conditions modeling the thin layer. Numerical tests for 1-D models with constant layer thickness allow us to choose an asymptotic model with good precision and easy to inverse.

Based on the choice of the pertinent approximate transmission conditions and asymptotic models in Chapter 3, in Chapter 4 we build and numerically validate the asymptotic models for layers with variable thickness. Then an inversion algorithm is proposed for thickness reconstruction and tested by some numerical examples.

We complement our work in Chapter 5 by an extension to the 3-D case. We build the eddy current model for the vector potentials and formulate the corresponding inversion algorithm with the same idea as in Chapter 2. To apply the geometrical shape optimization method, it is crucial here to derive the material derivative of the solution with respect to a small shape perturbation. A joint work with K. Riahi on numerical reconstruction is ongoing and already provides some encouraging preliminary results.

Part I

Eddy current inspection with axisymmetric deposits on tubes

Simulation of eddy current probe

Contents

1.1	Axisymmetric model	11
1.1.1	Asymptotic behavior for large r	12
1.1.2	Radial cut-off for eddy current simulations	14
1.2	DtN operator and cut-off in the longitudinal direction	16
1.2.1	Analysis of the non-selfadjoint eigenvalue problem	17
1.2.2	Spectral decomposition of the DtN operator	20
1.2.3	On the analysis of spectral error truncation	24
1.3	Numerical test	27
1.3.1	Error of domain cut-off in the radial direction	28
1.3.2	Error introduced by the DtN maps	29
1.4	Appendix: Some properties of the weighted spaces	34
1.4.1	Proof of Lemma 1.1.1	34
1.4.2	Proof of Lemma 1.1.6	36
1.4.3	Proof of Lemma 1.2.1	37
1.5	Appendix: Proof of Proposition 1.1.5	39
1.6	Appendix: Local boundary conditions for radial cut-off	42
1.6.1	Dirichlet boundary condition	42
1.6.2	Robin boundary condition	44
1.7	Appendix: 1-D Calibration	45

In order to simulate an eddy current testing experiment, one needs to solve the forward problem for any probe position one wants to incorporate into the measurements. For an iterative inversion method based on the exploitation of this forward problem, the number of required simulation is also proportional to the number of iterations. Given the large number of tubes to be probed, one easily understands the crucial importance of designing a fast (and reliable) numerical simulation of the forward problem. We consider here the eddy current problem under axisymmetric assumption (see for instance Bermúdez et al. [13]) and investigate strategies to bound the computational domain. While for the radial direction, cut-off with brute model for the boundary condition such as Neumann boundary condition would be sufficient due to the conductivity of the tube and the decay of the solution, in the axial direction this strategy requires some fictitious boundaries far from the sources. We rather propose to compute the exact Dirichlet-to-Neumann (DtN) operator for the region outside the source term and apply it as an exact boundary condition on the fictitious boundaries. This would allow the latter to be as close

as needed to the source term. The main difficulty here is in justifying the analytical expansion of this DtN map. We shall rely on results from perturbation theory for the spectrum of compactly perturbed selfadjoint operators. We also study the error due to truncation in the expression of the DtN operator and relate this to the regularity of the problem parameters. Indeed the latter is important from the computational point of view since this truncation is needed in practice. The DtN expansion relies on some eigenvalues and eigenfunctions that are not known analytically and should be numerically approximated. This may be expensive if a high degree of precision is required. However these calculations can be done off-line and therefore would not affect the speed of solving the problem.

There is a large literature on eddy current problems and without being exhaustive we may refer to the book of Alonso Rodríguez – Valli [4] for a recent survey on the problem, including an introduction to the eddy current phenomenon, the mathematical justification of the eddy current approximation and different formulations and numerical approaches for the three-dimensional problems. For axisymmetric configurations we refer to the work of [7] for the study of the theoretic tools for the Maxwell's equations in three dimensions, and to the works of Bermúdez et al. [13], Chaboudez et al. [24] for the discussion of the eddy current problem with bounded conductive components in the meridian half-plane, the numerical analysis and some numerical experiments applied to the induction heating system.

This chapter is organized as follows. In Section 1.1, we briefly recall the eddy current model in the cylindrical coordinate system corresponding to the rotational symmetry with respect to the axis of the tube (see Figure 1.1) and discuss existence and uniqueness of solution to this problem in its equivalent variational formulation in properly defined weighted function spaces.

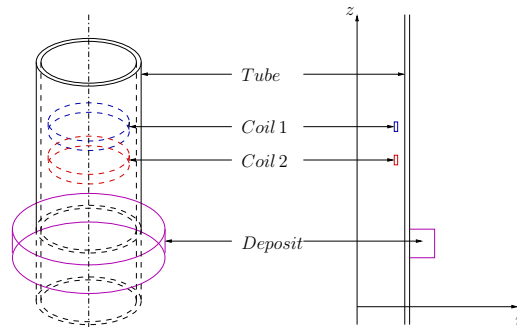


Figure 1.1: Three- and two-dimensional geometric representations of a steam generator tube covered with deposits and a probe consisting of two coils.

We then introduce cut-offs of the domain in the radial-direction by introducing some local boundary conditions (see Section 1.1.1) and then in the axial-direction by constructing the DtN boundary operator (see Section 1.2). We validate our analytical theory by several numerical tests that are motivated by ECT experiments as done in practice and present these numerical results in Section 1.3.

1.1 Axisymmetric model

Let us briefly outline the origin of the considered model. We consider the time-harmonic Maxwell's equations for the electric field \mathbf{E} and the magnetic field \mathbf{H}

$$\begin{cases} \operatorname{curl} \mathbf{H} + (i\omega\epsilon - \sigma)\mathbf{E} = \mathbf{J} & \text{in } \mathbb{R}^3, \\ \operatorname{curl} \mathbf{E} - i\omega\mu\mathbf{H} = 0 & \text{in } \mathbb{R}^3, \end{cases} \quad (1.1)$$

where \mathbf{J} is the applied electric current density such that $\operatorname{div} \mathbf{J} = 0$, and ω , ϵ , μ , σ respectively denote the frequency, the electrical permittivity, the magnetic permeability and the conductivity. In an axisymmetric (i.e., rotationally invariant) setting, for a vector field \mathbf{a} we denote by $\mathbf{a}_m = a_r \mathbf{e}_r + a_z \mathbf{e}_z$ its meridian and by $\mathbf{a}_\theta = a_\theta \mathbf{e}_\theta$ its azimuthal component. A vector field \mathbf{a} is called axisymmetric if, in the sense of distributions, $\partial_\theta \mathbf{a}$ vanishes. According to [7, Lemma 2.2], the Maxwell equations (1.1) decouple into two systems, one for $(\mathbf{H}_\theta, \mathbf{E}_m)$, and the other for $(\mathbf{H}_m, \mathbf{E}_\theta)$. The solution to the first system vanishes if \mathbf{J} is axisymmetric. Substituting \mathbf{H}_m in the second system yields the second-order equation for $\mathbf{E}_\theta = E_\theta \mathbf{e}_\theta$,

$$\frac{\partial}{\partial r} \left(\frac{1}{\mu r} \frac{\partial}{\partial r} (r E_\theta) \right) + \frac{\partial}{\partial z} \left(\frac{1}{\mu} \frac{\partial E_\theta}{\partial z} \right) + \omega^2 (\epsilon + i\sigma/\omega) E_\theta = -i\omega J_\theta \quad \text{in } \mathbb{R}_+^2, \quad (1.2)$$

with $\mathbb{R}_+^2 := \{(r, z) : r > 0, z \in \mathbb{R}\}$. The eddy current approximation corresponds to low frequency regimes and high conductivities: $\omega\epsilon \ll \sigma$. From (1.2) and the above assumption we get the eddy current model

$$\frac{\partial}{\partial r} \left(\frac{1}{\mu r} \frac{\partial}{\partial r} (r E_\theta) \right) + \frac{\partial}{\partial z} \left(\frac{1}{\mu} \frac{\partial E_\theta}{\partial z} \right) + i\omega\sigma E_\theta = -i\omega J_\theta \quad \text{in } \mathbb{R}_+^2, \quad (1.3)$$

with a Dirichlet boundary condition at $r = 0$ due to symmetry: $E_\theta|_{r=0} = 0$, and a decay condition $E_\theta \rightarrow 0$ as $r^2 + z^2 \rightarrow \infty$ at infinity. From now on, we denote $u = E_\theta$. We introduce operators $\nabla := (\partial_r, \partial_z)^t$ and $\operatorname{div} := \nabla \cdot$ on the half-plane \mathbb{R}_+^2 and the axis of symmetry $\Gamma_0 := \{(r, z) : r = 0, z \in \mathbb{R}\}$. Then the axisymmetric eddy current model reads

$$\begin{cases} -\operatorname{div} \left(\frac{1}{\mu r} \nabla (ru) \right) - i\omega\sigma u = i\omega J & \text{in } \mathbb{R}_+^2, \\ u = 0 & \text{on } \Gamma_0, \\ u \rightarrow 0 & \text{as } r^2 + z^2 \rightarrow \infty. \end{cases} \quad (1.4)$$

We shall assume that μ and σ are in $L^\infty(\mathbb{R}_+^2)$ such that $\mu \geq \mu_0 > 0$ on \mathbb{R}_+^2 and that $\sigma \geq 0$ and $\sigma = 0$ for $r \geq r_0$ sufficiently large. For $\lambda > 1$ and $\Omega \subset \mathbb{R}_+^2$, we define the weighted function spaces $L_{1/2, \lambda}^2(\Omega)$, $H_{1/2, \lambda}^1(\Omega)$ and the norms

$$L_{1/2, \lambda}^2(\Omega) := \{v : r^{1/2}(1+r^2)^{-\lambda/2} v \in L^2(\Omega)\}, \quad H_{1/2, \lambda}^1(\Omega) := \{v \in L_{1/2, \lambda}^2(\Omega) : r^{-1/2} \nabla(rv) \in L^2(\Omega)\},$$

$$\|v\|_{L_{1/2, \lambda}^2(\Omega)} = \left\| \sqrt{\frac{r}{(1+r^2)^\lambda}} v \right\|_{L^2(\Omega)}, \quad \|v\|_{H_{1/2, \lambda}^1(\Omega)}^2 = \|v\|_{L_{1/2, \lambda}^2(\Omega)}^2 + \left\| r^{-1/2} \nabla(rv) \right\|_{L^2(\Omega)}^2.$$

The following lemma gives a Poincaré-type inequality related to functions in $H_{1/2, \lambda}^1(\mathbb{R}_+^2)$. The proof uses classical arguments and is given in Appendix 1.4.1 for the convenience of the reader. Note that the trace $v|_{\Gamma_0}$ is well-defined since functions in $H_{1/2, \lambda}^1(\mathbb{R}_+^2)$ belong to $H^1(\{0 < r < r_0\})$ for all $r_0 > 0$.

Lemma 1.1.1. *Let $\lambda > 1$. Any function v in $H_{1/2,\lambda}^1(\mathbb{R}_+^2)$ satisfies $v = 0$ on Γ_0 . Moreover, there exists a constant $C_\lambda > 0$ such that for all v in $H_{1/2,\lambda}^1(\mathbb{R}_+^2)$,*

$$\|v\|_{H_{1/2,\lambda}^1(\mathbb{R}_+^2)} \leq C_\lambda \left\| r^{-1/2} \nabla(rv) \right\|_{L^2(\mathbb{R}_+^2)}. \quad (1.5)$$

One observes that if $u \in L_{1/2,\lambda}^2(\mathbb{R}_+^2)$ for all $\lambda > 1$ then u satisfies the decay condition at infinity in (1.4). Then with the help of the first part of Lemma 1.1.1, one easily verifies by integration by parts that u in $H_{1/2,\lambda}^1(\mathbb{R}_+^2)$ is solution of the two first equations of problem (1.4) if and only if u satisfies

$$\alpha(u, v) := \int_{\mathbb{R}_+^2} \frac{1}{\mu r} \nabla(ru) \cdot \nabla(r\bar{v}) \, dr \, dz - \int_{\mathbb{R}_+^2} i\omega\sigma u \bar{v} r \, dr \, dz = \int_{\mathbb{R}_+^2} i\omega J \bar{v} r \, dr \, dz \quad \forall v \in H_{1/2,\lambda}^1(\mathbb{R}_+^2). \quad (1.6)$$

Proposition 1.1.2. *Assume that $J \in L_{1/2,\lambda}^2(\mathbb{R}_+^2)$ has compact support. Then the variational problem (1.6) admits a unique solution u in $H_{1/2,\lambda}^1(\mathbb{R}_+^2)$ for all $\lambda > 1$.*

Proof. The proof is a direct application of the Lax-Milgram Theorem thanks to (1.5) which yields the coercivity of the sesquilinear form on the left of (1.6):

$$\Re \alpha(v, v) = \int_{\mathbb{R}_+^2} \frac{1}{\mu r} |\nabla(rv)|^2 \geq \frac{1}{\|\mu\|_\infty C_\lambda^2} \|v\|_{H_{1/2,\lambda}^1(\mathbb{R}_+^2)}^2,$$

where C_λ is the constant given in (1.5). □

Remark 1.1.3. *The source J has compact support bounded away from Γ_0 in \mathbb{R}_+^2 in the real problem. We have in particular that J vanishes for $r > r_0$ and $|z| > z_0$, where $r_0 > 0$ and $z_0 > 0$ are large enough.*

1.1.1 Asymptotic behavior for large r

We are interested here in a more precise evaluation of the decay the solution u for large argument r . We shall assume in addition to the hypothesis from Proposition 1.1.2 that the source J and the conductivity σ vanish and that the permeability μ is constant for $r > r_0$ where $r_0 > 0$ is some constant. One then gets from (1.4) that

$$r^2 \frac{\partial^2 u}{\partial r^2} + r \frac{\partial u}{\partial r} - u + r^2 \frac{\partial^2 u}{\partial z^2} = 0 \quad \text{for } r > r_0.$$

We then apply the Fourier transform with respect to the variable z and get

$$r^2 \frac{\partial^2 \hat{u}}{\partial r^2} + r \frac{\partial \hat{u}}{\partial r} - (1 + 4\pi^2 \xi^2 r^2) \hat{u} = 0, \quad \text{where } \hat{u}(\cdot, \xi) := \int_{-\infty}^{+\infty} u(\cdot, z) e^{-2\pi i \xi z} \, dz, \quad \xi \in \mathbb{R}. \quad (1.7)$$

The fundamental solutions of (1.7) for fixed ξ are the two modified Bessel functions $I_1(2\pi|\xi|r)$ and $K_1(2\pi|\xi|r)$ when $\xi \neq 0$, or the functions r and $1/r$ when $\xi = 0$. Since $u \in L_{1/2,\lambda}^2(\mathbb{R}_+^2)$ for all

$\lambda > 1$, the asymptotic behavior for large argument of the modified Bessel functions implies that u has the following expression for $r > r_0$,

$$\widehat{u}(r, \xi) = \begin{cases} \widehat{u}(r_0, \xi) \frac{K_1(2\pi|\xi|r)}{K_1(2\pi|\xi|r_0)} & \xi \neq 0, \\ \widehat{u}(r_0, 0) \frac{r_0}{r} & \xi = 0. \end{cases} \quad (1.8)$$

Let us also quote that $z \mapsto u(r, z) \in H^{1/2}(\mathbb{R})$ for $r > 0$ since $u \in H_{1/2, \lambda}^1(\mathbb{R}_+^2)$.

Proposition 1.1.4. *The solution $u \in H_{1/2, \lambda}^1(\mathbb{R}_+^2)$ to (1.6) satisfies*

$$\|u(r, \cdot)\|_{L^2(\mathbb{R})} \leq \frac{r_0}{r} \|u(r_0, \cdot)\|_{L^2(\mathbb{R})}, \quad \|u(r, \cdot)\|_{H^{1/2}(\mathbb{R})} \leq \frac{r_0}{r} \|u(r_0, \cdot)\|_{H^{1/2}(\mathbb{R})} \quad \forall r > r_0.$$

Proof. By the Plancherel theorem and the Cauchy-Schwarz inequality, we have

$$\|u(r, \cdot)\|_{L^2(\mathbb{R})}^2 = \|\widehat{u}(r, \cdot)\|_{L^2(\mathbb{R})}^2 \leq \|\widehat{u}(r_0, \cdot)\|_{L^2(\mathbb{R})}^2 \left\| \frac{K_1(2\pi|\cdot|r)}{K_1(2\pi|\cdot|r_0)} \right\|_{L^\infty(\mathbb{R})}^2.$$

We note that $K_1(x) \sim 1/x$ as $0 < x \rightarrow 0$. Therefore,

$$g_d(\xi; r_0, r) := \frac{K_1(2\pi\xi r)}{K_1(2\pi\xi r_0)} \rightarrow \frac{r_0}{r} \quad \text{as } 0 < \xi \rightarrow 0. \quad (1.9)$$

On the other hand, the derivative of g_d with respect to ξ is

$$\begin{aligned} g_d'(\xi; r_0, r) &= \frac{2\pi r K_1'(2\pi\xi r) K_1(2\pi\xi r_0) - 2\pi r_0 K_1(2\pi\xi r) K_1'(2\pi\xi r_0)}{K_1^2(2\pi\xi r_0)} \\ &= \frac{2\pi [-r K_0(2\pi\xi r) K_1(2\pi\xi r_0) + r_0 K_1(2\pi\xi r) K_0(2\pi\xi r_0)]}{K_1^2(2\pi\xi r_0)}, \end{aligned}$$

where the last equality follows from the recurrence formulas for Bessel functions. From the integral representation (see [48, (2.1)] and its references)

$$\frac{x K_0(x)}{K_1(x)} = \frac{4}{\pi^2} \int_0^{+\infty} \frac{x^2}{x^2 + t^2} \frac{t^{-1} dt}{J_1^2(t) + Y_1^2(t)}, \quad x > 0.$$

one concludes that the function $x K_0(x)/K_1(x)$ is increasing in $x > 0$, which implies in our case that

$$\frac{r_0 K_0(2\pi\xi r_0)}{K_1(2\pi\xi r_0)} \leq \frac{r K_0(2\pi\xi r)}{K_1(2\pi\xi r)} \quad \text{and therefore} \quad g_d'(\xi; r_0, r) \leq 0, \quad \xi > 0.$$

Consequently

$$g_d(\xi; r_0, r) \leq g_d(0+; r_0, r) = \frac{r_0}{r}, \quad \forall \xi > 0,$$

which gives the first inequality of the Proposition using the Plancherel theorem. The second one can be proved with the same arguments. \square

Using more involved computations and estimates on Bessel functions one can also prove the following result. The technical details of the proof are given in Appendix 1.5.

Proposition 1.1.5. *The solution $u \in H_{1/2,\lambda}^1(\mathbb{R}_+^2)$ to (1.6) satisfies*

$$\left\| \frac{\partial}{\partial r}(ru)(r, \cdot) \right\|_{H^{-1/2}(\mathbb{R})} \leq C \frac{r_0}{r} \|u(r_0, \cdot)\|_{H^{1/2}(\mathbb{R})} \quad \forall r > r_0$$

for some constant $C > 0$ independent of r and u .

1.1.2 Radial cut-off for eddy current simulations

The decay in radial direction suggests that reasonable accuracy can be obtained by truncating the computational domain at $r = r_*$ sufficiently large. In fact, for the application we are interested in, this is also justified by the high conductivity of the tube that would absorb most of the energy delivered by the coil inside the tube. We shall analyze in the sequel the error resulting from radial cut-off independently from the absorption. It turns out in this case that the boundary conditions that lead to reasonable error estimates are Neumann or Robin boundary conditions. The case of Dirichlet boundary conditions lead to slower convergence rates that will be confirmed by our numerical examples. We present in this section only the case of Neumann boundary conditions. The cases of Dirichlet and Robin boundary conditions are treated in Appendix 1.6.

For $R \geq 0$ we denote

$$B_R := \{(r, z) : 0 < r < R, z \in \mathbb{R}\} \quad \text{and} \quad \Gamma_R = \{(r, z) : r = R, z \in \mathbb{R}\},$$

and shall use the short notation

$$\begin{aligned} L_{1/2}^2(\Omega) &:= L_{1/2,0}^2(\Omega) = \{v : v\sqrt{r} \in L^2(\Omega)\}, \\ H_{1/2}^1(\Omega) &:= H_{1/2,0}^1(\Omega) = \{v \in L_{1/2}^2(\Omega) : r^{-1}\nabla(rv) \in L_{1/2}^2(\Omega)\}. \end{aligned}$$

Moreover, with $H^s(\mathbb{R})$ denoting the usual Sobolev space on \mathbb{R} and for sufficiently regular function v defined in a neighborhood of Γ_R we set

$$\|v\|_{H^s(\Gamma_R)} := \|v(R, \cdot)\|_{H^s(\mathbb{R})}.$$

Let $r_* > 0$ be sufficiently large such that the support of the source term J is included in B_{r_*} . Then the problem on the cut-off domain with Neumann boundary conditions on Γ_{r_*} consists into seeking $u_n \in H_{1/2}^1(B_{r_*})$ satisfying

$$\begin{cases} -\operatorname{div} \left(\frac{1}{\mu r} \nabla(ru_n) \right) - i\omega\sigma u_n = i\omega J & \text{in } B_{r_*}, \\ u_n = 0 & \text{on } \Gamma_0, \\ \frac{\partial}{\partial r}(ru_n) = 0 & \text{on } \Gamma_{r_*}. \end{cases} \quad (1.10)$$

The well-posedness of this problem is guaranteed thanks to the following lemma which will also be useful in quantifying error estimates. The proof of this Lemma is given in Appendix 1.4.2.

Lemma 1.1.6. *Let $r_* > 0$. Any function $v \in H_{1/2}^1(B_{r_*})$ satisfies $v = 0$ on Γ_0 . Moreover, we have the Poincaré-type inequality*

$$\|v\|_{L_{1/2}^2(B_{r_*})} \leq \frac{r_*}{\sqrt{2}} \left\| \frac{1}{r} \nabla(rv) \right\|_{L_{1/2}^2(B_{r_*})} \quad \forall v \in H_{1/2}^1(B_{r_*}), \quad (1.11)$$

and a trace estimate

$$\|v\|_{H^{1/2}(\Gamma_{r_*})} \leq \sqrt{\frac{3}{r_*}} \left\| \frac{1}{r} \nabla(rv) \right\|_{L_{1/2}^2(B_{r_*})} \quad \forall v \in H_{1/2}^1(B_{r_*}). \quad (1.12)$$

One then can prove the following result.

Proposition 1.1.7. *Assume that the source $J \in L^2(\mathbb{R}_+^2)$ has compact support and let $r_* > 0$ be so large that the support of J is included in B_{r_*} . Then problem (1.10) has a unique solution $u_n \in H_{1/2}^1(B_{r_*})$. Assume in addition that there exists $0 < r_0 < r_*$ such that J and the conductivity σ vanish and the permeability μ is constant for $r > r_0$. Then there exists a constant C that depends only on J , r_0 , μ and σ such that*

$$\left\| \frac{1}{r} \nabla(r(u_n - u)) \right\|_{L_{1/2}^2(B_{r_*})} \leq C/r_*^{3/2} \quad \text{and} \quad \|u_n - u\|_{H_{1/2}^1(B_{r_*})} \leq C/r_*^{1/2},$$

where u is the solution to (1.6).

Proof. The proof of the first part is similar to the proof of Proposition 1.1.2 thanks to Lemma 1.1.6. Let us set $w_n := u - u_n \in H_{1/2}^1(B_{r_*})$ such that

$$\int_{B_{r_*}} \frac{1}{\mu r} \nabla(rw_n) \cdot \nabla(r\bar{v}) - i\omega\sigma w_n \bar{v} r = \int_{\Gamma_{r_*}} \frac{1}{\mu} \frac{\partial}{\partial r}(ru) \bar{v} dz \quad \forall v \in H_{1/2}^1(B_{r_*}),$$

where the integral on Γ_{r_*} should be understood as a $H^{-1/2} - H^{1/2}$ duality pairing. Taking $v = \bar{w}_n$, we obtain

$$\left| \int_{B_{r_*}} \frac{1}{\mu r} |\nabla(rw_n)|^2 - i\omega\sigma |w_n|^2 r \right| = \left| \int_{\Gamma_{r_*}} \frac{1}{\mu} \frac{\partial}{\partial r}(ru) \bar{w}_n dz \right| \leq \frac{1}{\mu(r_*)} \left\| \frac{\partial}{\partial r}(ru) \right\|_{H^{-1/2}(\Gamma_{r_*})} \|w_n\|_{H^{1/2}(\Gamma_{r_*})}.$$

Using (1.12) we deduce

$$\begin{aligned} \frac{1}{\|\mu\|_\infty} \left\| \frac{1}{r} \nabla(rw_n) \right\|_{L_{1/2}^2(B_{r_*})}^2 &\leq \left| \int_{B_{r_*}} \frac{1}{\mu r} |\nabla(rw_n)|^2 - i\omega\sigma |w_n|^2 r \right| \\ &\leq \frac{1}{\mu(r_*)} \left\| \frac{\partial}{\partial r}(ru) \right\|_{H^{-1/2}(\Gamma_{r_*})} \sqrt{\frac{3}{r_*}} \left\| \frac{1}{r} \nabla(rw_n) \right\|_{L_{1/2}^2(B_{r_*})}. \end{aligned}$$

Therefore,

$$\left\| \frac{1}{r} \nabla(rw_n) \right\|_{L_{1/2}^2(B_{r_*})} \leq \frac{\|\mu\|_\infty}{\mu(r_*)} \sqrt{\frac{3}{r_*}} \left\| \frac{\partial}{\partial r}(ru) \right\|_{H^{-1/2}(\Gamma_{r_*})}.$$

The first estimate then follows from Proposition 1.1.5 and the second one can be deduced using (1.11). \square

Remark 1.1.8. *As indicated in the beginning of this section, the case of Robin boundary conditions leads to error estimates similar to those of Proposition 1.1.7. However, if one uses Dirichlet boundary conditions on Γ_{r_*} then one loses half an order of magnitude for the convergence rate in terms of $1/r_*$ (see Appendix 1.6). This means for instance that convergence in $H^{1/2}(\Gamma_{r_*})$ or in $L^2_{1/2}(\Gamma_{r_*})$ is not guaranteed in general in this case. This is in fact corroborated by our numerical experiments in Section 1.3.1.*

1.2 DtN operator and cut-off in the longitudinal direction

We discuss in this section the domain cut-off in the longitudinal direction, i.e., the z -direction, whenever a cut-off has been applied before in the radial direction. We therefore consider the solution u_n of (1.10) and in order to shorten notation we abusively denote this solution by u . Recall that the variational formulation of problem (1.10) is to find $u \in H^1_{1/2}(B_{r_*})$ such that

$$\int_{B_{r_*}} \frac{1}{\mu} \frac{1}{r} \nabla(ru) \cdot \frac{1}{r} \nabla(r\bar{v}) \, dr \, dz - \int_{B_{r_*}} i\omega\sigma u \bar{v} r \, dr \, dz = \int_{B_{r_*}} i\omega J \bar{v} r \, dr \, dz \quad \forall v \in H^1_{1/2}(B_{r_*}), \quad (1.13)$$

where $r_* > 0$ is as in Proposition 1.1.7. The idea how to cut off the domain in the z -direction is to explicitly compute the DtN map for the regions above and below the source and inhomogeneities in the coefficients μ and σ using the method of separation of variables. The main difficulty to cope with here is to prove that this is feasible even though the main operator is not selfadjoint.

We cut the domain by two horizontal boundaries

$$\Gamma_{\pm} := \{z = \pm z_*\}$$

for some $z_* > 0$ large enough such that the source is compactly supported in

$$B_{r_*, z_*} := \{(r, z) \in B_{r_*} : |z| < z_*\}.$$

We then assume in addition that μ and σ only depends on the variable r in the complementary region

$$B_{r_*, z_*}^{\pm} := \{(r, z) \in B_{r_*} : z \gtrless \pm z_*\}.$$

Since in B_{r_*, z_*}^{\pm} it holds that

$$-\operatorname{div} \left(\frac{1}{\mu r} \nabla(ru) \right) - i\omega\sigma u = 0,$$

a solution of the form $u(r, z) = \rho(r)\zeta(z)$ has to satisfy

$$\frac{1}{\zeta} \frac{d^2\zeta}{dz^2} = -\frac{1}{\rho} \frac{d}{dr} \left(\frac{1}{\mu r} \frac{d}{dr}(r\rho) \right) - i\omega\sigma = \nu,$$

where $\nu \in \mathbb{C}$ is some eigenvalue that we will estimate. For the first equation, we obtain

$$\frac{d^2\zeta}{dz^2} - \nu\zeta = 0,$$

which has as solutions $\zeta(z) = c \exp(\pm\sqrt{\nu}z)$ if $\nu \neq 0$, while for the second equation we are led to consider the eigenvalue problem

$$\begin{aligned} \mathcal{S}_\mu^\sigma \rho &:= -\frac{d}{dr} \left(\frac{1}{\mu r} \frac{d}{dr} (r\rho) \right) - i\omega\sigma\rho = \nu\rho \quad \text{in } I := \{r \in \mathbb{R} : 0 < r < r_*\}, \\ \rho(0) = 0, \frac{d}{dr} (r\rho) \Big|_{r=r_*} &= 0. \end{aligned} \quad (1.14)$$

We first formally observe from (1.14) (after multiplication by $r\bar{\rho}$ and integration by parts) that $\Im(\nu) \leq 0$ and $\Re(\nu) > 0$. Choosing $\sqrt{\nu}$ such that $\Re\sqrt{\nu} > 0$, we get that $\zeta(z) = c \exp(\pm\sqrt{\nu}z)$ on B_{r_*, z_*}^\mp are the only admissible solutions due to their boundedness at infinity. The only missing point that would allow the construction of a solution on B_{r_*, z_*}^\mp is to prove that the set of eigenfunctions associated with (1.14) forms a complete set for the traces of the solutions to problem (1.13).

1.2.1 Analysis of the non-selfadjoint eigenvalue problem

We consider the spaces

$$L_{1/2}^2(I) := \{\phi : \phi\sqrt{r} \in L^2(I)\}, \quad H_{1/2}^1(I) := \{\phi \in L_{1/2}^2(I) : \frac{1}{r} \frac{\partial}{\partial r} (r\phi) \in L_{1/2}^2(I)\}.$$

For convenience, we shall denote in the sequel by (\cdot, \cdot) the $L_{1/2}^2(I)$ scalar product.

Lemma 1.2.1. *The embedding $H_{1/2}^1(I) \hookrightarrow L_{1/2}^2(I)$ is dense and compact. Any $\phi \in H_{1/2}^1(I)$ is continuous in the closure of I and satisfies $\phi = 0$ at $r = 0$. Moreover, the following Poincaré-type inequalities hold,*

$$\|\phi\|_{L^2(I)} \leq \sqrt{r_*} \left\| \frac{1}{r} \nabla(r\phi) \right\|_{L_{1/2}^2(I)} \quad \text{and} \quad \|\phi\|_{L_{1/2}^2(I)} \leq \frac{r_*}{\sqrt{2}} \left\| \frac{1}{r} \nabla(r\phi) \right\|_{L_{1/2}^2(I)} \quad \forall \phi \in H_{1/2}^1(I). \quad (1.15)$$

Proof. The proof of the compact embedding is a simple application of [18, Corollaire IV.26]. For the detailed proof, see Appendix 1.4.3. The proof of the property $\phi(0) = 0$ and the inequalities is the same as for Lemma 1.1.6. \square

Since $H_{1/2}^1(I)$ is dense in $L_{1/2}^2(I)$ one can define the unbounded operator $\mathcal{A}_\mu : D(\mathcal{A}_\mu) \subset L_{1/2}^2(I) \rightarrow L_{1/2}^2(I)$, where

$$D(\mathcal{A}_\mu) = \left\{ u \in H_{1/2}^1(I) : \mathcal{A}_\mu u = \frac{d}{dr} \left(\frac{1}{\mu r} \frac{d}{dr} (ru) \right) \in L_{1/2}^2(I), \frac{d}{dr} (ru) \Big|_{r=r_*} = 0 \right\}.$$

Then we have $D(\mathcal{A}_\mu) \subset H_{1/2}^1(I)$. For $\phi \in H_{1/2}^1(I)$, $\mathcal{A}_\mu \phi$ is defined by

$$(\mathcal{A}_\mu \phi, \psi) = \int_0^{r_*} \frac{1}{\mu r} \frac{d}{dr} (r\phi) \frac{d}{dr} (r\bar{\psi}) dr \quad \forall \psi \in H_{1/2}^1(I). \quad (1.16)$$

It is clear from this definition that \mathcal{A}_μ is closed and selfadjoint and according to Lemma 1.2.1, it has a compact resolvent. Moreover, the second inequality in Lemma 1.2.1 shows that

$$(\mathcal{A}_\mu \phi, \phi) \geq c \|\phi\|_{H_{1/2}^1(I)}^2 \quad \forall \phi \in H_{1/2}^1(I)$$

for some positive constant c independent of ϕ .

We then deduce (see for instance [35, Chapter VIII, Theorem 7]) that \mathcal{A}_μ has positive eigenvalues $\{\lambda_k\}_{k \in \mathbb{N}^*}$ with corresponding $L_{1/2}^2$ -complete orthonormal eigenprojectors $\{P_k\}_{k \in \mathbb{N}^*}$ such that

$$0 < \lambda_1 < \lambda_2 < \dots < \lambda_k \rightarrow \infty \quad (k \rightarrow \infty),$$

and $\forall \phi \in P_k(H_{1/2}^1(I))$

$$(\mathcal{A}_\mu \phi, \psi) = \lambda_k (\phi, \psi) \quad \forall \psi \in H_{1/2}^1(I). \quad (1.17)$$

Since \mathcal{S}_μ^σ is formally only a compact perturbation of \mathcal{A}_μ by using the perturbation theory one can relate the spectrum of \mathcal{S}_μ^σ to the spectrum of \mathcal{A}_μ . We first need to have estimates on the eigenvalues $\{\lambda_k\}_{k \in \mathbb{N}^*}$. For that purpose we shall consider first the case of constant μ . We observe from (1.17) (after interpreting in the distributional sense), that if a couple (λ^1, ϕ) is an eigenpair of \mathcal{A}_1 then

$$\begin{aligned} -\frac{d}{dr} \left(\frac{1}{r} \frac{d}{dr} (r\phi) \right) &= \lambda^1 \phi \quad 0 < r < r_*, \\ \phi(0) = 0 \text{ and } \frac{d}{dr} (r\phi) \Big|_{r_*} &= 0. \end{aligned} \quad (1.18)$$

Rewriting the first equation in the form of a Bessel's differential equation, after setting $\zeta = \sqrt{\lambda^1}$,

$$r^2 \phi'' + r \phi' + (\zeta^2 r^2 - 1) \phi = 0$$

and using the regularity of ϕ , we obtain that solutions are proportional to the Bessel functions of the first kind $\{J_1(\frac{j_{0,k}}{r_*} r)\}_{k \in \mathbb{N}^*}$ where $j_{0,k} > 0$ is the k^{th} zero of Bessel function J_0 . It is easy to verify that $\{J_1(\frac{j_{0,k}}{r_*} r)\}_{k \in \mathbb{N}^*}$ is a orthogonal family of $L_{1/2}^2(I)$. This corresponding eigenvalues are

$$\lambda_k^1 = \left(\frac{j_{0,k}}{r_*} \right)^2 \quad \text{for } k \in \mathbb{N}^*. \quad (1.19)$$

Using McMahon's expansions for large zeros of Bessel functions (see [1, 9.5.12]):

$$j_{\nu,k} \sim \beta - \frac{4\nu^2 - 1}{8\beta} - \frac{4(4\nu^2 - 1)(28\nu^2 - 31)}{(8\beta)^3} + O(\beta^{-5}) \quad (k \rightarrow \infty),$$

$$\text{where } \beta = \beta(k) = \left(k + \frac{1}{4} \right) \pi, \quad \nu = 0, 1, \dots$$

we observe that the eigenvalues λ_k^1 grow like k^2 as $k \rightarrow \infty$. Now set

$$\mu_{\inf} := \inf \mu \text{ and } \mu_{\sup} := \sup \mu,$$

which are positive finite constants by assumptions. One obviously has

$$\frac{1}{\mu_{\sup}} \frac{(\mathcal{A}_1 \phi, \phi)}{\|\phi\|_{L^2_{1/2}(I)}^2} \leq \frac{(\mathcal{A}_\mu \phi, \phi)}{\|\phi\|_{L^2_{1/2}(I)}^2} \leq \frac{1}{\mu_{\inf}} \frac{(\mathcal{A}_1 \phi, \phi)}{\|\phi\|_{L^2_{1/2}(I)}^2}.$$

From the Courant-Fischer-Weyl min-max theorem, we deduce

$$\frac{1}{\mu_{\sup}} \lambda_k^1 \leq \lambda_k \leq \frac{1}{\mu_{\inf}} \lambda_k^1. \quad (1.20)$$

We therefore obtain the following result.

Lemma 1.2.2. *The difference $\lambda_k - \lambda_{k-1} \rightarrow +\infty$ as $k \rightarrow \infty$. Moreover, if*

$$\frac{\mu_{\sup}}{\mu_{\inf}} < \min_{k \geq 1} \frac{\lambda_{k+1}}{\lambda_k},$$

then all eigenvalues λ_k are simple.

Now let us consider the operator $\mathcal{S}_\mu^\sigma = \mathcal{A}_\mu + \mathcal{M}^\sigma$ defined in (1.14). Since the multiplication operator

$$\mathcal{M}^\sigma : \phi \mapsto -i\omega\sigma\phi, \quad \forall \phi \in L^2_{1/2}(I),$$

is bounded on $L^2_{1/2}(I)$, the theory for perturbed selfadjoint operators [50, Theorem V-4.15a and Remark V-4.16a] implies:

Proposition 1.2.3. *Under the assumptions of Lemma 1.2.2, the unbounded operator $\mathcal{S}_\mu^\sigma : L^2_{1/2}(I) \rightarrow L^2_{1/2}(I)$ is closed with compact resolvent and its eigenvalues and eigenprojectors can be indexed as $\{\nu_{0j}, \nu_k\}$ and $\{Q_{0j}, Q_k\}$ respectively, where $j = 1, \dots, m < \infty$ and $k = n+1, n+2, \dots$ with $n \geq 0$ such that the following results hold:*

1. *the sequence $|\nu_k - \lambda_k|$ is bounded as $k \rightarrow \infty$.*
2. *there exists a bounded operator W on $L^2_{1/2}(I)$ with bounded inverse W^{-1} such that*

$$Q_0 := \sum_{j=1}^m Q_{0j} = W^{-1} \left(\sum_{k \leq n} P_k \right) W \quad \text{and} \quad Q_k = W^{-1} P_k W \quad \text{for } k > n. \quad (1.21)$$

Moreover, $\{Q_{0j}, Q_k\}$ is a complete family in the sense that

$$\sum_{j=1}^m Q_{0j} + \sum_{k > n} Q_k = 1. \quad (1.22)$$

1.2.2 Spectral decomposition of the DtN operator

We are now in position to provide explicit expression for the DtN operator that will be used to cut off the domain in the z -direction. We first need to specify the space of traces on Γ_{\pm} of functions in $H_{1/2}^1(B_{r_*})$. From the definition of the spectral decomposition of \mathcal{A}_1 we immediately deduce that for $\phi \in H_{1/2}^1(I)$

$$\|\phi\|_{L_{1/2}^2(I)}^2 = \sum_{k \geq 1} \|P_k^1 \phi\|_{L_{1/2}^2(I)}^2 \quad \text{and} \quad \|\phi\|_{H_{1/2}^1(I)}^2 = \sum_{k \geq 1} (1 + \lambda_k^1) \|P_k^1 \phi\|_{L_{1/2}^2(I)}^2$$

where $\{P_k^1\}_{k \in \mathbb{N}^*}$ denotes the complete orthonormal eigenprojectors family associated with \mathcal{A}_1 . For $\theta \in [0, 1]$, we define $H_{1/2}^{\theta}(I)$ as the θ interpolation space $[H_{1/2}^1(I), L_{1/2}^2(I)]_{\theta}$ (see [53, Définition 2.1] for interpolation spaces) with norms

$$\|\phi\|_{H_{1/2}^{\theta}(I)}^2 = \sum_{k \geq 1} (1 + \lambda_k^1)^{\theta} \|P_k^1 \phi\|_{L_{1/2}^2(I)}^2 \quad (1.23)$$

and define $H_{1/2}^{-\theta}(I)$ as the dual space of $H_{1/2}^{\theta}(I)$ with pivot space $L_{1/2}^2(I)$. The norm in $H_{1/2}^{-\theta}(I)$ can be defined as in (1.23) replacing θ by $-\theta$. The definition of the spaces $H_{1/2}^{\pm\theta}(\Gamma_+)$ and $H_{1/2}^{\pm\theta}(\Gamma_-)$ are obtained from $H_{1/2}^{\pm\theta}(I)$ by identifying Γ_{\pm} with I using the obvious isometry. Let v be a regular function of B_{r_*} . We denote the trace mapping by

$$\gamma^{\pm} : v \mapsto v|_{\Gamma_{\pm}}.$$

Theorem 1.2.4. *The trace mapping γ^{\pm} can be extended to a continuous and surjective mapping from $H_{1/2}^1(B_{r_*, z_*})$ onto $H_{1/2}^{1/2}(\Gamma_{\pm})$ and from $H_{1/2}^1(B_{r_*, z_*}^{\pm})$ onto $H_{1/2}^{1/2}(\Gamma_{\pm})$.*

Proof. Obviously we have the equivalent definition

$$H_{1/2}^1(B_{r_*, z_*}) = \left\{ v : v \in L^2((-z_*, z_*); H_{1/2}^1(I)), \frac{\partial v}{\partial z} \in L^2((-z_*, z_*); L_{1/2}^2(I)) \right\},$$

with the same norm. Therefore the trace mapping properties for $H_{1/2}^1(B_{r_*, z_*})$ is a direct application of classical theory for trace spaces: [53, Théorème 3.2]. Similar considerations apply for $H_{1/2}^1(B_{r_*, z_*}^{\pm})$. \square

Let us also mention the following result that will be useful later

Lemma 1.2.5. *Let $\theta \in [0, 1]$. The norm*

$$\|\phi\|_{H_{1/2}^{\theta, \mu}} := \sum_{k=1}^{\infty} (1 + \lambda_k)^{\theta} \|P_k \phi\|_{L_{1/2}^2(I)}^2$$

defines an equivalent norm on $H_{1/2}^{\theta}(I)$.

Proof. From interpolation theory, it is sufficient to prove the result for $\theta = 0$ and $\theta = 1$. The case of $\theta = 0$ is obvious. The case $\theta = 1$ follows from the identity

$$\sum_{k=1}^{\infty} \lambda_k \|P_k \phi\|_{L_{1/2}^2(I)}^2 = (\mathcal{A}_{\mu} \phi, \phi)$$

and noting that $(\psi, \phi) \mapsto (\mathcal{A}_{\mu} \psi, \phi)$ is continuous and coercive on $H_{1/2}^1(I) \times H_{1/2}^1(I)$. \square

Let ϕ^\pm in $H_{1/2}^1(\Gamma_\pm)$ and denote by μ^\pm and σ^\pm the restrictions of μ and σ to B_{r_*, z_*}^\pm . Thanks to Theorem 1.2.4 one can uniquely define $u^\pm \in H_{1/2}^1(B_{r_*, z_*}^\pm)$ solution of

$$\begin{cases} -\operatorname{div}\left(\frac{1}{\mu^\pm r}\nabla(ru^\pm)\right) - i\omega\sigma^\pm u^\pm = 0 & \text{in } B_{r_*, z_*}^\pm, \\ u^\pm|_{r=0} = 0 \text{ and } \frac{1}{\mu^\pm}\frac{\partial}{\partial r}(ru^\pm)|_{r=r_*} = 0, \\ u^\pm = \phi^\pm & \text{on } \Gamma_\pm. \end{cases} \quad (1.24)$$

The construction of u^\pm can be done for instance by using some continuous lifting linear operators $\mathcal{R}^\pm : H_{1/2}^1(\Gamma_\pm) \rightarrow H_{1/2}^1(B_{r_*, z_*}^\pm)$ such that $\gamma^\pm \mathcal{R}^\pm(\phi) = \phi$ (these operators exist according to Theorem 1.2.4). The $H_{1/2}^1(B_{r_*, z_*}^\pm)$ norm of u^\pm indeed continuously depends on the $H_{1/2}^1(\Gamma_\pm)$ norm of the boundary data ϕ^\pm (respectively).

Definition 1.2.6. We define the DtN operators $\mathcal{T}^\pm : H_{1/2}^1(\Gamma_\pm) \rightarrow H_{1/2}^{-1/2}(\Gamma_\pm)$ by

$$\langle \mathcal{T}^\pm \phi^\pm, \psi^\pm \rangle = \int_{B_{r_*, z_*}^\pm} \frac{1}{\mu^\pm r} \nabla(ru^\pm) \nabla(r\overline{\mathcal{R}^\pm \psi^\pm}) \, dr \, dz + \int_{B_{r_*, z_*}^\pm} \operatorname{div}\left(\frac{1}{\mu r} \nabla(ru^\pm)\right) \overline{\mathcal{R}^\pm \psi^\pm} r \, dr \, dz$$

for all $\psi^\pm \in H_{1/2}^1(\Gamma_\pm)$, where $u^\pm \in H^1(B_{r_*, z_*}^\pm)$ is the unique solution of problem (1.24) and where $\langle \cdot, \cdot \rangle$ denotes the $H_{1/2}^{-1/2} - H_{1/2}^1$ duality product that coincides with (\cdot, \cdot) for $L_{1/2}^2$ functions.

Indeed

$$\langle \mathcal{T}^\pm \phi^\pm, \psi^\pm \rangle = \int_{B_{r_*, z_*}^\pm} \frac{1}{\mu^\pm r} \nabla(ru^\pm) \nabla(r\overline{\mathcal{R}^\pm \psi^\pm}) \, dr \, dz - \int_{B_{r_*, z_*}^\pm} i\omega\sigma^\pm u \overline{\mathcal{R}^\pm \psi^\pm} r \, dr \, dz \quad (1.25)$$

and therefore, from the definition of \mathcal{R}^\pm and the continuity property for the solutions u^\pm ,

$$\langle \mathcal{T}^\pm \phi^\pm, \psi^\pm \rangle \leq C \|\phi^\pm\|_{H_{1/2}^1(\Gamma_\pm)} \|\psi^\pm\|_{H_{1/2}^1(\Gamma_\pm)}$$

for some constant C independent from ϕ and ψ . This proves that $\mathcal{T}^\pm : H_{1/2}^1(\Gamma_\pm) \rightarrow H_{1/2}^{-1/2}(\Gamma_\pm)$ are well-defined and are continuous. We remark that for sufficiently regular u^\pm , we have (using Green's formula)

$$\mathcal{T}^\pm \phi^\pm = \mp \frac{1}{\mu^\pm} \frac{\partial u^\pm}{\partial z} \Big|_{\Gamma_\pm}. \quad (1.26)$$

Since $\gamma^\pm - \gamma^\pm \mathcal{R}^\pm \gamma^\pm = 0$, we also observe, using Green's formula (and a density argument) that

$$\langle \mathcal{T}^\pm \phi^\pm, \gamma^\pm v \rangle = \int_{B_{r_*, z_*}^\pm} \frac{1}{\mu^\pm r} \nabla(ru^\pm) \nabla(r\bar{v}) \, dr \, dz + \int_{B_{r_*, z_*}^\pm} \operatorname{div}\left(\frac{1}{\mu r} \nabla(ru^\pm)\right) \bar{v} r \, dr \, dz^\pm$$

for all $v \in H_{1/2}^1(B_{r_*, z_*}^\pm)$. Therefore we also have

$$\langle \mathcal{T}^\pm \phi^\pm, \gamma^\pm v \rangle = \int_{B_{r_*, z_*}^\pm} \frac{1}{\mu^\pm r} \nabla(ru^\pm) \nabla(r\bar{v}) \, dr \, dz - \int_{B_{r_*, z_*}^\pm} i\omega\sigma^\pm u^\pm \bar{v} r \, dr \, dz$$

$\forall v \in H_{1/2}^1(B_{r^*, z^*}^\pm)$. Then it becomes clear from the variational formulation (1.13) that $u|_{B_{r^*, z^*}} \in H_{1/2}^1(B_{r^*, z^*})$ and satisfies

$$\begin{aligned} & \int_{B_{r^*, z^*}} \frac{1}{\mu} \nabla(ru) \cdot \frac{1}{r} \nabla(r\bar{v}) \, dr \, dz - \int_{B_{r^*, z^*}} i\omega\sigma u \bar{v} r \, dr \, dz \\ & + \langle \mathcal{T}^+ \gamma^+ u, \gamma^+ v \rangle + \langle \mathcal{T}^- \gamma^- u, \gamma^- v \rangle = \int_{B_{r^*, z^*}} i\omega J \bar{v} r \, dr \, dz \quad \forall v \in H_{1/2}^1(B_{r^*, z^*}). \end{aligned} \quad (1.27)$$

We immediately get the following equivalence result.

Proposition 1.2.7. *A function $u \in H_{1/2}^1(B_{r^*})$ is solution of (1.13) if and only if $u|_{B_{r^*, z^*}} \in H_{1/2}^1(B_{r^*, z^*})$ and is solution of (1.27) and $u = u^\pm$ on B_{r^*, z^*}^\pm where $u^\pm \in H_{1/2}^1(B_{r^*, z^*}^\pm)$ are solution of (1.24) with $\phi^\pm = \gamma^\pm(u|_{B_{r^*, z^*}})$.*

Formulation (1.27) is the one that we would like to use in practice. Proposition 1.2.7 and the well-posedness of (1.13) show that (1.27) is also well-posed. To be numerically effective one needs explicit expressions for \mathcal{T}^\pm . We shall use for that purpose Proposition 1.2.3. We are then led to consider the spectral decompositions of $\mathcal{S}_{\mu^+}^{\sigma^+}$ and $\mathcal{S}_{\mu^-}^{\sigma^-}$ that correspond to the one in Proposition 1.2.3 for $(\mu, \sigma) = (\mu^+, \sigma^+)$ and $(\mu, \sigma) = (\mu^-, \sigma^-)$ respectively. Since the treatment of both cases is the same and in order to simplify the notation we shall use the same notation for the spectral decomposition of $\mathcal{S}_{\mu^+}^{\sigma^+}$ and $\mathcal{S}_{\mu^-}^{\sigma^-}$.

For $\phi^\pm \in H_{1/2}^1(\Gamma_\pm)$ we have the spectral decomposition

$$\phi^\pm = \sum_{j=1}^m Q_{0j}(\phi^\pm) + \sum_{k>n} Q_k(\phi^\pm).$$

By definition of Q_{0j} and Q_k the functions u^\pm defined on B_{r^*, z^*}^\pm by

$$u^\pm(r, z) = \sum_{j=1}^m Q_{0j}(\phi^\pm)(r) \exp(\mp \sqrt{\nu_{0j}}(z \mp z_*)) + \sum_{k>n} Q_k(\phi^\pm)(r) \exp(\mp \sqrt{\nu_k}(z \mp z_*)) \quad \text{in } B_{r^*, z^*}^\pm, \quad (1.28)$$

(the square root is determined as the one with positive real part) formally satisfy (1.24). In order to rigorously prove this, one only needs to verify that this function is in $H_{1/2}^1(B_{r^*, z^*}^\pm)$. Since the eigenfunctions $Q_{0j}(\phi^\pm)$ and $Q_k(\phi^\pm)$ are in $H_{1/2}^1(I)$, one easily checks that

$$u_N^\pm(r, z) := \sum_{j=1}^m Q_{0j}(\phi^\pm)(r) \exp(\mp \sqrt{\nu_{0j}}(z \mp z_*)) + \sum_{k=n+1}^N Q_k(\phi^\pm)(r) \exp(\mp \sqrt{\nu_k}(z \mp z_*)) \quad \text{in } B_{r^*, z^*}^\pm, \quad (1.29)$$

is in $H_{1/2}^1(B_{r^*, z^*}^\pm)$ and verifies (1.24) with boundary data on Γ_\pm equal

$$\phi_N^\pm = \sum_{j=1}^m Q_{0j}(\phi^\pm) + \sum_{k=n+1}^N Q_k(\phi^\pm).$$

We then can conclude using the following lemma.

Lemma 1.2.8. *Let $\phi \in H_{1/2}^{1/2}(I)$ and set for $N > n$,*

$$\phi_N = \sum_{j=1}^m Q_{0j}(\phi) + \sum_{k=n+1}^N Q_k(\phi).$$

Then, $\|\phi_N - \phi\|_{H_{1/2}^{1/2}(I)} \rightarrow 0$ as $N \rightarrow \infty$.

The proof of this Lemma is itself a straightforward consequence of the following result since, using the notation of the Lemma below,

$$\|\phi_N - \phi\|_{\widetilde{H_{1/2}^{1/2}(I)}}^2 = \sum_{k>N} (1 + |\nu_k|)^{1/2} \|P_k W \phi\|_{L_{1/2}^2(I)}^2.$$

Lemma 1.2.9. *Let $\theta \in [0, 1]$ and let $\nu_* \in \mathbb{R}$. The norm defined by*

$$\|\phi\|_{\widetilde{H_{1/2}^\theta(I)}}^2 := \sum_{k=1}^{\infty} (1 + |\nu_k|)^\theta \|P_k W \phi\|_{L_{1/2}^2(I)}^2$$

where $\nu_k, k > n$, are the eigenvalues of \mathcal{S}_μ^σ as defined in Proposition 1.2.3 and $\nu_k = \nu_$ for $k \leq n$, defines an equivalent norm on $H_{1/2}^\theta(I)$.*

Proof. We first observe that thanks to Lemma 1.2.5, the result is obvious for $\theta = 0$ since $\|\cdot\|_{H_{1/2}^{0,\mu}(I)}$ is a equivalent norm of $L_{1/2}^2(I)$ and

$$\|\phi\|_{L_{1/2}^2(I)}^2 = \|W \phi\|_{H_{1/2}^{0,\mu}(I)}^2$$

and $W : L_{1/2}^2(I) \rightarrow L_{1/2}^2(I)$ is an isomorphism. Using interpolation theory one then only needs to prove the result for $\theta = 1$. The case of $\theta = 1$ will also be proved using interpolation theory since, using again Lemma 1.2.5 and the definition of \mathcal{A}_μ , we have $H_{1/2}^1(I) = [D(\mathcal{A}_\mu), L_{1/2}^2(I)]_{1/2}$. Therefore it is sufficient to prove that

$$\|\phi\|_{D(\mathcal{A}_\mu)}^2 = \|\phi\|_{L_{1/2}^2(I)}^2 + \|\mathcal{A}_\mu \phi\|_{L_{1/2}^2(I)}^2 = \sum_{k=1}^{\infty} (1 + \lambda_k^2) \|P_k \phi\|_{L_{1/2}^2(I)}^2$$

is equivalent to

$$\|\phi\|_{\widetilde{H_{1/2}^2(I)}}^2 := \sum_{k=1}^{\infty} (1 + |\nu_k|^2) \|P_k W \phi\|_{L_{1/2}^2(I)}^2.$$

Using the identity $P_k(W \mathcal{S}_\mu^\sigma \phi) = \nu_k P_k W \phi$ for $k > n$, we observe that

$$\|\phi\|_{\widetilde{H_{1/2}^2(I)}}^2 = \|\phi\|_{L_{1/2}^2(I)}^2 + \|\mathcal{S}_\mu^\sigma(\phi - Q_0 \phi)\|_{L_{1/2}^2(I)}^2 + |\nu_*|^2 \|Q_0 \phi\|_{L_{1/2}^2(I)}^2. \quad (1.30)$$

Since

$$\|\mathcal{S}_\mu^\sigma(Q_0 \phi)\|_{L_{1/2}^2(I)}^2 \leq C \|Q_0 \phi\|_{L_{1/2}^2(I)}^2$$

with $C = \sup\{|\nu_{0j}|^2, j = 1, m\}$, then $\mathcal{S}_\mu^\sigma(I - Q_0) = \mathcal{A}_\mu + \mathcal{M}_0$, where $\mathcal{M}_0 := \mathcal{M}^\sigma - \mathcal{S}_\mu^\sigma Q_0$ is a bounded operator on $L_{1/2}^2(I)$. Therefore, with C denoting a constant independent of ϕ but whose value may change from a line to another, and using the first part of the proof,

$$\|\phi\|_{D(\mathcal{A}_\mu)}^2 \leq 2\|\mathcal{S}_\mu^\sigma(\phi - Q_0\phi)\|_{L_{1/2}^2(I)}^2 + 2\|\mathcal{M}_0\phi\|_{L_{1/2}^2(I)}^2 + \|\phi\|_{L_{1/2}^2(I)}^2 \leq C\|\phi\|_{\widetilde{H}_{1/2}^2(I)}^2$$

and

$$\|\phi\|_{\widetilde{H}_{1/2}^2(I)}^2 \leq 2\|\mathcal{A}_\mu\phi\|_{L_{1/2}^2(I)}^2 + 2\|\mathcal{M}_0\phi\|_{L_{1/2}^2(I)}^2 + (1 + |\nu_*|^2)\|\phi\|_{L_{1/2}^2(I)}^2 \leq C\|\phi\|_{D(\mathcal{A}_\mu)}^2,$$

which proves the desired equivalence of norms and concludes the proof. \square

The expression of u_N^\pm in B_{r_*, z_*}^\pm (1.29) yields,

$$\mp \frac{\partial u_N^\pm}{\partial z} \Big|_{\Gamma_\pm} = \sum_{j=1}^m \sqrt{\nu_{0j}} Q_{0j}(\phi^\pm) + \sum_{n < k \leq N} \sqrt{\nu_k} Q_k(\phi^\pm).$$

Therefore, using (1.26) and letting $N \rightarrow \infty$ we obtain (explicitly specifying in the notation the dependence on Γ_\pm on the spectral decomposition)

$$\mathcal{T}^\pm(\phi^\pm) = \frac{1}{\mu^\pm} \left(\sum_{j=1}^{m^\pm} \sqrt{\nu_{0j}^\pm} Q_{0j}^\pm \phi^\pm + \sum_{k > n^\pm} \sqrt{\nu_k^\pm} Q_k^\pm \phi^\pm \right). \quad (1.31)$$

1.2.3 On the analysis of spectral error truncation

For numerical simulations the spectral representation of operators \mathcal{T}^\pm should be truncated. We shall give here some estimates on the error due to this truncation. For $N > n^\pm$, we define the projectors

$$\mathcal{Q}_N^\pm := \sum_{j=1}^{m^\pm} \mathcal{Q}_{0j}^\pm + \sum_{n^\pm < k \leq N} \mathcal{Q}_k^\pm,$$

and the truncated DtN operators

$$\mathcal{T}_N^\pm := \mathcal{T}^\pm \mathcal{Q}_N^\pm = \frac{1}{\mu^\pm} \left(\sum_{j=1}^{m^\pm} \sqrt{\nu_{0j}^\pm} \mathcal{Q}_{0j}^\pm + \sum_{n^\pm < k \leq N} \sqrt{\nu_k^\pm} \mathcal{Q}_k^\pm \right). \quad (1.32)$$

According to Lemma 1.2.9, $\mathcal{Q}_N^\pm : H^{1/2}(\Gamma_\pm) \rightarrow H^{1/2}(\Gamma_\pm)$ are continuous and therefore $\mathcal{T}_N^\pm : H^{1/2}(\Gamma_\pm) \rightarrow H^{-1/2}(\Gamma_\pm)$ are also continuous. We are interested in considering $u_N \in H_{1/2}^1(B_{r_*, z_*})$ solving

$$\begin{aligned} & \int_{B_{r_*, z_*}} \frac{1}{\mu} \nabla(r u_N) \cdot \frac{1}{r} \nabla(r \bar{v}) \, dr \, dz - \int_{B_{r_*, z_*}} i\omega \sigma u_N \bar{v} r \, dr \, dz \\ & + \langle \mathcal{T}_N^+ \gamma^+ u_N, \mathcal{Q}_N^+ \gamma^+ v \rangle + \langle \mathcal{T}_N^- \gamma^- u_N, \mathcal{Q}_N^- \gamma^- v \rangle = \int_{B_{r_*, z_*}} i\omega J \bar{v} r \, dr \, dz \quad \forall v \in H_{1/2}^1(B_{r_*, z_*}). \end{aligned} \quad (1.33)$$

This variational problem is well-posed for all N as indicated in the following. Using the Riesz representation theorem, we introduce $A_0 : H_{1/2}^1(B_{r_*, z_*}) \rightarrow H_{1/2}^1(B_{r_*, z_*})$, $A : H_{1/2}^1(B_{r_*, z_*}) \rightarrow H_{1/2}^1(B_{r_*, z_*})$ and $A_N : H_{1/2}^1(B_{r_*, z_*}) \rightarrow H_{1/2}^1(B_{r_*, z_*})$ defined by

$$\begin{aligned} (A_0 w, v)_{H_{1/2}^1(B_{r_*, z_*})} &= \int_{B_{r_*, z_*}} \frac{1}{\mu} \nabla(rw) \cdot \frac{1}{r} \nabla(r\bar{v}) - i\omega\sigma w \bar{v} r \, dr \, dz, \\ (Aw, v)_{H_{1/2}^1(B_{r_*, z_*})} &= (A_0 w, v)_{H_{1/2}^1(B_{r_*, z_*})} + \langle \mathcal{T}^+ \gamma^+ w, \gamma^+ v \rangle + \langle \mathcal{T}^- \gamma^- w, \gamma^- v \rangle, \quad \text{and} \\ (A_N w, v)_{H_{1/2}^1(B_{r_*, z_*})} &= (A_0 w, v)_{H_{1/2}^1(B_{r_*, z_*})} + \langle \mathcal{T}^+ \mathcal{Q}_N^+ \gamma^+ w, \mathcal{Q}_N^+ \gamma^+ v \rangle + \langle \mathcal{T}^- \mathcal{Q}_N^- \gamma^- w, \mathcal{Q}_N^- \gamma^- v \rangle, \end{aligned}$$

for all $v \in H_{1/2}^1(B_{r_*, z_*})$, respectively. We recall that the operator A_0 is coercive, and more precisely

$$\Re(A_0 w, w)_{H_{1/2}^1(B_{r_*, z_*})} \geq a_0 \|w\|_{H_{1/2}^1(B_{r_*, z_*})}^2$$

for some positive constant a_0 independent of w . We observe from (1.25) that

$$\Re \langle \mathcal{T}^\pm \phi^\pm, \phi^\pm \rangle \geq 0,$$

and therefore

$$\Re(A_N w, w)_{H_{1/2}^1(B_{r_*, z_*})} \geq a_0 \|w\|_{H_{1/2}^1(B_{r_*, z_*})}^2.$$

This means in particular, thanks to the Lax-Milgram theorem that A_N is bijective and also

$$\|A_N^{-1}\| \leq 1/a_0.$$

Consequently problem (1.33) has a unique solution $u_N \in H_{1/2}^1(B_{r_*, z_*})$ that continuously depends on J with a modulus of continuity independent of N .

From the continuity of \mathcal{T}^\pm we easily obtain

$$\|(A - A_N)w\|_{H_{1/2}^1(B_{r_*, z_*})} \leq C \left(\|\gamma^+ w - \mathcal{Q}_N^+ \gamma^+ w\|_{H_{1/2}^{1/2}(\Gamma_+)} + \|\gamma^- w - \mathcal{Q}_N^- \gamma^- w\|_{H_{1/2}^{1/2}(\Gamma_-)} \right) \quad (1.34)$$

for some constant C independent of N and $w \in H_{1/2}^1(B_{r_*, z_*})$. Therefore, using Lemma 1.2.9,

$$\lim_{N \rightarrow \infty} \|(A - A_N)w\|_{H_{1/2}^1(B_{r_*, z_*})} = 0 \quad \forall w \in H_{1/2}^1(B_{r_*, z_*}).$$

With $u \in H_{1/2}^1(B_{r_*, z_*})$ denoting the solution of (1.27), we observe that

$$Au = A_N u_N.$$

Therefore,

$$u - u_N = A_N^{-1}(A_N u - Au).$$

This proves in particular that

$$\|u - u_N\|_{H_{1/2}^1(B_{r_*, z_*})} \leq 1/a_0 \|(A - A_N)u\|_{H_{1/2}^1(B_{r_*, z_*})} \rightarrow 0 \text{ as } N \rightarrow \infty. \quad (1.35)$$

We can summarize these results in the following proposition

Proposition 1.2.10. *Under the same assumptions as in Proposition 1.1.7, the variational problem (1.33) has a unique solution $u_N \in H_{1/2}^1(B_{r_*, z_*})$. Moreover, if $u \in H_{1/2}^1(B_{r_*, z_*})$ is the solution of (1.27), then*

$$\|u - u_N\|_{H_{1/2}^1(B_{r_*, z_*})} \rightarrow 0 \text{ as } N \rightarrow \infty.$$

We shall now give some indication on the rate of convergence under some additional regularity assumptions on the source term J and the coefficients μ and σ . Obviously, from (1.34) and (1.35)

$$\|u - u_N\|_{H_{1/2}^1(B_{r_*, z_*})} \leq C/a_0 \left(\|\gamma^+ u - \mathcal{Q}_N^+ \gamma^+ u\|_{H_{1/2}^{1/2}(\Gamma_+)} + \|\gamma^- u - \mathcal{Q}_N^- \gamma^- u\|_{H_{1/2}^{1/2}(\Gamma_+)} \right). \quad (1.36)$$

Therefore the speed of convergence will depend on the regularity of $\gamma^\pm u$. Considering problem (1.10) satisfied by u in the unbounded domain B_{r_*} and differentiating the equations with respect to z (i.e. considering the equation satisfied $(u(r, z + \Delta z) - u(r, z))/\Delta z$, then letting $\Delta z \rightarrow 0$) one easily observes from the well-posedness of problem (1.10) that if in addition

$$\frac{\partial^m J}{\partial z^m} \in L^2(B_{r_*}), \quad \frac{\partial^m \sigma}{\partial z^m} \in L^\infty(B_{r_*}) \text{ and } \frac{\partial^m \mu^{-1}}{\partial z^m} \in L^\infty(B_{r_*}),$$

for some integer $m \geq 0$, then

$$\frac{\partial^m u}{\partial z^m} \in H_{1/2}^1(B_{r_*}).$$

Consequently, if this holds with $m = 2$, then the first equation in (1.10) yields

$$\gamma^\pm \mathcal{S}_{\mu^\pm}^{\sigma^\pm} u = -\frac{1}{\mu^\pm} \gamma^\pm \frac{\partial^2 u}{\partial z^2} \in L_{1/2}^2(\Gamma_\pm).$$

With the help of Lemma 1.2.9, we can then estimate,

$$\begin{aligned} \|\gamma^\pm u - \mathcal{Q}_N^\pm \gamma^\pm u\|_{H_{1/2}^{1/2}(\Gamma_\pm)}^2 &\leq C_1 \sum_{k=N+1}^{\infty} (1 + |\nu_k^\pm|)^{1/2} \|P_k^\pm W^\pm \phi\|_{L_{1/2}^2(I)}^2 \\ &\leq \frac{C_2}{(1 + |\nu_N^\pm|)^{3/2}} \sum_{k=N+1}^{\infty} (1 + |\nu_k^\pm|)^2 \|P_k^\pm W^\pm \phi\|_{L_{1/2}^2(I)}^2 \\ &\leq \frac{C_3}{(1 + |\nu_N^\pm|)^{3/2}} \left(\|\phi\|_{L_{1/2}^2(\Gamma_\pm)}^2 + \|\mathcal{S}_{\mu^\pm}^{\sigma^\pm} u\|_{L_{1/2}^2(\Gamma_\pm)}^2 \right) \end{aligned}$$

where the constants C_1 , C_2 and C_3 are independent of N and where we used in the second inequality the fact that $|\nu_k| \rightarrow \infty$ as $k \rightarrow \infty$. According to Proposition 1.2.3 and inequalities (1.20),

$$|\nu_N| \geq CN^2$$

for some constant $C > 0$ independent from N . From the discussion above we then can deduce the following theorem.

Theorem 1.2.11. *Under the assumptions as in Proposition 1.1.7 and the additional assumptions that*

$$\frac{\partial^m J}{\partial z^m} \in L^2(B_{r_*}), \quad \frac{\partial^m \sigma}{\partial z^m} \in L^\infty(B_{r_*}) \quad \text{and} \quad \frac{\partial^m \mu^{-1}}{\partial z^m} \in L^\infty(B_{r_*}),$$

for $m = 0, 1, 2$, there exists a constant C that only depends on J , μ , σ , r_* and z_* such that

$$\|u - u_N\|_{H_{1/2}^1(B_{r_*, z_*})} \leq \frac{C}{N^{3/2}},$$

where $u \in H_{1/2}^1(B_{r_*, z_*})$ and $u_N \in H_{1/2}^1(B_{r_*, z_*})$ are the respective solutions of (1.27) and (1.33).

We end this section with a remark on the case of Dirichlet boundary conditions.

Remark 1.2.12. *The results and proofs of this section apply also to the case where the Neumann boundary conditions on $r = r_*$ are replaced with Dirichlet boundary conditions. The only modification would be the replacement of $H_{1/2}^1(B)$ by $H_{1/2,0}^1(B) := \{u \in H_{1/2}^1(B); u = 0 \text{ on } r = r_*\}$ where B stands for B_{r_*} or B_{r_*, z_*} . The eigenvalues λ_k^1 are in this case*

$$\lambda_k^1 = \left(\frac{j_{1,k}}{r_*} \right)^2$$

where $j_{1,k} > 0$ is the k^{th} positive zero of the Bessel function J_1 .

1.3 Numerical test

We recall the two-dimensional geometric representation of the eddy current testing procedure in the Orz plan from Figure 1.1 or, more precisely, Figure 1.2a. In the following examples, the two coils involved are represented by two rectangles with 0.67mm in length (radial direction) and 2mm in height (longitudinal direction). They are located 7.83mm away from the z -axis and have a distance of 0.5mm between them. The SG tube measures 9.84mm in radius for the interior interface and 11.11mm for the exterior interface. We assume some deposit with a rectangular shape on the shell side of the tube with 2mm in length and 6cm in height. The probe coils and the deposit are placed symmetrically with regard to the r -axis. The permeabilities and conductivities of the materials are given in Table 1.1. The background permeability μ_0 is the permeability of vacuum.

	vacuum	tube	deposit
permeability	$\mu_v = \mu_0$	$\mu_t = 1.01\mu_0$	$\mu_d = 10\mu_0$
conductivity (in $S \cdot m^{-1}$)	$\sigma_v = 0$	$\sigma_t = 1 \times 10^3$	$\sigma_d = 1 \times 10^4$

Table 1.1: Values of the physical parameters for the numerical examples.

To approximate solutions to the original eddy current problem (1.6) on the unbounded domain \mathbb{R}_+^2 by numerical simulations, we use a domain $B_{R,Z}$ with very large cut-off parameters

$R = 300mm$, $Z = 100mm$ and we set Neumann conditions on these boundaries. These values of R and Z are large enough to ensure that the corresponding reference solution is close enough to the true solution to be able to study the (non-)convergence of the different domain cut-offs presented above. All numerical examples are done using the open-source finite element software *FreeFem++*. The computation of the reference solution uses a mesh that is adaptively refined with respect to this solution with a maximum edge size $h_{\max} = 2mm$ as well as P1 finite elements on the mesh. The degrees of freedom of the finite element space are about 49900 for $B_{R,Z}$ with $R = 300mm$ and $Z = 100mm$.

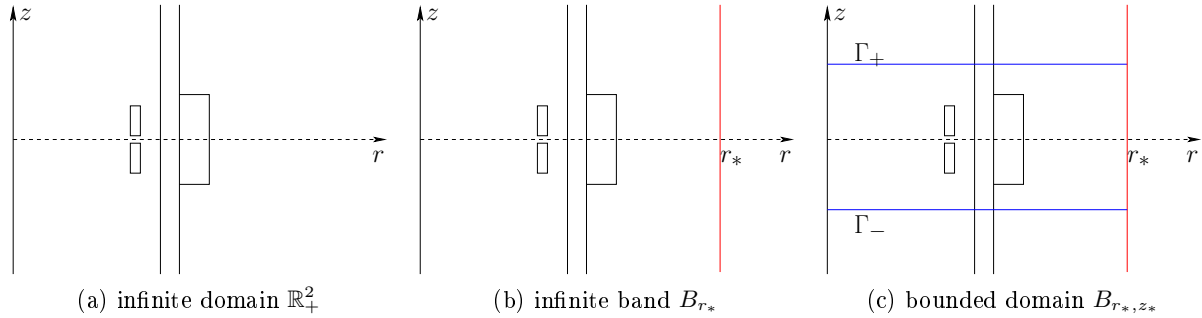


Figure 1.2: Domain cut-off in the radial and longitudinal directions.

1.3.1 Error of domain cut-off in the radial direction

Next we cut off the computational domain much closer to the tube at $r = r_*$, see Figure 1.2b by setting Dirichlet or Neumann boundary conditions on $\Gamma_{r_*} = \{r = r_*\}$. Using the same physical parameters as above and setting again $Z = 100mm$ to approximate solutions to the truncated problem on B_{r_*} on the domain $B_{r_*,Z}$; again, the value for Z gave sufficient numerical accuracy in our tests. In Figure 1.3 we show the numerical results corresponding to the convergence results of Proposition 1.1.7 and Proposition 1.6.3. As r_* increases, both the relative error of the Dirichlet problem (1.43) and that of the Neumann problem (1.10) tend to zero in the semi-norm $|\cdot|_{H_{1/2}^1(B_{r_*,Z})}$, though with different rates (Figure 1.3a). In the norm $\|\cdot\|_{L_{1/2}^2(B_{r_*,Z})}$, the error of the Neumann problem tends to zero, while the error of the Dirichlet problem is bounded away from zero (Figure 1.3b). The latter observation precisely corresponds to our theoretical results above, see Remark 1.1.8. The advantage of truncating the computational domain in the radial direction using a Neumann instead of a Dirichlet boundary condition is clearly confirmed by these examples.

In eddy current testing, one is interested in particular in measurements of impedances, which only depend on the solution inside the deposit domain Ω_D . To this end, we also compare the relative error of solution only on Ω_D due to the radial domain cut-off. From Figures 1.3c and 1.3d, at a cutting position $r_* = 50mm$, the relative errors issued from the Neumann problem in the semi-norm of $H_{1/2}^1(\Omega_d)$ and in the norm of $L_{1/2}^2(\Omega_d)$ are less than 0.5%. Therefore we conclude that simulations computed in a domain cut at $r = r_* = 50mm$ using Neumann boundary conditions are sufficiently precise for iterative reconstruction algorithms, since the noise level in the measurements would most probably be higher than the numerical error. Concerning the

finite element space on $B_{r_*,Z}$, this cut-off reduced the degrees of freedom in our experiments to about 16000.

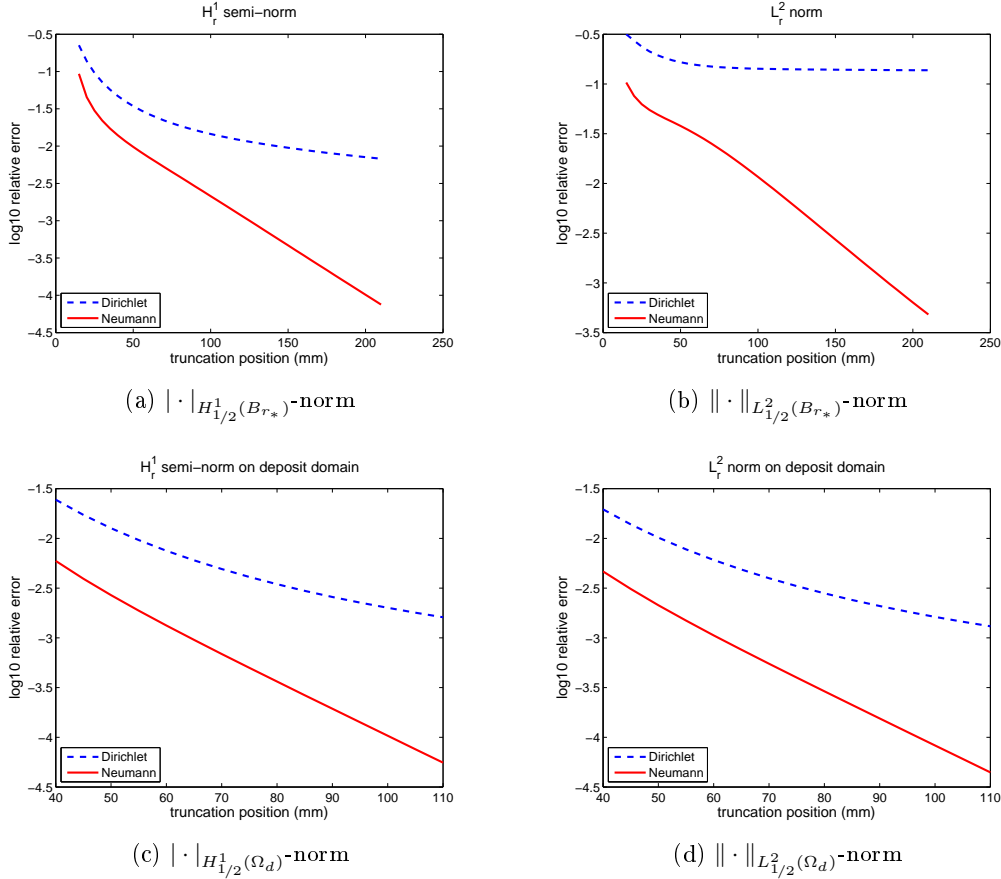


Figure 1.3: Relative errors with different cut-off position in the radial direction.

1.3.2 Error introduced by the DtN maps

In the following, we denote by u_{exact} a reference solution for the eddy current problem computed on the cut-off infinite band B_{r_*} with $r = r_* = 50\text{mm}$ using Neumann boundary conditions on Γ_{r_*} , compare Figure 1.2b. To compute u_{exact} numerically, we resolve the problem in a domain bounded $B_{r_*,Z}$ with $Z = 100\text{mm}$, as explained above. Then $B_{r_*,Z}$ is cut off into the bounded domain B_{r_*,z_*} with $\Gamma_{\pm} = \{0 < r < r_*, z = \pm z_* = \pm 5\text{mm}\}$, compare Figure 1.2c. The degrees of freedom of the P1 finite element space reduced by this cut-off to about 3500 elements. We set different boundary conditions – Dirichlet, Neumann or DtN boundary conditions – on the top and bottom boundaries Γ_{\pm} and solve the corresponding variational problems again using the finite element software package *FreeFem++*. The solutions are denoted by $u_{\text{Dirichlet}}$, u_{Neumann} and u_{DtN} in the following.

To build the DtN maps, we first discretize the interval $I = (0, r_*)$ (that has the same length as Γ_{\pm}) using 5000 boundary elements and use an eigenvalue solver (more precisely, the

function `eigs` in *Matlab*) to compute the first eigenpairs $(\nu_{0j}^\pm, Q_{0j}^\pm)$ and (ν_k^\pm, Q_k^\pm) corresponding to the physical parameters μ^\pm and σ^\pm . We then interpolate the boundary elements on I in the boundary element space on Γ_\pm of the finite element space on the computational domain (141 elements on each boundary) to get numerical approximations to the truncated DtN maps introduced in (1.32).

Choose of truncation order N for DtN operators

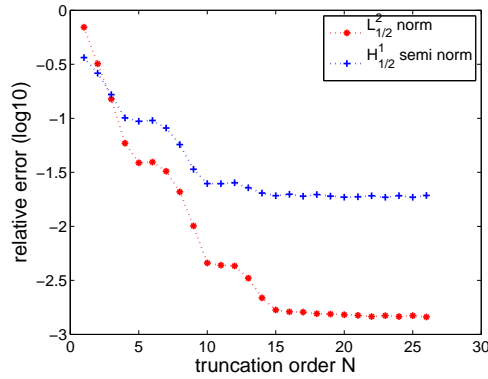


Figure 1.4: Relative errors for eddy current simulations using DtN maps with different truncation orders N .

Figure 1.4 illustrates the relative errors of u_{DtN} using different truncation parameters N for the DtN operator \mathcal{T}_N^\pm , see (1.32), with respect to u_{exact} in the $\|\cdot\|_{L^2_{1/2}(B_{r^*,z^*})}$ -norm and the $|\cdot|_{H^1_{1/2}(B_{r^*,z^*})}$ -semi-norms. The relative error decreases as the truncation order N increases before saturating at about $N = 16$. For $N = 20$, the errors are sufficiently small.

Comparison with other boundary conditions

Figure 1.5 illustrates real and imaginary parts of for the three different horizontal cutting-off techniques (Dirichlet, Neumann, and DtN) we investigated above. It shows in particular that the domain cut-off using DtN maps constructed with the first 20 eigenvalues and eigenprojections approaches the most the exact model. Moreover, Table 1.2 indicates the relative errors of the eddy current simulations on the cut-off domain in the $\|\cdot\|_{L^2_{1/2}(B_{r^*,z^*})}$ -norm and the $|\cdot|_{H^1_{1/2}(B_{r^*,z^*})}$ -semi-norm compared to the reference solution. Again, one clearly observes that using the DtN maps for the horizontal cut-off introduces a reasonably small error compared to the reference solution u_{exact} while truncating using Dirichlet- or Neumann boundary conditions on horizontal boundaries close to the coils and the deposit yields unacceptable errors. In particular, merely pre-computed DtN maps can ensure fast simulations of non-destructive eddy current measurements when many forward problems need to be solved. As mentioned in the introduction, such fast simulations are crucial for, e.g., iterative solution methods for the inversion of these measurements.

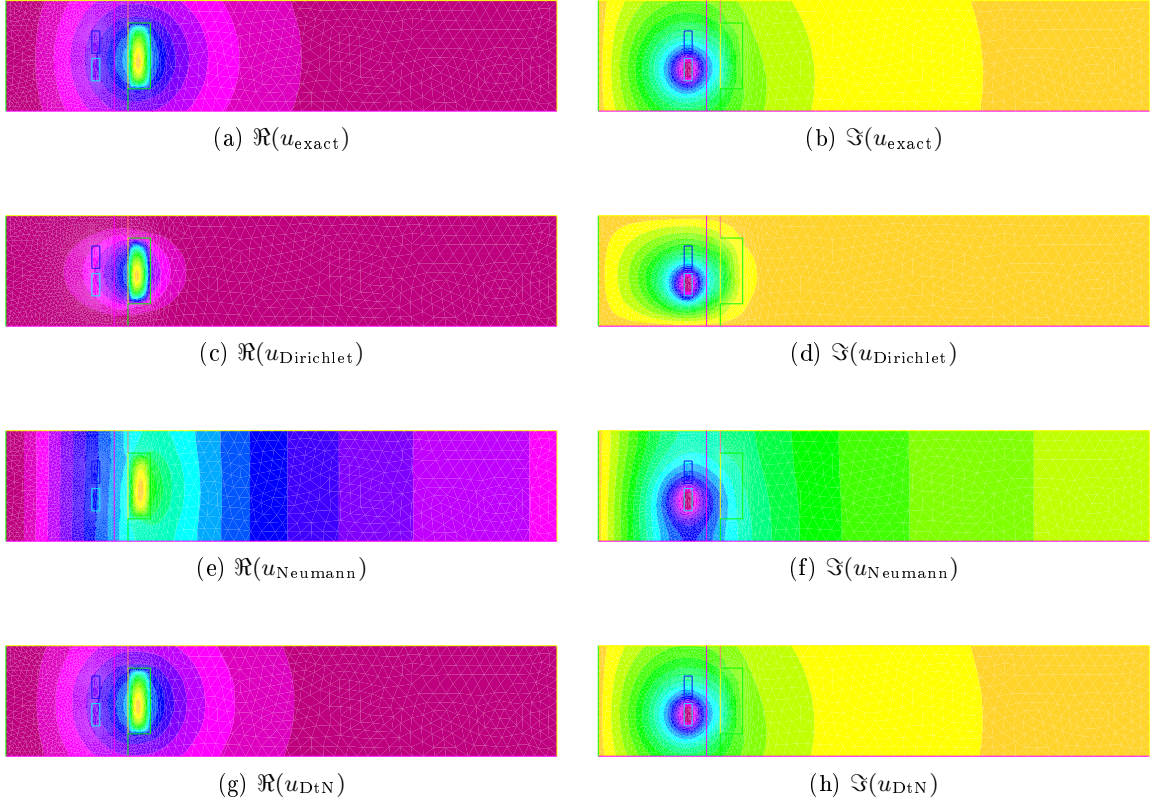


Figure 1.5: Real and imaginary parts of u fields on cut-off domain using different boundary conditions. DtN maps of truncation order $N = 20$.

	b. c.	Dirichlet	Neumann	DtN
norm				
$\ \cdot\ _{L^2_{1/2}(B_{r^*,z^*})}$		55.73%	181.57%	0.15%
$ \cdot _{H^1_{1/2}(B_{r^*,z^*})}$		28.79%	49.26%	1.86%

Table 1.2: Errors of longitudinal domain cut-off with different boundary conditions. DtN maps of truncation order $N = 20$.

Influence of the conductivity of tube on the DtN operators

We build the DtN operators with tubes of different conductivities σ_t and fixed permeability $\mu_t = 1.01\mu_0$. Figure 1.6 shows the first 20 eigenvalues of the operator \mathcal{S}_μ^σ (see Problem (1.14)) on the complex plane beginning from the one with the least absolute value which is closest to the original. In Figure 1.6a one observes that all the eigenvalues are real if $\sigma_t = 0$, since the perturbation operator $\mathcal{M}^\sigma = 0$ and therefore operator \mathcal{S}_μ^σ becomes selfadjoint and admits only real eigenvalues. In Figure 1.6b, we compare the eigenvalues for the different tube conductivities

σ_t . As σ_t increases, the perturbation term \mathcal{M}^σ becomes more and more important and the corresponding eigenvalues move farther and farther away from the real axis.

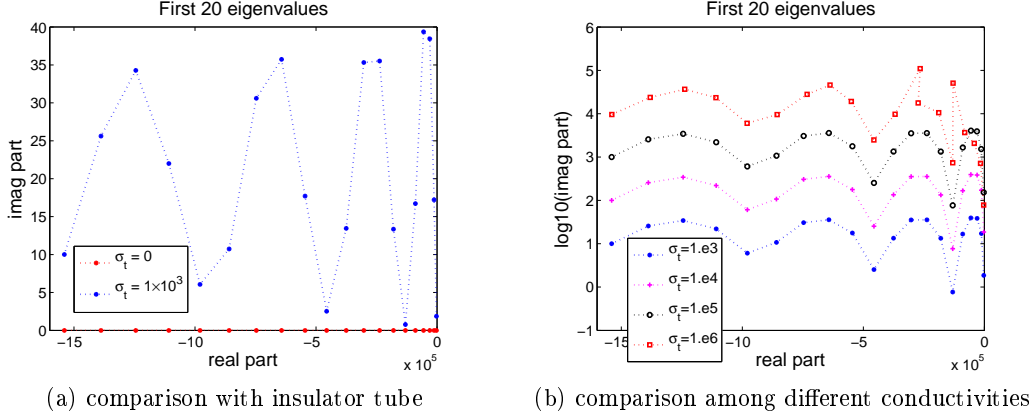


Figure 1.6: First 20 eigenvalues for different tube conductivities.

Table 1.3 gives the cut-off error with different DtN maps built with the corresponding tube conductivities. One remarks that the error due to the cut-off grows as the tube conductivity increases. This is due to the fact that when the perturbation term \mathcal{M}^σ becomes non-negligible in the operator \mathcal{S}_μ^σ , the number of the non-orthogonal eigenprojections Q_{0j} grows and then the first terms in the spectral decomposition of the DtN operators (see (1.31)) are not exact.

σ_t (S/m)	0	10^3	10^4	10^5	10^6
norm					
$\ \cdot\ _{L^2_{1/2}(B_{r^*,z^*})}$	0.12%	0.15%	0.93%	8.55%	14.86%
$ \cdot _{H^1_{1/2}(B_{r^*,z^*})}$	1.87%	1.86%	1.88%	3.86%	7.69%

Table 1.3: Errors of longitudinal domain cut-off with different DtN maps for different tube conductivities; DtN maps truncation order $N = 20$.

Influence of the permeability of tube on the DtN operators

In Figure 1.7 we illustrate the first 20 eigenvalues of \mathcal{S}_μ^σ with different permeabilities of tube μ_t but with the same conductivity $\sigma_t = 10^3 S/m$. As μ_t grows, some eigenvalues move far away from the real axis, which we have expected in Section 1.2.1 with the estimate (1.20).

Table 1.4 gives the error of domain cut-offs with different DtN maps built with the corresponding tube permeabilities. The error due to domain cut-off grows as the tube permeability goes far away from μ_0 .

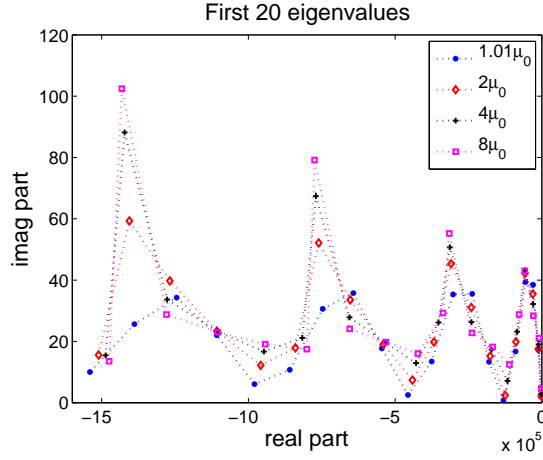


Figure 1.7: First 20 eigenvalues for different tube permeabilities.

μ_t	$1.01\mu_0$	$2\mu_0$	$4\mu_0$	$8\mu_0$
$\ \cdot\ _{L^2_{1/2}(B_{r^*,z^*})}$	0.15%	1.56%	2.67%	3.49%
$ \cdot _{H^1_{1/2}(B_{r^*,z^*})}$	1.86%	2.70%	4.55%	10.33%

Table 1.4: Errors of longitudinal domain cut-off with different DtN maps for different tube permeabilities; DtN maps truncation order $N = 20$.

Influence of the deposit shape on the domain cut-off error

In the reconstruction of deposits in the following chapter, we will evolve the deposit shape at each loop in an iterative algorithm. The DtN maps remain however unchanged in the iteration. So the deposit shape should not have impact on the precision of domain cut-off with the DtN maps. We test four different deposit shapes shown in Figure 1.8. Using the DtN operators with truncation order $N = 20$, we give the truncation errors in Table 1.5. We conclude that the deposit shape have no influence on the exactness of domain cut-off with DtN maps.

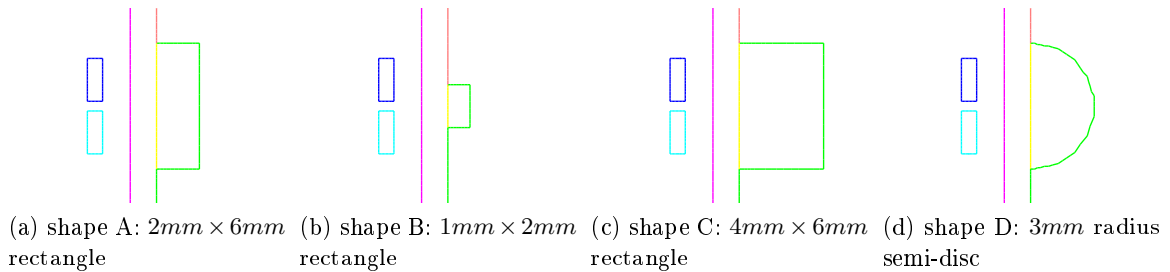


Figure 1.8: Different deposit shapes.

deposit shape	A	B	C	D
norm				
$\ \cdot\ _{L^2_{1/2}(B_{r_*,z_*})}$	0.15%	0.16%	0.16%	0.15%
$ \cdot _{H^1_{1/2}(B_{r_*,z_*})}$	1.86%	2.33%	2.01%	2.11%

Table 1.5: Errors of longitudinal domain cut-off with DtN maps for different deposit shapes; truncation order $N = 20$.

1.4 Appendix: Some properties of the weighted spaces

We recall the definition of the following spaces and corresponding norms. Let $\Omega \subset \mathbb{R}_+^2 := \{(r, z) : r > 0, z \in \mathbb{R}\}$ an open set. For $\lambda > 1$,

$$L^2_{1/2,\lambda}(\Omega) := \{v : r^{1/2}(1+r^2)^{-\lambda/2}v \in L^2(\Omega)\}, \quad H^1_{1/2,\lambda}(\Omega) := \{v \in L^2_{1/2,\lambda}(\Omega) : r^{-1/2}\nabla(rv) \in L^2(\Omega)\},$$

$$\|v\|_{L^2_{1/2,\lambda}(\Omega)} = \left\| \sqrt{\frac{r}{(1+r^2)^\lambda}} v \right\|_{L^2(\Omega)}, \quad \|v\|_{H^1_{1/2,\lambda}(\Omega)}^2 = \|v\|_{L^2_{1/2,\lambda}(\Omega)}^2 + \left\| r^{-1/2}\nabla(rv) \right\|_{L^2(\Omega)}^2.$$

For $\lambda = 0$, we define

$$L^2_{1/2}(\Omega) := L^2_{1/2,0}(\Omega) = \{v : v\sqrt{r} \in L^2(\Omega)\},$$

$$H^1_{1/2}(\Omega) := H^1_{1/2,0}(\Omega) = \{v \in L^2_{1/2}(\Omega) : r^{-1}\nabla(rv) \in L^2_{1/2}(\Omega)\}.$$

We shall also use the short notation

$$|v|_{H^1_{1/2}(\Omega)}^2 = \left\| r^{-1/2}\nabla(rv) \right\|_{L^2(\Omega)}^2.$$

For $r_* > 0$ and an interval $I = \{r \in \mathbb{R} : 0 < r < r_*\}$ we define

$$L^2_{1/2}(I) := \{\phi : \phi\sqrt{r} \in L^2(I)\}, \quad H^1_{1/2}(I) := \{\phi \in L^2_{1/2}(I) : r^{-1}\partial_r(r\phi) \in L^2_{1/2}(I)\}.$$

1.4.1 Proof of Lemma 1.1.1

Proof. Given $0 < \epsilon < r_*$, we set $B_{r_*}^\epsilon := \{(r, z) \in B_{r_*} : r \geq \epsilon\}$ and $I^\epsilon := \{r \in \mathbb{R} : \epsilon < r < r_*\}$. One easily observes that $L^2_{1/2,\lambda}(B_{r_*}^\epsilon) \subset L^2(B_{r_*}^\epsilon)$ and $H^1_{1/2,\lambda}(B_{r_*}^\epsilon) \subset H^1(B_{r_*}^\epsilon) \subset L^2(\mathbb{R}, H^1((\epsilon, r_*)))$. Since $H^1((\epsilon, r_*)) \subset \mathcal{C}((\epsilon, r_*))$, for $0 < \epsilon < r < r' < r_*$ and for almost all $z \in \mathbb{R}$, we can write for $v \in H^1_{1/2,\lambda}(B_{r_*}^\epsilon)$,

$$|r'v(r', z) - rv(r, z)| = \left| \int_r^{r'} \frac{\partial}{\partial s}(sv(s, z)) ds \right| \leq |r' - r| \left(\int_r^{r'} s \frac{1}{s} \left| \frac{\partial}{\partial s}(sv(s, z)) \right|^2 ds \right)^{1/2}$$

$$\leq |r' - r| \sqrt{r_*} |v(\cdot, z)|_{H^1_{1/2}(I^\epsilon)}$$

$$\int_{\mathbb{R}} |r'v(r', z) - rv(r, z)|^2 dz \leq |r' - r|^2 r_* \int_{\mathbb{R}} |v(\cdot, z)|_{H^1_{1/2}(I^\epsilon)}^2 dz \leq |r' - r|^2 r_* |v|_{H^1_{1/2}(B_{r_*}^\epsilon)}^2.$$

Thus, for $r_n \rightarrow 0$ ($n \rightarrow \infty$), $\{r_n v(r_n, \cdot)\}_{n \in \mathbb{N}^*}$ is a Cauchy sequence in $L^2(\mathbb{R})$. Since $L^2(\mathbb{R})$ is complete, the sequence converges and we denote the $L^2(\mathbb{R})$ -norm of its limit by $l \geq 0$. Now we will show that $l = 0$. If not, due to the continuity of rv on r for almost all z , one should have

$$\exists \delta > 0 \quad \forall 0 < r < \delta \quad \int_{\mathbb{R}} |rv(r, z)|^2 dz \geq \frac{l^2}{2}.$$

For $0 < \epsilon < \delta < r_*$, with Fubini's theorem,

$$\begin{aligned} \|v\|_{L^2_{1/2, \lambda}(B_{r_*}^\epsilon)}^2 &\geq \|v\|_{L^2_{1/2, \lambda}(B_\delta^\epsilon)}^2 \\ &= \int_{\mathbb{R}} \left(\int_\epsilon^\delta \frac{1}{r(1+r^2)^{1/2, \lambda}} |rv(r, z)|^2 dr \right) dz = \int_\epsilon^\delta \frac{1}{r(1+r^2)^\lambda} \left(\int_{\mathbb{R}} |rv(r, z)|^2 dz \right) dr \\ &\geq \frac{l^2}{2} \frac{1}{(1+\delta^2)^\lambda} \int_\epsilon^\delta \frac{1}{r} dr \xrightarrow{\epsilon \rightarrow 0} \infty, \end{aligned}$$

which contradicts the fact that $v \in L^2_{1/2, \lambda}(B_{r_*}^\epsilon) \subset L^2_{1/2, \lambda}(\mathbb{R}_+^2)$. So

$$\lim_{r \rightarrow 0} \|rv(r, \cdot)\|_{L^2(\mathbb{R})} = l = 0.$$

Therefore, for almost all $z \in \mathbb{R}$ and $v \in H^1_{1/2, \lambda}(B_{r_*}^\epsilon) \subset L^2(\mathbb{R}, H^1((\epsilon, r_*)))$,

$$\begin{aligned} |v(r, z)|^2 &= \frac{1}{r^2} |rv|^2 = \frac{1}{r^2} \left| \int_0^r \frac{\partial}{\partial s} (sv(s, z)) ds \right|^2 \leq \frac{1}{r} \left| \int_0^r \frac{1}{\sqrt{s}} \frac{\partial}{\partial s} (sv(s, z)) ds \right|^2 \\ &\leq \frac{1}{r} \int_0^r \left| \frac{1}{\sqrt{s}} \frac{\partial}{\partial s} (sv(s, z)) \right|^2 ds = \int_0^r \left| \frac{1}{\sqrt{s}} \frac{\partial}{\partial s} (sv(s, z)) \right|^2 ds \\ &\leq \int_0^\infty \left| \frac{1}{\sqrt{r}} \frac{\partial}{\partial r} (rv(r, z)) \right|^2 dr. \end{aligned}$$

We have

$$\|v(r, \cdot)\|_{L^2(\mathbb{R})}^2 = \int_{\mathbb{R}} |v(r, z)|^2 dz \leq \int_{\mathbb{R}} \int_0^r \left| \frac{1}{\sqrt{s}} \frac{\partial}{\partial s} (sv(s, z)) \right|^2 ds dz.$$

By the dominated convergence theorem, let $r \rightarrow 0$ in the above inequality, we get $\|v(0, \cdot)\|_{L^2(\mathbb{R})} = 0$, which means $v|_{r=0}$ vanishes almost everywhere. Now we consider

$$\begin{aligned} \int_{\mathbb{R}_+^2} \frac{r}{(1+r^2)^\lambda} |v|^2 dr dz &= \int_{-\infty}^\infty \int_0^\infty \frac{r}{(1+r^2)^\lambda} |v(r, z)|^2 dr dz \\ &\leq \int_{-\infty}^\infty \left(\int_0^\infty \frac{r}{(1+r^2)^\lambda} dr \int_0^\infty \left| \frac{1}{\sqrt{r}} \frac{\partial}{\partial r} (rv(r, z)) \right|^2 dr \right) dz \\ &= \int_0^\infty \frac{r}{(1+r^2)^\lambda} dr \int_{\mathbb{R}_+^2} \left| \frac{1}{\sqrt{r}} \frac{\partial}{\partial r} (rv(r, z)) \right|^2 dr dz = \left(\int_0^\infty \frac{r}{(1+r^2)^\lambda} dr \right) \|v\|_{H^1_{1/2}(\mathbb{R}_+^2)}^2. \end{aligned}$$

Therefore, the inequality is proved by setting

$$C = \sqrt{1 + \int_0^\infty \frac{r}{(1+r^2)^\lambda} dr}.$$

□

1.4.2 Proof of Lemma 1.1.6

Proof. The first part of the proof is similar to the proof of Lemma 1.1.1. Given $0 < \epsilon < r_*$, we note $B_{r_*}^\epsilon = \{(r, z) \in B_{r_*} : r \geq \epsilon\}$. It is easy to show that the space $L^2_{1/2}(B_{r_*}^\epsilon)$ is equivalent to $L^2(B_{r_*}^\epsilon)$ and $H^1_{1/2}(B_{r_*}^\epsilon)$ to $H^1(B_{r_*}^\epsilon) \subset L^2(\mathbb{R}, H^1((\epsilon, r_*)))$. Since $H^1((\epsilon, r_*)) \subset \mathcal{C}((\epsilon, r_*))$, for $0 < \epsilon < r < r' < r_*$ and for almost all $z \in \mathbb{R}$, we can write for $v \in H^1_{1/2}(B_{r_*}^\epsilon)$

$$\begin{aligned} |r'v(r', z) - rv(r, z)| &= \left| \int_r^{r'} \frac{\partial}{\partial s}(sv(s, z)) \, ds \right| \leq |r' - r| \left(\int_r^{r'} s \frac{1}{s} \left| \frac{\partial}{\partial s}(sv(s, z)) \right|^2 \, ds \right)^{1/2} \\ &\leq |r' - r| \sqrt{r_*} |v(\cdot, z)|_{H^1_{1/2}(I)}, \end{aligned}$$

$$\int_{\mathbb{R}} |r'v(r', z) - rv(r, z)|^2 \, dz \leq |r' - r|^2 r_* \int_{\mathbb{R}} |v(\cdot, z)|^2_{H^1_{1/2}(I)} \, dz \leq |r' - r|^2 r_* \|v\|^2_{H^1_{1/2}(B_{r_*})}.$$

Thus, for $r_n \rightarrow 0$ ($n \rightarrow \infty$), $\{r_n v(r_n, \cdot)\}_{n \in \mathbb{N}^*}$ is a Cauchy sequence in $L^2(\mathbb{R})$. Since $L^2(\mathbb{R})$ is complete, the sequence converges and we denote the $L^2(\mathbb{R})$ -norm of its limit by $l \geq 0$. Now we will show that $l = 0$. If not, due to the continuity of rv on r for almost all z , we should have

$$\exists \delta > 0 \quad \forall 0 < r < \delta \quad \int_{\mathbb{R}} |rv(r, z)|^2 \, dz \geq \frac{l^2}{2}.$$

For $0 < \epsilon < \delta$, with Fubini's theorem,

$$\|v(\cdot, z)\|^2_{L^2_{1/2}(B_{r_*})} \geq \int_{\mathbb{R}} \left(\int_\epsilon^\delta \frac{1}{r} |rv(r, z)|^2 \, dr \right) \, dz = \int_\epsilon^\delta \frac{1}{r} \left(\int_{\mathbb{R}} |rv(r, z)|^2 \, dz \right) \, dr \geq \frac{l^2}{2} \int_\epsilon^\delta \frac{1}{r} \, dr \xrightarrow{\epsilon \rightarrow 0} \infty,$$

which contradicts the fact that $v \in L^2_{1/2}(B_{r_*})$. So $l = 0$. For almost all $z \in \mathbb{R}$ and $v \in L^2(\mathbb{R}, H^1((\epsilon, r_*)))$,

$$\begin{aligned} |v(r, z)|^2 &= \left| \frac{1}{r}(rv(r, z)) \right|^2 = \left| \frac{1}{r} \int_0^r \frac{\partial}{\partial s}(sv(s, z)) \, ds \right|^2 = \frac{1}{r} \left| \int_0^r \frac{1}{\sqrt{r}} \frac{\partial}{\partial s}(sv(s, z)) \, ds \right|^2 \\ &\leq \frac{1}{r} \cdot r \int_0^r \frac{1}{r} \left| \frac{\partial}{\partial s}(sv(s, z)) \right|^2 \, ds \leq \int_0^r \frac{1}{s} \left| \frac{\partial}{\partial s}(sv(s, z)) \right|^2 \, ds = |v(\cdot, z)|^2_{H^1_{1/2}((0, r))} \\ &\leq |v(\cdot, z)|^2_{H^1_{1/2}(I)}. \end{aligned}$$

By the dominated convergence theorem, let $r \rightarrow 0$ in the above inequality, we get $\|v(0, \cdot)\|_{L^2(\mathbb{R})} = 0$, which means $v(0, z)$ vanishes almost everywhere for $z \in \mathbb{R}$. Otherwise,

$$\|v(\cdot, z)\|^2_{L^2_{1/2}(I)} \leq \int_0^{r_*} r \, dr |v(\cdot, z)|^2_{H^1_{1/2}(I)} = \frac{r_*^2}{2} |v(\cdot, z)|^2_{H^1_{1/2}(I)}.$$

Therefore, we get

$$\|v\|^2_{L^2_{1/2}(B_{r_*})} = \left\| \|v(\cdot, z)\|_{L^2_{1/2}(I)} \right\|^2_{L^2(\mathbb{R})} \leq \frac{r_*^2}{2} \left\| |v(\cdot, z)|^2_{H^1_{1/2}(I)} \right\|^2_{L^2(\mathbb{R})} \leq \frac{r_*^2}{2} \|v\|^2_{H^1_{1/2}(B_{r_*})}.$$

By setting $C_p = r_*/\sqrt{2}$, the first Poincaré-type inequality (1.11) is proved.

To evaluate the trace, we calculate

$$\begin{aligned}
\|v\|_{H^{1/2}(\Gamma_{r_*})}^2 &= \frac{1}{r_*} \|\sqrt{r_*} v(r_*, \cdot)\|_{H^{1/2}(\mathbb{R})}^2 = \frac{1}{r_*} \left(r_* \int_{\mathbb{R}} (1 + |\xi|^2)^{1/2} |\hat{v}(r_*, \xi)|^2 d\xi \right) \\
&\leq \frac{1}{r_*} \left(r_* \int_{\mathbb{R}} |\hat{v}(r_*, \xi)|^2 d\xi + r_* \int_{\mathbb{R}} |\xi| |\hat{v}(r_*, \xi)|^2 d\xi \right) \\
&= \frac{1}{r_*} \left(\frac{1}{r_*} \int_{\mathbb{R}} |r_* \hat{v}(r_*, \xi)|^2 d\xi + \int_{\mathbb{R}} |\xi| \int_0^{r_*} \frac{\partial}{\partial r} (r |\hat{v}|^2) dr d\xi \right) \\
&= \frac{1}{r_*} \left(\frac{1}{r_*} \int_{\mathbb{R}} \left| \int_0^{r_*} \frac{\partial}{\partial r} (r \hat{v}) dr \right|^2 d\xi + \int_{\mathbb{R}} |\xi| \int_0^{r_*} 2\Re \left(\hat{v} \overline{\frac{\partial}{\partial r} (r \hat{v})} \right) dr d\xi \right) \\
&\leq \frac{1}{r_*} \left(\int_{\mathbb{R}} \left| \int_0^{r_*} \frac{1}{\sqrt{r}} \frac{\partial}{\partial r} (r \hat{v}) dr \right|^2 d\xi + 2 \int_{\mathbb{R}} \int_0^{r_*} |\xi| |\sqrt{r} \hat{v}| \left| \frac{1}{\sqrt{r}} \frac{\partial}{\partial r} (r \hat{v}) \right| dr d\xi \right) \\
&\leq \frac{1}{r_*} \left(|v|_{H_{1/2}^1(B_{r_*})}^2 + 2 \left(\int_{\mathbb{R}} \int_0^{r_*} |\xi|^2 |\sqrt{r} \hat{v}|^2 dr d\xi + \int_{\mathbb{R}} \int_0^{r_*} \left| \frac{1}{\sqrt{r}} \frac{\partial}{\partial r} (r \hat{v}) \right|^2 dr d\xi \right) \right) \\
&= \frac{1}{r_*} \left(|v|_{H_{1/2}^1(B_{r_*})}^2 + 2 \left(\int_{\mathbb{R}} \int_0^{r_*} \left| \frac{1}{\sqrt{r}} \frac{\partial}{\partial z} (r v) \right|^2 dr dz + \int_{\mathbb{R}} \int_0^{r_*} \left| \frac{1}{\sqrt{r}} \frac{\partial}{\partial r} (r v) \right|^2 dr dz \right) \right) \\
&= 3 \frac{1}{r_*} |v|_{H_{1/2}^1(B_{r_*})}^2.
\end{aligned}$$

Therefore, we get (1.12). □

1.4.3 Proof of Lemma 1.2.1

Proof. We suppose \mathcal{B} is a unit ball in $H_{1/2}^1(I)$. To prove the compactness of \mathcal{B} in $L_{1/2}^2(I)$, it is sufficient to show that $\tilde{\mathcal{B}} := \{\phi(\cdot)\sqrt{\cdot} : \phi \in \mathcal{B}\}$ is compact in $L^2(I)$. We use [18, Corollaire IV.26].

We suppose for arbitrary $\eta > 0$ small enough, $\omega \subset]\eta, r_* - \eta[$ is strongly included in I , written as $\omega \subset\subset I$. We note τ_h the translation operator: $(\tau_h \phi)(r) = \phi(r + h)$.

First of all, we shall show

$$\forall h \in \mathbb{R} \quad \text{with} \quad |h| < \eta \quad \text{and} \quad \forall \psi = \phi(\cdot)\sqrt{\cdot} \in \tilde{\mathcal{B}}, \quad \|\tau_h \psi - \psi\|_{L^2(\omega)} \xrightarrow{h \rightarrow 0} 0.$$

For $r \in \omega$, we have $|h| < \eta < r$. For $h > 0$,

$$\begin{aligned}
|\psi(r+h) - \psi(r)|^2 &= |\phi(r+h)\sqrt{r+h} - \phi(r)\sqrt{r}|^2 \\
&= |\phi(r+h)(r+h) - \phi(r)r + \phi(r+h)\sqrt{r+h}(\sqrt{r} - \sqrt{r+h})|^2 \frac{1}{r} \\
&\leq |\phi(r+h)(r+h) - \phi(r)r|^2 \frac{1}{r} + |\phi(r+h)|^2 (\sqrt{r+h} - \sqrt{r})^2 \frac{r+h}{r} \\
&= \left| \int_r^{r+h} \frac{d}{ds}(s\phi(s)) ds \right|^2 \frac{1}{r} + |\phi(r+h)|^2 \left(\frac{h}{\sqrt{r+h} + \sqrt{r}} \right)^2 \frac{r+h}{r} \\
&\leq \frac{h}{r} \int_r^{r+h} \left| \frac{d}{ds}(s\phi(s)) \right|^2 ds + |\phi(r+h)|^2 \left(\frac{h}{2\sqrt{r}} \right)^2 \frac{2r}{r} \\
&\leq 2h \int_r^{r+h} \frac{1}{r+h} \left| \frac{d}{ds}(s\phi(s)) \right|^2 ds + \frac{h}{2} |\phi(r+h)|^2 \\
&\leq 2h \int_r^{r+h} \frac{1}{s} \left| \frac{d}{ds}(s\phi(s)) \right|^2 ds + \frac{h}{2} |\phi(r+h)|^2 \\
&\leq 2h |\phi|_{H_{1/2}^1(I)}^2 + \frac{h}{2} |\phi(r+h)|^2,
\end{aligned}$$

thus by Lemma 1.2.1 and the fact that $\phi \in \mathcal{B}$

$$\|\tau_h \psi - \psi\|_{L^2(\omega)}^2 \leq 2hr_* |\phi|_{H_{1/2}^1(I)}^2 + \frac{h}{2} \|\phi\|_{L^2(I)}^2 \leq 2hr_* |\phi|_{H_{1/2}^1(I)}^2 + \frac{h}{2} r_* |\phi|_{H_{1/2}^1(I)}^2 \leq \frac{5h}{2} r_* \xrightarrow{h \rightarrow 0} 0.$$

For $h < 0$, we note always $h > 0$ but we calculate

$$\begin{aligned}
|\psi(r-h) - \psi(r)|^2 &= |\phi(r-h)\sqrt{r-h} - \phi(r)\sqrt{r}|^2 \\
&= |\phi(r)r - \phi(r-h)(r-h) - \phi(r-h)\sqrt{r-h}(\sqrt{r} - \sqrt{r-h})|^2 \frac{1}{r} \\
&\leq |\phi(r)r - \phi(r-h)(r-h)|^2 \frac{1}{r} + |\phi(r-h)|^2 (\sqrt{r} - \sqrt{r-h})^2 \frac{r-h}{r} \\
&= \left| \int_{r-h}^r \frac{d}{ds}(s\phi(s)) ds \right|^2 \frac{1}{r} + |\phi(r-h)|^2 \left(\frac{h}{\sqrt{r} + \sqrt{r-h}} \right)^2 \frac{r-h}{r} \\
&\leq \frac{h}{r} \int_{r-h}^r \left| \frac{d}{ds}(s\phi(s)) \right|^2 ds + |\phi(r-h)|^2 \left(\frac{h}{2\sqrt{r-h}} \right)^2 \frac{r-h}{r} \\
&\leq h \int_{r-h}^r \frac{1}{s} \left| \frac{d}{ds}(s\phi(s)) \right|^2 ds + \frac{h}{4} |\phi(r-h)|^2 \\
&\leq h |\phi|_{H_{1/2}^1(I)}^2 + \frac{h}{4} |\phi(r-h)|^2
\end{aligned}$$

again by Lemma 1.2.1 we have

$$\|\tau_{-h} \psi - \psi\|_{L^2(\omega)}^2 \leq hr_* |\phi|_{H_{1/2}^1(I)}^2 + \frac{h}{4} r_* |\phi|_{H_{1/2}^1(I)}^2 \leq \frac{5h}{4} r_* \xrightarrow{h \rightarrow 0} 0.$$

It remains to prove that

$$\forall \epsilon > 0 \quad \exists \omega \subset\subset I \quad \text{such that} \quad \|\phi(\cdot)\sqrt{\cdot}\|_{L^2(I \setminus \omega)} < \epsilon \quad \forall \phi \in \mathcal{B}.$$

If we take $\omega = (\eta, r_* - \eta)$, then by Lemma 1.2.1

$$\|\phi(\cdot)\sqrt{\cdot}\|_{L^2(I \setminus \omega)}^2 = \|\phi\|_{L^2_{1/2}((0, \eta))}^2 + \|\phi\|_{L^2_{1/2}((r_* - \eta, r_*))}^2 \leq \frac{\eta^2}{2} |\phi|_{H^1_{1/2}((0, \eta))}^2 + \frac{\eta^2}{2} |\phi|_{H^1_{1/2}((r_* - \eta, r_*))}^2 \leq \frac{\eta^2}{2}.$$

By setting η small enough we obtain the result.

So the conditions of [18, Corollaire IV.26] are satisfied, and \mathcal{B} is relatively compact in $L^2_{1/2}(I)$. The embedding $H^1_{1/2}(I) \hookrightarrow L^2_{1/2}(I)$ is hence compact. \square

1.5 Appendix: Proof of Proposition 1.1.5

Before the proof, we introduce some preliminaries. With the Fourier-transformed representation (1.8), we have

$$\frac{\partial}{\partial r}(r\hat{u})(r, \xi) = \begin{cases} \hat{u}(r_0, \xi)(-2\pi|\xi|r) \frac{K_0(2\pi|\xi|r)}{K_1(2\pi|\xi|r_0)} & \xi \neq 0, \\ 0 & \xi = 0. \end{cases} \quad (1.37)$$

Before the estimate, we introduce some properties for the functions

$$h(x; a, b) = \frac{1 + x^2}{2 + x^2} \left[ax \frac{K_1(ax)}{K_0(ax)} - bx \frac{K_0(bx)}{K_1(bx)} \right], \quad (1.38)$$

with $x > 0$, $a > b > 0$.

Lemma 1.5.1. *Let $a > b > 0$. The function $h(x; a, b)$ defined by (1.38) is positive and increasing in $x \in \mathbb{R}^+$. Moreover, for fixed b , the unique solution of $h(\cdot; a, b) = 1$, denoted by $x^*(a)$, has the asymptotic behavior $x^*(a) \sim O(a^{-1})$ when $a \rightarrow +\infty$.*

Proof. As $a > b > 0$ and $K_1(\cdot) > K_0(\cdot)$ for positive arguments, $h(\cdot; a, b)$ is positive on \mathbb{R}^+ . Since the function $(1 + x^2)/(2 + x^2)$ is positive and increasing, it is sufficient to discuss the monotonicity of

$$\tilde{h}(x; a, b) = ax \frac{K_1(ax)}{K_0(ax)} - bx \frac{K_0(bx)}{K_1(bx)}.$$

Its derivative writes

$$\tilde{h}'(x; a, b) = a^2 x \left(\frac{K_1^2(ax)}{K_0^2(ax)} - 1 \right) + b^2 x \left(1 - \frac{K_0^2(bx)}{K_1^2(bx)} \right) - 2b \frac{K_0(bx)}{K_1(bx)}.$$

We want to show that $\tilde{h}'(x; a, b) > 0$ for $x > 0$. It is equivalent to say $x\tilde{h}'(x; a, b) > 0$ for $x > 0$. If we denote $ax = A$, $bx = B$, then we are going to show

$$A^2 \left(\frac{K_1^2(A)}{K_0^2(A)} - 1 \right) + B^2 \left(1 - \frac{K_0^2(B)}{K_1^2(B)} \right) > 2B \frac{K_0(B)}{K_1(B)}, \quad A > B > 0.$$

[10, Theorem 2] implies the following inequality

$$\frac{1}{x} \cdot K_0^2(x) < K_1^2(x) - K_0^2(x), \quad x > 0.$$

We have

$$\frac{K_1^2(x)}{K_0^2(x)} - 1 > \frac{1}{x},$$

and

$$\frac{K_1^2(x)}{K_0^2(x)} > \frac{1+x}{x} \Rightarrow \frac{K_0^2(x)}{K_1^2(x)} < \frac{x}{1+x} \Rightarrow 1 - \frac{K_0^2(x)}{K_1^2(x)} > \frac{1}{1+x}.$$

With the above inequalities, we have

$$A^2 \left(\frac{K_1^2(A)}{K_0^2(A)} - 1 \right) + B^2 \left(1 - \frac{K_0^2(B)}{K_1^2(B)} \right) > A + \frac{B^2}{B+1} > B + \frac{B^2}{B+1} \geq 2B \sqrt{\frac{B}{B+1}} > 2B \frac{K_0(B)}{K_1(B)}.$$

Thus, we have shown that $h(x; a, b)$ is increasing. With the known limiting form of K_0 and K_1 for small and big arguments, we have

$$\begin{aligned} \lim_{x \rightarrow 0^+} h(x; a, b) &= \lim_{x \rightarrow 0^+} \frac{1}{2} \left[ax \frac{\frac{1}{ax}}{-\ln(ax)} - bx \frac{-\ln(bx)}{\frac{1}{bx}} \right] = 0, \\ \lim_{x \rightarrow +\infty} h(x; a, b) &= \lim_{x \rightarrow +\infty} x \frac{aK_1(ax)K_1(bx) - bK_0(ax)K_0(bx)}{K_0(ax)K_1(bx)} \\ &= \lim_{x \rightarrow +\infty} x \frac{\sqrt{\frac{\pi}{2ax}} \sqrt{\frac{\pi}{2bx}} e^{-(a+b)x} (a - b + O(\frac{1}{x}))}{\sqrt{\frac{\pi}{2ax}} \sqrt{\frac{\pi}{2bx}} e^{-(a+b)x} (1 + O(\frac{1}{x}))} = +\infty. \end{aligned}$$

Therefore, the monotonicity and continuity of $h(x; a, b)$ ensures that $h(x; a, b) = 1$ admits one unique solution x^* .

Given $b > 0$, we shall study the asymptotic behavior of $x^*(a)$ when $a \rightarrow +\infty$. First of all, we will prove by contradiction that $x^*(a) \rightarrow 0$ when $a \rightarrow +\infty$. If

$$\exists \epsilon > 0, \forall M > 0, \exists a > M, \text{ such that } x^*(a) > \epsilon,$$

then

$$\begin{aligned} 1 = h(x^*(a); a, b) &= \frac{1 + x^*(a)^2}{2 + x^*(a)^2} \cdot x^*(a) \cdot \left[a \frac{K_1(ax^*(a))}{K_0(ax^*(a))} - b \frac{K_0(bx^*(a))}{K_1(bx^*(a))} \right] \\ &\geq \frac{1}{2} \cdot \epsilon \cdot [M - b] \xrightarrow{M \rightarrow +\infty} +\infty. \end{aligned}$$

So $\lim_{a \rightarrow +\infty} x^*(a) = 0$. Now we will prove that $x^*(a) \sim O(a^{-1})$ ($a \rightarrow +\infty$).

1. If there exists a sequence $\{a_n\}$ tending to infinity such that $\lim_{n \rightarrow \infty} a_n x^*(a_n) = 0$, then

$$\begin{aligned} [1, 2] \ni \frac{2 + x^*(a_n)^2}{1 + x^*(a_n)^2} &= a_n x^*(a_n) \frac{K_1(a_n x^*(a_n))}{K_0(a_n x^*(a_n))} - b x^*(a_n) \frac{K_0(b x^*(a_n))}{K_1(b x^*(a_n))} \\ &\sim a_n x^*(a_n) \frac{\frac{1}{a_n x^*(a_n)}}{-\ln(a_n x^*(a_n))} - b x^*(a_n) \frac{-\ln(b x^*(a_n))}{\frac{1}{b x^*(a_n)}} \xrightarrow{n \rightarrow \infty} \infty. \end{aligned}$$

So there exists $l_{\min} > 0$ such that $a x^*(a) > l_{\min}$.

2. If there exists a sequence $\{a_n\}$ tending to infinity such that $\lim_{n \rightarrow \infty} a_n x^*(a_n) = +\infty$, then

$$\begin{aligned} [1, 2] \ni \frac{2 + x^*(a_n)^2}{1 + x^*(a_n)^2} &= a_n x^*(a_n) \frac{K_1(a_n x^*(a_n))}{K_0(a_n x^*(a_n))} - b x^*(a_n) \frac{K_0(b x^*(a_n))}{K_1(b x^*(a_n))} \\ &\sim a_n x^*(a_n) - b x^*(a_n) \frac{-\ln(b x^*(a_n))}{\frac{1}{b x^*(a_n)}} \xrightarrow{n \rightarrow \infty} \infty. \end{aligned}$$

So there exists $l_{\max} > 0$ such that $ax^*(a) < l_{\max}$. The needed asymptotic behavior is proved. \square

Proof of Proposition 1.1.5. From (1.37), we have

$$\begin{aligned} \left\| \frac{\partial}{\partial r}(ru)(r, \cdot) \right\|_{H^{-1/2}(\mathbb{R})}^2 &= \left\| (1 + |\cdot|^2)^{-1/4} \frac{\partial}{\partial r}(r\widehat{u})(r, \cdot) \right\|_{L^2(\mathbb{R})}^2 \\ &= \int_{-\infty}^{\infty} (1 + |\xi|^2)^{1/2} |\widehat{u}(r_0, \xi)|^2 (1 + |\xi|^2)^{-1} (2\pi|\xi|r)^2 \frac{K_0^2(2\pi|\xi|r)}{K_1^2(2\pi|\xi|r_0)} d\xi \\ &\leq \|u(r_0, \cdot)\|_{H^{1/2}(\mathbb{R})}^2 \left\| \frac{2\pi r |\cdot|}{(1 + |\cdot|^2)^{1/2}} \frac{K_0(2\pi r |\cdot|)}{K_1(2\pi r_0 |\cdot|)} \right\|_{L^\infty(\mathbb{R})}^2 \\ &= \|u(r_0, \cdot)\|_{H^{1/2}(\mathbb{R})}^2 \|g_n(\cdot; r_0, r)\|_{L^\infty(\mathbb{R}_\xi^+)}, \end{aligned}$$

where

$$g_n(\xi; r_0, r) := \frac{2\pi r \xi}{(1 + \xi^2)^{1/2}} \frac{K_0(2\pi r \xi)}{K_1(2\pi r_0 \xi)}, \quad \xi > 0. \quad (1.39)$$

We would like to find the maximum of the function g_n . We compute

$$\begin{aligned} &g_n'(\xi; r_0, r) \cdot (2\pi r)^{-1} (1 + \xi^2)^{\frac{3}{2}} K_1^2(2\pi r_0 \xi) \\ &= \left[K_0(2\pi r \xi) + \xi 2\pi r K_0'(2\pi r \xi) \right] (1 + \xi^2) K_1(2\pi r_0 \xi) - \xi K_0(2\pi r \xi) \left[\xi K_1(2\pi r_0 \xi) + (1 + \xi^2) 2\pi r_0 K_1'(2\pi r_0 \xi) \right] \\ &= \left[K_0(2\pi r \xi) - \xi 2\pi r K_1(2\pi r \xi) \right] (1 + \xi^2) K_1(2\pi r_0 \xi) \\ &\quad - \xi K_0(2\pi r \xi) \left[\xi K_1(2\pi r_0 \xi) - (1 + \xi^2) \left(2\pi r_0 K_0(2\pi r_0 \xi) + \frac{1}{\xi} K_1(2\pi r_0 \xi) \right) \right] \\ &= 2\pi \xi (1 + \xi^2) \left[r_0 K_0(2\pi r_0 \xi) K_0(2\pi r \xi) - r K_1(2\pi r_0 \xi) K_1(2\pi r \xi) \right] + (2 + \xi^2) K_0(2\pi r \xi) K_1(2\pi r_0 \xi) \\ &= -A(\xi) + B(\xi), \end{aligned}$$

where

$$\begin{aligned} A(\xi) &= 2\pi \xi (1 + \xi^2) \left[r K_1(2\pi r_0 \xi) K_1(2\pi r \xi) - r_0 K_0(2\pi r_0 \xi) K_0(2\pi r \xi) \right], \\ B(\xi) &= (2 + \xi^2) K_0(2\pi r \xi) K_1(2\pi r_0 \xi). \end{aligned}$$

Obviously,

$$\frac{A(\xi)}{B(\xi)} = h(\xi; 2\pi r, 2\pi r_0).$$

From Lemma 1.5.1, $g'(\xi; r_0, r)$ admits only one zero (when $A(\xi)/B(\xi) = 1$), which we denote by $\xi^*(r)$. Moreover, we have

$$\xi^*(r) \sim O\left(\frac{1}{r}\right) \quad r \rightarrow \infty. \quad (1.40)$$

Therefore,

$$g_n(\xi^*(r); r_0, r) \sim O\left(\frac{1}{K_1(r_0/r)}\right) \sim O\left(\frac{r_0}{r}\right) \quad r \rightarrow \infty,$$

which yields the claimed estimate. \square

1.6 Appendix: Comparison of different local boundary conditions for radial cut-off

1.6.1 Dirichlet boundary condition

Definition 1.6.1. We build a lifting operator $\mathcal{R}_{r_*} : H^{1/2}(\mathbb{R}) \rightarrow H_{1/2}^1(B_{r_0})$ such that its Fourier transform satisfies

$$\widehat{(\mathcal{R}_{r_*}\phi)}(r, \xi) = \frac{I_1(2\pi|\xi|r)}{I_1(2\pi|\xi|r_*)} \hat{\phi}(\xi),$$

where I_1 is the modified Bessel function.

We verify easily that $(\mathcal{R}_{r_*}\phi)|_{r=0} = 0$, $(\mathcal{R}_{r_*}\phi)|_{r=r_*} = \phi$ and

$$-\operatorname{div}\left(\frac{1}{r}\nabla(r\mathcal{R}_{r_*}\phi)\right) = 0 \quad \text{in } B_{r_*}.$$

By multiplying the above equation with $\overline{r\mathcal{R}_{r_*}\phi}$ and integrating by parts, we get

$$\begin{aligned} \|r^{-1}\nabla(r\mathcal{R}_{r_*}\phi)\|_{L_{1/2}^2(B_{r_*})}^2 &= \int_{\Gamma_{r_*}} \frac{\partial}{\partial r}(r\mathcal{R}_{r_*}\phi)\overline{\mathcal{R}_{r_*}\phi} \, ds = \int_{\mathbb{R}} \left(\frac{\partial}{\partial r}(r\mathcal{R}_{r_*}\phi)\right)(r_*, z)\bar{\phi}(z) \, dz \\ &= \int_{\mathbb{R}} \left(\frac{\partial}{\partial r}(r\widehat{\mathcal{R}_{r_*}\phi})\right)(r_*, \xi)\bar{\hat{\phi}}(\xi) \, d\xi = \int_{\mathbb{R}} 2\pi r_* \frac{I_0(2\pi|\xi|r_*)}{I_1(2\pi|\xi|r_*)} |\xi| |\hat{\phi}(\xi)|^2 \, d\xi \\ &\leq 2\pi r_* \frac{I_0(2\pi|\xi|r_*)}{I_1(2\pi|\xi|r_*)} \int_{\mathbb{R}} (1 + |\xi|^2)^{1/2} |\hat{\phi}(\xi)|^2 \, d\xi \\ &= 2\pi r_* \frac{I_0(2\pi|\xi|r_*)}{I_1(2\pi|\xi|r_*)} \|\phi\|_{H^{1/2}(\mathbb{R})}^2. \end{aligned}$$

So we verified that $\mathcal{R}_{r_*}\phi \in H_{1/2}^1(B_{r_*})$, and

$$\|r^{-1}\nabla(r\mathcal{R}_{r_*}\phi)\|_{L_{1/2}^2(B_{r_*})}^2 \leq C(r_*) \|\phi\|_{H^{1/2}(\mathbb{R})}^2 \quad \text{with } C(r_*) = \sqrt{2\pi r_* \frac{I_0(2\pi|\xi|r_*)}{I_1(2\pi|\xi|r_*)}}. \quad (1.41)$$

Considering the asymptotic behavior of I_0 , I_1 with big argument, we have

$$C(r_*) \sim O(\sqrt{r_*}) \quad r_* \rightarrow \infty. \quad (1.42)$$

So the lifting operator \mathcal{R}_{r_*} grows with a rate of $(r_*)^{1/2}$ when r_* tends to infinity. Now we introduce a lemma.

Remark 1.6.2. Lemma 1.1.6 and (1.42) show that the lifting \mathcal{R}_{r_*} is “minimal” in the sense that its norm grows with the least rate, i.e. as $(r_*)^{1/2}$ when r_* tends to infinity.

The problem with Dirichlet boundary condition on $\Gamma_{r_*} = \{r = r_*\}$ writes:

$$\begin{cases} -\operatorname{div}\left(\frac{1}{\mu r}\nabla(ru_d)\right) - i\omega\sigma u_d = i\omega J & \text{in } B_{r_*}, \\ u_d = 0, & \text{on } \Gamma_0, \\ u_d = 0, & \text{on } \Gamma_{r_*}. \end{cases} \quad (1.43)$$

Proposition 1.6.3. Let $r_* > 0$ be sufficiently large so that the support of the source term $J \in L^2(\mathbb{R}_+^2)$ is included in B_{r_*} . Then problem (1.43) has a unique solution $u_d \in H_{1/2,0}^1(B_{r_*})$. Assume in addition that there exists positive $r_0 < r_*$ such that the source J and the conductivity σ vanish and the permeability μ is constant for $r > r_0$. Then there exists a constant C that depends only on J , r_0 , μ and σ such that

$$\left\| \frac{1}{r}\nabla(r(u_d - u)) \right\|_{L_{1/2}^2(B_{r_*})} \leq C/r_*^{1/2},$$

where u is the solution of (1.6) (in Proposition 1.1.2).

Proof. The proof of the first part is similar to the proof of Proposition 1.1.2 thanks to Lemma 1.1.6. Let us set $w_d = u - u_d$. Then $w_d \in H_{1/2}^1(B_{r_*})$ and satisfies

$$\begin{cases} -\operatorname{div}\left(\frac{1}{\mu r}\nabla(rw_d)\right) - i\omega\sigma w_d = 0 & \text{in } B_{r_*}, \\ w_d = 0, & \text{on } \Gamma_0, \\ w_d = u, & \text{on } \Gamma_{r_*}, \end{cases} \quad (1.44)$$

Using the lifting operator \mathcal{R}_{r_*} , then $\tilde{w}_d := w_d - \mathcal{R}_{r_*}(u|_{\Gamma_{r_*}})$ satisfies: $\forall v \in H_{1/2,0}^1(B_{r_*})$,

$$\begin{aligned} & \int_{B_{r_*}} \frac{1}{\mu r} \nabla(r\tilde{w}_d) \cdot \nabla(r\bar{v}) - i\omega\sigma\tilde{w}_d\bar{v}r \, dr \, dz \\ &= \int_{B_{r_*}} \frac{1}{\mu r} \nabla(r\mathcal{R}_{r_*}(u|_{r_*})) \cdot \nabla(r\bar{v}) - i\omega\sigma\mathcal{R}_{r_*}(u|_{r_*})\bar{v}r \, dr \, dz \end{aligned} \quad (1.45)$$

A similar argument to the proof of Proposition 1.1.2 thanks to Lemma 1.1.6 yields the the existence and uniqueness of $\tilde{w}_d \in H_{1/2,0}^1(B_{r_*})$, thus the existence and uniqueness of the solution $w_d \in H_{1/2}^1(B_{r_*})$. By taking $v = \tilde{w}_d$ in the variational formulation (1.45), we get the following estimates

$$\begin{aligned} & \frac{1}{\|\mu\|_\infty} \left\| \frac{1}{r}\nabla(r\tilde{w}_d) \right\|_{L_{1/2}^2(B_{r_*})}^2 \leq \left| \int_{B_{r_*}} \frac{1}{\mu r} |\nabla(r\tilde{w}_d)|^2 - i\omega\sigma|\tilde{w}_d|^2 \, dr \, dz \right| \\ &= \left| \int_{B_{r_*}} \frac{1}{\mu r} \nabla(r\mathcal{R}_{r_*}(u|_{r_*})) \cdot \nabla(r\bar{\tilde{w}}_d) - i\omega\sigma\mathcal{R}_{r_*}(u|_{r_*})\bar{\tilde{w}}_d r \, dr \, dz \right| \\ &\leq \frac{1}{\inf|\mu|} \left\| \frac{1}{r}\nabla(r\mathcal{R}_{r_*}(u|_{r_*})) \right\|_{L_{1/2}^2(B_{r_*})} \left\| \frac{1}{r}\nabla(r\tilde{w}_d) \right\|_{L_{1/2}^2(B_{r_*})} \\ &+ \omega\|\sigma\|_\infty \|\mathcal{R}_{r_*}(u|_{r_*})\|_{L_{1/2}^2(B_{r_0})} \|\tilde{w}_d\|_{L_{1/2}^2(B_{r_0})}. \end{aligned}$$

The last inequality is due to the fact that σ vanishes for $r > r_0$. Thanks to the Poincaré type inequality (1.11), we have

$$\|\tilde{w}_d\|_{L^2_{1/2}(B_{r_0})} \leq \frac{r_0}{\sqrt{2}} \left\| \frac{1}{r} \nabla(r\tilde{w}_d) \right\|_{L^2_{1/2}(B_{r_0})}^2 \leq \frac{r_0}{\sqrt{2}} \left\| \frac{1}{r} \nabla(r\tilde{w}_d) \right\|_{L^2_{1/2}(B_{r_*})}^2.$$

Thus

$$\|r^{-1} \nabla(r\tilde{w}_d)\|_{L^2_{1/2}(B_{r_*})} \leq C(r_0, \mu, \sigma) \|r^{-1} \nabla(r\mathcal{R}_{r_*}(u|_{r_*}))\|_{L^2_{1/2}(B_{r_*})}.$$

Considering (1.41), (1.42) and Proposition 1.1.4, we have

$$\begin{aligned} \|r^{-1} \nabla(rw_d)\|_{L^2_{1/2}(B_{r_*})} &= \|r^{-1} \nabla(r(\tilde{w}_d + \mathcal{R}_{r_*}u|_{r_*}))\|_{L^2_{1/2}(B_{r_*})} \\ &\leq (1 + C(r_0, \mu, \sigma)) \|r^{-1} \nabla(r\mathcal{R}_{r_*}u|_{r_*})\|_{L^2_{1/2}(B_{r_*})} \leq (1 + C(r_0, \mu, \sigma)) C(r_*) \|u|_{r_*}\|_{H^{1/2}(\mathbb{R})} \\ &\leq C/r_*^{1/2}, \end{aligned}$$

where C depends only on r_0, J, μ, σ . □

Remark 1.6.4. *Considering the Poincaré type inequality (1.11) with $C_p = r_*/2$, we do not have the convergence of u_d to u in $L^2_{1/2}(B_{r_*})$ as $r_* \rightarrow \infty$.*

1.6.2 Robin boundary condition

We consider a problem with a Robin boundary condition on Γ_{r_*} :

$$\begin{cases} -\operatorname{div} \left(\frac{1}{\mu r} \nabla(ru_r) \right) - i\omega\sigma u_r = i\omega J & \text{in } B_{r_*}, \\ u_r = 0, & \text{on } \Gamma_0, \\ \frac{\partial}{\partial r}(ru_r) = \alpha u_r, & \text{on } \Gamma_{r_*}, \end{cases} \quad (1.46)$$

where $\alpha = \alpha(r_*)$ is a constant which can be dependent on r_* . We want to discuss the possibility of obtaining a better approximation model by setting appropriate Robin coefficient α .

The error $w_r = u - u_r$ satisfies

$$\begin{cases} -\operatorname{div} \left(\frac{1}{\mu r} \nabla(rw_r) \right) - i\omega\sigma w_r = 0 & \text{in } B_{r_*}, \\ w_r = 0, & \text{on } \Gamma_0, \\ \frac{\partial}{\partial r}(rw_r) = \alpha w_r + \frac{\partial}{\partial r}(ru) - \alpha u, & \text{on } \Gamma_{r_*}. \end{cases} \quad (1.47)$$

The equivalent variational form of problem (1.47) writes: $\forall v \in H_r^1(B_{r_*})$

$$\int_{B_{r_*}} \frac{1}{\mu r} \nabla(rw_r) \cdot \nabla(r\bar{v}) - i\omega\sigma w_r \bar{v} r - \int_{\Gamma_{r_*}} \frac{1}{\mu} \alpha w_r \bar{v} \, ds = \int_{\Gamma_{r_*}} \frac{1}{\mu} \left(\frac{\partial}{\partial r}(ru) - \alpha u \right) \bar{v} \, ds$$

Similar to the error estimate for Neumann problem above, we need to study the asymptotic behavior of $\|(\partial_r(ru) - \alpha u)(r_*, \cdot)\|_{H^{-1/2}(\mathbb{R})}$ while r_* tends to infinity. From Propositions 1.1.4 and 1.1.5 and the functions g_d and g_r defined in (1.9) and (1.39) respectively, we know that for $r_* > r_0$,

$$\left\| \left(\frac{\partial}{\partial r}(ru) - \alpha u \right) (r_*, \cdot) \right\|_{H^{-1/2}(\mathbb{R})} \leq \|u(r_0, \cdot)\|_{H^{1/2}(\mathbb{R})} \|g_r(\cdot; r_0, r_*)\|_{L^\infty(\mathbb{R}_\xi^+)},$$

where

$$g_r(\xi; r_0, r_*) = g_n(\xi; r_0, r_*) + \alpha \frac{1}{(1 + \xi^2)^{1/2}} g_d(\xi; r_0, r_*), \quad \xi > 0.$$

As $g_n(0+; r_0, r_*) = 0$,

$$\|g_r(\cdot; r_0, r_*)\|_{L^\infty(\mathbb{R}_\xi^+)} \geq |g_r(0+; r_0, r_*)| = |\alpha g_d(0+; r_0, r_*)| = |\alpha| \frac{r_0}{r_*}.$$

In order to have better approximation than the Neumann problem, we will need at least that

$$\alpha = \alpha(r_*) \sim o(1) \quad r_* \rightarrow \infty.$$

If we take $\xi = \xi^*(r_*)$ the maximal point of $g_n(\cdot; r_0, r_*)$, we have

$$\begin{aligned} g_r(\xi^*(r_*); r_0, r_*) &\sim O\left(\frac{1}{r_*}\right) \quad r_* \rightarrow \infty, \\ 0 \leq g_d(\xi^*(r_*); r_0, r_*) &\leq g_d(0; r_0, r_*) \sim O\left(\frac{1}{r_*}\right) \quad r_* \rightarrow \infty, \end{aligned}$$

we have

$$\begin{aligned} g_r(\xi^*(r_*); r_0, r_*) &= g_r(\xi^*(r_*); r_0, r_*) + \alpha(r_*) g_d(\xi^*(r_*); r_0, r_*), \\ \|g_r(\cdot; r_0, r_*)\|_{L^\infty(\mathbb{R}_\xi^+)} &\geq |g_r(\xi^*(r_*); r_0, r_*)| \sim O\left(\frac{1}{r_*}\right) \quad r_* \rightarrow \infty. \end{aligned}$$

Therefore, the approximation model with Robin boundary condition converges at most as fast as the model with Neumann boundary condition.

1.7 Appendix: 1-D Calibration

1-D models, which result from the invariance in the z -direction and who have known analytical solutions, can justify the eddy current approximation and calibrate the 2-D solution.

We take a line applied electric current at $\Gamma_s = \{r = r_s\}$, i.e. a Dirac distribution $J_\theta = J\delta_{r_s}$ and suppose a deposit-free case. The two interfaces where ϵ , μ and/or σ change are the inner and outer surfaces of the tube $\Gamma_{t1} = \{r = r_{t1}\}$, $\Gamma_{t2} = \{r = r_{t2}\}$. The z -invariance assumption, the second order Maxwell equation (1.2) and the second order eddy current equation (1.3) yield

$$\frac{\partial}{\partial r} \left(\frac{1}{\mu r} \frac{\partial}{\partial r}(ru) \right) + \omega^2(\epsilon + i\sigma/\omega)u = -i\omega J\delta_{r_s}(r), \quad (1.48)$$

where $\epsilon = 0$ for eddy current model. In each region of $0 < r < r_s$, $r_s < r < r_{t1}$, $r_{t1} < r < r_{t2}$ and $r > r_{t2}$, (1.48) writes

$$r^2 u'' + ru' + (r^2 k^2 - 1)u = 0, \quad (1.49)$$

with $k^2 = \omega^2 \mu (\epsilon + i\sigma/\omega)$ for the Maxwell model or $k^2 = i\omega \mu \sigma$ for the eddy current model. At Γ_s , we have two interface conditions. The first one is the continuity of the electric field

$$[u]_{\Gamma_s} = 0. \quad (1.50)$$

The second one is given by applying (1.48) in the sense of distribution to any test functions $\phi \in \mathcal{C}_c^\infty(\mathbb{R}^+)$:

$$\begin{aligned} \left[\frac{1}{r} \frac{\partial}{\partial r} (ru) \phi \right]_{\Gamma_s} &= \left\langle \frac{\partial}{\partial r} \left(\frac{1}{r} \frac{\partial}{\partial r} (ru) \right) + k^2 u, \phi \right\rangle = -i\omega \mu J \phi(r_s), \\ \left[\frac{1}{r} \frac{\partial}{\partial r} (ru) \right]_{\Gamma_s} &= -i\omega \mu J. \end{aligned} \quad (1.51)$$

If $k \neq 0$, (1.49) admits elementary solutions as Bessel functions $J_1(kr)$ and $Y_1(kr)$ or $H_1^{(i)}(kr)$, $i = 1, 2$. When $k = 0$, its elementary solutions are r and $1/r$. Considering the Dirichlet condition at $r = 0$ due to axisymmetry and the radiation condition at infinity, the solution to the Maxwell equation (1.2) writes

$$u_M(r) = \begin{cases} \alpha_1 J_1(k_1 r) & 0 < r < r_s, \\ \alpha_2 J_1(k_1 r) + \alpha_3 Y_1(k_1 r) & r_s < r < r_{t1}, \\ \alpha_4 J_1(k_2 r) + \alpha_5 Y_1(k_2 r) & r_{t1} < r < r_{t2}, \\ \alpha_6 H_1^{(i)}(k_1 r) \quad i = 1, 2 & r > r_{t2}, \end{cases}$$

with $k_1^2 = \omega^2 \epsilon_v \mu_v$ $k_2^2 = \omega^2 \mu_t (\epsilon_t + i\sigma_t/\omega)$,

where we choose between $i = 1, 2$ corresponding to the choice of argument of k_1 so that u_M satisfies the radiation condition. Similarly, the solution to the eddy current equation writes

$$u_{EC}(r) = \begin{cases} \beta_1 r & 0 < r < r_s, \\ \beta_2 r + \beta_3 \frac{1}{r} & r_s < r < r_{t1}, \\ \beta_4 J_1(k_3 r) + \beta_5 Y_1(k_3 r) & r_{t1} < r < r_{t2}, \\ \beta_6 \frac{1}{r} & r > r_{t2}, \end{cases}$$

with $k_3^2 = i\omega \mu_t \sigma_t$.

We use the interface conditions at the applied electric current line Γ_s (1.50), (1.51) and the jump conditions at interfaces Γ_{t1} , Γ_{t2} ($[u]_\Gamma = 0$, $[\frac{1}{\mu} \frac{\partial}{\partial n} (ru)]_\Gamma = 0$) to resolve the linear systems for coefficients $\boldsymbol{\alpha} = (\alpha_1, \dots, \alpha_6)^T$, $\boldsymbol{\beta} = (\beta_1, \dots, \beta_6)^T$:

$$\begin{aligned} A_M \boldsymbol{\alpha} &= \mathbf{b}, & A_{EC} \boldsymbol{\beta} &= \mathbf{b}, \\ \mathbf{b} &= (0, -i\omega \mu J, 0, \dots, 0)^T, \end{aligned}$$

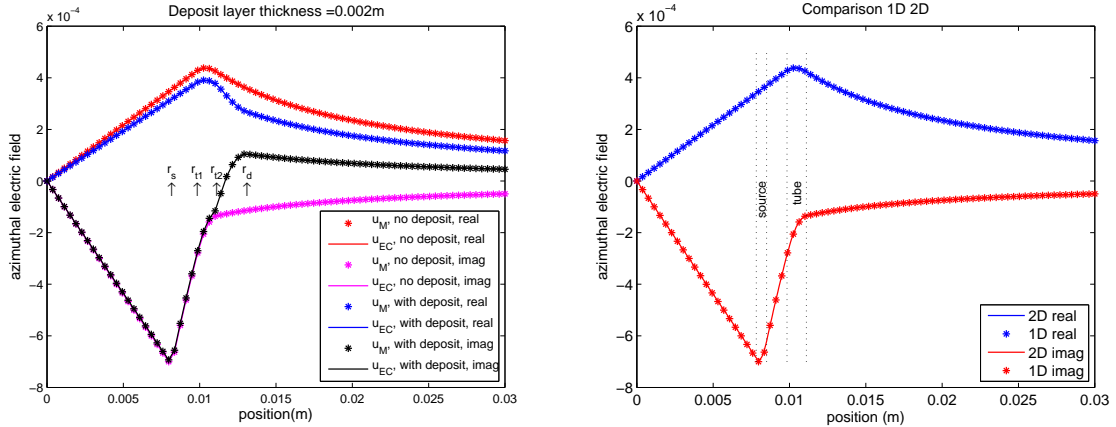
with

$$A_M = \begin{pmatrix} J_1(k_1 r_s) & -J_1(k_1 r_s) & -Y_1(k_1 r_s) & 0 & 0 & 0 \\ k_1 J_0(k_1 r_s) & -k_1 J_0(k_1 r_s) & -k_1 Y_0(k_1 r_s) & 0 & 0 & 0 \\ 0 & J_1(k_1 r_{t_1}) & Y_1(k_1 r_{t_1}) & -J_1(k_2 r_{t_1}) & -Y_1(k_2 r_{t_1}) & 0 \\ 0 & \frac{k_1 J_0(k_1 r_{t_1})}{\mu_v} & \frac{k_1 Y_0(k_1 r_{t_1})}{\mu_v} & \frac{-k_2 J_0(k_2 r_{t_1})}{\mu_t} & \frac{-k_2 Y_0(k_2 r_{t_1})}{\mu_t} & 0 \\ 0 & 0 & 0 & J_1(k_2 r_{t_2}) & Y_1(k_2 r_{t_2}) & -H_1^{(i)}(k_1 r_{t_2}) \\ 0 & 0 & 0 & \frac{k_2 J_0(k_2 r_{t_2})}{\mu_t} & \frac{k_2 Y_0(k_2 r_{t_2})}{\mu_t} & \frac{-k_1 H_0^{(i)}(k_1 r_{t_2})}{\mu_v} \end{pmatrix},$$

and

$$A_{EC} = \begin{pmatrix} r_s & -r_s & -\frac{1}{r_s} & 0 & 0 & 0 \\ 2 & -2 & 0 & 0 & 0 & 0 \\ 0 & r_{t_1} & \frac{1}{r_{t_1}} & -J_1(k_3 r_{t_1}) & -Y_1(k_3 r_{t_1}) & 0 \\ 0 & \frac{2}{\mu_v} & 0 & \frac{-k_3 J_0(k_3 r_{t_1})}{\mu_t} & \frac{-k_3 Y_0(k_3 r_{t_1})}{\mu_t} & 0 \\ 0 & 0 & 0 & J_1(k_3 r_{t_2}) & Y_1(k_3 r_{t_2}) & -\frac{1}{r_{t_2}} \\ 0 & 0 & 0 & \frac{k_3 J_0(k_3 r_{t_2})}{\mu_t} & \frac{k_3 Y_0(k_3 r_{t_2})}{\mu_t} & 0 \end{pmatrix}.$$

Figure 1.9a compares u_M and u_{EC} in the above deposit-free case and in other 1-D configurations, which shows that the Eddy current model is a good approximation of the Maxwell equation model.



(a) comparison of u_M and u_{EC} in 1-D

(b) comparison of fields from 2-D and 1-D models

Figure 1.9: Comparison of azimuthal electric fields.

Finally, Figure 1.9b shows the numerical calibration of the 2-D Eddy current model by the 1-D model.

Identification of lowly-conductive deposits

Contents

2.1	Modeling of ECT signal for axisymmetric configurations	50
2.2	Shape derivative of the impedance measurements	53
2.2.1	Shape and material derivatives of the solution	53
2.2.2	Shape derivative of the impedance	59
2.2.3	Expression of the impedance shape derivative using the adjoint state	61
2.3	Shape reconstruction of deposits using a gradient method	63
2.3.1	Objective function	63
2.3.2	Regularization of the descent direction	64
2.3.3	Inversion algorithm	65
2.3.4	Numerical tests	65
2.4	On the reconstruction of the deposit conductivity and permeability	72
2.4.1	The cost functional derivative with respect to the conductivity	72
2.4.2	Derivative with respect to the magnetic permeability	73
2.4.3	Numerical tests	74
2.5	On the reconstruction of the shape and physical parameters	76

In this chapter, we first aim to estimate the deposit shape given ECT signals by supposing that the physical nature of deposit is *a priori* known. We shall employ for that purpose a shape optimization scheme based on evaluation of the shape derivative of the measured signal with respect to the deposit shape. We may refer to Murat and Simon [63, 64], Zolésio [85] and Allaire [2] for a general introduction to shape optimization. The work of Pantz [67] on shape derivatives of heat equation with jumps of conductivity inspires our derivation of material derivative of eddy current equation. We remind that there exist other inversion methods based on shape optimization, such as inversion based on topological derivative (Guzina and Bonnet [16, 40]) or the level-set approach (Santosa [75], Dorn and Lesselier [37]). From engineering point of view, Trillon et al. [84] proposed a contrast source inverse method to retrieve flaws from eddy current signals.

The proposed inversion scheme via shape optimization then employs a standard gradient descent strategy to minimize a least square cost functional. In order to stabilize the gradient we regularize the descent direction by solving a Laplace-Beltrami problem on the deposit boundary. Similar regularization methods are discussed and applied in the works of Nicolas [65] and Chaulet

[28]. We validate our procedure through some numerical experiments that clearly demonstrate that the ECT signals are capable to provide good estimates on the deposit shapes.

We then discuss the case where the physical parameters are not known. While we show that retrieving either the conductivity or the magnetic permeability would be possible if the geometry is known, retrieving both parameters cannot in principle be accurately estimated without very good initial guesses. Retrieving the shape and one of the parameters is also very sensitive to the initial guess. However we show that the sensitivity with respect to geometry is much more robust. For instance reasonably accurate estimates of the deposits shape can be obtained with a small error on the physical parameters.

Overview: In Section 2.1 we recall the eddy current model for axisymmetric configurations and explain different impedance measurement modes and how to evaluate them from axisymmetric eddy current model solutions. Section 2.2 is then dedicated to characterizing the shape derivative of the solution and the impedance measurements with respect to the deposit shape. We also give a representation of the impedance derivative using the adjoint state technique. The shape inversion scheme and numerical validating experiments are given in Section 2.3. We then analyze in Section 2.4 the reconstruction of physical parameters for known geometries of the deposit. Finally, we discuss simultaneous shape and physical parameters reconstructions in Section 2.5.

2.1 Modeling of ECT signal for axisymmetric configurations

The ECT experiment settings and geometrical configurations are depicted in Figure 2.1.

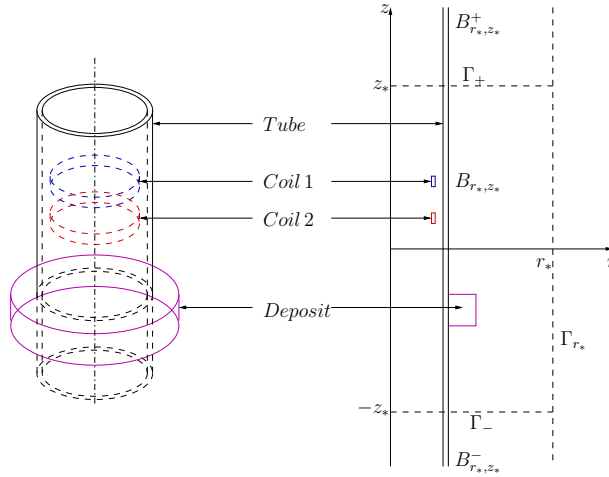


Figure 2.1: 3-D and 2-D geometrical representations of a SG tube covered with deposits and a probe consisting of two coils.

Active coils generate an electric field \mathbf{E} and a magnetic field \mathbf{H} that satisfy the Maxwell system

$$\begin{cases} \operatorname{curl} \mathbf{H} + (i\omega\epsilon - \sigma)\mathbf{E} = \mathbf{J} & \text{in } \mathbb{R}^3, \\ \operatorname{curl} \mathbf{E} - i\omega\mu\mathbf{H} = 0 & \text{in } \mathbb{R}^3, \end{cases} \quad (2.1)$$

where \mathbf{J} is the applied electric current density (satisfying $\operatorname{div} \mathbf{J} = 0$), and ω , ϵ , μ , σ respectively denote the frequency, the electrical permittivity, the magnetic permeability and the conductivity.

In the ECT experiment we are interested in, the probe is done with two coils that move along the axis of the SG tube from vertical position z_{\min} to z_{\max} . At each position ζ , we get an impedance measurement (ECT signal) $Z_{meas}(\zeta)$. According to [8, (10a)], in the 3-D case the impedance measured in the coil k when the electromagnetic field is induced by the coil l writes

$$\Delta Z_{kl} = \frac{1}{I^2} \int_{\partial\Omega_d^{3D}} (\mathbf{E}_l^0 \times \mathbf{H}_k - \mathbf{E}_k \times \mathbf{H}_l^0) \cdot \mathbf{n} \, dS,$$

where $\Omega_d^{3D} \subset \mathbb{R}^3$ is the deposit domain, \mathbf{E}_l^0 and \mathbf{H}_l^0 are respectively the electric field and the magnetic field in the deposit-free case with corresponding permeability and conductivity distributions μ^0, σ^0 , while $\mathbf{E}_k, \mathbf{H}_k$ are those in the case with some deposits. Using the divergence theorem, we also have

$$\begin{aligned} \Delta Z_{kl} &= \frac{1}{I^2} \int_{\Omega_d^{3D}} \operatorname{div} (\mathbf{E}_l^0 \times \mathbf{H}_k - \mathbf{E}_k \times \mathbf{H}_l^0) \, dx \\ &= \frac{1}{I^2} \int_{\Omega_d^{3D}} (\operatorname{curl} \mathbf{E}_l^0 \cdot \mathbf{H}_k - \mathbf{E}_l^0 \cdot \operatorname{curl} \mathbf{H}_k - \operatorname{curl} \mathbf{E}_k \cdot \mathbf{H}_l^0 + \mathbf{E}_k \cdot \operatorname{curl} \mathbf{H}_l^0) \, dx \\ &= \frac{1}{i\omega I^2} \int_{\Omega_d^{3D}} \left(\left(\frac{1}{\mu} - \frac{1}{\mu^0} \right) \operatorname{curl} \mathbf{E}_k \cdot \operatorname{curl} \mathbf{E}_l^0 - (i\omega(\sigma - \sigma^0) + \omega^2(\epsilon - \epsilon^0)) \mathbf{E}_k \cdot \mathbf{E}_l^0 \right) \, dx. \end{aligned}$$

The eddy current approximation corresponds to low frequency regimes and high conductivities: $\omega\epsilon \ll \sigma$. In this case

$$\Delta Z_{kl} \simeq \frac{1}{i\omega I^2} \int_{\Omega_d^{3D}} \left(\left(\frac{1}{\mu} - \frac{1}{\mu^0} \right) \operatorname{curl} \mathbf{E}_k \cdot \operatorname{curl} \mathbf{E}_l^0 - i\omega(\sigma - \sigma^0) \mathbf{E}_k \cdot \mathbf{E}_l^0 \right) \, dx. \quad (2.2)$$

In an axisymmetric (i.e., rotationally invariant) setting, for a vector field \mathbf{a} we denote by $\mathbf{a}_m = a_r \mathbf{e}_r + a_z \mathbf{e}_z$ its meridian and by $\mathbf{a}_\theta = a_\theta \mathbf{e}_\theta$ its azimuthal component. A vector field \mathbf{a} is called axisymmetric if $\partial_\theta \mathbf{a}$ vanishes. Then the Maxwell equations (2.1) decouple into two systems, a first one for $(\mathbf{H}_\theta, \mathbf{E}_m)$, and a second one for $(\mathbf{H}_m, \mathbf{E}_\theta)$. The solution to the first system vanishes if \mathbf{J} is axisymmetric. Substituting \mathbf{H}_m in the second system yields the second-order equation for $\mathbf{E}_\theta = E_\theta \mathbf{e}_\theta$,

$$\frac{\partial}{\partial r} \left(\frac{1}{\mu r} \frac{\partial}{\partial r} (r E_\theta) \right) + \frac{\partial}{\partial z} \left(\frac{1}{\mu} \frac{\partial E_\theta}{\partial z} \right) + \omega^2(\epsilon + i\sigma/\omega) E_\theta = -i\omega J_\theta \quad \text{in } \mathbb{R}_+^2, \quad (2.3)$$

with $\mathbb{R}_+^2 := \{(r, z) : r > 0, z \in \mathbb{R}\}$. Under the eddy current approximation this equation simplifies to

$$\frac{\partial}{\partial r} \left(\frac{1}{\mu r} \frac{\partial}{\partial r} (r E_\theta) \right) + \frac{\partial}{\partial z} \left(\frac{1}{\mu} \frac{\partial E_\theta}{\partial z} \right) + i\omega\sigma E_\theta = -i\omega J_\theta \quad \text{in } \mathbb{R}_+^2, \quad (2.4)$$

with a Dirichlet boundary condition at $r = 0$ due to symmetry: $E_\theta|_{r=0} = 0$, and a decay condition $E_\theta \rightarrow 0$ as $r^2 + z^2 \rightarrow \infty$ at infinity. We then obtain

$$\begin{aligned} \Delta Z_{kl} &= \frac{2\pi}{i\omega I^2} \int_{\Omega_d} \left(\left(\frac{1}{\mu} - \frac{1}{\mu^0} \right) \frac{1}{r} \nabla(r E_{\theta,k}) \cdot \nabla(r E_{\theta,l}^0) - i\omega(\sigma - \sigma^0) E_{\theta,k} E_{\theta,l}^0 r \right) \, dr \, dz \\ &= \frac{2\pi}{i\omega I^2} \int_{\Omega_d} \left(\left(\frac{1}{\mu} - \frac{1}{\mu^0} \right) \frac{\nabla w_k \cdot \nabla w_l^0}{r} - i\omega(\sigma - \sigma^0) \frac{w_k w_l^0}{r} \right) \, dr \, dz, \end{aligned} \quad (2.5)$$

where we have set

$$w_j := rE_{\theta,j}, \quad w_j^0 := rE_{\theta,j}^0, \quad j = 1, 2.$$

We shall assume that μ and σ are in $L^\infty(\mathbb{R}_+^2)$ such that $\mu \geq \mu_v > 0$ on \mathbb{R}_+^2 and that $\sigma \geq 0$ and $\sigma = 0$ for $r \geq r_0$ sufficiently large. Then problem (2.4) has a unique solution $E_\theta \in H(\mathbb{R}_+^2)$ if one assumes for instance that $J_\theta \in L^2(\mathbb{R}_+^2)$ with compact support where we used the notation for any $\Omega \subset \mathbb{R}_+^2$

$$H(\Omega) := \left\{ v : r^{1/2}(1+r^2)^{-\lambda/2}v \in L^2(\Omega), r^{-1/2}\nabla(rv) \in L^2(\Omega) \right\}$$

where λ can be any real > 1 and where $\nabla := (\partial_r, \partial_z)^t$. In the following it will be more convenient to work with $w := rE_\theta \in \tilde{H}(\Omega) := \{v : rv \in H(\Omega)\}$. This field satisfies the variational formulation

$$a(w, \varphi) := \int_\Omega \left(\frac{1}{\mu r} \nabla w \cdot \nabla \bar{\varphi} - \frac{i\omega\sigma}{r} w \bar{\varphi} \right) dr dz = \int_\Omega i\omega J \bar{\varphi} dr dz \quad \forall \varphi \in \tilde{H}(\Omega) \quad (2.6)$$

with $\Omega = \mathbb{R}_+^2$. The solution to (2.6) satisfies (in the weak sense)

$$-\operatorname{div} \left(\frac{\nabla w}{\mu r} \right) - i\omega\sigma \frac{w}{r} = i\omega J \quad \text{in } \Omega. \quad (2.7)$$

Let us already indicate that for numerical purposes, the computational domain will be truncated in radial direction at $r = r_*$ where r_* is sufficiently large and impose a Neumann boundary condition on $r = r_*$ (see Figure 2.1). Then the solution for the truncated problem would satisfy (2.6) with $\Omega = B_{r_*} := \{(r, z) \in \mathbb{R}^2 : 0 \leq r \leq r_*\}$. This is why we shall use in the sequel the variational formulation (2.6) with the generic notation for the variational space $\tilde{H}(\Omega)$ with Ω denoting \mathbb{R}_+^2 or B_{r_*} . We also recall that the variational formulation with $\Omega = B_{r_*}$ can be equivalently reduced to a variational formulation posed on $B_{r_*, z_*} = \{(r, z) \in \mathbb{R}^2 : 0 \leq r \leq r_*, |z| < z_*\}$ by introducing appropriate Dirichlet-to-Neumann operators on $z = \pm z_*$. This would be convenient for accelerating numerical evaluation of the solution (see Chapter 1). As a corollary of the well-posedness of the problem for E_θ we can state: We have

Corollary 2.1.1. *Assume that the source $J \in L^2(\Omega)$ with compact support. Then the variational formulation (2.6) has a unique solution w in $\tilde{H}(\Omega)$.*

Let us finally note that in practice, the impedances are measured either in the absolute mode, denoted by Z_{FA} , or in the differential mode, denoted by Z_{F3} . From [70], we have

$$\begin{cases} Z_{FA} = \frac{i}{2}(\Delta Z_{11} + \Delta Z_{21}) & \text{absolute mode,} \\ Z_{F3} = \frac{i}{2}(\Delta Z_{11} - \Delta Z_{22}) & \text{differential mode.} \end{cases} \quad (2.8)$$

To have an illustration of the impedance measurements without giving the experimental details, Figure 2.2 shows the ECT signals deformed by an axisymmetric deposit covering 10mm of the shell side of the tube in the axial direction. We denote by $Z(\Omega_d; \zeta)$ either Z_{F3} or Z_{FA} the impedance simulated with a deposit form Ω_d at the probe position ζ .

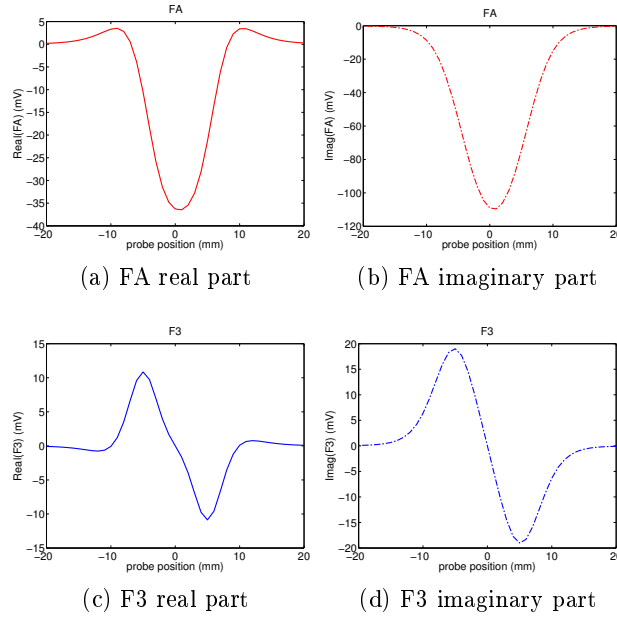


Figure 2.2: ECT signals of a rectangular deposit.

Notation: In the 2-D axisymmetric configuration in the Orz plan, the tube is represented by $\Omega_t := \{(r, z) \in \Omega : r_{t1} < r < r_{t2}\}$ with $0 < r_{t1} < r_{t2}$ the inner and outer radius of the tube wall. We denote by Ω_s the domain inside the tube ($r < r_{t1}$) which contains the support of the source: $\text{supp}J \subset \Omega_s$. The deposit is at the shell side of the tube, that is $\Omega_d \subset \{(r, z) \in \Omega : r > r_{t2}\}$. We denote by Ω_v the vacuum domain outside the tube $\Omega_v := \{(r, z) \in \Omega : r > r_{t2}\} \setminus \Omega_d$. Then we have $\Omega = \cup_{i \in \Lambda} \Omega_i$ where $\Lambda = \{s, t, d, v\}$ is a set of indices designating the above subdomains of Ω . We will also use the notation Ω_d for the complement set of Ω_d in Ω ($\Omega_d^c = \Omega \setminus \Omega_d = \Omega_s \cup \Omega_t \cup \Omega_v$).

2.2 Shape derivative of the impedance measurements

The expression of ΔZ_{kl} the impedance measurements (2.5) is an integral on the deposit domain Ω_d with integrand (or precisely w_k the solution of the eddy current problem (2.6) also depending on Ω_d). To have an expression for the shape derivative of impedance measurements of Ω_d , we shall first study the derivatives of the shape-dependent function w which is the solution to problem (2.6) (and satisfies (2.7)).

2.2.1 Shape and material derivatives of the solution

For \mathcal{Q} a regular open subset of Ω , we can define a domain deformation as a perturbation of the identity

$$\text{Id} + \theta : \mathcal{Q} \rightarrow \mathcal{Q}_\theta = (\text{Id} + \theta)\mathcal{Q},$$

where $\theta \in W^{1,\infty}(\mathcal{Q}, \mathcal{Q})^2$ is a perturbation field. In our problem, an admissible deformation should keep the domains Ω_t and Ω_s invariant, i.e.

$$\text{supp}\theta \cap \Omega_s = \text{supp}\theta \cap \Omega_t = \emptyset.$$

Indeed we are mainly interested in perturbation fields θ with support located in vicinity of the interface $\Gamma := \overline{\partial\Omega_d} \cap \overline{\partial\Omega_v}$ between the deposit and the vacuum region outside the tube. We denote by $[\cdot]$ the jump operator across Γ , i.e. for any $f(x)$ ($x = (r, z)$) defined in a vicinity of Γ and any $x_0 = (r_0, z_0) \in \Gamma$

$$\begin{aligned} [f](x_0) &:= f_+(x_0) - f_-(x_0), \\ \text{with } f_+(x_0) &= \lim_{\Omega_v \ni x \rightarrow x_0} f(x) \quad \text{and} \quad f_-(x_0) = \lim_{\Omega_d \ni x \rightarrow x_0} f(x). \end{aligned}$$

Following [2, Section 6.3.3] we give the following definitions for material (Lagrangian) and shape (Eulerian) derivatives.

Definition 2.2.1. *Let $v = v(\mathcal{Q})$ be a shape-dependent function that belongs to some Banach space B (that may depend on \mathcal{Q}). If $\tilde{v}(\theta) := v(\mathcal{Q}_\theta) \circ (\text{Id} + \theta) \in B$, then the material (Lagrangian) derivative $V(\theta)$ of v is defined as a linear functional with respect to θ with values in B such that*

$$\tilde{v}(\theta) = \tilde{v}(0) + V(\theta) + o(\theta) \quad \text{in } \mathcal{Q},$$

where $\lim_{\theta \rightarrow 0} \frac{\|o(\theta)\|_B}{\|\theta\|_{1,\infty}} = 0$. The shape (Eulerian) derivative $v'(\theta)$ of v is defined by

$$v'(\theta) = V(\theta) - \theta \cdot \nabla v(\mathcal{Q}). \quad (2.9)$$

In the sequel we shall adopt the generic notation $o(\theta)$ to design a function such that $\|o(\theta)\|/\|\theta\|_{1,\infty} \rightarrow 0$ as $\theta \rightarrow 0$ where the norm $\|\cdot\|$ for $o(\theta)$ should be clear from the context.

Remark 2.2.2. *It is readily seen from Definition 2.2.1, using the definition of \tilde{v} and the chain rule, that formally*

$$v(\mathcal{Q}_\theta) = v(\mathcal{Q}) + v'(\theta) + o(\theta) \quad \text{in } \omega \subset \mathcal{Q} \cap \mathcal{Q}_\theta.$$

Proposition 2.2.3. *Under the same assumptions as Corollary 2.1.1, for an admissible shape perturbation $\theta \in W^{1,\infty}(\Omega, \Omega)^2$, the solution $w(\Omega) \in \tilde{H}(\Omega)$ (2.6) has material derivative $W(\theta)$ that is defined by*

$$\begin{aligned} a(W(\theta), \phi) &= L_\theta(\phi) \quad \forall \phi \in \tilde{H}(\Omega), \\ \text{where } L_\theta(\phi) &:= \int_{\Omega} \left\{ \frac{1}{\mu} \left(-\text{div}(\theta/r)I + \frac{\nabla\theta + \nabla\theta^t}{r} \right) \nabla w \cdot \nabla \bar{\phi} + i\omega\sigma \text{div}(\theta/r)w\bar{\phi} + i\omega \text{div}(J\theta)\bar{\phi} \right\} dr dz. \end{aligned} \quad (2.10)$$

Proof. We consider the change of variables

$$(\text{Id} + \theta)^{-1} : \Omega_\theta \rightarrow \Omega, \quad y \mapsto x,$$

and in particular the fact that

$$(\nabla v) \circ (\text{Id} + \theta) = (I + \nabla \theta)^{-t} \nabla(v \circ (\text{Id} + \theta)) = (I + \nabla \theta)^{-t} \nabla \tilde{v}(\theta) \quad \forall v \in \tilde{H}(\Omega_\theta),$$

where $\nabla \theta$ is the Jacobian matrix of θ . Since $w(\Omega_\theta)$ satisfies the variational problem (2.6) in Ω_θ , one gets after the change of variable (2.11),

$$\begin{aligned} & \int_{\Omega} \left(\frac{1}{r} + \nabla \frac{1}{r} \cdot \theta + o(\theta) \right) \left(\frac{1}{\mu} A(\theta) \nabla \tilde{w}(\theta) \cdot \bar{\phi} - i\omega \sigma \tilde{w}(\theta) \bar{\phi} | \det(I + \nabla \theta) | \right) dr dz \\ &= \int_{\Omega} i\omega J \circ (\text{Id} + \theta) \bar{\phi} | \det(I + \nabla \theta) | dr dz, \end{aligned} \quad (2.11)$$

where we have set

$$A(\theta) := |\det(I + \nabla \theta)| (I + \nabla \theta)^{-1} ((I + \nabla \theta)^{-1})^t \quad (2.12)$$

and $\phi := \varphi \circ (\text{Id} + \theta)$. Expanding the above formulation with respect to θ and using the identities

$$\begin{aligned} \det(I + \theta) &= 1 + \text{div} \theta + o(\theta), \\ (I + \nabla \theta)^{-1} &= I - \nabla \theta + o(\theta), \end{aligned}$$

the terms of order zero with respect to θ give exactly the variational formulation on Ω (2.6), while the first order terms with respect to θ yield the formulation (2.10). Since the sesquilinear form $a(\cdot, \cdot)$ is continuous and coercive, the variational formulation (2.10) has a unique solution. \square

To simplify the variational formulation (2.10), we shall prove some preliminary technical results. For any $\mathcal{Q} \subset \Omega$, we define a shape-dependent sesquilinear form

$$\alpha(\mathcal{Q})(u(\mathcal{Q}), v(\mathcal{Q})) := \int_{\mathcal{Q}} \left(\frac{1}{\mu r} \nabla u \cdot \nabla \bar{v} - \frac{i\omega \sigma}{r} u \bar{v} \right) dr dz \quad \forall (u, v) \in \tilde{H}(\mathcal{Q})^2. \quad (2.13)$$

In the Orz plane with (r, z) -coordinates, we denote by $n = (n_r, n_z)^t$ the unit out normal vector on the boundary $\partial \mathcal{Q}$ and by $\tau = (-n_z, n_r)^t$ the tangential vector on $\partial \mathcal{Q}$. The tangential gradient operator on $\partial \mathcal{Q}$ is defined by $\nabla_\tau := \nabla - n \partial_n = \tau (\tau \cdot \nabla)$. Then we have in particular on $\partial \mathcal{Q}$ $\nabla u \cdot \nabla v = \partial_n u \partial_n v + \nabla_\tau u \cdot \nabla_\tau v$.

Lemma 2.2.4. *Assume that μ and σ are constant in \mathcal{Q} . Let $u(\mathcal{Q}) \in \tilde{H}(\mathcal{Q})$ satisfying in the weak sense*

$$-\text{div} \left(\frac{1}{\mu r} \nabla u \right) - \frac{i\omega \sigma}{r} u = 0 \quad \text{in } \mathcal{Q} \quad (2.14)$$

and $v(\mathcal{Q}) \in \tilde{H}(\mathcal{Q})$ and assume that their material derivatives $(u'(\theta), v'(\theta))$ and shape derivatives $(U(\theta), V(\theta))$ exist. We assume in addition that $D^2 u$ and $D^2 v$ are in $L^2(\mathcal{Q} \cap \{\Omega_v \cup \Omega_d\})$. Then the shape derivative of $\alpha(\mathcal{Q})(u(\mathcal{Q}), v(\mathcal{Q}))$, denoted by $\beta(\theta)$ exists for all admissible perturbations θ and is given by

$$\begin{aligned} \beta(\theta) &= \alpha(\mathcal{Q})(u'(\theta), v(\mathcal{Q})) + \alpha(\mathcal{Q})(u(\mathcal{Q}), V(\theta)) \\ &+ \int_{\partial \mathcal{Q}} \left\{ (\theta \cdot n) \left(\frac{1}{\mu r} \nabla_\tau u \cdot \nabla_\tau \bar{v} - \frac{i\omega \sigma}{r} u \bar{v} \right) - \left(\frac{1}{\mu r} \partial_n u (\theta \cdot \nabla_\tau \bar{v}) \right) \right\} ds. \end{aligned} \quad (2.15)$$

Proof. We recall that $\beta(\theta)$ is formally defined as

$$\beta(\theta) = \alpha(\mathcal{Q}_\theta)(u(\mathcal{Q}_\theta), v(\mathcal{Q}_\theta)) - \alpha(\mathcal{Q})(u(\mathcal{Q}), v(\mathcal{Q})) + o(\theta).$$

We consider the change of variables from \mathcal{Q}_θ to \mathcal{Q} with $(\text{Id} + \theta)^{-1}$ and rewrite de shape-dependent form $\alpha(\mathcal{Q}_\theta)(u(\mathcal{Q}_\theta), v(\mathcal{Q}_\theta))$ as an integral on \mathcal{Q} . Using the same notations as in Definition 2.2.1 for $\tilde{u}(\theta)$, $\tilde{v}(\theta)$, we have

$$\begin{aligned} & \alpha(\mathcal{Q}_\theta)(u(\mathcal{Q}_\theta), v(\mathcal{Q}_\theta)) \\ &= \int_{\mathcal{Q}} \left(\frac{1}{r} + \theta \cdot \nabla \left(\frac{1}{r} \right) + o(\theta) \right) \left(\frac{1}{\mu} A(\theta) \nabla \tilde{u}(\theta) \cdot \nabla \overline{\tilde{v}(\theta)} - i\omega\sigma \tilde{u}(\theta) \overline{\tilde{v}(\theta)} | \det(I + \nabla\theta) | \right) dr dz, \end{aligned}$$

where $A(\theta)$ is given in (2.12). By definition of the material derivative, we have the developments

$$\begin{aligned} \tilde{u}(\theta) &= \tilde{u}(0) + U(\theta) + o(\theta) = u(\mathcal{Q}) + U(\theta) + o(\theta), \\ \tilde{v}(\theta) &= \tilde{v}(0) + V(\theta) + o(\theta) = v(\mathcal{Q}) + V(\theta) + o(\theta). \end{aligned}$$

Thus one obtains

$$\begin{aligned} & \alpha(\mathcal{Q}_\theta)(u(\mathcal{Q}_\theta), v(\mathcal{Q}_\theta)) \\ &= \alpha(\mathcal{Q})(u(\mathcal{Q}), v(\mathcal{Q})) + \alpha(\mathcal{Q})(U(\theta), v(\mathcal{Q})) + \alpha(\mathcal{Q})(u(\mathcal{Q}), V(\theta)) \\ &+ \int_{\mathcal{Q}} \left\{ \frac{1}{\mu} \left(\theta \cdot \nabla \frac{1}{r} + \frac{1}{r} (\text{div } \theta - \nabla\theta - (\nabla\theta)^t) \right) \nabla u \nabla \bar{v} - i\omega\sigma \left(\theta \cdot \nabla \frac{1}{r} + \frac{\text{div } \theta}{r} \right) u \bar{v} \right\} dr dz + o(\theta) \\ &= \alpha(\mathcal{Q})(u(\mathcal{Q}), v(\mathcal{Q})) + \alpha(\mathcal{Q})(U(\theta), v(\mathcal{Q})) + \alpha(\mathcal{Q})(u(\mathcal{Q}), V(\theta)) \\ &+ \int_{\mathcal{Q}} \left\{ \frac{1}{\mu} \left(\text{div } (\theta/r) - \frac{1}{r} (\nabla\theta + (\nabla\theta)^t) \right) \nabla u \nabla \bar{v} - i\omega\sigma \text{div } (\theta/r) u \bar{v} \right\} dr dz + o(\theta). \end{aligned}$$

Therefore, from the definition of $\beta(\theta)$, one has

$$\beta(\theta) = \alpha(\mathcal{Q})(U(\theta), v) + \alpha(\mathcal{Q})(u, V(\theta)) + \mathcal{I}_1 + \mathcal{I}_2 + \mathcal{I}_3 + \mathcal{I}_4, \quad (2.16)$$

with

$$\begin{aligned} \mathcal{I}_1 &= \int_{\mathcal{Q}} \frac{1}{\mu} \text{div } (\theta/r) \nabla u \nabla \bar{v} dr dz, \\ \mathcal{I}_2 &= \int_{\mathcal{Q}} \frac{1}{\mu} \left(-\frac{\nabla\theta}{r} \right) \nabla u \nabla \bar{v} dr dz, \\ \mathcal{I}_3 &= \int_{\mathcal{Q}} \frac{1}{\mu} \left(-\frac{(\nabla\theta)^t}{r} \right) \nabla u \nabla \bar{v} dr dz, \\ \mathcal{I}_4 &= \int_{\mathcal{Q}} (-i\omega\sigma) \text{div } (\theta/r) u \bar{v} dr dz. \end{aligned}$$

We compute using integration by parts

$$\begin{aligned}
\mathcal{I}_1 &= - \int_{\mathcal{Q}} \frac{1}{\mu r} \theta \cdot \nabla (\nabla u \cdot \nabla \bar{v}) \, dr \, dz + \int_{\partial \mathcal{Q}} \frac{(\theta \cdot n)}{\mu r} \nabla u \cdot \nabla \bar{v} \, ds \\
&= - \int_{\mathcal{Q}} \frac{1}{\mu r} \theta \cdot (D^2 u \nabla \bar{v} + D^2 \bar{v} \nabla u) \, dr \, dz + \int_{\partial \mathcal{Q}} \frac{(\theta \cdot n)}{\mu r} \nabla u \cdot \nabla \bar{v} \, ds \\
&= - \int_{\mathcal{Q}} \frac{1}{\mu r} (\nabla (\nabla u \cdot \theta) \cdot \nabla \bar{v} - (\nabla \theta)^t \nabla u \cdot \nabla \bar{v} + \theta \cdot D^2 \bar{v} \nabla u) \, dr \, dz \\
&\quad + \int_{\partial \mathcal{Q}} \frac{(\theta \cdot n)}{\mu r} (\partial_n u \partial_n \bar{v} + \nabla_\tau u \cdot \nabla_\tau \bar{v}) \, ds,
\end{aligned}$$

and

$$\begin{aligned}
\mathcal{I}_2 &= - \int_{\mathcal{Q}} \frac{1}{\mu r} ((\nabla \theta_r \cdot \nabla u) \partial_r \bar{v} + (\nabla \theta_z \cdot \nabla u) \partial_z \bar{v}) \, dr \, dz \\
&= \int_{\mathcal{Q}} \frac{1}{\mu} \left(\operatorname{div} \left(\frac{\nabla u}{r} \partial_r \bar{v} \right) \theta_r + \operatorname{div} \left(\frac{\nabla u}{r} \partial_z \bar{v} \right) \theta_z \right) \, dr \, dz - \int_{\partial \mathcal{Q}} \frac{1}{\mu r} \partial_n u (\theta \cdot \nabla \bar{v}) \, ds \\
&= \int_{\mathcal{Q}} \left\{ \frac{1}{\mu} \operatorname{div} \left(\frac{\nabla u}{r} \right) (\theta \cdot \nabla \bar{v}) + \frac{1}{\mu r} \nabla u \cdot (\nabla (\partial_r \bar{v}) \theta_r + \nabla (\partial_z \bar{v}) \theta_z) \right\} \, dr \, dz \\
&\quad - \int_{\partial \mathcal{Q}} \frac{1}{\mu r} \partial_n u ((\theta \cdot n) \partial_n \bar{v} + (\theta \cdot \nabla_\tau \bar{v})) \, ds \\
&= \int_{\mathcal{Q}} \left\{ -\frac{i\omega\sigma}{r} u (\theta \cdot \nabla \bar{v}) + \frac{1}{\mu r} \nabla u \cdot D^2 \bar{v} \theta \right\} \, dr \, dz - \int_{\partial \mathcal{Q}} \frac{1}{\mu r} \partial_n u ((\theta \cdot n) \partial_n \bar{v} + (\theta \cdot \nabla_\tau \bar{v})) \, ds.
\end{aligned}$$

We observe that the last equality is due to (2.14). Finally,

$$\mathcal{I}_4 = \int_{\mathcal{Q}} \frac{i\omega\sigma}{r} ((\theta \cdot \nabla u) \bar{v} + u (\theta \cdot \nabla \bar{v})) \, dr \, dz - \int_{\partial \mathcal{Q}} (\theta \cdot n) \frac{i\omega\sigma}{r} u \bar{v} \, ds.$$

Thus, putting together all previous expressions, one gets

$$\begin{aligned}
\mathcal{I}_1 + \mathcal{I}_2 + \mathcal{I}_3 + \mathcal{I}_4 &= - \int_{\mathcal{Q}} \left\{ \frac{1}{\mu r} \nabla (\theta \cdot \nabla u) \cdot \nabla \bar{v} - \frac{i\omega\sigma}{r} (\theta \cdot \nabla u) \bar{v} \right\} \, dr \, dz \\
&\quad + \int_{\partial \mathcal{Q}} \left\{ (\theta \cdot n) \left(\frac{1}{\mu r} \nabla_\tau u \cdot \nabla_\tau \bar{v} - \frac{i\omega\sigma}{r} u \bar{v} \right) - \left(\frac{1}{\mu r} \partial_n u (\theta \cdot \nabla_\tau \bar{v}) \right) \right\} \, ds. \tag{2.17}
\end{aligned}$$

Since $U(\theta) - \theta \cdot \nabla u = u'(\theta)$ (see (2.9)), by substituting (2.17) in (2.16), we get the result (2.15). \square

Proposition 2.2.5. *Under the same assumptions as in Proposition 2.2.3, if we assume in addition that (μ, σ) are piecewise constant and equal to constants (μ_i, σ_i) on each subdomains Ω_i ($i \in \Lambda$) of Ω , and that $\theta \in W^{1,\infty}(\Omega, \Omega)^2$ is an admissible perturbation, then the material derivative $W(\theta)$ of w satisfies*

$$\begin{aligned}
a(W(\theta), \phi) &= \int_{\Gamma} (\theta \cdot n) \left(\left[\frac{1}{\mu} \right] \frac{1}{r} \nabla_\tau w \cdot \nabla_\tau \bar{\phi} - \frac{i\omega[\sigma]}{r} w \bar{\phi} \right) \, ds \\
&\quad + \int_{\Omega_d \cup \Omega_d^c} \left(\frac{1}{\mu r} \nabla (\theta \cdot \nabla w) \cdot \nabla \bar{\phi} - \frac{i\omega\sigma}{r} (\theta \cdot \nabla w) \bar{\phi} \right) \, dr \, dz \quad \forall \phi \in \tilde{H}(\Omega). \tag{2.18}
\end{aligned}$$

Remark 2.2.6. For the right-hand-side of the variational formulation (2.18), the notation $\int_{\Omega_d \cup \Omega_v}$ means the integrals on Ω_d and on Ω_d^c are evaluated separately. This is because $(\theta \cdot \nabla w)$ is not in the function space $\tilde{H}(\Omega)$. In fact, the jump of μ through the interface Γ yields the transmission condition $[\mu^{-1} \partial_n w] = 0$ on Γ . Thus $(\theta \cdot \nabla w)$ is discontinuous on Γ

$$[(\theta \cdot \nabla w)] = [(\theta \cdot n) \partial_n w + (\theta \cdot \nabla_\tau w)] = (\theta \cdot n) [\partial_n w] = (\theta \cdot n) [\mu] (\mu^{-1} \partial_n w). \quad (2.19)$$

However, we locally have $(\theta \cdot \nabla w)|_{\Omega_i} \in \tilde{H}(\Omega_i)$ for $i \in \{s, t, d, v\}$. We may refer to [53] for a detailed discussion on local regularities of PDE solution on subdomains with piecewise regular coefficients.

Proof. We write the sesquilinear form $a(\cdot, \cdot)$ in (2.6) as the sum of forms on subdomains where μ and σ are constant

$$a(w, \varphi) = \sum_{i \in \Lambda} \alpha_i(\Omega_i)(w, \varphi),$$

where $\alpha_i(\mathcal{Q})(\cdot, \cdot)$ is defined as $\alpha(\mathcal{Q})(\cdot, \cdot)$ in (2.13) with $\mu = \mu_i$ and $\sigma = \sigma_i$. We will also denote by $\beta_i(\theta)$ the shape derivative associated with α_i . We choose the test function φ on Ω_θ such that $\phi = \varphi \circ (\text{Id} + \theta)$ on Ω . Thus, the material derivative of φ vanishes. Considering that the support of θ is contained in $\Omega_d \cup \Omega_v$, that $w'(\theta) = W(\theta) - \theta \cdot \nabla w$ on Ω_d and on Ω_d^c , and that the solution w satisfies the transmission conditions $[w] = [\mu^{-1} \partial_n w] = 0$ on Γ , from Lemma (2.2.4) one gets shape derivative of $a(w, \varphi)$ is given by

$$\begin{aligned} \sum_{i \in \Lambda} \beta_i(\theta) &= \sum_{i \in \Lambda} \alpha_i(\Omega_i)(w'(\theta), \phi) \\ &\quad - \int_{\Gamma} \left[(\theta \cdot n) \left(\frac{1}{\mu r} \nabla_\tau w \cdot \nabla_\tau \bar{\phi} - \frac{i\omega\sigma}{r} w \bar{\phi} \right) - \left(\frac{1}{\mu r} \partial_n w (\theta \cdot \nabla_\tau \bar{\phi}) \right) \right] ds \\ &= \sum_{i \in \Lambda} \alpha_i(\Omega_i)(W(\theta), \phi) - \sum_{i \in \{d, v\}} \alpha_i(\Omega_i)(\theta \cdot \nabla w, \phi) \\ &\quad - \int_{\Gamma} \left\{ (\theta \cdot n) \left(\left[\frac{1}{\mu r} \nabla_\tau w \right] \cdot \nabla_\tau \bar{\phi} - \frac{i\omega}{r} [\sigma w] \bar{\phi} \right) - \left[\frac{1}{\mu r} \partial_n w \right] (\theta \cdot \nabla_\tau \bar{\phi}) \right\} ds \\ &= a(W(\theta), \phi) - \int_{\Omega_d \cup \Omega_d^c} \left(\frac{1}{\mu r} \nabla(\theta \cdot \nabla w) \cdot \nabla \bar{\phi} - \frac{i\omega\sigma}{r} (\theta \cdot \nabla w) \bar{\phi} \right) dr dz \\ &\quad - \int_{\Gamma} (\theta \cdot n) \left(\left[\frac{1}{\mu} \right] \frac{1}{r} \nabla_\tau w \cdot \nabla_\tau \bar{\phi} - \frac{i\omega[\sigma]}{r} w \bar{\phi} \right) ds. \end{aligned}$$

On the other hand, since the support of the source J is contained in Ω_s , the shape derivative of the right-hand-side of the variational formulation (2.6) vanishes. Hence, we get the result (2.18). \square

Remark 2.2.7. $w'(\theta)$ is not in $\tilde{H}(\Omega)$ due to its discontinuity on Γ as we have discussed in Remark 2.2.6. From (2.19) we have

$$[w'(\theta)] = -[\theta \cdot \nabla w] = -(\theta \cdot n) [\mu] (\mu^{-1} \partial_n w). \quad (2.20)$$

Thus, one should consider a function space which is less regular than $\tilde{H}(\Omega)$

$$\tilde{H}(\Omega_d \cup \Omega_d^c) = \{v : v|_{\Omega_d} \in \tilde{H}(\Omega_d), \quad v|_{\Omega_d^c} \in \tilde{H}(\Omega_d^c)\}$$

and a sesquilinear form similar to $a(\cdot, \cdot)$

$$\check{a}(u, v) := \int_{\Omega_d \cup \Omega_d^c} \left(\frac{1}{\mu r} \nabla u \cdot \nabla \bar{v} - \frac{i\omega\sigma}{r} u \bar{v} \right) dr dz \quad \forall (u, v) \in \tilde{H}(\Omega_d \cup \Omega_d^c)^2.$$

One obtains immediately from Proposition 2.2.5 that the shape derivative $w'(\theta)$ of w satisfies

$$\check{a}(w'(\theta), \phi) = \int_{\Gamma} (\theta \cdot n) \left(\left[\frac{1}{\mu} \right] \frac{1}{r} \nabla_{\tau} w \cdot \nabla_{\tau} \bar{\phi} - \frac{i\omega[\sigma]}{r} w \bar{\phi} \right) ds \quad \forall \phi \in \tilde{H}(\Omega). \quad (2.21)$$

To complete (2.21), one should take into account the discontinuity of $w'(\theta)$ on Γ . One possibility would be to consider a lifting in $\tilde{H}(\Omega_d \cup \Omega_d^c)$ of $-\partial_n w$ and then write a variational formulation for the difference which is an element of $\tilde{H}(\Omega)$.

2.2.2 Shape derivative of the impedance

Now that we have the shape and material derivatives of the solution, we can compute the shape derivative of the measured impedances. Let w be the solution of problem (2.6) with coefficients (μ, σ) and w^0 the solution in a deposit free-case, i.e. with coefficients $(\mu, \sigma) = (\mu^0, \sigma^0)$. We shall denote by $\alpha_0(\mathcal{Q})$ the sesquilinear form $\alpha(\mathcal{Q})$ for $(\mu, \sigma) = (\mu^0, \sigma^0)$. Following (2.5) we define the impedance measurement as

$$\Delta Z(\Omega) = \frac{2\pi}{i\omega I^2} \int_{\Omega_d} \left(\left(\frac{1}{\mu} - \frac{1}{\mu^0} \right) \frac{\nabla w \cdot \nabla w^0}{r} - i\omega(\sigma - \sigma^0) \frac{w w^0}{r} \right) dr dz. \quad (2.22)$$

Proposition 2.2.8. *Under the same assumptions as Proposition 2.2.5 for μ, σ and θ , the shape derivative of the impedance ΔZ is well defined and is given by*

$$\begin{aligned} \Delta Z'(\theta) &= \frac{2\pi}{i\omega I^2} \int_{\Omega_d} \left(\left(\frac{1}{\mu} - \frac{1}{\mu^0} \right) \frac{1}{r} \nabla w'(\theta) \cdot \nabla w^0 - \frac{i\omega(\sigma - \sigma^0)}{r} w'(\theta) w^0 \right) dr dz \\ &\quad + \frac{2\pi}{i\omega I^2} \int_{\Gamma} (\theta \cdot n) \left(\left(\frac{1}{\mu} - \frac{1}{\mu^0} \right) \frac{1}{r} \nabla w \cdot \nabla w^0 - \frac{i\omega(\sigma - \sigma^0)}{r} w w^0 \right) ds \\ &= \frac{2\pi}{i\omega I^2} \int_{\Omega_d} \left(\left(\frac{1}{\mu} - \frac{1}{\mu^0} \right) \frac{1}{r} \nabla (W(\theta) - \theta \cdot \nabla w) \cdot \nabla w^0 - \frac{i\omega(\sigma - \sigma^0)}{r} (W(\theta) - \theta \cdot \nabla w) w^0 \right) dr dz \\ &\quad + \frac{2\pi}{i\omega I^2} \int_{\Gamma} (\theta \cdot n) \left(\left(\frac{1}{\mu} - \frac{1}{\mu^0} \right) \frac{1}{r} \nabla w \cdot \nabla w^0 - \frac{i\omega(\sigma - \sigma^0)}{r} w w^0 \right) ds. \end{aligned} \quad (2.23)$$

where $w'(\theta)$ and $W(\theta)$ are respectively the shape and material derivative of w (the solution of problem (2.6)).

Proof. Since in Ω_d , μ, σ, μ^0 and σ^0 are constant, from (2.5) and the definition of the sesquilinear form α in (2.13) we have

$$\frac{i\omega I^2}{2\pi} \Delta Z = \alpha(\Omega_d)(w, \overline{w^0}) - \alpha(\Omega_d)(w^0, \overline{w}).$$

The field w^0 for the deposit-free case is invariant under the shape deformation $(\text{Id} + \theta)$ (since μ^0 and σ^0 are invariant under the shape deformation $(\text{Id} + \theta)$). Thus its shape derivative is zero and consequently its material derivative

$$W^0(\theta) = \theta \cdot \nabla w^0.$$

In Ω_d the field w satisfies equation (2.14) with μ, σ . So does the field w^0 in Ω_d with μ^0, σ^0 . Hence, Lemma 2.2.4 implies

$$\begin{aligned} \frac{i\omega I^2}{2\pi} \Delta Z'(\theta) &= \alpha(\Omega_d)(w', \overline{w^0}) + \alpha(\Omega_d)(w, \overline{W^0}) - \alpha_0(\Omega_d)(w^0, \overline{W}) \\ &\quad + \int_{\Gamma} \left\{ (\theta \cdot n) \left(\frac{1}{\mu r} \nabla_{\tau} w \cdot \nabla_{\tau} w^0 - \frac{i\omega\sigma}{r} w w^0 \right) - \left(\frac{1}{\mu r} \partial_n w (\theta \cdot \nabla_{\tau} w^0) \right) \right\} ds \\ &\quad - \int_{\Gamma} \left\{ (\theta \cdot n) \left(\frac{1}{\mu^0 r} \nabla_{\tau} w^0 \cdot \nabla_{\tau} w - \frac{i\omega\sigma^0}{r} w^0 w \right) - \left(\frac{1}{\mu^0 r} \partial_n w^0 (\theta \cdot \nabla_{\tau} w) \right) \right\} ds. \end{aligned}$$

We evaluate term by term the right-hand-side of above equality. By integration by parts,

$$\begin{aligned} \alpha(\Omega_d)(w, \overline{W^0}) &= \alpha(\Omega_d)(w, \overline{\theta \cdot \nabla w^0}) \\ &= \int_{\Omega_d} \left(\frac{1}{\mu r} \nabla w \cdot \nabla (\theta \cdot \nabla w^0) - \frac{i\omega\sigma}{r} w (\theta \cdot \nabla w^0) \right) dr dz \\ &= \int_{\Omega_d} \left(-\text{div} \left(\frac{1}{\mu r} \nabla w \right) - \frac{i\omega\sigma}{r} w \right) (\theta \cdot \nabla w^0) dr dz + \int_{\Gamma} \frac{1}{\mu r} \partial_n w (\theta \cdot \nabla w^0) ds \\ &= \int_{\Gamma} \frac{1}{\mu r} \partial_n w ((\theta \cdot n) \partial_n w^0 + (\theta \cdot \nabla_{\tau} w^0)) ds. \end{aligned}$$

From the definition of the sesquilinear form,

$$\alpha_0(\Omega_d)(w^0, \overline{W}) = \alpha_0(\Omega_d)(W, \overline{w^0}).$$

Using the partial differential equation satisfied by w^0 in Ω_d we get

$$\begin{aligned} &\int_{\Gamma} \frac{1}{\mu^0 r} \partial_n w^0 (\theta \cdot \nabla_{\tau} w) ds \\ &= \int_{\Gamma} \frac{1}{\mu^0 r} \partial_n w^0 (\theta \cdot \nabla w - (\theta \cdot n) \partial_n w) ds \\ &= \int_{\Omega_d} \text{div} \left(\frac{1}{\mu^0 r} \nabla w^0 (\theta \cdot \nabla w) \right) dr dz - \int_{\Gamma} (\theta \cdot n) \frac{1}{\mu^0 r} \partial_n w \partial_n w^0 ds \\ &= \int_{\Omega_d} \left\{ \text{div} \left(\frac{1}{\mu^0 r} \nabla w^0 \right) (\theta \cdot \nabla w) + \frac{1}{\mu^0 r} \nabla w^0 \cdot \nabla (\theta \cdot \nabla w) \right\} dr dz - \int_{\Gamma} (\theta \cdot n) \frac{1}{\mu^0 r} \partial_n w \partial_n w^0 ds \\ &= \int_{\Omega_d} \left\{ \left(-\frac{i\omega\sigma^0}{r} w^0 \right) (\theta \cdot \nabla w) + \frac{1}{\mu^0 r} \nabla w^0 \cdot \nabla (\theta \cdot \nabla w) \right\} dr dz - \int_{\Gamma} (\theta \cdot n) \frac{1}{\mu^0 r} \partial_n w \partial_n w^0 ds \\ &= \alpha_0(\Omega_d)(\theta \cdot \nabla w, w^0) - \int_{\Gamma} (\theta \cdot n) \frac{1}{\mu^0 r} \partial_n w \partial_n w^0 ds. \end{aligned}$$

Finally, with the above results, one obtains

$$\begin{aligned} \frac{i\omega I^2}{2\pi} \Delta Z'(\theta) &= \alpha(\Omega_d)(w', \overline{w^0}) - \alpha_0(\Omega_d)(W, \overline{w^0}) + \alpha_0(\Omega_d)((\theta \cdot \nabla w), w^0) \\ &\quad + \int_{\Gamma} (\theta \cdot n) \left\{ \left(\frac{1}{\mu} - \frac{1}{\mu^0} \right) \frac{1}{r} (\nabla_{\tau} w \cdot \nabla_{\tau} w^0 + \partial_n w \partial_n w^0) - \frac{i\omega(\sigma - \sigma^0)}{r} w w^0 \right\} ds \\ &= \alpha(\Omega_d)(w', \overline{w^0}) - \alpha_0(\Omega_d)(w', \overline{w^0}) \\ &\quad + \int_{\Gamma} (\theta \cdot n) \left(\left(\frac{1}{\mu} - \frac{1}{\mu^0} \right) \frac{1}{r} \nabla w \cdot \nabla w^0 - \frac{i\omega(\sigma - \sigma^0)}{r} w w^0 \right) ds. \end{aligned}$$

This is exactly expression (2.23). \square

2.2.3 Expression of the impedance shape derivative using the adjoint state

The expression of the gradient $\Delta Z'(\theta)$ shown in (2.23) contains not only a boundary integral on Γ whose integrand depends explicitly on the shape perturbation θ , but also a volume integral on Ω_d with the shape or material derivative of w in the integrand which depends implicitly on θ via the variational problem (2.18). We shall consider here the Hadamard representation of cost functional derivatives using an appropriately defined adjoint state which allows to have an expression of $\Delta Z'(\theta)$ as a boundary integral on Γ with integrand explicitly dependent on θ . This expression is much more appropriate for the numerical scheme that we shall use for the inverse problem.

We define the sesquilinear form

$$a^*(u, v) := \overline{a(v, u)} \quad \forall (u, v) \in \tilde{H}(\Omega)^2. \quad (2.24)$$

and we introduce the adjoint problem associated with w^0 as finding $p \in \tilde{H}(\Omega)$ such that

$$a^*(p, q) = \int_{\Omega_d} \left(\left(\frac{1}{\mu} - \frac{1}{\mu^0} \right) \frac{1}{r} \nabla \overline{w^0} \cdot \nabla \overline{q} + \frac{i\omega(\sigma - \sigma^0)}{r} \overline{w^0} \overline{q} \right) dr dz \quad \forall q \in \tilde{H}(\Omega). \quad (2.25)$$

In particular, p satisfies in the weak sense:

$$\left\{ \begin{array}{ll} -\operatorname{div} \left(\frac{1}{\mu r} \nabla p \right) + \frac{i\omega\sigma}{r} p = -\operatorname{div} \left(\left(\frac{1}{\mu} - \frac{1}{\mu^0} \right) \frac{1}{r} \nabla \overline{w^0} \right) + \frac{i\omega(\sigma - \sigma^0)}{r} \overline{w^0} & \text{in } \Omega_d, \\ -\operatorname{div} \left(\frac{1}{\mu r} \nabla p \right) + \frac{i\omega\sigma}{r} p = 0 & \text{in } \Omega_d^c, \\ [p] = 0 & \text{on } \Gamma, \\ [\mu^{-1} \partial_n p] = -\left(\frac{1}{\mu} - \frac{1}{\mu^0} \right) \partial_n \overline{w^0} & \text{on } \Gamma. \end{array} \right. \quad (2.26)$$

Problem (2.25) has the same structure as (2.6) and therefore one can conclude:

Proposition 2.2.9. *Let $w^0 \in \tilde{H}(\Omega)$ be the solution to the eddy current problem (2.6) in a deposit-free case, i.e. with (μ^0, σ^0) instead of (μ, σ) . Then, under the same assumptions as in Corollary 2.1.1 for μ and σ , the variational formulation (2.25) has a unique solution p in $\tilde{H}(\Omega)$.*

Then we have the following result.

Proposition 2.2.10. *Under the same assumptions as in Proposition 2.2.8, if p is the adjoint state satisfying the adjoint problem (2.25), then the shape derivative of the impedance ΔZ given by (2.5) has the following expression*

$$\begin{aligned} \Delta Z'(\theta) = & \frac{2\pi}{i\omega I^2} \int_{\Gamma} \frac{(\theta \cdot n)}{r} \left\{ \left[\frac{1}{\mu} \right] \nabla_{\tau} w \cdot \nabla_{\tau} (\bar{p} - w^0) \right. \\ & \left. - [\mu] (\mu^{-1} \partial_n w) \left((\mu^0)^{-1} (\partial_n \bar{p})_+ - (\mu^0)^{-1} \partial_n w^0 \right) - i\omega [\sigma] w (\bar{p} - w^0) \right\} ds, \end{aligned} \quad (2.27)$$

where w (resp. w^0) is the solution to the weighted eddy current problem (2.6) with (resp. without) deposits.

Proof. We take $q = W(\theta) \in \tilde{H}(\Omega)$ as test function in (2.25) and get

$$\begin{aligned} a(W(\theta), p) &= \overline{a^*(p, W(\theta))} \\ &= \int_{\Omega_d} \left(\left(\frac{1}{\mu} - \frac{1}{\mu^0} \right) \frac{1}{r} \nabla w^0 \cdot \nabla W(\theta) - \frac{i\omega(\sigma - \sigma^0)}{r} w^0 W(\theta) \right) dr dz. \end{aligned} \quad (2.28)$$

We consider the function space $\tilde{H}(\Omega_d \cup \Omega_d^c)$ and the sesquilinear form $\check{a}(\cdot, \cdot)$ defined in Remark 2.2.7. We denote by $\check{a}^*(\cdot, \cdot)$ a sesquilinear form similar to $a^*(\cdot, \cdot)$

$$\check{a}^*(u, v) := \overline{\check{a}(v, u)} \quad \forall (u, v) \in \tilde{H}(\Omega_d \cup \Omega_d^c)^2.$$

Using (2.26), we have for $q \in \tilde{H}(\Omega_d \cup \Omega_d^c)$

$$\begin{aligned} \check{a}^*(p, q) &+ \int_{\Gamma} \left[\frac{1}{r} (\mu^{-1} \partial_n p) \bar{q} \right] ds \\ &= \int_{\Omega_d} \left(\left(\frac{1}{\mu} - \frac{1}{\mu^0} \right) \frac{1}{r} \nabla \bar{w}^0 \cdot \nabla \bar{q} + \frac{i\omega(\sigma - \sigma^0)}{r} \bar{w}^0 \bar{q} \right) dr dz - \int_{\Gamma} \left(\frac{1}{\mu} - \frac{1}{\mu^0} \right) \partial_n \bar{w}^0 \bar{q} ds, \end{aligned}$$

and therefore

$$\check{a}^*(p, q) = \int_{\Omega_d} \left(\left(\frac{1}{\mu} - \frac{1}{\mu^0} \right) \frac{1}{r} \nabla \bar{w}^0 \cdot \nabla \bar{q} + \frac{i\omega(\sigma - \sigma^0)}{r} \bar{w}^0 \bar{q} \right) dr dz - \int_{\Gamma} \frac{1}{r} (\mu^{-1} \partial_n p)_+ [\bar{q}] ds.$$

From Remark 2.2.6, $(\theta \cdot \nabla w)$ is in $\tilde{H}(\Omega_d \cup \Omega_d^c)$. Taking $q = (\theta \cdot \nabla w)$ in the above formulation and considering the jump condition (2.19), one gets

$$\begin{aligned} \check{a}((\theta \cdot \nabla w), p) &= \overline{\check{a}^*(p, (\theta \cdot \nabla w))} \\ &= \int_{\Omega_d} \left(\left(\frac{1}{\mu} - \frac{1}{\mu^0} \right) \frac{1}{r} \nabla w^0 \cdot \nabla (\theta \cdot \nabla w) - \frac{i\omega(\sigma - \sigma^0)}{r} w^0 (\theta \cdot \nabla w) \right) dr dz \\ &\quad - \int_{\Gamma} (\theta \cdot n) \frac{[\mu]}{r} (\mu^{-1} \partial_n \bar{p})_+ (\mu^{-1} \partial_n w) ds. \end{aligned} \quad (2.29)$$

Taking $\phi = p$ in (2.18) yields

$$a(W(\theta), p) = \int_{\Gamma} \frac{(\theta \cdot n)}{r} \left(\left[\frac{1}{\mu} \right] \nabla_{\tau} w \cdot \nabla_{\tau} \bar{p} - i\omega [\sigma] w \bar{p} \right) ds + \check{a}((\theta \cdot \nabla w), p). \quad (2.30)$$

From (2.28) – (2.30) one has

$$\begin{aligned} & \int_{\Omega_d} \left(\left(\frac{1}{\mu} - \frac{1}{\mu^0} \right) \frac{1}{r} \nabla w'(\theta) \cdot \nabla w^0 - \frac{i\omega(\sigma - \sigma^0)}{r} w'(\theta) w^0 \right) dr dz \\ &= \int_{\Gamma} \frac{(\theta \cdot n)}{r} \left\{ \left[\frac{1}{\mu} \right] \nabla_{\tau} w \cdot \nabla_{\tau} \bar{p} - [\mu] (\mu^{-1} \partial_n w) ((\mu^0)^{-1} (\partial_n \bar{p})_+) - i\omega[\sigma] w \bar{p} \right\} ds. \end{aligned} \quad (2.31)$$

Since μ^0, σ^0 are the background coefficients for the deposit-free case, we have

$$\left[\frac{1}{\mu} \right] = \frac{1}{\mu^0} - \frac{1}{\mu}, \quad [\mu] = \mu^0 - \mu, \quad [\sigma] = \sigma^0 - \sigma.$$

On Γ we have

$$\begin{aligned} \left(\frac{1}{\mu} - \frac{1}{\mu^0} \right) \nabla w \cdot \nabla w^0 &= \left(\frac{1}{\mu} - \frac{1}{\mu^0} \right) (\nabla_{\tau} w \cdot \nabla_{\tau} w^0 + \partial_n w \partial_n w^0) \\ &= \left(\frac{1}{\mu} - \frac{1}{\mu^0} \right) \nabla_{\tau} w \cdot \nabla_{\tau} w^0 + (\mu^0 - \mu) (\mu^{-1} \partial_n w) ((\mu^0)^{-1} \partial_n w^0) \\ &= - \left[\frac{1}{\mu} \right] \nabla_{\tau} w \cdot \nabla_{\tau} w^0 + [\mu] (\mu^{-1} \partial_n w) ((\mu^0)^{-1} \partial_n w^0) \end{aligned} \quad (2.32)$$

Finally, from (2.23), (2.31) and (2.32), we conclude the result (2.27). \square

2.3 Shape reconstruction of deposits using a gradient method

2.3.1 Objective function

We denote by Z the impedance measurement either in absolute mode (Z_{FA}) or in differential mode (Z_{F3}). Giving the ECT signals $Z_{meas}(\zeta)$ for $\zeta \in [z_{\min}, z_{\max}]$, the inverse problem aims to approximate the real deposit domain by an estimate Ω_d in simulation so that the ETC signals $Z(\Omega_d, \zeta)$ reproduced with Ω_d approach $Z_{meas}(\zeta)$. This naturally motivates us to define a least square cost functional

$$\mathcal{J}(\Omega_d) = \int_{z_{\min}}^{z_{\max}} |Z(\Omega_d; \zeta) - Z_{meas}(\zeta)|^2 d\zeta \quad (2.33)$$

and apply the shape optimization method to minimize it. To obtain the gradient of the cost functional $\mathcal{J}(\Omega_d)$, one should compute its shape derivative

$$\mathcal{J}'(\theta) = \int_{z_{\min}}^{z_{\max}} 2\Re(Z'(\theta) \overline{(Z(\Omega_d; \zeta) - Z_{meas}(\zeta))}) d\zeta,$$

$Z'(\theta)$ (which is either $Z'_{FA}(\theta)$ or $Z'_{F3}(\theta)$ according to the measuring mode) is a linear combination of $\Delta Z'_{kl}$ where according to (2.27)

$$\begin{aligned} \Delta Z'_{kl}(\theta) &= \frac{2\pi}{i\omega I^2} \int_{\Gamma} \frac{(\theta \cdot n)}{r} \left\{ \left[\frac{1}{\mu} \right] \nabla_{\tau} w_k \cdot \nabla_{\tau} (\bar{p}_l - w_l^0) \right. \\ &\quad \left. - [\mu] (\mu^{-1} \partial_n w_k) \left((\mu^0)^{-1} (\partial_n \bar{p}_l)_+ - (\mu^0)^{-1} \partial_n w_l^0 \right) - i\omega[\sigma] w_k (\bar{p}_l - w_l^0) \right\} ds, \end{aligned}$$

where w_k and w_l^0 are as defined in Section 2.1 and where the adjoint state p_l is the solution of (2.25) with $w^0 = w_l^0$.

The shape derivative of the cost functional \mathcal{J} can be written as

$$\mathcal{J}'(\Omega_d)(\theta) = \frac{2\pi}{\omega I^2} \int_{\Gamma} (n \cdot \theta) g \, ds,$$

where according to the measuring mode

$$g = \begin{cases} g_{11} + g_{21} & \text{absolute mode,} \\ g_{11} - g_{22} & \text{differential mode,} \end{cases}$$

with

$$g_{kl} = \int_{z_{\min}}^{z_{\max}} \Re \left\{ \overline{(Z(\Omega_d; \zeta) - Z_{meas}(\zeta))} \frac{1}{r} \left(\begin{bmatrix} 1 \\ \mu \end{bmatrix} \nabla_{\tau} w_k \cdot \nabla_{\tau} (\bar{p}_l - w_l^0) - [\mu](\mu^{-1} \partial_n w_k) \left(\frac{1}{\mu^0} (\partial_n \bar{p}_l)_+ - \frac{1}{\mu^0} \partial_n w_l^0 \right) - i\omega[\sigma] w_k (\bar{p}_l - w_l^0) \right) \Big|_{\zeta} \right\} d\zeta. \quad (2.34)$$

We remark in particular that if one choose θ such that

$$\theta = -\gamma g n \quad \text{on } \Gamma, \quad (2.35)$$

where γ is a positive constant, then

$$\mathcal{J}'(\Omega_d)(\theta) = -\gamma \frac{2\pi}{\omega I^2} \int_{\Gamma} |g|^2 \, ds \leq 0.$$

This means that $\mathcal{J}(\Omega_{d\theta}) \leq \mathcal{J}(\Omega_d)$ for γ sufficiently small.

2.3.2 Regularization of the descent direction

For an arbitrary parametrization of Ω_d , a regularization of the descent direction is in general needed since the shape increment given by (2.35) may cause singularity on Γ (see the numerical experiments below). We propose to use the $H^1(\Gamma)$ boundary regularization by solving the following problem for $\lambda \in H^1(\Gamma)^2$:

$$\lambda - \alpha \Delta_{\tau} \lambda = \theta \quad \text{on } \Gamma, \quad (2.36)$$

where Δ_{τ} is the boundary Laplace-Beltrami operator and $\alpha > 0$ is a regularization parameter. The equivalent variational formulation of (2.36) is,

$$\forall \psi \in H^1(\Gamma)^2 \quad \int_{\Gamma} (\lambda \cdot \psi + \alpha \nabla_{\tau} \lambda \cdot \nabla_{\tau} \psi) \, ds = \int_{\Gamma} \theta \cdot \psi \, ds. \quad (2.37)$$

Therefore, λ is two order more regular than θ . It is also a descent direction since

$$\mathcal{J}'(\Omega_d)(\lambda) = -\frac{2\pi}{\gamma \omega I^2} \int_{\Gamma} (|\lambda|^2 + \alpha |\nabla_{\tau} \lambda|^2) \, ds \leq 0. \quad (2.38)$$

2.3.3 Inversion algorithm

The inversion procedure is done as follows:

- Initialization with a deposit domain Ω_d^0 .
- Step k :
 1. Solve the direct problems (2.6) for the different positions ζ of the coils using the deposit shape Ω_d^k and test the stopping rule

$$\mathcal{J}(\Omega_d^k) \leq \delta \int_{z_{\min}}^{z_{\max}} |Z_{meas}(\zeta)|^2 d\zeta$$

where δ is a chosen threshold.

2. Solve the adjoint problems (2.25) for the different coil positions and for the deposit shape Ω_d^k then evaluate the corresponding g .
3. Get a regularized descent direction λ^k (see (2.36) or (2.37)). The parameter γ in (2.35) is evaluated at the first step ($k = 1$) such that $\gamma \max g \leq \epsilon$ where ϵ is a chosen threshold, then it is kept fixed for next iterations.
4. Go to step $k + 1$ with a deposit domain

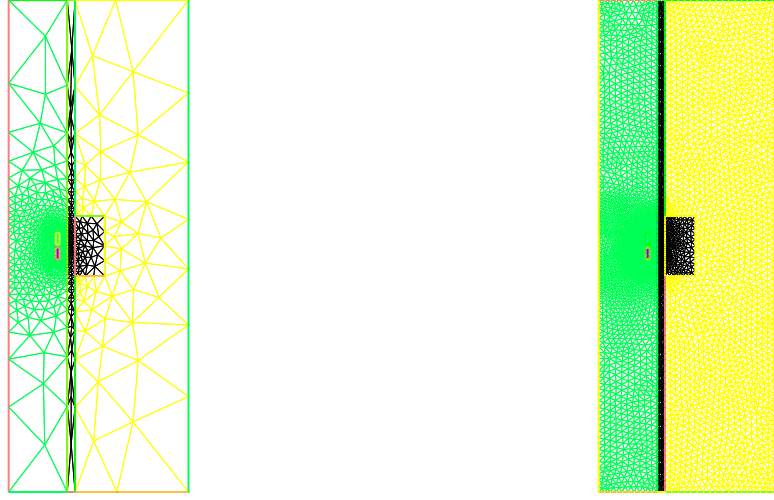
$$\Omega_d^{k+1} = (\text{Id} + \lambda^k)\Omega_d^k.$$

2.3.4 Numerical tests

We shall consider here some numerical inversion tests for deposits for geometrical configurations depicted in Figure 2.1. The physical parameters are close to real experiments and are as follows:

- The tube is defined by $\Omega_t = \{(r, z) : r_{t_1} \leq r \leq r_{t_2}\}$ with $r_{t_1} = 9.84mm$, Its conductivity is $\sigma_t = 9.7 \times 10^5 S/m$ and its magnetic permeability is $\mu_t = 1.01\mu_v$, where μ_v is the permeability of vacuum.
- The deposit has in general a relatively low conductivity: $\sigma_d = 1 \times 10^4 S/m$. It can be magnetic: permeability $\mu_d = 10\mu_v$ or non-magnetic: $\mu_d = \mu_v$.
- The operating frequency for the coils is $\omega = 100kHz$, the dimensions of one coil are $0.67mm$ in length (radial direction) and $2mm$ in height (axial direction). Both the two coils are located $7.83mm$ away from the z -axis and there is a distance of $0.5mm$ between them.

The numerical forward problem is set on a bounded domain B_{r_*, z_*} with $r_* = 30mm$ and $z_* = 41mm$. It is solved using *FreeFem++* with P1 finite elements and an adapted mesh (using the command `adaptmesh`). The number of degrees of freedom is around 1000 (see Figure 2.3a). To avoid “crime inverse”, we use a refined mesh to generate the impedance measurements as given observation data (see Figure 2.3b). The number of degrees of freedom of P1 finite element on this mesh is about 6000.



(a) adapted mesh for forward problem in inverse algorithm (b) refined mesh for generating observation data

Figure 2.3: Examples of mesh.

For the inversion we use impedance measurements either in the pseudo-absolute mode (FA) or in the differential mode (F3). The number of used vertical positions will be specified for each experiment. The algorithm parameters for the stopping rule and the increment magnitude are set to $\delta = 10^{-4}$ and $\epsilon = 5 \times 10^{-4}$.

Finally let us note that in all subsequent figures, the target deposit shape is shown in green while the reconstructed shape using the inverse algorithm is in red.

Parameterized shape reconstruction

Non-magnetic deposits We first consider a non-magnetic deposit. We assume that the deposit is rectangular in the semi-plan \mathbb{R}_+^2 . Then its shape can be parameterized by its thickness in the r -direction and the positions in the z -direction of its two horizontal sides. The target shape has $5mm$ in thickness, and its horizontal sides are at $\pm 5mm$.

In Figure 2.4 the only unknown parameter is the thickness of the rectangular deposit. We use the FA signal at only one probe position for the reconstructions. We initialize the inverse algorithm with either a small guess (Figure 2.4a) or a large one (Figure 2.4c). The reconstruction resulting from the small initialization after 108 iterations is shown in Figure 2.4b. We also observe the decrease of the cost functional as well as those of the gradient (in absolute value) and of the thickness relative error during the iteration in Figure 2.4e. Figure 2.4d gives the reconstruction result from the large guess initialization after 14 iterations. Figure 2.4f show the similar decrease behavior of the cost functional, the gradient and the thickness relative error during iterations.

To reconstruct both the thickness and the two vertical positions of the horizontal sides of the rectangular deposit, we use either FA or F3 signals at 41 probe positions with a distance of $1mm$

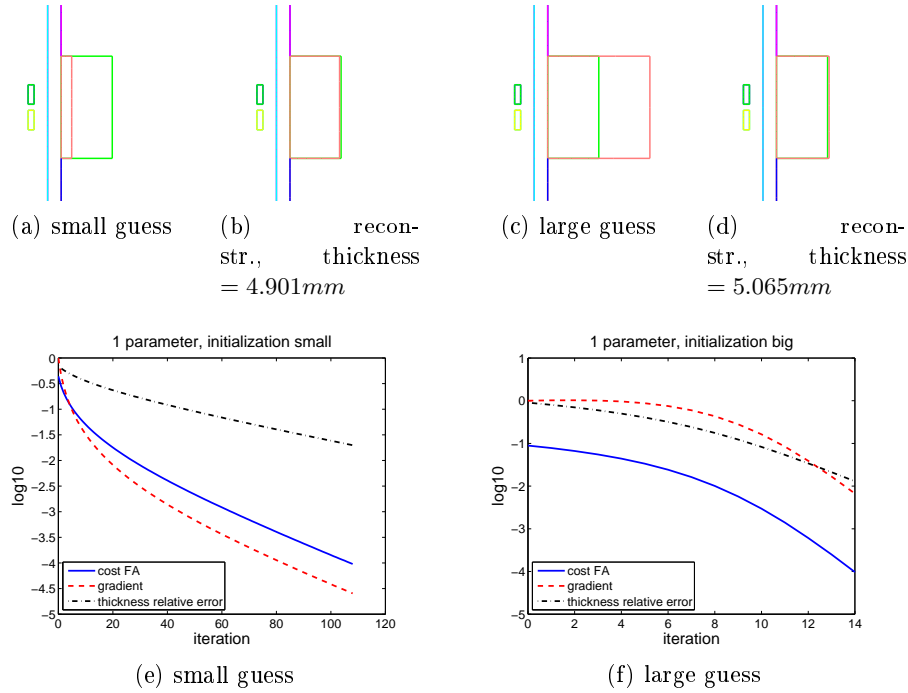
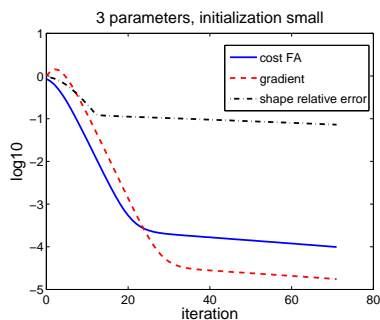
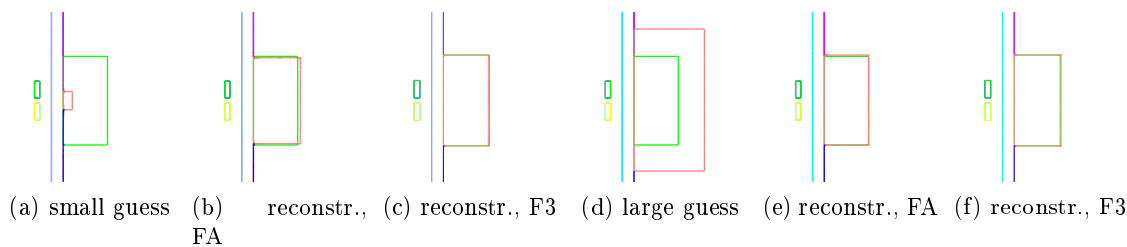


Figure 2.4: Results of thickness reconstruction of a rectangular non-magnetic deposit.

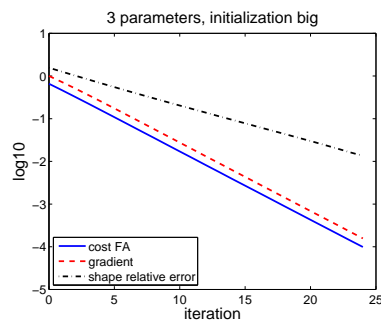
between two neighboring positions. Figure 2.5 and Table 2.1 show the results. We initialize the inverse algorithm with either a small guess (Figure 2.5a) or a large one (Figure 2.5d). The result from the small guess using FA signal after 71 iterations is shown in Figure 2.5b, and that using F3 signal after 43 iterations is shown in Figure 2.5c. From a large guess, we get the reconstruction result in Figure 2.5e using FA signal after 24 iterations, and that in Figure 2.5e using F3 signal after 112 iterations. In Figures 2.5g, 2.5h, 2.5i and 2.5j we observe the decrease of the cost functional and the gradient (in absolute value) during iterations. However, the decrease of the shape relative error (the difference of the characteristic functions of the target deposit domain and the reconstructed domain, taking in L^2 norm) may stagnate around 10%, which means that the information from the impedance measurements is no longer sufficient to distinguish the reconstructed shape from the target shape.

	thickness	vertical position 1	vertical position 2
target shape	5mm	5mm	-5mm
from small guess, FA	5.236mm	4.872mm	-4.870mm
from small guess, F3	4.882mm	5.017mm	-5.017mm
from large guess, FA	5.015mm	5.041mm	-5.039mm
from large guess, F3	5.123mm	4.983mm	-4.982mm

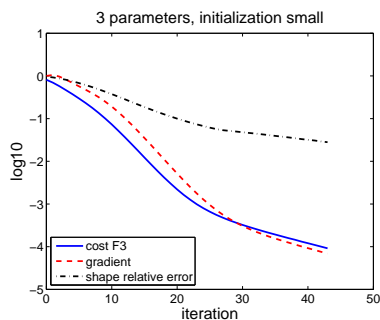
Table 2.1: Parameter reconstructions of a rectangular non-magnetic deposit.



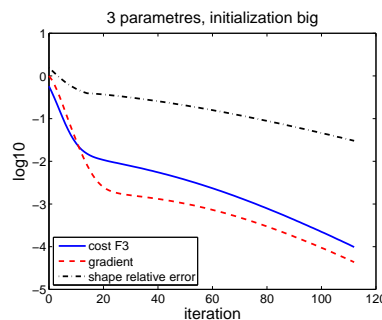
(g) small guess, FA



(h) large guess, FA



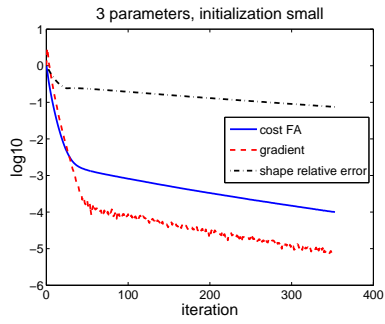
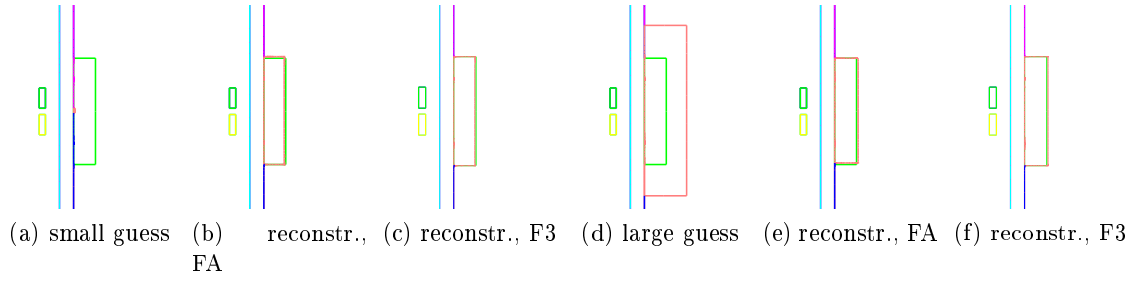
(i) small guess, F3



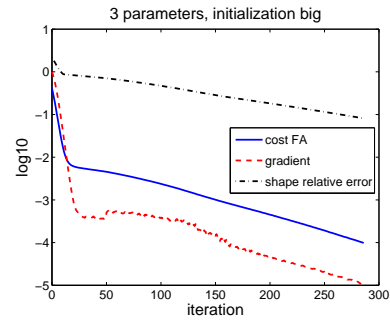
(j) large guess, F3

Figure 2.5: Parameter reconstructions of a rectangular non-magnetic deposit.

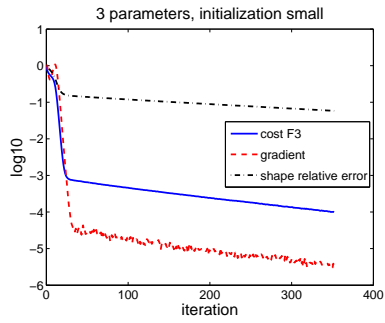
Magnetic deposits We consider here the reconstruction of the three parameters (thickness and two vertical positions of the horizontal sides) of a rectangular magnetic deposit: see Figure 2.6 and Table 2.2. With a small rectangle as initial guess (Figure 2.6a) we get the result in Figure 2.6b after 353 iterations with the FA signal and that in Figure 2.6c after 352 iterations using the F3 signal. While the inversion algorithm beginning from a large initial guess (Figure 2.6d) gives the result either shown in Figure 2.6e after 286 iterations using FA signal or in Figure 2.6f after 462 iterations using F3 signal. The decreasing behavior of the cost functional, the absolute value of the gradient and the relative error of the deposit shape is shown in Figures 2.6g, 2.6h, 2.6i and 2.6j for the four reconstructions respectively.



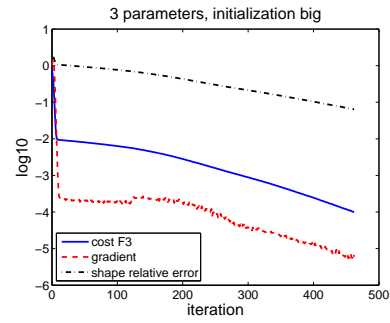
(g) small guess, FA



(h) large guess, FA



(i) small guess, F3



(j) large guess, F3

Figure 2.6: Parameter reconstructions of a rectangular magnetic deposit.

	thickness	vertical position 1	vertical position 2
target shape	$2mm$	$5mm$	$-5mm$
from small guess, FA	$1.875mm$	$5.068mm$	$-5.062mm$
from small guess, F3	$1.887mm$	$4.992mm$	$-4.992mm$
from large guess, FA	$2.138mm$	$4.934mm$	$-4.941mm$
from large guess, F3	$2.124mm$	$5.009mm$	$-5.007mm$

Table 2.2: Parameter reconstructions of a rectangular magnetic deposit.

Reconstruction of deposits with arbitrary shapes

In this section we consider the reconstruction of the deposit without *a priori* knowledge on its shape.

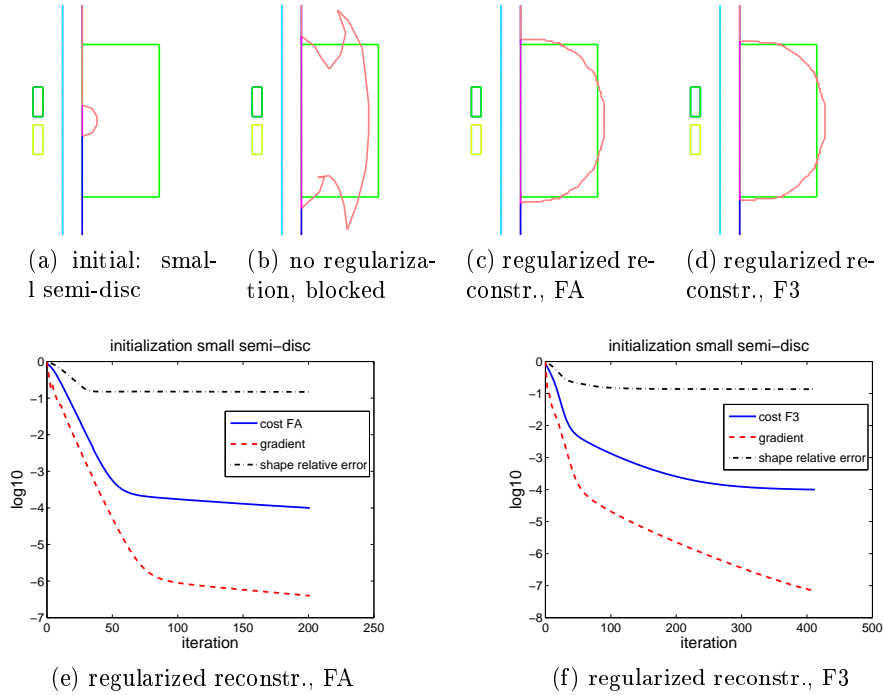


Figure 2.7: Reconstruction of a rectangular non-magnetic deposit.

In Figure 2.7 the target non-magnetic deposit shape is a rectangle. Since we do not have any information of the shape, we take a small semi-disc as the initial guess in the inversion algorithm. We use either FA or F3 signals for inversion at 41 probe positions with a distance of 1mm between each two neighboring positions. The algorithm without boundary regularization using FA signal is blocked due to singularities on the interface between the deposit and the vacuum (Figure 2.7b).

To regularize the gradient using the method in Section 2.3.2, we take $\alpha = 1 \times 10^{-5}$ as the regularization parameter in the boundary regularization problem (2.36). The regularized algorithm using FA signals ends after 201 iterations with a good estimate (Figure 2.7c) and that using F3 signals gives the result shown in Figure 2.7d after 412 iterations. We also show in Figures 2.7e and 2.7f the decrease of the cost functional, the absolute value of gradient and the relative error on the shape during iterations.

In Figure 2.8 we show the reconstructions of a non-magnetic semi-disc issued from different initial shapes (Figures 2.8a or 2.8c) using FA signals. The corresponding reconstruction results shown in Figure 2.8b (37 iterations) and in Figure 2.8d (52 iterations) for the non-magnetic deposits are satisfying, as we can observe the decrease of the cost functional, the absolute value of the gradient and the shape relative error in Figures 2.8e and 2.8f.

Finally Figure 2.9 shows the reconstruction of a non convex deposit shape using differential mode (F3) impedance signals. For the non-magnetic deposit (Figures 2.9a – 2.9b), we choose the stopping threshold $\delta = 4 \times 10^{-4}$ (which means a 2% relative error of impedance measurements) and the algorithm ends after 145 iterations. For the magnetic deposit (Figures 2.9c – 2.9d), with $\delta = 9 \times 10^{-4}$ (a 3% relative error of impedance measurements), the algorithm ends after

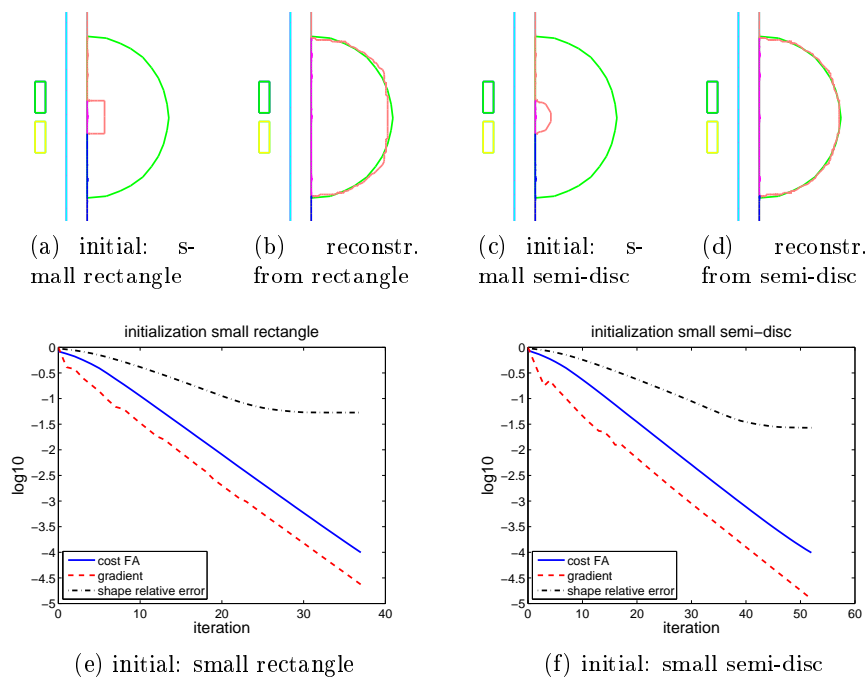


Figure 2.8: Reconstruct some non-magnetic deposit in semi-disc shape.

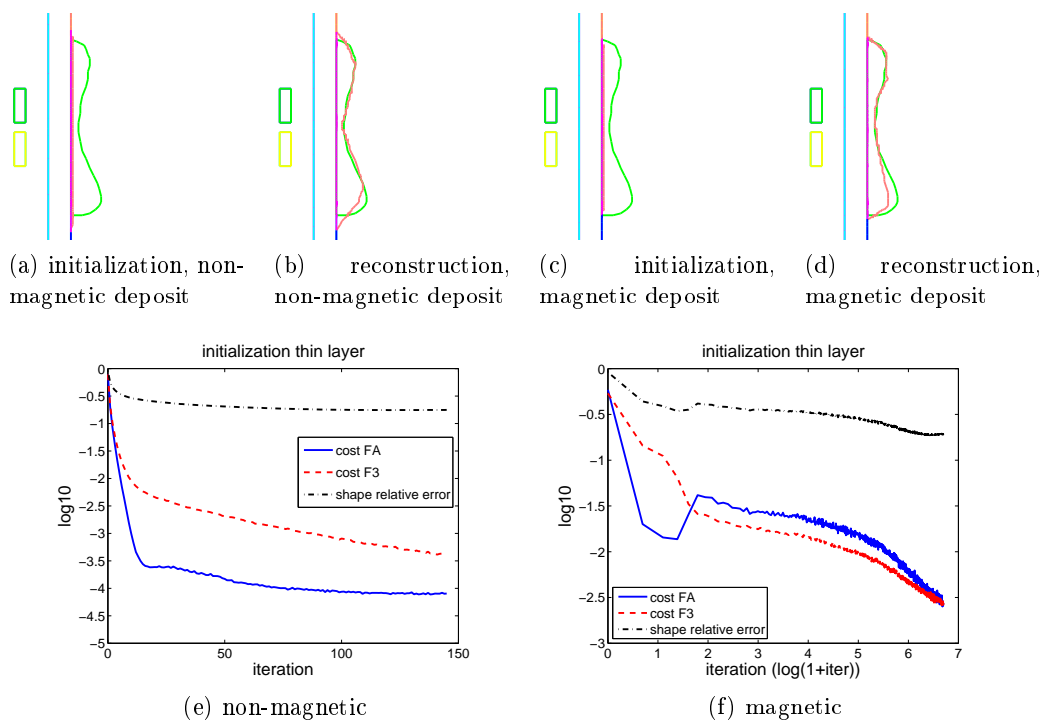


Figure 2.9: Reconstruction of a deposit with a non convex shape.

810 iterations.

2.4 On the reconstruction of the deposit conductivity and permeability

The conductivity and the permeability are the two critical physical parameters which characterize the material nature of the deposit. The exact values of these parameters, crucial for the modeling, the simulation and the reconstruction of the deposit is usually not known with a high precision in the industrial context. In this section we discuss the reconstruction of these parameters for known shapes. The simultaneous reconstruction of the parameters and the shape is discussed in the last section.

2.4.1 The cost functional derivative with respect to the conductivity

We consider the variational formulation of the eddy current problem (2.6). We denote by δw the variation of w due to a small increment of the conductivity $\sigma_d \rightarrow \sigma_d + \delta\sigma_d$ of the deposit that is assumed to be constant. Therefore, we have $\forall \varphi \in \tilde{H}(\Omega)$:

$$\int_{\Omega} \left(\frac{1}{\mu r} \nabla(w + \delta w) \cdot \nabla \bar{\varphi} - \frac{i\omega(\sigma + \delta\sigma_d \chi_{\Omega_d})}{r} (w + \delta w) \bar{\varphi} \right) dr dz = \int_{\Omega} i\omega J \bar{\varphi} dr dz,$$

where χ_{Ω_d} is the index function of the domain Ω_d . After developing this formulation, the terms of order zero of the variation give the original problem (2.6). We denote by $(\partial_{\sigma} w)$ the derivative of w with respect to σ_d :

$$\partial_{\sigma} w := \lim_{\delta\sigma_d \rightarrow 0} \delta w / \delta\sigma_d$$

where the limit holds in $\tilde{H}(\Omega)$. Then the terms of first order of the variation in the above formulation as $\delta\sigma_d$ goes to zero imply

$$\int_{\Omega} \left(\frac{1}{\mu r} \nabla(\partial_{\sigma} w) \cdot \nabla \bar{\varphi} - \frac{i\omega\sigma}{r} (\partial_{\sigma} w) \bar{\varphi} \right) dr dz = \int_{\Omega_d} \frac{i\omega}{r} w \bar{\varphi} dr dz. \quad (2.39)$$

Now we consider the impedance measurement given by (2.5). We denote by $\partial_{\sigma}(\Delta Z_{kl})$ its derivative with respect to σ_d . Then we have

$$\partial_{\sigma}(\Delta Z_{kl}) = \frac{2\pi}{i\omega I^2} \int_{\Omega_d} \left(\left(\frac{1}{\mu} - \frac{1}{\mu^0} \right) \frac{\nabla(\partial_{\sigma} w_k) \cdot \nabla w^0}{r} - i\omega(\sigma - \sigma^0) \frac{(\partial_{\sigma} w_k) w^0}{r} - i\omega \frac{w_k w^0}{r} \right) dr dz. \quad (2.40)$$

Similarly, we denote by $\partial_{\sigma} \mathcal{J}$ the derivative of the cost functional \mathcal{J} given by (2.33) with respect to the variation of σ_d . We get

$$\partial_{\sigma} \mathcal{J} = \int_{z_{\min}}^{z_{\max}} 2\Re \left\{ \partial_{\sigma} Z(\Omega_d; \zeta) \overline{(Z(\Omega_d; \zeta) - Z_{meas}(\zeta))} \right\} d\zeta, \quad (2.41)$$

where according to the impedance measuring mode,

$$\partial_\sigma Z(\Omega_d; \zeta) = \begin{cases} \partial_\sigma Z_{FA} = \frac{i}{2}(\partial_\sigma(\Delta Z_{11}) + \partial_\sigma(\Delta Z_{21})), \\ \partial_\sigma Z_{F3} = \frac{i}{2}(\partial_\sigma(\Delta Z_{11}) - \partial_\sigma(\Delta Z_{22})). \end{cases}$$

To minimize the cost functional with respect to σ_d we shall use a descent gradient method based of a numerical evaluation of the derivative provided by (2.41).

2.4.2 Derivative with respect to the magnetic permeability

Similarly to the previous section, we consider here a small increment of the deposit magnetic permeability $\mu_d \rightarrow \mu_d + \delta\mu_d$ which leads to a small variation of the field $w \rightarrow \delta w$. Then from (2.6) we derive

$$\int_\Omega \left(\frac{1}{(\mu + \delta\mu_d \chi_{\Omega_d})r} \nabla(w + \delta w) \cdot \nabla \bar{\varphi} - \frac{i\omega\sigma}{r}(w + \delta w)\bar{\varphi} \right) dr dz = \int_\Omega i\omega J \bar{\varphi} dr dz.$$

If we denote by

$$\partial_\mu w := \lim_{\delta\mu_d \rightarrow 0} \delta w / \delta\mu_d,$$

where the limit is understood with respect the $\tilde{H}(\Omega)$ norm, then one easily verify that $\partial_\mu w$ satisfies $\forall \varphi \in \tilde{H}(\Omega)$

$$\int_\Omega \left(\frac{1}{\mu r} \nabla(\partial_\mu w) \cdot \nabla \bar{\varphi} - \frac{i\omega\sigma}{r}(\partial_\mu w)\bar{\varphi} \right) dr dz = \int_{\Omega_d} \frac{1}{\mu^2 r} \nabla w \cdot \nabla \bar{\varphi} dr dz. \quad (2.42)$$

Then the derivative of the impedance measurement ΔZ_{kl} with regard to the deposit magnetic permeability, which we denote by $\partial_\mu \Delta Z_{kl}$, is given by the following expression:

$$\partial_\mu(\Delta Z_{kl}) = \frac{2\pi}{i\omega I^2} \int_{\Omega_d} \left(\left(\frac{1}{\mu} - \frac{1}{\mu^0} \right) \frac{\nabla(\partial_\mu w_k) \cdot \nabla w_l^0}{r} - i\omega(\sigma - \sigma^0) \frac{(\partial_\mu w_k)w_l^0}{r} - \frac{1}{\mu^2 r} \nabla w_k \cdot \nabla w_l^0 \right) dr dz. \quad (2.43)$$

If $\partial_\mu \mathcal{J}$ represents the derivative of the cost functional \mathcal{J} with respect to the variation of μ_d , then from (2.33),

$$\partial_\mu \mathcal{J} = \int_{z_{\min}}^{z_{\max}} 2\Re \left\{ \partial_\mu Z(\Omega_d; \zeta) \overline{(Z(\Omega_d; \zeta) - Z_{meas}(\zeta))} \right\} d\zeta, \quad (2.44)$$

where according to the impedance measurement mode,

$$\partial_\mu Z(\Omega_d; \zeta) = \begin{cases} \partial_\mu Z_{FA} = \frac{i}{2}(\partial_\mu(\Delta Z_{11}) + \partial_\mu(\Delta Z_{21})), \\ \partial_\mu Z_{F3} = \frac{i}{2}(\partial_\mu(\Delta Z_{11}) - \partial_\mu(\Delta Z_{22})). \end{cases}$$

To minimize the cost functional with respect to μ_d we shall also use a descent gradient method based of a numerical evaluation of the derivative provided by (2.44).

2.4.3 Numerical tests

Reconstruction of conductivity

We consider the reconstruction of the conductivity of a non-magnetic deposit ($\mu_d = \mu_v$) with $\sigma_d = 1 \times 10^4 S/m$ in a known shape (a $5mm \times 10mm$ rectangle) at the shell side of the tube. We initialize the inversion algorithm with either a small guess of the conductivity ($5 \times 10^3 S/m$) or a large guess ($3 \times 10^4 S/m$). The reconstruction results using FA signals at one probe position are given in Figure 2.10.

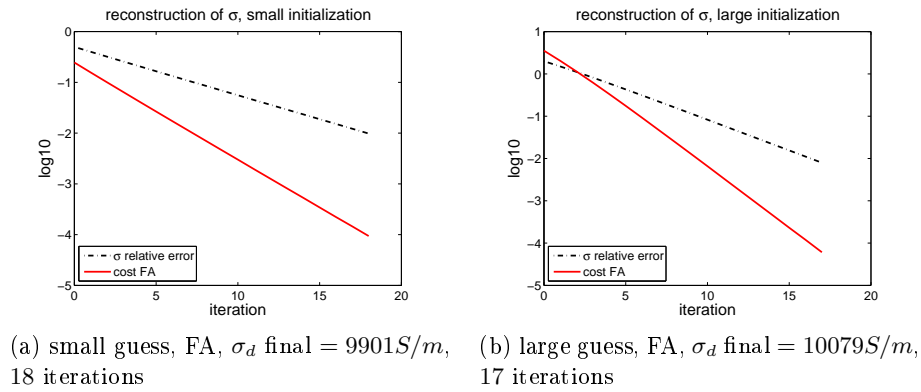


Figure 2.10: Reconstruction of the conductivity.

Reconstruction of magnetic permeability

We want to find here the magnetic permeability of a magnetic deposit with $\sigma_d = 1 \times 10^4 S/m$, $\mu_d = 10\mu_v$ and in a known shape (a $2mm \times 10mm$ rectangle) at the shell side of the tube. We initialize the inversion algorithm with either a small guess of the magnetic permeability ($2\mu_v$) or a large guess ($15\mu_v$). The reconstruction results using FA signals at one probe position are given in Figure 2.11.

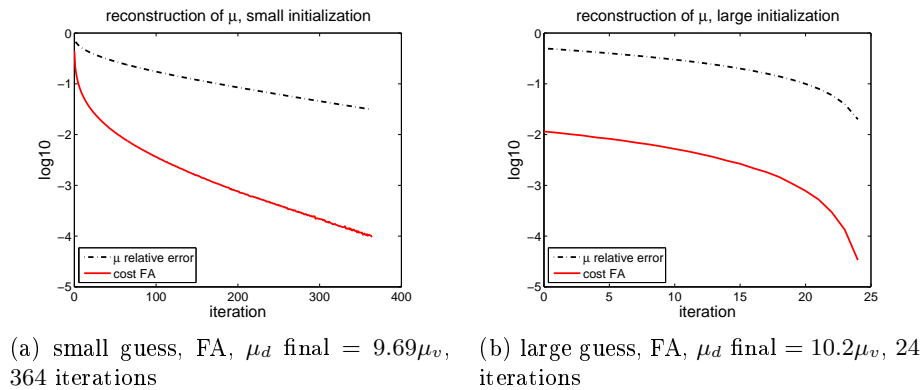


Figure 2.11: Reconstruct of magnetic permeability.

Simultaneous reconstruction of conductivity and the magnetic permeability

We try to reconstruct here both the conductivity and the magnetic permeability with FA signals at one probe position. The conductivity and the magnetic permeability of the target rectangular deposit ($2\text{mm} \times 10\text{mm}$) are respectively $\sigma_t = 1 \times 10^4 \text{S/m}$, $\mu_t = 10\mu_v$. The initialization of these two parameters can be either small or large. The results are shown in Figure 2.12 and Table 2.3.

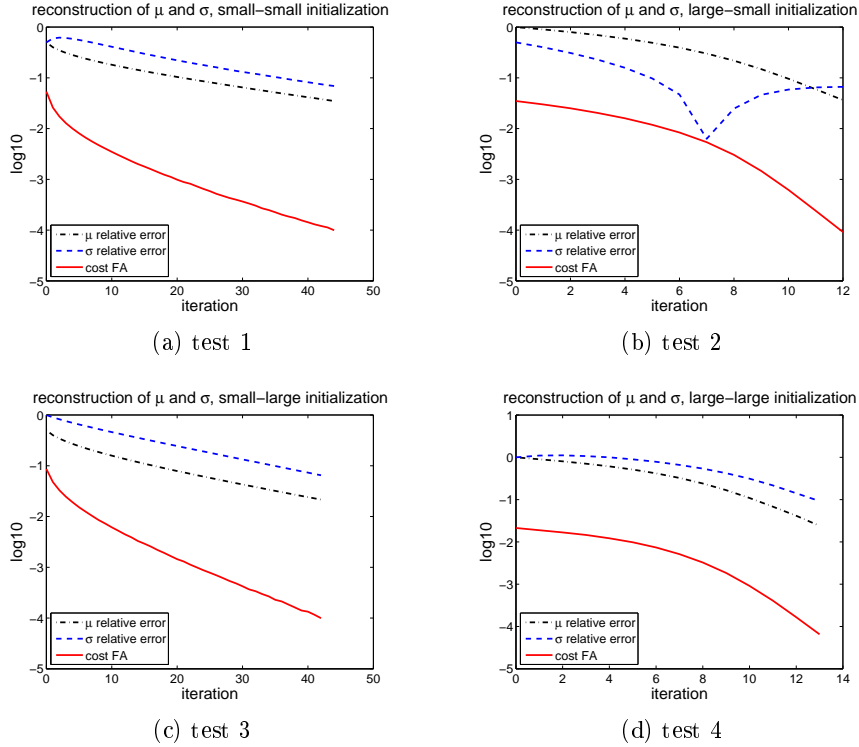


Figure 2.12: Reconstruction of both the conductivity and the magnetic permeability using FA signals.

	initial guess	reconstructed	number of iterations
target deposit		(10000, 10)	
test 1	(5000, 5)	(9309, 9.65)	44
test 2	(5000, 20)	(10666, 10.37)	12
test 3	(20000, 5)	(10649, 9.78)	42
test 4	(20000, 20)	(10921, 10.24)	13

Table 2.3: Reconstruction of the conductivity and the relative magnetic permeability ($\sigma_d(\text{S/m}), \mu_d$) using FA signals.

We observe that the reconstruction results are not accurate even if the normalized cost func-

tional is under 10^{-4} . This is explained by the extremely low dependence of the cost functional with respect to simultaneous variations of the two parameters. This is clearly indicated by Figure 2.13. We hence conclude that these eddy-current measurements are not really suited to determine physical parameters.

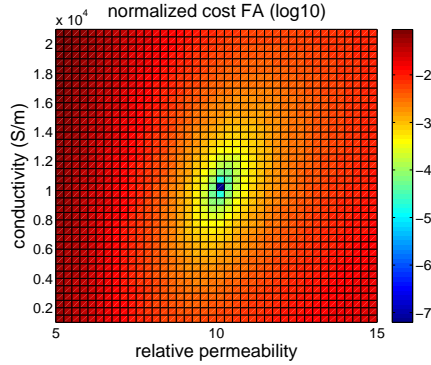


Figure 2.13: Interference between conductivity and magnetic permeability.

2.5 On the reconstruction of the shape and physical parameters

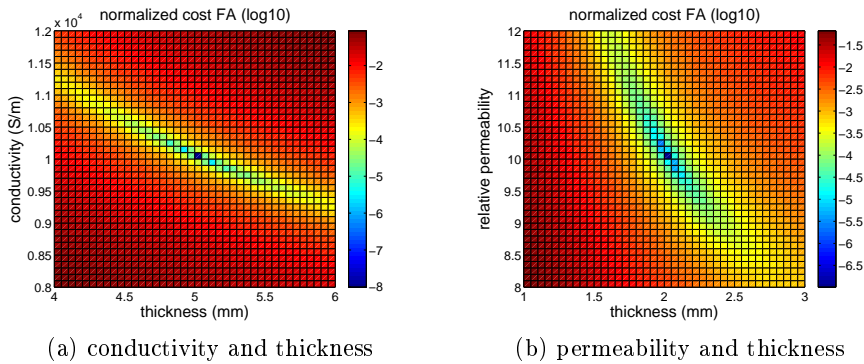


Figure 2.14: Interference between physical parameters and shape parameter.

We would like to discuss here the possibility of reconstructing simultaneously the conductivity (or the magnetic permeability) and the shape of the deposit by coupling the inversion algorithm for shape reconstruction in Section 2.3.3 and that for conductivity (magnetic permeability) reconstruction. We consider the most simple cases in which the deposit shape is a rectangle with unknown thickness but with fixed horizontal sides.

In the first case with unknown conductivity and thickness, the target deposit is a $5\text{mm} \times 10\text{mm}$ rectangle with the $\sigma_d = 10^4\text{S/m}$ and $\mu_d = \mu_v$. For rectangular deposits with the range of thickness from 4mm to 6mm and the range of conductivity from $8 \times 10^3\text{S/m}$ to $1.2 \times 10^4\text{S/m}$, we show in Figure 2.14a the value (in \log_{10}) of the cost functional of the absolute mode impedance measurements (FA) normalized with regard to the FA impedance measurement of the target

deposit.

In the second case where the magnetic permeability and the thickness are to reconstruct, the target deposit is a $2mm \times 10mm$ rectangle with $\sigma_d = 10^4 S/m$ and $\mu_d = 10\mu_v$. For rectangular deposits with the range of thickness from $1mm$ to $3mm$ and the range of relative magnetic permeability from 8 to 12, we show similarly the normalized cost functional for FA signals in Figure 2.14b.

In both two cases the interferences between the physical parameters and the geometrical parameter (the thickness) are too important to hope obtaining a precise reconstruction. For instance, $\sigma = 0.95 \times 10^4 S/m$ and a thickness = $5.6mm$ would lead to a relative magnitude of the cost functional of order 10^{-4} which reaches the stopping threshold of the inversion algorithm. Similarly, $\mu = 0.95\mu_v$ and a thickness = $2.2mm$ would lead to a relative magnitude of the cost functional of order 10^{-4} .

	$\sigma(S/m)$	μ/μ_v	initial guess	reconstruction
target deposit	1×10^4	10	$2mm$	
test 1	0.98×10^4	10	$0.5mm$	$1.91mm$
test 2	0.98×10^4	10	$4mm$	$2.08mm$
test 3	1×10^4	9.8	$0.5mm$	$1.96mm$
test 4	1×10^4	9.8	$4mm$	$2.13mm$

Table 2.4: Reconstruction of thickness of a rectangular deposit with wrong values of the conductivity or the magnetic permeability using FA signals.

However, with a good initial guess of the conductivity and the permeability, shape reconstruction of deposits yields reasonable results. We observe in Table 2.4 that a small error in σ or in μ (2%) would still lead to accurate reconstruction of deposit shape.

Part II

Asymptotic models for axisymmetric thin copper layers

Some asymptotic models for thin and highly conducting deposits

Contents

3.1 Settings for asymptotic models	82
3.1.1 Rescaled in-layer eddy current model	82
3.1.2 Taylor developments for u_{\pm}^{δ}	83
3.1.3 Transmission conditions between \tilde{u} (or \tilde{w}) and u_{\pm}^{δ}	85
3.1.4 Procedure for obtaining approximate transmission conditions $\mathcal{Z}_{m,n}$ between u_{\pm}^{δ}	86
3.2 Asymptotic models for deposits with constant thickness	86
3.2.1 Rescaling of the in-layer problem	86
3.2.2 Transmission conditions between \tilde{u} (or \tilde{w}) and u_{\pm}^{δ}	88
3.2.3 Computing algorithm for the rescaled in-layer field \tilde{u} (or \tilde{w})	90
3.2.4 Computation of some approximate transmission conditions $\mathcal{Z}_{m,n}$	92
3.2.5 Numerical tests for 1-D models	102

Other than deposits such as the magnetite which have a relatively comparable electrical conductivity to that of the SG tube, it is also possible that some thin layer of copper deposit covers the shell side of the tube and therefore modify the eddy current signal. These deposits are characterized by a very high conductivity (as compared to SG tubes) and a very small thickness, see Table 3.1. This type of deposits does not directly effect the safety of SG. However their presence may mask other type of problematic faults such as cracks. This is why it is important to be able to detect them.

	tube wall	copper layer
conductivity (in $S \cdot m^{-1}$)	$\sigma_t = 0.97 \times 10^6$	$\sigma_c = 58.0 \times 10^6$
thickness (in mm)	$r_{t_2} - r_{t_1} = 1.27$	$0.005 \sim 0.1$

Table 3.1: Conductivity and scale differences between tube wall and copper layer.

A major numerical challenge to deal with this problem in the full model is the expensive computing cost resulting from the fact that the domain discretization should use a very fine mesh with the size adapted to the thin layer. To reduce the numerical cost, we replace the thin deposit layer by some transmission conditions using the asymptotic expansion of the solution with respect to the thickness of the deposit. According to the choice of a rescaling parameter

m and the asymptotic expansion order n , we build a family of transmission conditions $\mathcal{Z}_{m,n}$ linking up the solutions at the two sides of the deposit layer. There is a rich literature on asymptotic models. We may refer to Tordeux [82], Claeys [30], Delourme [36], Poignard [71] and the references therein for different approaches and various applications.

The objective of this chapter is to choose the transmission conditions, or the parameters (m, n) , with which the direct asymptotic model not only gives a good approximation of the full model, but also allows us to reduce the inversion cost. For this purpose, we shall consider here a simplified case where the deposit layer has constant thickness, and compute the explicit expressions of $\mathcal{Z}_{m,n}$. We then compare the errors of the asymptotic models using different $\mathcal{Z}_{m,n}$ with regard to the full model via several numerical tests and discuss the appropriate choice of $\mathcal{Z}_{m,n}$.

Although mainly considering here the case of deposit with constant thickness, we shall introduce the asymptotic method for a general shape of the deposit. This will be useful for the next chapter where this case is considered with the appropriate scaling for the conductivities.

3.1 Settings for asymptotic models

3.1.1 Rescaled in-layer eddy current model

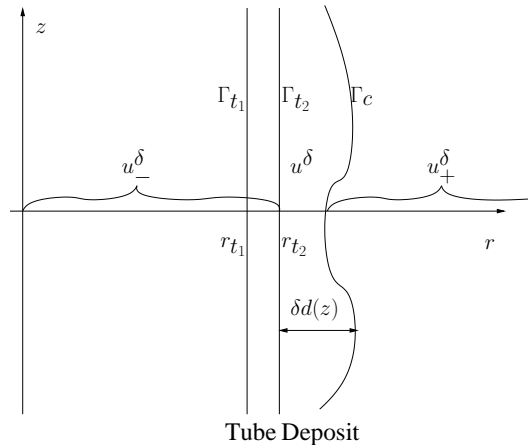


Figure 3.1: Representation of a thin layer deposit.

On the domain of problem Ω , we set

$$\Omega_{\pm} := \{(r, z) \in \Omega : r \gtrless r_{t_2}\}$$

We consider a thin layer of deposit with high conductivity (in our case, a layer of copper) covering axisymmetrically (a part of) the shell side of the tube. The deposit thin layer is depicted by the domain $\Omega_c^{\delta} \subset \Omega_+$. We denote by u_{\pm}^{δ} the electric fields outside the deposit layer, with u_-^{δ} in Ω_- and u_+^{δ} in $\Omega_+ \setminus \Omega_c^{\delta}$ (at the shell side of the deposit layer), and by u^{δ} the in-layer electric field, i.e. in Ω_c^{δ} (see Figure 3.1). We assume that the thickness $f_{\delta}(z)$ at the vertical position z is of the order δ

$$f_{\delta}(z) = \delta d(z),$$

where δ is a small parameter and $d(z)$ is independent of δ . Assuming that the deposit conductivity is of the form

$$\sigma_c = \frac{\sigma_m}{\delta^m} \quad m \in \mathbb{N}, \quad (3.1)$$

where σ_m is an appropriately rescaled conductivity and m is the rescaling parameter. We will particularly interest in the cases where $m = 0, 1, 2$. Therefore, the eddy current equation in the deposit layer writes

$$-\operatorname{div} \left(\frac{1}{\mu_c r} \nabla(ru) \right) - i\omega \frac{\sigma_m}{\delta^m} u = 0 \quad \text{on } \Omega_c^\delta \quad (3.2)$$

We rescale also the distance dimension in the direction r to represent the thin layer

$$\rho = \frac{r - r_{t_2}}{\delta}, \quad \rho \in [0, d(z)],$$

and we denote by $\tilde{u} = \tilde{u}(\rho, z) := u^\delta(r_{t_2} + \delta\rho, z)$ the rescaled in-layer solution.

3.1.2 Taylor developments for u_+^δ

We would like to extend the solution outside the deposit layer u_+^δ through the layer domain till the interface Γ_{t_2} , i.e. from $\Omega_+ \setminus \Omega_c^\delta$ to Ω_+ , such that the transmission conditions on Γ_c between u and u_+^δ could be expressed by terms of u_+^δ on Γ_{t_2} . As u_+^δ satisfies the eddy current equation with coefficients $\mu = \mu_v$ and $\sigma = \sigma_v = 0$ in $\Omega_+ \setminus \Omega_c^\delta$, it is natural to assume that its extension to Ω_c^δ satisfies the same equation

$$-\operatorname{div} \left(\frac{1}{\mu_v r} \nabla(ru_+^\delta) \right) = 0 \quad \text{in } \Omega_+.$$

Using the variable substitution $\nu = r - r_{t_2}$, one rewrites the above equation in the following form

$$\sum_{j=0}^4 \nu^j \mathcal{A}_j(\nu\partial_\nu, \partial_z) u_+^\delta = 0, \quad (3.3)$$

where

$$\begin{aligned} \mathcal{A}_0(\nu\partial_\nu, \partial_z) &= (\nu\partial_\nu)^2 - \nu\partial_\nu, \\ \mathcal{A}_1(\nu\partial_\nu, \partial_z) &= \frac{2}{r_{t_2}} (\nu\partial_\nu)^2 - \frac{1}{r_{t_2}} \nu\partial_\nu, \\ \mathcal{A}_2(\nu\partial_\nu, \partial_z) &= \frac{1}{r_{t_2}^2} (\nu\partial_\nu)^2 - \frac{1}{r_{t_2}^2} + \partial_z^2, \\ \mathcal{A}_3(\nu\partial_\nu, \partial_z) &= \frac{2}{r_{t_2}} \partial_z^2, \\ \mathcal{A}_4(\nu\partial_\nu, \partial_z) &= \frac{1}{r_{t_2}^2} \partial_z^2. \end{aligned}$$

The asymptotic expansion of u_+^δ with respect to δ is in the form

$$u_+^\delta(r, z) = \sum_{n=0}^{\infty} \delta^n u_+^n(r, z).$$

Obviously each term $u_+^n(r, z)$ verifies the same equation (3.3). With Taylor series expansion, one has

$$u_+^n(r_{t_2} + \nu, z) = \sum_{k=0}^{\infty} \nu^k u_+^{n,k}(z) \quad \text{where} \quad u_+^{n,k}(z) = \frac{1}{k!} \left(\partial_\nu^k u_+^n \right) (r_{t_2}, z).$$

Since

$$\nu \partial_\nu \left(\nu^k u_+^{n,k}(z) \right) = k \left(\nu^k u_+^{n,k}(z) \right),$$

we can indeed write $\mathcal{A}_i(\nu \partial_\nu, \partial_z)$ as $\mathcal{A}_i(k, \partial_z)$ while it is applied to $\left(\nu^k u_+^{n,k}(z) \right)$. Thus, from (3.3)

$$\sum_{j=0}^4 \sum_{k=0}^{\infty} \mathcal{A}_j(k, \partial_z) (\nu^{k+j} u_+^{n,k}) = 0.$$

The equality at order $\mathcal{O}(\nu^k)$ gives

$$\mathcal{A}_0(k, \partial_z) u_+^{n,k} = - \sum_{j=1}^4 \mathcal{A}_j(k-j, \partial_z) u_+^{n,k-j},$$

with $u_+^{n,-1} = u_+^{n,-2} = u_+^{n,-3} = u_+^{n,-4} = 0$. Now we consider $\mathcal{A}_0(k, \partial_z) = k^2 - k$. For $k \geq 2$, $\mathcal{A}_0(k, \partial_z) \neq 0$, thus invertible with its inverse $\mathcal{A}_0^{-1}(k, \partial_z) = \frac{1}{k^2 - k}$. So we have

$$u_+^{n,k} = -\mathcal{A}_0^{-1}(k, \partial_z) \left(\sum_{j=1}^4 \mathcal{A}_j(k-j, \partial_z) u_+^{n,k-j} \right), \quad k \geq 2. \quad (3.4)$$

Now we define recurrently two families of operators $\{\mathcal{S}_k^0(\partial_z), \mathcal{S}_k^1(\partial_z)\}$:

$$\begin{aligned} \mathcal{S}_0^0 &:= \text{Id}, & \mathcal{S}_0^1 &:= 0, & \mathcal{S}_1^0 &:= 0, & \mathcal{S}_1^1 &:= \text{Id}, \\ k \geq 2 & \left\{ \begin{array}{l} \mathcal{S}_k^0 := -\mathcal{A}_0^{-1}(k, \partial_z) \left(\sum_{j=1}^4 \mathcal{A}_j(k-j, \partial_z) \mathcal{S}_{k-j}^0(\partial_z) \right), \\ \mathcal{S}_k^1 := -\mathcal{A}_0^{-1}(k, \partial_z) \left(\sum_{j=1}^4 \mathcal{A}_j(k-j, \partial_z) \mathcal{S}_{k-j}^1(\partial_z) \right). \end{array} \right. \end{aligned} \quad (3.5)$$

From the recurrent relation (3.4), one observes

$$u_+^{n,k}(z) = \mathcal{S}_k^0(\partial_z) u_+^n(r_{t_2}, z) + \mathcal{S}_k^1(\partial_z) \partial_r u_+^n(r_{t_2}, z).$$

Therefore we have the following developments

$$\begin{cases} u_+^n(r_{t_2} + \nu, z) = \sum_{k=0}^{\infty} \nu^k \left(\mathcal{S}_k^0(\partial_z) u_+^n + \mathcal{S}_k^1(\partial_z) \partial_r u_+^n \right) (r_{t_2}, z), \\ \partial_r u_+^n(r_{t_2} + \nu, z) = \sum_{k=0}^{\infty} \nu^k (k+1) \left(\mathcal{S}_{k+1}^0(\partial_z) u_+^n + \mathcal{S}_{k+1}^1(\partial_z) \partial_r u_+^n \right) (r_{t_2}, z). \end{cases}$$

We also define the operators

$$\begin{cases} \tilde{\mathcal{S}}_k^0 = \mathcal{S}_k^0 - \frac{1}{r_{t_2}} \mathcal{S}_k^1, \\ \tilde{\mathcal{S}}_k^1 = \frac{1}{r_{t_2}} \mathcal{S}_k^1. \end{cases} \quad (3.6)$$

Then the Taylor series expansions write

$$\begin{cases} u_+^n(r_{t_2} + \nu, z) = \sum_{k=0}^{\infty} \nu^k \left(\tilde{\mathcal{S}}_k^0(\partial_z) u_+^n + \tilde{\mathcal{S}}_k^1 \partial_r (r u_+^n) \right) (r_{t_2}, z), \\ \partial_r (r u_+^n)(r_{t_2} + \nu, z) = \sum_{k=0}^{\infty} \nu^k (k+1) \left((r_{t_2} \tilde{\mathcal{S}}_{k+1}^0 + \tilde{\mathcal{S}}_k^0) u_+^n + (r_{t_2} \tilde{\mathcal{S}}_{k+1}^1 + \tilde{\mathcal{S}}_k^1) \partial_r (r u_+^n) \right) (r_{t_2}, z). \end{cases} \quad (3.7)$$

3.1.3 Transmission conditions between \tilde{u} (or \tilde{w}) and u_{\pm}^{δ}

The transmission conditions between the fields in domains representing different materials link them on the interfaces where the conductivity σ and/or the permeability μ change. The transmission conditions between the field inside the tube u_{-}^{δ} and the in-layer field u on Γ_{t_2} are

$$\begin{cases} u_{-}^{\delta}|_{r_{t_2}} = u|_{r_{t_2}}, \end{cases} \quad (3.8a)$$

$$\begin{cases} \frac{1}{\mu_t} \partial_r (r u_{-}^{\delta}) \Big|_{r_{t_2}} = \frac{1}{\mu_c} \partial_r (r u) \Big|_{r_{t_2}}. \end{cases} \quad (3.8b)$$

The transmission conditions between the field outside the deposit layer u_{+}^{δ} and the in-layer field u on Γ_c write

$$\begin{cases} u_{+}^{\delta}|_{\Gamma_c} = u|_{\Gamma_c}, \end{cases} \quad (3.9a)$$

$$\begin{cases} \frac{1}{\mu_v} \partial_n (r u_{+}^{\delta}) \Big|_{\Gamma_c} = \frac{1}{\mu_c} \partial_n (r u) \Big|_{\Gamma_c}. \end{cases} \quad (3.9b)$$

The unit normal and tangential vectors on Γ_c at the point $(r_{t_2} + \delta d(z), z)$ are

$$n = \frac{(1, -\delta d'(z))}{\sqrt{1 + (\delta d'(z))^2}}, \quad \tau = \frac{(\delta d'(z), 1)}{\sqrt{1 + (\delta d'(z))^2}}.$$

The first transmission condition (3.9a) implies a continuous condition of the tangential derivatives of u_{+}^{δ} and u

$$\begin{aligned} \tau \cdot \nabla u_{+}^{\delta} \Big|_{r_{t_2} + \delta d} &= \tau \cdot \nabla u \Big|_{r_{t_2} + \delta d} \\ \left(\delta d' \partial_r (r u_{+}^{\delta}) + \partial_z (r u_{+}^{\delta}) \right) \Big|_{r_{t_2} + \delta d} &= \left(\delta d' \partial_r (r u) + \partial_z (r u) \right) \Big|_{r_{t_2} + \delta d}, \end{aligned} \quad (3.10)$$

While the second transmission condition (3.9b) yields

$$\begin{aligned} \frac{1}{\mu_v} \partial_n(ru_+^\delta) \Big|_{r_{t_2}+\delta d} &= \frac{1}{\mu_c} \partial_n(ru) \Big|_{r_{t_2}+\delta d} \\ \frac{1}{\mu_v} \left(\partial_r(ru_+^\delta) - \delta d' \partial_z(ru_+^\delta) \right) \Big|_{r_{t_2}+\delta d} &= \frac{1}{\mu_c} \left(\partial_r(ru) - \delta d' \partial_z(ru) \right) \Big|_{r_{t_2}+\delta d}. \end{aligned} \quad (3.11)$$

(3.10) and (3.11) yield the transmission conditions on Γ_c

$$\begin{cases} u|_{r_{t_2}+\delta d} = u_+^\delta|_{r_{t_2}+\delta d}, & (3.12a) \\ \partial_r(ru)|_{r_{t_2}+\delta d} = \left(\frac{\frac{\mu_c}{\mu_v} + (\delta d')^2}{1 + (\delta d')^2} \partial_r(ru_+^\delta) + \left(1 - \frac{\mu_c}{\mu_v}\right) \frac{\delta d'}{1 + (\delta d')^2} \partial_z(ru_+^\delta) \right) \Big|_{r_{t_2}+\delta d}. & (3.12b) \end{cases}$$

3.1.4 Procedure for obtaining approximate transmission conditions $\mathcal{Z}_{m,n}$ between u_\pm^δ

Given a rescaling parameter $m \in \mathbb{N}$ in (3.1), we write the rescaled in-layer eddy current problem (3.2) as a Cauchy problem for the rescaled in-layer solution \tilde{u} with initial values given by the transmission conditions (3.8) between \tilde{u} and u_-^δ on Γ_{t_2} . The boundary values of \tilde{u} on Γ_c should match the transmission conditions (3.12) between \tilde{u} and u_+^δ on Γ_c , which yields the transmission conditions between u_-^δ and u_+^δ on Γ_{t_2} by considering the Taylor series expansion (3.7) which allows us to extend u_+^δ to the interface Γ_{t_2} (3.12).

In asymptotic expansions, we develop u_\pm^δ and \tilde{u} with respect to δ :

$$u_\pm^\delta = \sum_{n=0}^{\infty} \delta^n u_\pm^n, \quad \tilde{u} = \sum_{n=0}^{\infty} \delta^n u^n.$$

We denote by $\mathcal{Z}_{m,n}$ the approximate transmission conditions between u_\pm^δ on Γ_{t_2} with rescaling parameter m at order n in the asymptotic expansion ($\mathcal{O}(\delta^n)$). Therefore, we can obtain a family of asymptotic models with different approximate transmission conditions $\mathcal{Z}_{m,n}$ according to the choice of (m, n) .

3.2 Asymptotic models for deposits with constant thickness

To determine (m, n) with which the asymptotic model using $\mathcal{Z}_{m,n}$ is both a good approximation and easy to deduce inverse methods, we study a simplified case where the deposit layer on the shell side of the tube has constant thickness δ .

3.2.1 Rescaling of the in-layer problem

Since the deposit layer has constant thickness, we set the layer thickness $f_\delta(z) = \delta$, i.e. $d(z) = 1$. Therefore, we have

$$\rho = \frac{r - r_{t_2}}{\delta} \quad \rho \in [0, 1].$$

We denote by k_m the complex quantity with positive imaginary part such that

$$k_m^2 = i\omega\mu_c\sigma_m$$

We rewrite the differential equation for the in-layer field after rescaling

$$\tilde{u}(\rho, z) := u(r_{t_2} + \delta\rho, z)$$

according to the different rescaling parameter m .

1. $m = 0$.

From the eddy current equation in the deposit layer (3.2), we get

$$\frac{r^2}{\delta^2}\partial_\rho^2\tilde{u} + \frac{r}{\delta}\partial_\rho\tilde{u} - \tilde{u} + r^2(\partial_z^2\tilde{u} + k_0^2\tilde{u}) = 0.$$

By substituting r with $r_{t_2} + \rho\delta$, we obtain

$$\partial_\rho^2\tilde{u} = -\delta\mathcal{B}_0^1\tilde{u} - \delta^2\mathcal{B}_0^2\tilde{u} - \delta^3\mathcal{B}_0^3\tilde{u} - \delta^4\mathcal{B}_0^4\tilde{u}, \quad (3.13)$$

with

$$\begin{aligned} \mathcal{B}_0^1 &= \frac{2\rho}{r_{t_2}}\partial_\rho^2 + \frac{1}{r_{t_2}}\partial_\rho, \\ \mathcal{B}_0^2 &= \frac{\rho^2}{r_{t_2}^2}\partial_\rho^2 + \frac{\rho}{r_{t_2}^2}\partial_\rho - \frac{1}{r_{t_2}^2} + \partial_z^2 + k_0^2, \\ \mathcal{B}_0^3 &= \frac{2\rho}{r_{t_2}}(\partial_z^2 + k_0^2), \\ \mathcal{B}_0^4 &= \frac{\rho^2}{r_{t_2}^2}(\partial_z^2 + k_0^2). \end{aligned}$$

2. $m = 1$.

From (3.2), we obtain

$$\frac{r^2}{\delta^2}\partial_\rho^2\tilde{u} + \frac{r}{\delta}\partial_\rho\tilde{u} - \tilde{u} + r^2\left(\partial_z^2\tilde{u} + \frac{k_1^2}{\delta}\tilde{u}\right) = 0.$$

By substituting r with $r_{t_2} + \rho\delta$, we get

$$\partial_\rho^2\tilde{u} = -\delta\mathcal{B}_1^1\tilde{u} - \delta^2\mathcal{B}_1^2\tilde{u} - \delta^3\mathcal{B}_1^3\tilde{u} - \delta^4\mathcal{B}_1^4\tilde{u}, \quad (3.14)$$

with

$$\begin{aligned} \mathcal{B}_1^1 &= \frac{2\rho}{r_{t_2}}\partial_\rho^2 + \frac{1}{r_{t_2}}\partial_\rho + k_1^2, \\ \mathcal{B}_1^2 &= \frac{\rho^2}{r_{t_2}^2}\partial_\rho^2 + \frac{\rho}{r_{t_2}^2}\partial_\rho - \frac{1}{r_{t_2}^2} + \partial_z^2 + \frac{2\rho}{r_{t_2}}k_1^2, \\ \mathcal{B}_1^3 &= \frac{2\rho}{r_{t_2}}\partial_z^2 + \frac{\rho^2}{r_{t_2}^2}k_1^2, \\ \mathcal{B}_1^4 &= \frac{\rho^2}{r_{t_2}^2}\partial_z^2. \end{aligned}$$

3. $m = 2$.

To facilitate further computations, we set a weighted in-layer field

$$w(r, z) := \sqrt{r}u(r, z),$$

and after rescaling one has

$$\tilde{w}(\rho, z) := w(r_{t_2} + \delta\rho, z)$$

So the eddy current equation for the in-layer field u (3.2) becomes here

$$\frac{1}{\delta^2} \partial_\rho^2 \tilde{w} - \frac{3}{4r^2} \tilde{w} + \frac{k_2^2}{\delta^2} \tilde{w} + \partial_z^2 \tilde{w} = 0.$$

By substituting r with $r_{t_2} + \rho\delta$, we obtain

$$(\partial_\rho^2 + k_2^2) \tilde{w} = -\delta \mathcal{B}_2^1 \tilde{w} - \delta^2 \mathcal{B}_2^2 \tilde{w} - \delta^3 \mathcal{B}_2^3 \tilde{w} - \delta^4 \mathcal{B}_2^4 \tilde{w}, \quad (3.15)$$

with

$$\begin{aligned} \mathcal{B}_2^1 &= \frac{2\rho}{r_{t_2}} (\partial_\rho^2 + k_2^2), \\ \mathcal{B}_2^2 &= \frac{\rho^2}{r_{t_2}^2} (\partial_\rho^2 + k_2^2) - \frac{3}{4r_{t_2}^2} + \partial_z^2, \\ \mathcal{B}_2^3 &= \frac{2\rho}{r_{t_2}} \partial_z^2, \\ \mathcal{B}_2^4 &= \frac{\rho^2}{r_{t_2}^2} \partial_z^2. \end{aligned}$$

The formal asymptotic development of w with respect to the order of parameter δ writes:

$$\tilde{w} = \sum_{n=0}^{\infty} w^n \cdot \delta^n.$$

3.2.2 Transmission conditions between \tilde{u} (or \tilde{w}) and u_\pm^δ

1. $m = 0, 1$.

The transmission conditions at Γ_{t_2} (3.8) yield

$$\begin{cases} u_-^\delta|_{r=r_{t_2}} = \tilde{u}|_{\rho=0}, \\ \frac{1}{\mu_T} \partial_r(ru_-^\delta)|_{r=r_{t_2}} = \frac{1}{\mu_c} \left(\frac{r_{t_2} + \delta\rho}{\delta} \partial_\rho \tilde{u} + \tilde{u} \right) \Big|_{\rho=0}, \end{cases}$$

which imply

$$\begin{cases} u^n|_{\rho=0} = u_-^n|_{r=r_{t_2}}, \end{cases} \quad (3.16a)$$

$$\begin{cases} \partial_\rho u^n|_{\rho=0} = -\frac{1}{r_{t_2}} u_-^{n-1}|_{r=r_{t_2}} + \frac{1}{r_{t_2}} \frac{\mu_c}{\mu_t} \partial_r(ru_-^{n-1})|_{r=r_{t_2}}. \end{cases} \quad (3.16b)$$

From the transmission conditions at Γ_c (3.12) we have

$$\begin{cases} u_+^\delta|_{r=r_{t_2}+\delta} = \tilde{u}|_{\rho=1}, \\ \frac{1}{\mu_v} \partial_r(ru_+^\delta)|_{r=r_{t_2}+\delta} = \frac{1}{\mu_c} \left(\frac{r_{t_2} + \delta\rho}{\delta} \partial_\rho \tilde{u} + \tilde{u} \right) \Big|_{\rho=1}. \end{cases}$$

Combined with the Taylor expansions (3.7), the above conditions yield

$$\begin{cases} u^n|_{\rho=1} = \sum_{k=0}^n \left(\tilde{\mathcal{S}}_k^0 u_+^{n-k} + \tilde{\mathcal{S}}_k^1 \partial_r(ru_+^{n-k}) \right) \Big|_{r=r_{t_2}}, & (3.17a) \\ \partial_\rho u^n|_{\rho=1} = \sum_{l=0}^{n-1} \sum_{k=0}^{n-l-1} \frac{(-1)^l}{r_{t_2}^{l+1}} \left\{ - \left(\tilde{\mathcal{S}}_k^0 u_+^{n-l-k-1} + \tilde{\mathcal{S}}_k^1 \partial_r(ru_+^{n-l-k-1}) \right) \right. \\ \left. + \frac{\mu_c}{\mu_v} (k+1) \left((r_{t_2} \tilde{\mathcal{S}}_{k+1}^0 + \tilde{\mathcal{S}}_k^0) u_+^{n-l-k-1} + (r_{t_2} \tilde{\mathcal{S}}_{k+1}^1 + \tilde{\mathcal{S}}_k^1) \partial_r(ru_+^{n-l-k-1}) \right) \right\} \Big|_{r_{t_2}}. & (3.17b) \end{cases}$$

2. $m = 2$.

From the definition of w , we have

$$\begin{cases} \tilde{w} = \sqrt{r_{t_2} + \rho\delta} \tilde{u}, \\ \partial_\rho \tilde{w} = \frac{\delta}{2\sqrt{r_{t_2} + \rho\delta}} \tilde{u} + \sqrt{r_{t_2} + \rho\delta} \partial_\rho \tilde{u}. \end{cases}$$

Then after some calculates, the transmission conditions at Γ_{t_2} (3.8) is transformed as

$$\begin{cases} \tilde{w}|_{\rho=0} = \sqrt{r_{t_2}} \tilde{u}|_{\rho=0} = \sqrt{r_{t_2}} u_-^\delta|_{r=r_{t_2}}, \\ \partial_\rho \tilde{w}|_{\rho=0} = \frac{\delta}{2\sqrt{r_{t_2}}} \tilde{u}|_{\rho=0} + \sqrt{r_{t_2}} \partial_\rho \tilde{u}|_{\rho=0} = -\frac{\delta}{2\sqrt{r_{t_2}}} u_-^\delta|_{r=r_{t_2}} + \frac{\mu_c}{\mu_t} \frac{\delta}{\sqrt{r_{t_2}}} \partial_r(ru_-^\delta) \Big|_{r=r_{t_2}}, \end{cases}$$

which yields

$$\begin{cases} w^n|_{\rho=0} = \sqrt{r_{t_2}} u_-^n|_{r=r_{t_2}}, & (3.18a) \\ \partial_\rho w^n|_{\rho=0} = \frac{1}{\sqrt{r_{t_2}}} \left(-\frac{1}{2} u_-^{n-1} + \frac{\mu_c}{\mu_t} \partial_r(ru_-^{n-1}) \right) \Big|_{r=r_{t_2}}. & (3.18b) \end{cases}$$

Similarly, the transmission conditions at Γ_c (3.12) become

$$\begin{cases} w|_{\rho=1} = \sqrt{r_{t_2} + \delta} u_+^\delta|_{r=r_{t_2}+\delta} \\ = \left(\sqrt{r_{t_2}} + \sum_{k=1}^{\infty} \frac{(-1)^{k-1} (2k-3)!!}{k!} \frac{r_{t_2}^{-\frac{2k-1}{2}}}{2^k} \delta^k \right) u_+^\delta|_{r=r_{t_2}+\delta} \\ \partial_\rho w|_{\rho=1} = \frac{\delta}{2\sqrt{r_{t_2} + \delta}} u|_{\rho=1} + \sqrt{r_{t_2} + \delta} \partial_\rho u|_{\rho=1} \\ = \delta \left(\sum_{k=0}^{\infty} \frac{(-1)^k (2k-1)!!}{k!} \frac{r_{t_2}^{-\frac{2k+1}{2}}}{2^k} \delta^k \right) \left(-\frac{1}{2} u_+^\delta + \frac{\mu_c}{\mu_v} \partial_r(ru_+^\delta) \right) \Big|_{r=r_{t_2}+\delta}. \end{cases}$$

Together with the Taylor developments (3.7), the above transmission conditions yield

$$\left\{ \begin{array}{l} w^n|_{\rho=1} = \sum_{k=0}^n a_k \sum_{l=0}^{n-k} \left(\tilde{\mathcal{S}}_l^0(\partial_z) u_+^{n-k-l} + \tilde{\mathcal{S}}_l^1(\partial_z) \partial_r (r u_+^{n-k-l}) \right) \Big|_{r=r_{t_2}}, \\ \partial_\rho w^n|_{\rho=1} = \sum_{k=0}^{n-1} b_k \sum_{l=0}^{n-k-1} \left\{ \left(-\frac{1}{2} \tilde{\mathcal{S}}_l^0 + \frac{\mu_c}{\mu_v} (l+1) (r_{t_2} \tilde{\mathcal{S}}_{l+1}^0 + \tilde{\mathcal{S}}_l^0) \right) u_+^{n-k-l-1} \right. \\ \left. + \left(-\frac{1}{2} \tilde{\mathcal{S}}_l^1 + \frac{\mu_c}{\mu_v} (l+1) (r_{t_2} \tilde{\mathcal{S}}_{l+1}^1 + \tilde{\mathcal{S}}_l^1) \right) \partial_r (r u_+^{n-k-l-1}) \right\} \Big|_{r=r_{t_2}}. \end{array} \right. \quad (3.19a)$$

where

$$a_0 = \sqrt{r_{t_2}}, \quad a_k|_{k \geq 1} = \frac{(-1)^{k-1} (2k-3)!!}{k!} \frac{r_{t_2}^{-\frac{2k-1}{2}}}{2^k},$$

$$b_k = \frac{(-1)^k (2k-1)!!}{k!} \frac{r_{t_2}^{-\frac{2k+1}{2}}}{2^k}.$$

3.2.3 Computing algorithm for the rescaled in-layer field \tilde{u} (or \tilde{w})

In this section, we follow the procedure in 3.1.4 and give the detailed computing steps. Given $m = 0, 1$ or 2 , we resolve the corresponding problem (3.13), (3.14) or (3.15) in the thin deposit layer to obtain the transmission conditions between u_-^n and u_+^n (or between w_-^n and w_+^n) on Γ_{t_2} from the transmission conditions (3.16) - (3.17) between u^n and u_\pm^n (or the transmission conditions (3.18) - (3.19) between w^n and w_\pm^n).

1. $m = 0, 1$.

We consider a general Cauchy problem with an arbitrary second member f for the same differential equation as in (3.13) or in (3.14):

$$\partial_\rho^2 \tilde{u} = f \quad \rho \in [0, 1].$$

With the initial values at $\rho = 0$, the solution \tilde{u} writes

$$\tilde{u}(\rho) = \tilde{u}|_{\rho=0} + \partial_\rho \tilde{u}|_{\rho=0} \rho + \int_0^\rho \int_0^s f(t) dt ds.$$

And at $\rho = 1$,

$$\left\{ \begin{array}{l} \tilde{u}|_{\rho=1} = \tilde{u}|_{\rho=0} + \partial_\rho \tilde{u}|_{\rho=0} + \int_0^1 \int_0^s f(t) dt ds, \\ \partial_\rho \tilde{u}|_{\rho=1} = \partial_\rho \tilde{u}|_{\rho=0} + \int_0^1 f(t) dt. \end{array} \right. \quad (3.20)$$

From the above resolvent and the rescaled eddy current equations (3.13) or (3.14), it follows that the asymptotic expansions u^n of \tilde{u} can be obtained recurrently via the following Cauchy

problems

$$\begin{aligned}
\partial_\rho^2 u^0 &= 0, \\
\partial_\rho^2 u^1 &= -\mathcal{B}_m^1 u^0, \\
\partial_\rho^2 u^2 &= -\mathcal{B}_m^1 u^1 - \mathcal{B}_m^2 u^0, \\
\partial_\rho^2 u^3 &= -\mathcal{B}_m^1 u^2 - \mathcal{B}_m^2 u^1 - \mathcal{B}_m^3 u^0, \\
\partial_\rho^2 u^4 &= -\mathcal{B}_m^1 u^3 - \mathcal{B}_m^2 u^2 - \mathcal{B}_m^3 u^1 - \mathcal{B}_m^4 u^0, \\
&\dots
\end{aligned}$$

with initial values given by the transmission conditions (3.16) at $\rho = 0$. Then the boundary values of u^n at $\rho = 1$ given by (3.20) should coincident with those given by the transmission conditions (3.17) on Γ_c . These equalities give recurrently the transmission conditions linking up u_\pm^n on Γ_{t2} .

2. $m = 2$.

We consider the Cauchy problem with the same operator as in problem (3.15) and an arbitrary second member f

$$(\partial_\rho^2 + k_2^2) \check{w} = f \quad \rho \in [0, 1],$$

with initial values at $\rho = 0$. Its solution \check{w} writes

$$\check{w} = (\check{w}|_{\rho=0} - (v \star f)|_{\rho=0}) \cos(k_2 \rho) + \frac{1}{k_2} \left(\partial_\rho \check{w}|_{\rho=0} - \partial_\rho (v \star f)|_{\rho=0} \right) \sin(k_2 \rho) + v \star f, \quad (3.21)$$

where $v = \frac{1}{2ik_2} e^{ik_2|\rho|}$ is the fundamental solution, i.e. the solution of the problem with a Dirac distribution as second member:

$$(\partial_\rho^2 + k_2^2) \check{w} = \delta_0.$$

One computes

$$\begin{aligned}
v \star f(\rho) &= \int_0^\rho \frac{1}{2ik_2} e^{ik_2(\rho-\xi)} f(\xi) d\xi + \int_\rho^1 \frac{1}{2ik_2} e^{ik_2(\xi-\rho)} f(\xi) d\xi, \\
\partial_\rho (v \star f)(\rho) &= \int_0^\rho \frac{1}{2} e^{ik_2(\rho-\xi)} f(\xi) d\xi - \int_\rho^1 \frac{1}{2} e^{ik_2(\xi-\rho)} f(\xi) d\xi, \\
v \star f(0) &= \int_0^1 \frac{1}{2ik_2} e^{ik_2\xi} f(\xi) d\xi = -\frac{1}{ik_2} \partial_\rho (v \star f)(0), \\
v \star f(1) &= \int_0^1 \frac{1}{2ik_2} e^{ik_2(1-\xi)} f(\xi) d\xi = \frac{1}{ik_2} \partial_\rho (v \star f)(1).
\end{aligned}$$

By substituting the above terms in (3.21), we obtain

$$\begin{cases}
\check{w}|_{\rho=1} = \cos(k_2) (\check{w} - v \star f)|_{\rho=0} + \frac{\sin(k_2)}{k_2} (\partial_\rho \check{w} + ik_2 v \star f)|_{\rho=0} + (v \star f)|_{\rho=1}, \\
\partial_\rho \check{w}|_{\rho=1} = -k_2 \sin(k_2) (\check{w} - v \star f)|_{\rho=0} + \cos(k_2) (\partial_\rho \check{w} + ik_2 v \star f)|_{\rho=0} + ik_2 (v \star f)|_{\rho=1}.
\end{cases} \quad (3.22)$$

Therefore, from the above resolvent procedure and the problem (3.15), the asymptotic expansions w^n of \tilde{w} verify recurrently the following Cauchy problems

$$\begin{aligned} (\partial_\rho^2 + k_2^2) w^0 &= 0, \\ (\partial_\rho^2 + k_2^2) w^1 &= -\mathcal{B}_2^1 w^0, \\ (\partial_\rho^2 + k_2^2) w^2 &= -\mathcal{B}_2^1 w^1 - \mathcal{B}_2^2 w^0, \\ (\partial_\rho^2 + k_2^2) w^3 &= -\mathcal{B}_2^1 w^2 - \mathcal{B}_2^2 w^1 - \mathcal{B}_2^3 w^0, \\ (\partial_\rho^2 + k_2^2) w^4 &= -\mathcal{B}_2^1 w^3 - \mathcal{B}_2^2 w^2 - \mathcal{B}_2^3 w^1 - \mathcal{B}_2^4 w^0, \\ &\dots \end{aligned}$$

with initial values given by the transmission conditions (3.18) at $\rho = 0$ (on Γ_{t_2}). Their solutions give the boundary values (3.22) that should coincide with the transmission conditions (3.19) at $\rho = 1$ (on Γ_{t_2}), which implies recurrently the transmission conditions connecting u_\pm^n on Γ_{t_2} .

3.2.4 Computation of some approximate transmission conditions $\mathcal{Z}_{m,n}$

In this section, we follow the computing algorithm described in the previous section 3.2.3 and give the transmission conditions $\mathcal{Z}_{m,n}$ on Γ_{t_2} for $m = 0, 1, 2$ and $n = 0, 1, 2$. We will use the first $\tilde{\mathcal{S}}_k^i(\partial_z)$ operators in the Taylor developments (3.7) with their explicit expressions

$$\begin{aligned} \tilde{\mathcal{S}}_0^0 &= \text{Id}, & \tilde{\mathcal{S}}_0^1 &= 0, \\ \tilde{\mathcal{S}}_1^0 &= -\frac{1}{r_{t_2}}, & \tilde{\mathcal{S}}_1^1 &= \frac{1}{r_{t_2}}, \\ \tilde{\mathcal{S}}_2^0 &= \frac{1}{r_{t_2}^2} - \frac{1}{2} \partial_z^2, & \tilde{\mathcal{S}}_2^1 &= -\frac{1}{2r_{t_2}^2}. \end{aligned}$$

We denote by u_\pm^δ the approximated fields of u_\pm^δ up to the asymptotic developments order, that is

$$\begin{aligned} u_\pm^\delta &= u_\pm^0 && \text{order 0,} \\ u_\pm^\delta &= u_\pm^0 + \delta u_\pm^1 && \text{order 1,} \\ u_\pm^\delta &= u_\pm^0 + \delta u_\pm^1 + \delta^2 u_\pm^2 && \text{order 2.} \end{aligned}$$

Readers may skip the fastidious computational details and refer to the following expressions for the corresponding approximate transmission conditions.

$\mathcal{Z}_{0,0}$	(3.29)	$\mathcal{Z}_{0,1}$	(3.36)	$\mathcal{Z}_{0,2}$	(3.41)
$\mathcal{Z}_{1,0}$	(3.47)	$\mathcal{Z}_{1,1}$	(3.52)	$\mathcal{Z}_{1,2}$	(3.56)
$\mathcal{Z}_{2,0}$	(3.60)	$\mathcal{Z}_{2,1}$	(3.64)	$\mathcal{Z}_{2,2}$	(3.68)

Rescaling parameter $m = 0$

1. Order $n = 0$.

From the asymptotic development (3.13) and the transmission conditions (3.16) on Γ_{t2} for u^0 , we have the differential equation for u^0

$$\begin{cases} \partial_\rho^2 u^0 = 0 & \rho \in [0, 1], \\ u^0|_{\rho=0} = u_-^0|_{r_{t2}}, \\ \partial_\rho u^0|_{\rho=0} = 0, \end{cases}$$

which yields

$$u^0(\rho) = u_-^0|_{r_{t2}} \quad \rho \in [0, 1].$$

Thus, with the first transmission condition (3.17a) on Γ_c for u^0 , which is

$$u^0|_{\rho=1} = \tilde{\mathcal{S}}_0^0 u_+^0|_{r_{t2}} + \tilde{\mathcal{S}}_0^1 \partial_r(r u_+^0)|_{r_{t2}} = u_+^0|_{r_{t2}}, \quad (3.23)$$

we have

$$u_-^0|_{r_{t2}} = u_+^0|_{r_{t2}}. \quad (3.24)$$

Similarly, considering (3.13) and the transmission conditions (3.16) on Γ_{t2} for u^1 , we write the differential problem for u^1 as

$$\begin{cases} \partial_\rho^2 u^1 = -\mathcal{B}_0^1 u^0 = 0 & \rho \in [0, 1], \\ u^1|_{\rho=0} = u_-^1|_{r_{t2}}, \\ \partial_\rho u^1|_{\rho=0} = -\frac{1}{r_{t2}} u_-^0|_{r_{t2}} + \frac{1}{r_{t2}} \frac{\mu_c}{\mu_t} \partial_r(r u_-^0)|_{r_{t2}}, \end{cases}$$

which implies

$$\partial_\rho u^1 = -\frac{1}{r_{t2}} \left(u_-^0|_{r_{t2}} - \frac{\mu_c}{\mu_t} \partial_r(r u_-^0)|_{r_{t2}} \right), \quad (3.25)$$

$$u^1 = u_-^1|_{r_{t2}} - \frac{1}{r_{t2}} \left(u_-^0|_{r_{t2}} - \frac{\mu_c}{\mu_t} \partial_r(r u_-^0)|_{r_{t2}} \right) \rho. \quad (3.26)$$

The second transmission condition (3.17b) on Γ_c for u^1 writes

$$\partial_\rho u^1|_{\rho=1} = -\frac{1}{r_{t2}} \left(u_+^0|_{r_{t2}} - \frac{\mu_c}{\mu_v} \partial_r(r u_+^0)|_{r_{t2}} \right). \quad (3.27)$$

Hence, the equalities (3.25) and (3.27) yield

$$\frac{1}{r_{t2}} \frac{\mu_c}{\mu_t} \partial_r(r u_-^0)|_{r_{t2}} = \frac{1}{r_{t2}} \frac{\mu_c}{\mu_v} \partial_r(r u_+^0)|_{r_{t2}}. \quad (3.28)$$

(3.24) and (3.28) imply the approximate transmission conditions at order 0 on Γ_{t2}

$$\mathcal{Z}_{0,0} \begin{cases} u_-^\delta = u_+^\delta, \\ \frac{1}{r_{t2}} \frac{\mu_c}{\mu_t} \partial_r(r u_-^\delta) = \frac{1}{r_{t2}} \frac{\mu_c}{\mu_v} \partial_r(r u_+^\delta). \end{cases} \quad (3.29a)$$

$$(3.29b)$$

We remark that $\mathcal{Z}_{0,0}$ for $u_\pm^\delta = u_\pm^0$ on Γ_{t2} given by (3.29) are simply the transmission conditions between the tube wall and the vacuum, as if the deposit layer does not exist.

2. Order $n = 1$.

The first transmission condition (3.17a) for u^1 on Γ_c

$$\begin{aligned} u^1|_{\rho=1} &= \tilde{\mathcal{S}}_0^0 u_+^1|_{r_{t_2}} + \tilde{\mathcal{S}}_0^1 \partial_r(ru_+^1)|_{r_{t_2}} + \tilde{\mathcal{S}}_1^0 u_+^0|_{r_{t_2}} + \tilde{\mathcal{S}}_1^1 \partial_r(ru_+^0)|_{r_{t_2}} \\ &= u_+^1|_{r_{t_2}} - \frac{1}{r_{t_2}} (u_+^0|_{r_{t_2}} - \partial_r(ru_+^0)|_{r_{t_2}}) \end{aligned} \quad (3.30)$$

together with the equality (3.26) imply

$$u_-^1|_{r_{t_2}} + \frac{1}{r_{t_2}} \frac{\mu_c}{\mu_t} \partial_r(ru_-^0)|_{r_{t_2}} = u_+^1|_{r_{t_2}} + \frac{1}{r_{t_2}} \partial_r(ru_-^0)|_{r_{t_2}}. \quad (3.31)$$

One get the differential problem for u^2 from (3.13) using the previous expansions u^0 , u^1 and the transmission conditions (3.16) on Γ_{t_2} for u^2

$$\begin{cases} \partial_\rho^2 u^2 = -\mathcal{B}_0^1 u^1 - \mathcal{B}_0^2 u^0 \\ \quad = \left(\frac{2}{r_{t_2}^2} - (\partial_z^2 + k_0^2) \right) u_-^0|_{r_{t_2}} - \frac{1}{r_{t_2}^2} \frac{\mu_c}{\mu_t} \partial_r(ru_-^0)|_{r_{t_2}} & \rho \in [0, 1], \\ u^2|_{\rho=0} = u_-^2|_{r_{t_2}}, \\ \partial_\rho u^2|_{\rho=0} = -\frac{1}{r_{t_2}} u_-^1|_{r_{t_2}} + \frac{1}{r_{t_2}} \frac{\mu_c}{\mu_t} \partial_r(ru_-^1)|_{r_{t_2}}. \end{cases}$$

Thus

$$\begin{aligned} \partial_\rho u^2 &= -\frac{1}{r_{t_2}} \left(u_-^1|_{r_{t_2}} - \frac{\mu_c}{\mu_t} \partial_r(ru_-^1)|_{r_{t_2}} \right) \\ &\quad + \left(\left(\frac{2}{r_{t_2}^2} - (\partial_z^2 + k_0^2) \right) u_-^0|_{r_{t_2}} - \frac{1}{r_{t_2}^2} \frac{\mu_c}{\mu_t} \partial_r(ru_-^0)|_{r_{t_2}} \right) \rho, \end{aligned} \quad (3.32)$$

$$\begin{aligned} u^2 &= u_-^2|_{r_{t_2}} - \frac{1}{r_{t_2}} \left(u_-^1|_{r_{t_2}} - \frac{\mu_c}{\mu_t} \partial_r(ru_-^1)|_{r_{t_2}} \right) \rho \\ &\quad + \left(\left(\frac{2}{r_{t_2}^2} - (\partial_z^2 + k_0^2) \right) u_-^0|_{r_{t_2}} - \frac{1}{r_{t_2}^2} \frac{\mu_c}{\mu_t} \partial_r(ru_-^0)|_{r_{t_2}} \right) \frac{\rho^2}{2}. \end{aligned} \quad (3.33)$$

The explicit expression of the second transmission condition (3.17b) on Γ_c for u^2 is

$$\partial_\rho u^2|_{\rho=1} = -\frac{1}{r_{t_2}} \left(u_+^1|_{r_{t_2}} - \frac{\mu_c}{\mu_v} \partial_r(ru_+^1)|_{r_{t_2}} \right) + \left(\frac{2}{r_{t_2}^2} - \frac{\mu_c}{\mu_v} \partial_z^2 \right) u_+^0|_{r_{t_2}} - \frac{1}{r_{t_2}^2} \partial_r(ru_+^0)|_{r_{t_2}}. \quad (3.34)$$

Thus, (3.32) and (3.34) imply

$$\frac{1}{r_{t_2}} \frac{\mu_c}{\mu_t} \partial_r(ru_-^1) - (k_0^2 + \partial_z^2) u_-^0 = \frac{1}{r_{t_2}} \frac{\mu_c}{\mu_v} \partial_r(ru_+^1) - \frac{\mu_c}{\mu_v} \partial_z^2 u_+^0. \quad (3.35)$$

(3.31) and (3.35) lead to the first order approximate transmission conditions

$$\mathcal{Z}_{0,1} \begin{cases} u_-^\delta + \frac{\delta}{r_{t_2}} \frac{\mu_c}{\mu_t} \partial_r(ru_-^\delta) = u_+^\delta + \frac{\delta}{r_{t_2}} \partial_r(ru_+^\delta), \end{cases} \quad (3.36a)$$

$$\begin{cases} \frac{1}{r_{t_2}} \frac{\mu_c}{\mu_t} \partial_r(ru_-^\delta) - \delta (k_0^2 + \partial_z^2) u_-^\delta = \frac{1}{r_{t_2}} \frac{\mu_c}{\mu_v} \partial_r(ru_+^\delta) - \delta \frac{\mu_c}{\mu_v} \partial_z^2 u_+^\delta. \end{cases} \quad (3.36b)$$

3. Order $n = 2$.

From (3.33) and the first transmission condition (3.17a) for u^2 on Γ_c , which is

$$u^2|_{\rho=1} = u_+^2|_{r_{t_2}} - \frac{1}{r_{t_2}} (u_+^1|_{r_{t_2}} - \partial_r(ru_+^1)|_{r_{t_2}}) \quad (3.37)$$

one gets

$$\begin{aligned} u_-^2|_{r_{t_2}} + \frac{1}{r_{t_2}} \frac{\mu_c}{\mu_t} \partial_r(ru_-^1)|_{r_{t_2}} + \frac{1}{2r_{t_2}^2} \frac{\mu_c}{\mu_t} \partial_r(ru_-^0)|_{r_{t_2}} - \frac{1}{2} k_0^2 u_-^0|_{r_{t_2}} \\ = u_+^2|_{r_{t_2}} + \frac{1}{r_{t_2}} \partial_r(ru_+^1)|_{r_{t_2}} + \frac{1}{2r_{t_2}^2} \partial_r(ru_+^0)|_{r_{t_2}}. \end{aligned} \quad (3.38)$$

To get the second transmission conditions connecting u_{\pm}^2 one has to consider the Cauchy problem for u^3 derived from (3.13) and the transmission conditions (3.16) on Γ_{t_2} for u^3

$$\left\{ \begin{array}{l} \partial_{\rho}^2 u^3 = -\mathcal{B}_0^1 u^2 - \mathcal{B}_0^2 u^1 - \mathcal{B}_0^3 u^0 \\ = \left(\frac{2}{r_{t_2}^2} - (\partial_z^2 + k_0^2) \right) u_-^1|_{r_{t_2}} - \frac{1}{r_{t_2}} \frac{\mu_c}{\mu_t} \partial_r(ru_-^1)|_{r_{t_2}} \\ + \rho \left(\frac{3}{r_{t_2}^3} - \frac{1}{r_{t_2}} (\partial_z^2 + k_0^2) \right) \left(-2u_-^0|_{r_{t_2}} + \frac{\mu_c}{\mu_t} \partial_r(ru_-^0)|_{r_{t_2}} \right) \quad \rho \in [0, 1], \\ u^3|_{\rho=0} = u_-^3|_{r_{t_2}}, \quad \partial_{\rho} u^3|_{\rho=0} = -\frac{1}{r_{t_2}} u_-^2|_{r_{t_2}} + \frac{1}{r_{t_2}} \frac{\mu_c}{\mu_t} \partial_r(ru_-^2)|_{r_{t_2}}. \end{array} \right.$$

On one hand, we get easily from the above Cauchy problem

$$\begin{aligned} \partial_{\rho} u^3|_{\rho=1} = -\frac{1}{r_{t_2}} u_-^2|_{r_{t_2}} + \frac{1}{r_{t_2}} \frac{\mu_c}{\mu_t} \partial_r(ru_-^2)|_{r_{t_2}} + \left(\frac{2}{r_{t_2}^2} - \frac{\mu_c}{\mu_v} \partial_z^2 \right) u_-^1|_{r_{t_2}} - \frac{1}{r_{t_2}^2} \frac{\mu_c}{\mu_t} \partial_r(ru_-^1)|_{r_{t_2}} \\ + \frac{1}{2} \left(\frac{3}{r_{t_2}^3} - \frac{1}{r_{t_2}} (\partial_z^2 + k_0^2) \right) \left(-2u_-^0|_{r_{t_2}} + \frac{\mu_c}{\mu_t} \partial_r(ru_-^0)|_{r_{t_2}} \right). \end{aligned}$$

On the other hand, the second transmission condition (3.17b) on Γ_c for u^3 writes explicitly

$$\begin{aligned} \partial_{\rho} u^3|_{\rho=1} = -\frac{1}{r_{t_2}} \left(u_+^2|_{r_{t_2}} - \frac{\mu_c}{\mu_v} \partial_r(ru_+^2)|_{r_{t_2}} \right) + \left(\frac{2}{r_{t_2}^2} - \partial_z^2 \right) u_+^1|_{r_{t_2}} - \frac{1}{r_{t_2}^2} \partial_r(ru_+^1)|_{r_{t_2}} \\ + \left(-\frac{3}{r_{t_2}^3} + \frac{1}{2r_{t_2}} \left(1 + \frac{\mu_c}{\mu_t} \right) \partial_z^2 \right) u_+^0|_{r_{t_2}} + \left(\frac{3}{2r_{t_2}^3} - \frac{1}{2r_{t_2}} \frac{\mu_c}{\mu_t} \partial_z^2 \right) \partial_r(ru_+^0)|_{r_{t_2}}. \end{aligned} \quad (3.39)$$

The above two equalities result in

$$\begin{aligned} \frac{1}{r_{t_2}} \frac{\mu_c}{\mu_t} \partial_r(ru_-^2) - (k_0^2 + \partial_z^2) u_-^1 + \frac{1}{2r_{t_2}} (k_0^2 + \partial_z^2) u_-^0 - \frac{1}{2r_{t_2}} \frac{\mu_c}{\mu_t} k_0^2 \partial_r(ru_-^0) \\ = \frac{1}{r_{t_2}} \frac{\mu_c}{\mu_v} \partial_r(ru_+^2) - \frac{\mu_c}{\mu_v} \partial_z^2 u_+^1 + \frac{1}{2r_{t_2}} \frac{\mu_c}{\mu_v} \partial_z^2 u_+^0. \end{aligned} \quad (3.40)$$

We derive from (3.38) considering the previous expansions u^0 , u^1 , u^2 and (3.40) the second order approximate transmission conditions

$$\mathcal{Z}_{0,2} \begin{cases} \left(1 - \frac{\delta^2}{2}k_0^2\right)u_-^\delta + \left(\frac{\delta}{r_{t_2}} + \frac{\delta^2}{2r_{t_2}^2}\right)\frac{\mu_c}{\mu_t}\partial_r(ru_-^\delta) = u_+^\delta + \left(\frac{\delta}{r_{t_2}} + \frac{\delta^2}{2r_{t_2}^2}\right)\partial_r(ru_+^\delta), \\ \left(\frac{1}{r_{t_2}} - \frac{\delta^2}{2r_{t_2}^2}k_0^2\right)\frac{\mu_c}{\mu_t}\partial_r(ru_-^\delta) + \left(-\delta + \frac{\delta^2}{2r_{t_2}^2}\right)(k_0^2 + \partial_z^2)u_-^\delta \\ = \frac{1}{r_{t_2}}\frac{\mu_c}{\mu_v}\partial_r(ru_+^\delta) + \left(-\delta + \frac{\delta^2}{2r_{t_2}^2}\right)\frac{\mu_c}{\mu_v}\partial_z^2u_+^\delta. \end{cases} \quad (3.41a)$$

$$(3.41b)$$

Rescaling parameter $m = 1$

1. Order $n = 0$.

The asymptotic development (3.14) and the transmission conditions (3.16) on Γ_{t_2} for u^0 lead to the Cauchy problem for u^0 with initial values at $\rho = 0$

$$\begin{cases} \partial_\rho^2 u^0 = 0 & \rho \in [0, 1], \\ u^0|_{\rho=0} = u_-^0|_{r_{t_2}}, \\ \partial_\rho u^0|_{\rho=0} = 0, \end{cases}$$

which yields

$$u^0(\rho) = u_-^0|_{r_{t_2}} \quad \rho \in [0, 1]. \quad (3.42)$$

Taking $\rho = 1$ in (3.42) and considering the transmission condition on Γ_c for u^0 (3.23), one gets

$$u_-^0|_{r_{t_2}} = u_+^0|_{r_{t_2}}. \quad (3.43)$$

Then we consider the Cauchy problem for u^1 given by the asymptotic development (3.14) and by the transmission conditions (3.16) on Γ_{t_2} for u^1

$$\begin{cases} \partial_\rho^2 u^1 = -\mathcal{B}_1^1 u^0 = -k_1^2 u_-^0|_{r_{t_2}} & \rho \in [0, 1], \\ u^1|_{\rho=0} = u_-^1|_{r_{t_2}}, \\ \partial_\rho u^1|_{\rho=0} = -\frac{1}{r_{t_2}}u_-^0|_{r_{t_2}} + \frac{1}{r_{t_2}}\frac{\mu_c}{\mu_t}\partial_r(ru_-^0)|_{r_{t_2}}, \end{cases}$$

which implies

$$\partial_\rho u^1 = -\frac{1}{r_{t_2}}\left(u_-^0|_{r_{t_2}} - \frac{\mu_c}{\mu_t}\partial_r(ru_-^0)|_{r_{t_2}}\right) - \rho k_1^2 u_-^0|_{r_{t_2}}, \quad (3.44)$$

$$u^1 = u_-^1|_{r_{t_2}} - \frac{\rho^2}{r_{t_2}}\left(u_-^0|_{r_{t_2}} - \frac{\mu_c}{\mu_t}\partial_r(ru_-^0)|_{r_{t_2}}\right) \rho - \frac{1}{2}k_1^2 u_-^0|_{r_{t_2}}. \quad (3.45)$$

(3.44) and the transmission condition on Γ_c for u^1 (3.27) imply

$$\frac{1}{r_{t_2}}\frac{\mu_c}{\mu_t}\partial_r(ru_-^0)|_{r_{t_2}} - k_1^2 u_-^0|_{r_{t_2}} = \frac{1}{r_{t_2}}\frac{\mu_c}{\mu_v}\partial_r(ru_+^0)|_{r_{t_2}}. \quad (3.46)$$

(3.43) and (3.46) give the approximate transmission conditions at order 0 on Γ_{t2} for u_{\pm}^{δ}

$$\mathcal{Z}_{1,0} \begin{cases} u_{-}^{\delta} = u_{+}^{\delta}, & (3.47a) \\ -k_1^2 u_{-}^{\delta} + \frac{1}{r_{t2}} \frac{\mu_c}{\mu_t} \partial_r(r u_{-}^{\delta}) = \frac{1}{r_{t2}} \frac{\mu_c}{\mu_v} \partial_r(r u_{+}^{\delta}). & (3.47b) \end{cases}$$

If we rewrite the second transmission condition (3.47b) as

$$\frac{1}{\mu_t} \partial_r(r u_{-}^{\delta}) = \frac{1}{\mu_v} \partial_r(r u_{+}^{\delta}) + i\omega \sigma_c \delta r_{t2} u_{-}^{\delta},$$

we remark that the transmission conditions $\mathcal{Z}_{1,0}$ given by (3.47) are indeed the classical boundary impedance conditions which take into account the deposit layer.

2. Order $n = 1$.

From (3.45) and the transmission condition on Γ_c for u^1 (3.30) we have

$$u_{-}^1|_{r_{t2}} + \frac{1}{r_{t2}} \frac{\mu_c}{\mu_t} \partial_r(r u_{-}^0)|_{r_{t2}} - \frac{1}{2} k_1^2 u_{-}^0|_{r_{t2}} = u_{+}^1|_{r_{t2}} + \frac{1}{r_{t2}} \partial_r(r u_{+}^0)|_{r_{t2}}. \quad (3.48)$$

Using the asymptotic development (3.14) and the transmission conditions (3.16) on Γ_{t2} for u^2 , we get

$$\begin{cases} \partial_{\rho}^2 u^2 = -\mathcal{B}_1^1 u^1 - \mathcal{B}_1^2 u^0 \\ \quad = -k_1^2 u_{-}^1|_{r_{t2}} + \left(\frac{2}{r_{t2}^2} - \partial_z^2\right) u_{-}^0|_{r_{t2}} - \frac{1}{r_{t2}^2} \frac{\mu_c}{\mu_t} \partial_r(r u_{-}^0)|_{r_{t2}} \\ \quad + \rho k_1^2 \left(\frac{2}{r_{t2}} u_{-}^0|_{r_{t2}} - \frac{1}{r_{t2}} \frac{\mu_c}{\mu_t} \partial_r(r u_{-}^0)|_{r_{t2}}\right) + \rho^2 \frac{k_1^4}{2} u_{-}^0|_{r_{t2}} \quad \rho \in [0, 1], \\ u^2|_{\rho=0} = u_{-}^2|_{r_{t2}}, \\ \partial_{\rho} u^2|_{\rho=0} = -\frac{1}{r_{t2}} u_{-}^1|_{r_{t2}} + \frac{1}{r_{t2}} \frac{\mu_c}{\mu_t} \partial_r(r u_{-}^1)|_{r_{t2}}. \end{cases}$$

So

$$\begin{aligned} \partial_{\rho} u^2 &= -\frac{1}{r_{t2}} \left(u_{-}^1|_{r_{t2}} - \frac{\mu_c}{\mu_t} \partial_r(r u_{-}^1)|_{r_{t2}} \right) \\ &\quad + \rho \left(-k_1^2 u_{-}^1|_{r_{t2}} + \left(\frac{2}{r_{t2}^2} - \partial_z^2\right) u_{-}^0|_{r_{t2}} - \frac{1}{r_{t2}^2} \frac{\mu_c}{\mu_t} \partial_r(r u_{-}^0)|_{r_{t2}} \right) \\ &\quad + \rho^2 \frac{k_1^2}{2} \left(\frac{2}{r_{t2}} u_{-}^0|_{r_{t2}} - \frac{1}{r_{t2}} \frac{\mu_c}{\mu_t} \partial_r(r u_{-}^0)|_{r_{t2}} \right) + \rho^3 \frac{k_1^4}{6} u_{-}^0|_{r_{t2}}, \end{aligned} \quad (3.49)$$

$$\begin{aligned} u^2 &= u_{-}^2|_{r_{t2}} - \frac{\rho}{r_{t2}} \left(u_{-}^1|_{r_{t2}} - \frac{\mu_c}{\mu_t} \partial_r(r u_{-}^1)|_{r_{t2}} \right) \\ &\quad + \rho^2 \frac{1}{2} \left(-k_1^2 u_{-}^1|_{r_{t2}} + \left(\frac{2}{r_{t2}^2} - \partial_z^2\right) u_{-}^0|_{r_{t2}} - \frac{1}{r_{t2}^2} \frac{\mu_c}{\mu_t} \partial_r(r u_{-}^0)|_{r_{t2}} \right) \\ &\quad + \rho^3 \frac{k_1^2}{6} \left(\frac{2}{r_{t2}} u_{-}^0|_{r_{t2}} - \frac{1}{r_{t2}} \frac{\mu_c}{\mu_t} \partial_r(r u_{-}^0)|_{r_{t2}} \right) + \rho^4 \frac{k_1^4}{24} u_{-}^0|_{r_{t2}}. \end{aligned} \quad (3.50)$$

Using (3.49) at $\rho = 1$ and the explicit expression of the transmission condition for u^2 on Γ_{t2} (3.34), one has on Γ_{t2}

$$-k_1^2 u_-^1 + \frac{1}{r_{t2}} \frac{\mu_c}{\mu_t} \partial_r(r u_-^1) - \left(\partial_z^2 - \frac{k_1^2}{2r_{t2}} - \frac{k_1^4}{6} \right) u_-^0 - \frac{k_1^2}{2r_{t2}} \frac{\mu_c}{\mu_t} \partial_r(r u_-^0) = \frac{1}{r_{t2}} \frac{\mu_c}{\mu_v} \partial_r(r u_+^1) - \frac{\mu_c}{\mu_v} \partial_z^2 u_+^0. \quad (3.51)$$

Therefore, (3.48) and (3.51) yield the approximate transmission conditions at order 1 between u_{\pm}^{δ} on Γ_{t2}

$$\mathcal{Z}_{1,1} \begin{cases} \left(1 - \frac{\delta}{2} k_1^2 \right) u_-^{\delta} + \frac{\delta}{r_{t2}} + \frac{\mu_c}{\mu_t} \partial_r(r u_-^{\delta}) = u_+^{\delta} + \frac{\delta}{r_{t2}} \partial_r(r u_+^{\delta}), & (3.52a) \\ \left(-k_1^2 - \delta \left(\partial_z^2 - \frac{k_1^2}{2r_{t2}} - \frac{k_1^4}{6} \right) \right) u_-^{\delta} + \left(\frac{1}{r_{t2}} - \delta \frac{k_1^2}{2r_{t2}} \right) \frac{\mu_c}{\mu_t} \partial_r(r u_-^{\delta}) \\ = -\delta \frac{\mu_c}{\mu_v} \partial_z^2 u_+^{\delta} + \frac{1}{r_{t2}} \frac{\mu_c}{\mu_v} \partial_r(r u_+^{\delta}). & (3.52b) \end{cases}$$

3. Order $n = 2$.

We derive from (3.50) and the transmission condition on Γ_c for u^1 (3.37)

$$\begin{aligned} u_-^2 - \frac{1}{2} k_1^2 u_-^1 + \frac{1}{r_{t2}} \frac{\mu_c}{\mu_t} \partial_r(r u_-^1) - \left(\frac{k_1^2}{6r_{t2}} - \frac{k_1^4}{24} \right) u_-^0 + \left(\frac{1}{2r_{t2}^2} - \frac{k_1^2}{6r_{t2}} \right) \frac{\mu_c}{\mu_t} \partial_r(r u_-^0) \\ = u_+^2 + \frac{1}{r_{t2}} \partial_r(r u_+^1) + \frac{1}{2r_{t2}^2} \partial_r(r u_+^0). \end{aligned} \quad (3.53)$$

Now we consider the Cauchy problem for u^3 with initial values at $\rho = 0$. From the asymptotic development (3.14) and the transmission conditions (3.16) on Γ_{t2} for u^3 , the Cauchy problem writes

$$\left\{ \begin{aligned} \partial_{\rho}^2 u^3 &= -\mathcal{B}_1^1 u^2 - \mathcal{B}_1^2 u^1 - \mathcal{B}_1^3 u^0 \\ &= -k_1^2 u^2|_{r_{t2}} + \left(\frac{2}{r_{t2}^2} - \partial_z^2 \right) u^1|_{r_{t2}} - \frac{1}{r_{t2}^2} \frac{\mu_c}{\mu_t} \partial_r(r u^1)|_{r_{t2}} \\ &\quad + \rho \left(k_1^2 \left(\frac{2}{r_{t2}} u^1|_{r_{t2}} - \frac{1}{r_{t2}} \frac{\mu_c}{\mu_t} \partial_r(r u^1)|_{r_{t2}} \right) \right. \\ &\quad \left. + \left(-\frac{6}{r_{t2}^3} + \frac{2}{r_{t2}} \partial_z^2 \right) u^0|_{r_{t2}} + \left(\frac{3}{r_{t2}^3} - \frac{1}{r_{t2}} \partial_z^2 \right) \frac{\mu_c}{\mu_t} \partial_r(r u^0)|_{r_{t2}} \right) \\ &\quad + \rho^2 \left(\frac{k_1^4}{2} u^1|_{r_{t2}} + k_1^2 \left(-\frac{9}{2r_{t2}^2} + \partial_z^2 \right) u^0|_{r_{t2}} + \frac{2k_1^2}{r_{t2}^2} \frac{\mu_c}{\mu_t} \partial_r(r u^0)|_{r_{t2}} \right) \\ &\quad + \rho^3 k_1^4 \left(-\frac{1}{2r_{t2}} u^0|_{r_{t2}} + \frac{1}{6r_{t2}} \frac{\mu_c}{\mu_t} \partial_r(r u^0)|_{r_{t2}} \right) - \rho^4 \frac{k_1^6}{24} u^0|_{r_{t2}} \quad \rho \in [0, 1], \\ u_{\rho=0}^3 &= u^3|_{r_{t2}}, \\ \partial_{\rho} u^3|_{\rho=0} &= -\frac{1}{r_{t2}} u^2|_{r_{t2}} + \frac{1}{r_{t2}} \frac{\mu_c}{\mu_t} \partial_r(r u^2)|_{r_{t2}}. \end{aligned} \right.$$

Then we obtain

$$\begin{aligned}
\partial_\rho u^3 &= -\frac{1}{r_{t_2}} u_-^2|_{r_{t_2}} + \frac{1}{r_{t_2}} \frac{\mu_c}{\mu_t} \partial_r(ru_-^2)|_{r_{t_2}} \\
&+ \rho \left(-k_1^2 u_-^2|_{r_{t_2}} + \left(\frac{2}{r_{t_2}^2} - \partial_z^2 \right) u_-^1|_{r_{t_2}} - \frac{1}{r_{t_2}^2} \frac{\mu_c}{\mu_t} \partial_r(ru_-^1)|_{r_{t_2}} \right) \\
&+ \frac{\rho^2}{2} \left(k_1^2 \left(\frac{2}{r_{t_2}} u_-^1|_{r_{t_2}} - \frac{1}{r_{t_2}} \frac{\mu_c}{\mu_t} \partial_r(ru_-^1)|_{r_{t_2}} \right) \right. \\
&\quad \left. + \left(-\frac{6}{r_{t_2}^3} + \frac{2}{r_{t_2}} \partial_z^2 \right) u_-^0|_{r_{t_2}} + \left(\frac{3}{r_{t_2}^3} - \frac{1}{r_{t_2}} \partial_z^2 \right) \frac{\mu_c}{\mu_t} \partial_r(ru_-^0)|_{r_{t_2}} \right) \\
&+ \frac{\rho^3}{3} \left(\frac{k_1^4}{2} u_-^1|_{r_{t_2}} + k_1^2 \left(-\frac{9}{2r_{t_2}^2} + \partial_z^2 \right) u_-^0|_{r_{t_2}} + \frac{2k_1^2}{r_{t_2}^2} \frac{\mu_c}{\mu_t} \partial_r(ru_-^0)|_{r_{t_2}} \right) \\
&+ \frac{\rho^4}{4} k_1^4 \left(-\frac{1}{2r_{t_2}} u_-^0|_{r_{t_2}} + \frac{1}{6r_{t_2}} \frac{\mu_c}{\mu_t} \partial_r(ru_-^0)|_{r_{t_2}} \right) - \rho^5 \frac{k_1^6}{120} u_-^0|_{r_{t_2}} \tag{3.54}
\end{aligned}$$

Taking $\rho = 1$ in (3.54) and considering the transmission condition for u^3 on Γ_{t_2} (3.39), we have

$$\begin{aligned}
&-k_1^2 u_-^2 + \frac{1}{r_{t_2}} \frac{\mu_c}{\mu_t} \partial_r(ru_-^2) - \left(\partial_z^2 - \frac{k_1^2}{2r_{t_2}} - \frac{k_1^4}{6} \right) u_-^1 - \frac{k_1^2}{2r_{t_2}} \frac{\mu_c}{\mu_t} \partial_r(ru_-^1) \\
&+ \left(\left(\frac{1}{2r_{t_2}} + \frac{k_1^2}{3} \right) \partial_z^2 - \left(\frac{2k_1^2}{3r_{t_2}^2} + \frac{k_1^4}{12r_{t_2}} + \frac{k_1^6}{120} \right) \right) u_-^0 + \left(\frac{k_1^2}{2r_{t_2}^2} + \frac{k_1^4}{24r_{t_2}} \right) \frac{\mu_c}{\mu_t} \partial_r(ru_-^0) \\
&= \frac{1}{r_{t_2}} \frac{\mu_c}{\mu_v} \partial_r(ru_+^2) - \partial_z^2 u_+^1 + \frac{1}{2r_{t_2}} \frac{\mu_c}{\mu_v} \partial_z^2 u_+^0. \tag{3.55}
\end{aligned}$$

From (3.53) and (3.55), we conclude the second order approximate transmission conditions for u_\pm^δ on Γ_{t_2}

$$\mathcal{Z}_{1,2} \left\{ \begin{aligned} &\left(1 - \frac{\delta}{2} k_1^2 - \delta^2 \left(\frac{k_1^2}{6r_{t_2}} - \frac{k_1^4}{24} \right) \right) u_-^\delta + \left(\frac{\delta}{r_{t_2}} + \delta^2 \left(\frac{1}{2r_{t_2}^2} - \frac{k_1^2}{6r_{t_2}} \right) \right) \frac{\mu_c}{\mu_t} \partial_r(ru_-^\delta) \\ &= u_+^\delta + \left(\frac{\delta}{r_{t_2}} + \frac{\delta^2}{2r_{t_2}^2} \right) \partial_r(ru_+^\delta), \tag{3.56a} \\ &\left(-k_1^2 - \delta \left(\partial_z^2 - \frac{k_1^2}{2r_{t_2}} - \frac{k_1^4}{6} \right) + \delta^2 \left(\left(\frac{1}{2r_{t_2}} + \frac{k_1^2}{3} \right) \partial_z^2 - \frac{2k_1^2}{3r_{t_2}^2} - \frac{k_1^4}{12r_{t_2}} - \frac{k_1^6}{120} \right) \right) u_-^\delta \\ &+ \left(\frac{1}{r_{t_2}} - \delta \frac{k_1^2}{2r_{t_2}} + \delta^2 \left(\frac{k_1^2}{2r_{t_2}^2} + \frac{k_1^4}{24r_{t_2}} \right) \right) \frac{\mu_c}{\mu_t} \partial_r(ru_-^\delta) \\ &= \left(-\delta + \frac{\delta^2}{2r_{t_2}} \frac{\mu_c}{\mu_v} \right) \partial_z^2 u_+^\delta + \frac{1}{r_{t_2}} \frac{\mu_c}{\mu_v} \partial_r(ru_+^\delta). \tag{3.56b} \end{aligned} \right.$$

Rescaling parameter $m = 2$

1. Order $n = 0$.

The asymptotic development (3.15) and the transmission conditions (3.18) on Γ_{t_2} for w^0 lead to the Cauchy problem for w^0 with initial values at $\rho = 0$

$$\begin{cases} (\partial_\rho^2 + k_2^2)w^0 = 0 & \rho \in [0, 1], \\ w^0|_{\rho=0} = \sqrt{r_{t_2}}u_-^0|_{r_{t_2}}, \\ \partial_\rho w^0|_{\rho=0} = 0. \end{cases}$$

The solution and its derivative writes

$$\begin{cases} w^0 = \sqrt{r_{t_2}}u_-^0|_{r_{t_2}} \cos(k_2\rho), & (3.57a) \\ \partial_\rho w^0 = -\sqrt{r_{t_2}}u_-^0|_{r_{t_2}} k_2 \sin(k_2\rho). & (3.57b) \end{cases}$$

We consider the transmission conditions (3.18) on Γ_c for w^0 , which writes explicitly

$$\begin{cases} w^0|_{\rho=1} = \sqrt{r_{t_2}}u_+^0|_{r_{t_2}}, & (3.58a) \\ \partial_\rho w^0|_{\rho=1} = 0. & (3.58b) \end{cases}$$

By taking $\rho = 1$ in (3.57) and by comparing them with (3.58), we get

$$u_-^0|_{r_{t_2}} = u_+^0|_{r_{t_2}} = 0. \quad (3.59)$$

Therefore, at order 0, the approximate transmission conditions $\mathcal{Z}_{2,0}$ for u_\pm^δ on Γ_{t_2} becomes Dirichlet boundary conditions

$$\mathcal{Z}_{2,0} \quad u_-^\delta = u_+^\delta = 0. \quad (3.60)$$

These conditions model the conductive deposit as a perfect conductor.

2. Order $n = 1$.

The Cauchy problem for w^1 writes

$$\begin{cases} (\partial_\rho^2 + k_2^2)w^1 = -\mathcal{B}_2^1 w^0 = 0 & \rho \in [0, 1], \\ w^1|_{\rho=0} = \sqrt{r_{t_2}}u_-^1|_{r_{t_2}}, \\ \partial_\rho w^1|_{\rho=0} = \frac{1}{\sqrt{r_{t_2}}} \left(-\frac{1}{2}u_-^0|_{r_{t_2}} + \frac{\mu_c}{\mu_t} \partial_r(ru_-^0)|_{r_{t_2}} \right), \end{cases}$$

where the initial values are just the transmission conditions (3.18) on Γ_{t_2} . Thus we have

$$\begin{cases} w^1 = \sqrt{r_{t_2}}u_-^1|_{r_{t_2}} \cos(k_2\rho) + \frac{1}{\sqrt{r_{t_2}}} \left(-\frac{1}{2}u_-^0 + \frac{\mu_c}{\mu_t} \partial_r(ru_-^0) \right) \Big|_{r_{t_2}} \frac{\sin(k_2\rho)}{k_2}, & (3.61a) \\ \partial_\rho w^1 = -\sqrt{r_{t_2}}u_-^1|_{r_{t_2}} k_2 \sin(k_2\rho) + \frac{1}{\sqrt{r_{t_2}}} \left(-\frac{1}{2}u_-^0 + \frac{\mu_c}{\mu_t} \partial_r(ru_-^0) \right) \Big|_{r_{t_2}} \cos(k_2\rho). & (3.61b) \end{cases}$$

Otherwise, the transmission conditions (3.18) on Γ_c for w^1 write

$$\begin{cases} w^1|_{\rho=1} = \sqrt{r_{t_2}}u_+^1|_{r_{t_2}} - \frac{1}{2\sqrt{r_{t_2}}}u_+^0|_{r_{t_2}} + \frac{1}{\sqrt{r_{t_2}}} \partial_r(ru_+^0)|_{r_{t_2}} & (3.62a) \\ \partial_\rho w^1|_{\rho=1} = -\frac{1}{2\sqrt{r_{t_2}}}u_+^0|_{r_{t_2}} + \frac{1}{\sqrt{r_{t_2}}} \frac{\mu_c}{\mu_v} \partial_r(ru_+^0)|_{r_{t_2}} & (3.62b) \end{cases}$$

Taking $\rho = 1$ in (3.61) and considering (3.62) imply

$$\begin{cases} \cos(k_2)u_-^1 + \frac{1}{r_{t_2}} \frac{\sin(k_2)}{k_2} \frac{\mu_c}{\mu_t} \partial_r(ru_-^0) = u_+^1 + \frac{1}{r_{t_2}} \partial_r(ru_+^0), & (3.63a) \\ -\sin(k_2)u_-^1 + \frac{1}{r_{t_2}} \frac{\cos(k_2)}{k_2} \frac{\mu_c}{\mu_t} \partial_r(ru_-^0) = \frac{1}{r_{t_2}} \frac{1}{k_2} \frac{\mu_c}{\mu_v} \partial_r(ru_+^0). & (3.63b) \end{cases}$$

So from (3.63) we obtain the first order approximate transmission conditions between u_{\pm}^{δ} on Γ_{t_2}

$$\mathcal{Z}_{2,1} \begin{cases} \cos(k_2)u_-^{\delta} + \frac{\delta}{r_{t_2}} \frac{\sin(k_2)}{k_2} \frac{\mu_c}{\mu_t} \partial_r(ru_-^{\delta}) = u_+^{\delta} + \frac{\delta}{r_{t_2}} \partial_r(ru_+^{\delta}), & (3.64a) \\ -\sin(k_2)u_-^{\delta} + \frac{\delta}{r_{t_2}} \frac{\cos(k_2)}{k_2} \frac{\mu_c}{\mu_t} \partial_r(ru_-^{\delta}) = \frac{\delta}{r_{t_2}} \frac{1}{k_2} \frac{\mu_c}{\mu_v} \partial_r(ru_+^{\delta}). & (3.64b) \end{cases}$$

3. Order $n = 2$.

With the transmission conditions (3.18) for w^2 on Γ_{t_2} as initial values, the Cauchy problem for w^2 writes

$$\begin{cases} (\partial_{\rho}^2 + k_2^2)w^2 = -\mathcal{B}_2^1 w^1 - \mathcal{B}_2^2 w^0 = \sqrt{r_{t_2}} \left(\frac{3}{4r_{t_2}^2} - \partial_z^2 \right) u_-^0|_{r_{t_2}} \cos(k_2 \rho) & \rho \in [0, 1], \\ w^2|_{\rho=0} = \sqrt{r_{t_2}} u_-^2|_{r_{t_2}}, \\ \partial_{\rho} w^2|_{\rho=0} = \frac{1}{\sqrt{r_{t_2}}} \left(-\frac{1}{2} u_-^1|_{r_{t_2}} + \frac{\mu_c}{\mu_t} \partial_r(ru_-^1)|_{r_{t_2}} \right), \end{cases}$$

Using the computing algorithm for $m = 2$ described in Section 3.2.3, in particular the formula (3.22), one obtains

$$\begin{cases} w^2|_{\rho=1} = \left(\sqrt{r_{t_2}} u_-^2 + \frac{1 - e^{i2k_2} - i2k_2}{8k_2^2} \sqrt{r_{t_2}} (\partial_z^2 - \frac{3}{4r_{t_2}^2}) u_-^0 \right) \Big|_{r_{t_2}} \cos(k_2) \\ + \left\{ \frac{1}{\sqrt{r_{t_2}}} \left(-\frac{1}{2} u_-^1 + \frac{\mu_c}{\mu_t} \partial_r(ru_-^1) \right) - \frac{i(1 - e^{i2k_2} - i2k_2)}{8k_2} \sqrt{r_{t_2}} (\partial_z^2 - \frac{3}{4r_{t_2}^2}) u_-^0 \right\} \Big|_{r_{t_2}} \frac{\sin(k_2)}{k_2} \\ + \left(\frac{i \sin k_2}{4k_2^2} + \frac{ie^{ik_2}}{4k_2} \right) \sqrt{r_{t_2}} (\partial_z^2 - \frac{3}{4r_{t_2}^2}) u_-^0|_{r_{t_2}}, & (3.65a) \\ \partial_{\rho} w^1 = - \left(\sqrt{r_{t_2}} u_-^2 + \frac{1 - e^{i2k_2} - i2k_2}{8k_2^2} \sqrt{r_{t_2}} (\partial_z^2 - \frac{3}{4r_{t_2}^2}) u_-^0 \right) \Big|_{r_{t_2}} k_2 \sin(k_2) \\ + \left\{ \frac{1}{\sqrt{r_{t_2}}} \left(-\frac{1}{2} u_-^1 + \frac{\mu_c}{\mu_t} \partial_r(ru_-^1) \right) - \frac{i(1 - e^{i2k_2} - i2k_2)}{8k_2} \sqrt{r_{t_2}} (\partial_z^2 - \frac{3}{4r_{t_2}^2}) u_-^0 \right\} \Big|_{r_{t_2}} \cos(k_2) \\ - \left(\frac{\sin k_2}{4k_2} + \frac{e^{ik_2}}{4} \right) \sqrt{r_{t_2}} (\partial_z^2 - \frac{3}{4r_{t_2}^2}) u_-^0|_{r_{t_2}}. & (3.65b) \end{cases}$$

Otherwise, the transmission conditions (3.19) for w^2 on Γ_c write

$$\left\{ \begin{array}{l} w^2|_{\rho=1} = \sqrt{r_{t_2}} u_+^2|_{r_{t_2}} - \frac{1}{2\sqrt{r_{t_2}}} u_+^1|_{r_{t_2}} + \frac{1}{\sqrt{r_{t_2}}} \partial_r(ru_+^1)|_{r_{t_2}} \\ \quad - \frac{\sqrt{r_{t_2}}}{2} \left(\partial_z^2 - \frac{3}{4r_{t_2}^2} \right) u_+^0|_{r_{t_2}}, \end{array} \right. \quad (3.66a)$$

$$\left\{ \begin{array}{l} \partial_\rho w^2|_{\rho=1} = -\frac{1}{2\sqrt{r_{t_2}}} u_+^1|_{r_{t_2}} + \frac{1}{\sqrt{r_{t_2}}} \frac{\mu_c}{\mu_v} \partial_r(ru_+^1)|_{r_{t_2}} \\ \quad - \sqrt{r_{t_2}} \left(\frac{\mu_c}{\mu_v} \partial_z^2 - \frac{3}{4r_{t_2}^2} \right) u_+^0|_{r_{t_2}} + \frac{1}{2r_{t_2}\sqrt{r_{t_2}}} \left(\frac{\mu_c}{\mu_v} - 1 \right) \partial_r(ru_+^0)|_{r_{t_2}}. \end{array} \right. \quad (3.66b)$$

From (3.65) and (3.66) we have

$$\left\{ \begin{array}{l} \cos(k_2)u_-^2 + \frac{1}{r_{t_2}} \frac{\sin(k_2)}{k_2} \frac{\mu_c}{\mu_t} \partial_r(ru_-^1) + \frac{1}{2r_{t_2}^2} \left(\frac{\csc(k_2)}{k_2} - \frac{\cos(k_2)}{k_2^2} \right) \frac{\mu_c}{\mu_t} \partial_r(ru_-^0) \\ \quad = u_+^2 + \frac{1}{r_{t_2}} \partial_r(ru_+^1) - \frac{1}{2r_{t_2}^2} \left[\left(\frac{1}{k_2^2} - \frac{\cot(k_2)}{k_2} \right) \frac{\mu_c}{\mu_v} - 1 \right] \partial_r(ru_+^0), \end{array} \right. \quad (3.67a)$$

$$\left\{ \begin{array}{l} -\sin(k_2)u_-^2 + \frac{1}{r_{t_2}} \frac{\cos(k_2)}{k_2} \frac{\mu_c}{\mu_t} \partial_r(ru_-^1) + \frac{1}{2r_{t_2}^2} \frac{\sin(k_2)}{k_2^2} \frac{\mu_c}{\mu_t} \partial_r(ru_-^0) \\ \quad = \frac{1}{r_{t_2}} \frac{1}{k_2} \frac{\mu_c}{\mu_v} \partial_r(ru_+^1) + \frac{1}{2r_{t_2}^2} \frac{1}{k_2} \partial_r(ru_+^0). \end{array} \right. \quad (3.67b)$$

Therefore, we conclude that the second order approximate transmission conditions $\mathcal{Z}_{2,2}$ between u_\pm^δ on Γ_{t_2} write

$$\mathcal{Z}_{2,2} \left\{ \begin{array}{l} \cos(k_2)u_-^\delta + \left(\frac{\delta}{r_{t_2}} \frac{\sin(k_2)}{k_2} + \frac{\delta^2}{2r_{t_2}^2} \left(\frac{\csc(k_2)}{k_2} - \frac{\cos(k_2)}{k_2^2} \right) \right) \frac{\mu_c}{\mu_t} \partial_r(ru_-^\delta) \\ \quad = u_+^\delta + \left[\frac{\delta}{r_{t_2}} - \frac{\delta^2}{2r_{t_2}^2} \left(\left(\frac{1}{k_2^2} - \frac{\cot(k_2)}{k_2} \right) \frac{\mu_c}{\mu_v} - 1 \right) \right] \partial_r(ru_+^\delta), \end{array} \right. \quad (3.68a)$$

$$\left\{ \begin{array}{l} -\sin(k_2)u_-^\delta + \left(\frac{\delta}{r_{t_2}} \frac{\cos(k_2)}{k_2} + \frac{\delta^2}{2r_{t_2}^2} \frac{\sin(k_2)}{k_2^2} \right) \frac{\mu_c}{\mu_t} \partial_r(ru_-^\delta) \\ \quad = \left(\frac{\delta}{r_{t_2}} \frac{1}{k_2} \frac{\mu_c}{\mu_v} + \frac{\delta^2}{2r_{t_2}^2} \frac{1}{k_2} \right) \partial_r(ru_+^\delta). \end{array} \right. \quad (3.68b)$$

3.2.5 Numerical tests for 1-D models

To choose the (m, n) with which the asymptotic model has a best approximation, we test numerically the asymptotic models by implementing the transmission conditions $\mathcal{Z}_{m,n}$ for $m = 0, 1, 2$ and $n = 0, 1, 2$ in the 1-D case, i.e. $\partial_z = 0$, since the 1-D eddy current models discussed in Section 1.7 have analytic solutions, which allow us to estimate modeling errors. We write the transmission conditions $\mathcal{Z}_{m,2}$ for $m = 0, 1, 2$ at order $n = 2$ in a general form

$$\begin{cases} \alpha_1^m u_-^\delta + \beta_1^m \partial_r(ru_-^\delta) = \gamma_1^m u_+^\delta + \eta_1^m \partial_r(ru_+^\delta), \\ \alpha_2^m u_-^\delta + \beta_2^m \partial_r(ru_-^\delta) = \gamma_2^m u_+^\delta + \eta_2^m \partial_r(ru_+^\delta). \end{cases} \quad (3.69)$$

The transmission conditions $\mathcal{Z}_{m,n}$ at order $n = 0, 1$ can be derived from $\mathcal{Z}_{m,2}$ by neglecting the high order terms. We give the coefficients α_j^m , β_j^m , γ_j^m and η_j^m , $m = 0, 1, 2$, $j = 1, 2$ as below.

1. $m = 0$.

From $\mathcal{Z}_{0,2}$ given by (3.41), we have

$$\begin{aligned} \alpha_1^0 &= 1 - \delta^2 \frac{k_0^2}{2}, & \alpha_2^0 &= -\delta k_0^2 + \delta^2 \frac{k_0^2}{2r_{t_2}}, \\ \beta_1^0 &= \delta \frac{1}{r_{t_2}} \frac{\mu_c}{\mu_t} + \delta^2 \frac{1}{2r_{t_2}^2} \frac{\mu_c}{\mu_t}, & \beta_2^0 &= \frac{1}{r_{t_2}} \frac{\mu_c}{\mu_t} - \delta^2 \frac{k_0^2}{2r_{t_2}} \frac{\mu_c}{\mu_t}, \\ \gamma_1^0 &= 1, & \gamma_2^0 &= 0, \\ \eta_1^0 &= \delta \frac{1}{r_{t_2}} + \delta^2 \frac{1}{2r_{t_2}^2}, & \eta_2^0 &= \frac{1}{r_{t_2}} \frac{\mu_c}{\mu_v}. \end{aligned}$$

One gets easily the coefficients corresponding to $\mathcal{Z}_{0,0}$ (see (3.29)) by considering only the terms on order $\mathcal{O}(1)$ of δ , and those corresponding to $\mathcal{Z}_{0,1}$ (see (3.36)) by neglecting the terms on order $\mathcal{O}(\delta^2)$.

2. $m = 1$.

The transmission conditions $\mathcal{Z}_{1,2}$ given by (3.56) yields

$$\begin{aligned} \alpha_1^1 &= 1 - \delta \frac{k_1^2}{2} - \delta^2 \left(\frac{k_1^2}{6r_{t_2}} - \frac{k_1^4}{24} \right), & \alpha_2^1 &= -k_1^2 + \delta \left(\frac{k_1^2}{2r_{t_2}} + \frac{k_1^4}{6} \right) - \delta^2 \left(\frac{2k_1^2}{3r_{t_2}^2} + \frac{k_1^4}{12r_{t_2}} + \frac{k_1^6}{120} \right), \\ \beta_1^1 &= \left(\frac{\delta}{r_{t_2}} + \delta^2 \left(\frac{1}{2r_{t_2}^2} - \frac{k_1^2}{6r_{t_2}} \right) \right) \frac{\mu_c}{\mu_t}, & \beta_2^1 &= \left(\frac{1}{r_{t_2}} - \delta \frac{k_1^2}{2r_{t_2}} + \delta^2 \left(\frac{k_1^2}{2r_{t_2}^2} + \frac{k_1^4}{24r_{t_2}} \right) \right) \frac{\mu_c}{\mu_t}, \\ \gamma_1^1 &= 1, & \gamma_2^1 &= 0, \\ \eta_1^1 &= \delta \frac{1}{r_{t_2}} + \delta^2 \frac{1}{2r_{t_2}^2}, & \eta_2^1 &= \frac{1}{r_{t_2}} \frac{\mu_c}{\mu_v}. \end{aligned}$$

For $\mathcal{Z}_{1,0}$ given by (3.47), one needs only to take the terms on order $\mathcal{O}(1)$ of δ in the above coefficients. For $\mathcal{Z}_{1,1}$ (see (3.52)), we neglect the terms on order $\mathcal{O}(\delta^2)$.

3. $m = 2$.

The transmission conditions $\mathcal{Z}_{2,2}$ (3.68) yield

$$\begin{aligned} \alpha_1^2 &= \cos(k_2), & \alpha_2^2 &= -\sin(k_2), \\ \beta_1^2 &= \left(\frac{\delta}{r_{t_2}} \frac{\sin k_2}{k_2} + \frac{\delta^2}{2r_{t_2}^2} \left(\frac{\csc(k_2)}{k_2} - \frac{\cos(k_2)}{k_2^2} \right) \right) \frac{\mu_c}{\mu_t}, & \beta_2^2 &= \left(\frac{\delta}{r_{t_2}} \frac{\cos(k_2)}{k_2} + \frac{\delta^2}{2r_{t_2}^2} \frac{\sin(k_2)}{k_2^2} \right) \frac{\mu_c}{\mu_t}, \\ \gamma_1^2 &= 1, & \gamma_2^2 &= 0, \\ \eta_1^2 &= \delta \frac{1}{r_{t_2}} - \delta^2 \frac{1}{2r_{t_2}^2} \left(\left(\frac{1}{k_2^2} - \frac{\cot(k_2)}{k_2} \right) \frac{\mu_c}{\mu_v} - 1 \right), & \eta_2^2 &= \delta \frac{1}{r_{t_2}} \frac{1}{k_2} \frac{\mu_c}{\mu_v} + \delta^2 \frac{1}{2r_{t_2}^2} \frac{1}{k_2}. \end{aligned}$$

We observe that terms on order $\mathcal{O}(1)$ of δ in the above coefficients gives the transmission conditions $\mathcal{Z}_{2,0}$ (see (3.60)). If we consider additionally the terms on $\mathcal{O}(\delta)$, then we obtain the transmission conditions $\mathcal{Z}_{2,1}$ (see (3.64)).

With these approximate transmission conditions $\mathcal{Z}_{m,n}$, we build the 1-D asymptotic models by supposing that there is no variation in the axial (z) direction. As shown in Section 1.7, we may introduce a Dirac distribution like applied electric current $J\delta_{r_s}$ at $r = r_s$, which yields the transmission conditions (1.50) – (1.51) at r_s . The analytic solution of the full 1-D model writes

$$u(r) = \begin{cases} c_1 r & 0 < r < r_s, \\ c_2 r + c_3 \frac{1}{r} & r_s < r < r_{t_1}, \\ c_4 J_1(k_t r) + c_5 Y_1(k_t r) & r_{t_1} < r < r_{t_2}, \\ c_6 J_1(k_c r) + c_7 Y_1(k_c r) & r_{t_2} < r < r_{t_2} + \delta, \\ c_8 \frac{1}{r} & r > r_{t_2} + \delta, \end{cases}$$

with $k_t^2 = i\omega\mu_t\sigma_t$ and $k_c^2 = i\omega\mu_c\sigma_c$.

With the transmission conditions $[u] = [\mu^{-1}\partial_r(ru)] = 0$ at $r = r_{t_1}$, r_{t_2} and $r_{t_2} + \delta$, the coefficients $\mathbf{c} = (c_1, \dots, c_8)^T$ can be obtained by resolving a linear system

$$A\mathbf{c} = (0, -i\omega\mu J, 0, \dots, 0)^T$$

and

$$A = \begin{pmatrix} r_s & -r_s & -\frac{1}{r_s} & 0 & 0 & 0 & 0 & 0 & 0 \\ 2 & -2 & 0 & 0 & 0 & 0 & 0 & 0 & 0 \\ 0 & r_{t_1} & \frac{1}{r_{t_1}} & -J_1(k_t r_{t_1}) & -Y_1(k_t r_{t_1}) & 0 & 0 & 0 & 0 \\ 0 & \frac{2}{\mu_v} & 0 & -\frac{k_t J_0(k_t r_{t_1})}{\mu_t} & -\frac{k_t Y_0(k_t r_{t_1})}{\mu_t} & 0 & 0 & 0 & 0 \\ 0 & 0 & 0 & \frac{J_1(k_t r_{t_2})}{k_3 J_0(k_3 r_{t_2})} & \frac{Y_1(k_t r_{t_2})}{k_3 Y_0(k_3 r_{t_2})} & -\frac{J_1(k_c r_{t_2})}{k_c J_0(k_c r_{t_2})} & -\frac{Y_1(k_c r_{t_2})}{k_c Y_0(k_c r_{t_2})} & 0 & 0 \\ 0 & 0 & 0 & \frac{\mu_t}{0} & \frac{\mu_t}{0} & \frac{\mu_c}{J_1(k_c(r_{t_2} + \delta))} & \frac{\mu_c}{Y_1(k_c(r_{t_2} + \delta))} & -\frac{1}{(r_{t_2} + \delta)} & 0 \\ 0 & 0 & 0 & 0 & 0 & \frac{k_c J_0(k_c(r_{t_2} + \delta))}{\mu_c} & \frac{k_c Y_0(k_c(r_{t_2} + \delta))}{\mu_c} & 0 & 0 \end{pmatrix}.$$

The analytic solution of the asymptotic models is in the form

$$u^\delta(r) = \begin{cases} u_-^\delta = \begin{cases} c_1^\delta r & 0 < r < r_s, \\ c_2^\delta r + c_3^\delta \frac{1}{r} & r_s < r < r_{t_1}, \\ c_4^\delta J_1(k_t r) + c_5^\delta Y_1(k_t r) & r_{t_1} < r < r_{t_2}, \end{cases} \\ u_+^\delta = c_6^\delta \frac{1}{r} & r > r_{t_2}. \end{cases}$$

With the transmission conditions $[u] = [\mu^{-1}\partial_r(ru)] = 0$ at $r = r_{t_1}$ and the approximate transmission conditions $\mathcal{Z}_{m,n}$ (3.69) at $r = r_{t_2}$ we obtain a linear system for the coefficients $\mathbf{c}^\delta = (c_1^\delta, \dots, c_6^\delta)$

$$A^\delta \mathbf{c}^\delta = (0, -i\omega\mu J, 0, \dots, 0)^T,$$

where

$$A^\delta = \begin{pmatrix} r_s & -r_s & -\frac{1}{r_s} & 0 & 0 & 0 \\ 2 & -2 & 0 & 0 & 0 & 0 \\ 0 & r_{t_1} & \frac{1}{r_{t_1}} & -J_1(k_t r_{t_1}) & -Y_1(k_t r_{t_1}) & 0 \\ 0 & \frac{2}{\mu_v} & 0 & -\frac{k_t J_0(k_t r_{t_1})}{\mu_t} & -\frac{k_t Y_0(k_t r_{t_1})}{\mu_t} & 0 \\ 0 & 0 & 0 & \alpha_1^m J_1(k_t r_{t_2}) + \beta_1^m k_t J_0(k_t r_{t_2}) & \alpha_1^m Y_1(k_t r_{t_2}) + \beta_1^m k_t Y_0(k_t r_{t_2}) & -\gamma_1^m \frac{1}{r_{t_2}} \\ 0 & 0 & 0 & \alpha_2^m J_1(k_t r_{t_2}) + \beta_2^m k_t J_0(k_t r_{t_2}) & \alpha_2^m Y_1(k_t r_{t_2}) + \beta_2^m k_t Y_0(k_t r_{t_2}) & -\gamma_2^m \frac{1}{r_{t_2}} \end{pmatrix}.$$

Tests with fixed rescaled conductivities

We first fix the rescaled conductivities of the thin layer deposits σ_m , $m = 0, 1, 2$. Ignoring the physical unities, we take in our tests

$$\begin{aligned} \sigma_0 &= 5 \times 10^6, \\ \sigma_1 &= 1 \times 10^3, \\ \sigma_2 &= 5 \times 10^{-1}. \end{aligned}$$

Then we evaluate the relative errors of the asymptotic models using $\mathcal{Z}_{m,n}$ ($n = 0, 1, 2$) approximate transmission conditions with respect to the full model. We remark that here the deposit conductivity in the full model is variable according to the layer thickness δ :

$$\sigma_c = \frac{\sigma_m}{\delta^m}.$$

We also recall that the permeability of the deposit is $\mu_c = \mu_v$, the conductivity of tube $\sigma_t = 9.7 \times 10^5 S/m$ and the permeability of tube $\mu_t = 1.01\mu_v$.

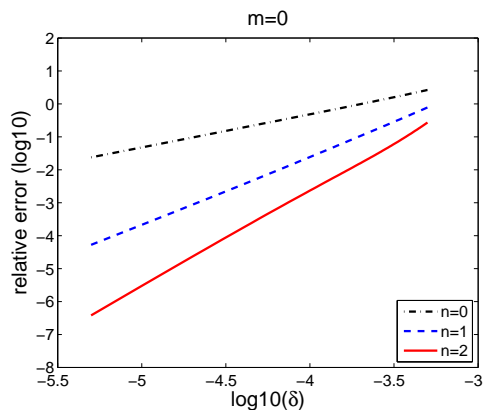
Figure 3.2 shows the relative errors in $L^2_{1/2}$ -norm of solutions of the asymptotic models with respect to the full model for fixed rescaled conductivities σ_m , $m = 0, 1, 2$. One observes that for a given rescaling parameter m , the asymptotic models approximate better the full model as the asymptotic expansion order n increases. The slopes given in the figure validate numerically the above asymptotic models using approximate transmission conditions $\mathcal{Z}_{m,n}$ with the corresponding orders of approximation.

Tests with real deposit conductivity

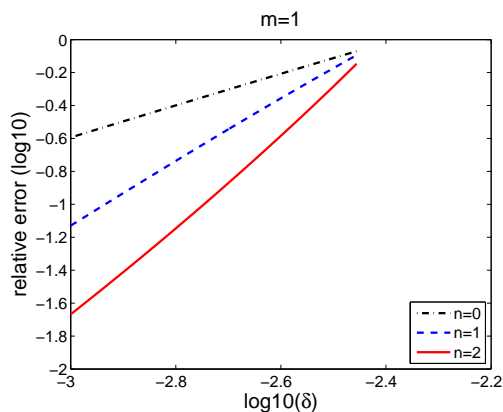
We consider a thin layer of copper covering the tube with constant thickness. The conductivity of copper is $\sigma_c = 5.8 \times 10^7 S/m$ and its permeability is $\mu_c = \mu_v$. σ_t and μ_t are the same as in the previous tests. We vary the thickness δ from $5\mu m$ to $200\mu m$ and evaluate the differences between the solutions u^δ of the asymptotic models with the solution u of the full model.

Figure 3.3 shows that with a given rescaling parameter $m = 0, 1, \text{ or } 2$, the approximation gets better as the asymptotic expansion order n increases. One observes in Figure 3.3c that for a layer thickness under $200\mu m$, the asymptotic model using the transmission conditions $\mathcal{Z}_{2,0}$ is not a good approximation. This is because the $\mathcal{Z}_{2,0}$ conditions model the thin layer as perfect conductor, which is not true for copper through which the electrical field can still penetrate.

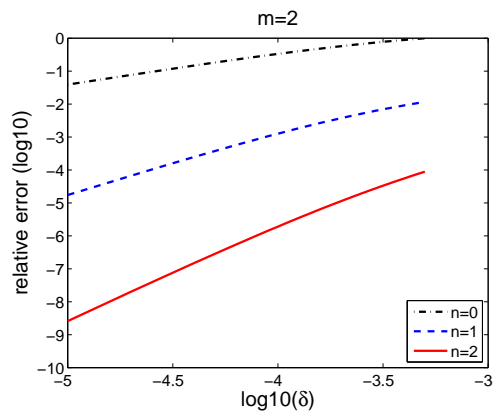
From the comparisons shown in Figure 3.4, we can conclude that for the asymptotic development order $n = 2$, the asymptotic model using the approximate transmission conditions



(a) $\sigma_0 = 5 \times 10^6$



(b) $\sigma_1 = 1 \times 10^3$



(c) $\sigma_2 = 5 \times 10^{-1}$

Figure 3.2: $L^2_{1/2}$ -norm relative errors of asymptotic models with $\mathcal{Z}_{m,n}$ transmission conditions with fixed re-scaled conductivities.

$\mathcal{Z}_{2,2}$ is the best approximation of the full model among the three choices of the rescaling parameter $m = 0, 1, 2$. However, we remark that in the corresponding coefficients $\alpha_j^2, \beta_j^2, \gamma_j^2$ and

η_j^2 , $j = 1, 2$, the layer thickness δ , which we would like to reconstruct in the inverse problem, appears not only as polynomial factors but also implicitly in the trigonometric terms $\sin(k_2)$ and $\cos(k_2)$, now that $k_2^2 = i\omega\mu_c\sigma_2 = i\omega\mu_c\sigma_c\delta^2$. Hence it will be difficult to deduce the inverse problems from direct asymptotic models using $\mathcal{Z}_{2,2}$.

Meanwhile, one observes that the asymptotic models using $\mathcal{Z}_{1,n}$ are good approximations of the full model. For instance, if we choose a threshold of 1% relative error to judge whether an asymptotic model is accurate, then one observes in Figure 3.3b that even the asymptotic model using $\mathcal{Z}_{1,0}$ gives a good approximation for thickness δ under $50\mu m$, which covers already a large range of interested thickness in industrial practice (see Table 3.1). The asymptotic model using $\mathcal{Z}_{1,1}$ ameliorates the precision for the full range of interested thickness (say, $\delta < 150\mu m$). With $m = 1$, the layer thickness δ appears only as polynomial factors in the coefficients α_j^1 , β_j^1 , γ_j^1 and η_j^1 , $j = 1, 2$, which facilitate the deduction of inverse method for the reconstruction of thickness.

Therefore, we will focus on the asymptotic models using $\mathcal{Z}_{1,n}$ with $n = 0, 1$ in the following discussion.

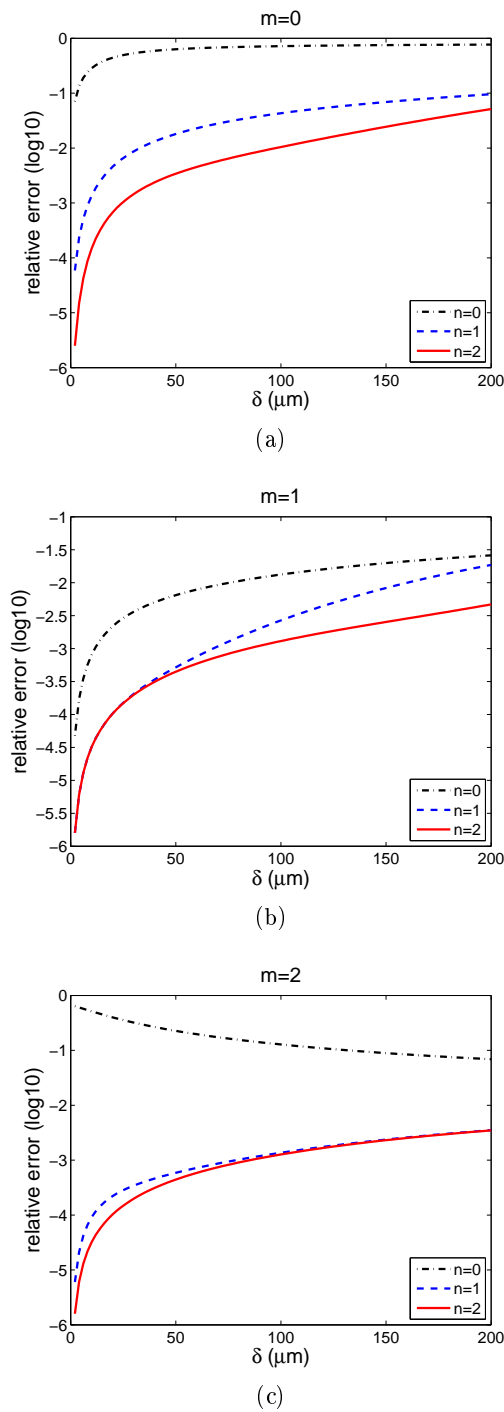
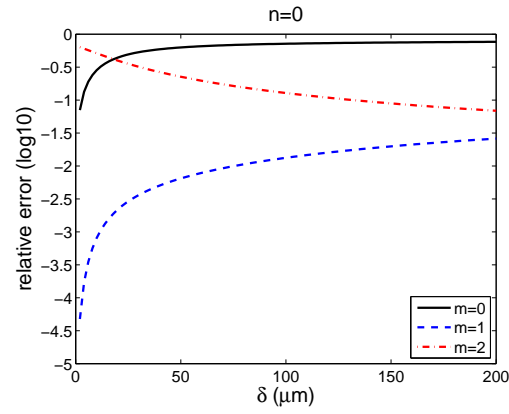
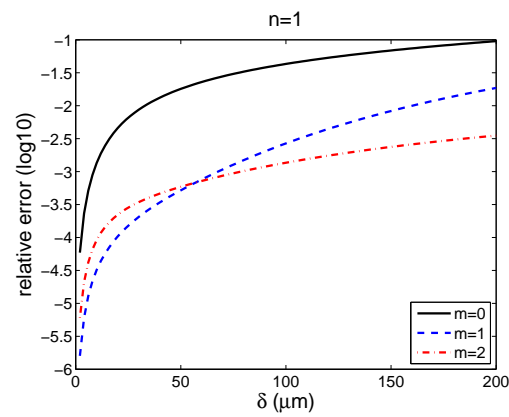


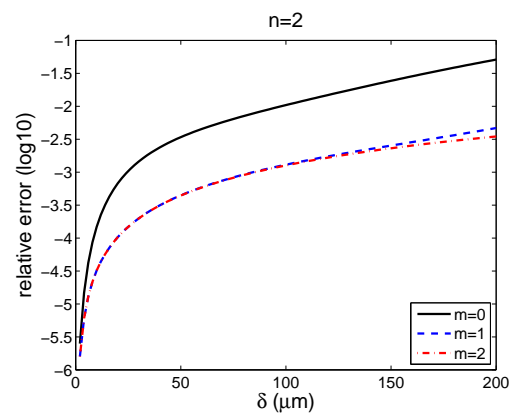
Figure 3.3: $L^2_{1/2}$ -norm relative errors of asymptotic models with $\mathcal{Z}_{m,n}$ transmission conditions. Comparison between different expansion order n , rescaling parameter m fixed.



(a)



(b)



(c)

Figure 3.4: $L^2_{1/2}$ -norm relative errors of asymptotic models with $\mathcal{Z}_{m,n}$ transmission conditions. Comparison between different rescaling parameters m , expansion order n fixed

Reconstruction of deposit thin layers via asymptotic models

Contents

4.1	Asymptotic models for deposits with variable layer thickness	112
4.1.1	Formal derivation of approximate transmission conditions $\mathcal{Z}_{1,0}$	112
4.1.2	The asymptotic model of order 0	113
4.1.3	Formal derivation of approximate transmission conditions $\mathcal{Z}_{1,1}$	114
4.1.4	Mixed formulation for the asymptotic model using $\mathcal{Z}_{1,1}$	116
4.1.5	Numerical validation of the 2-D asymptotic models	120
4.1.6	Approximation of the impedance measurements	121
4.1.7	Numerical tests on impedance measurements	123
4.2	Thickness reconstruction via asymptotic model using $\mathcal{Z}_{1,0}$	124
4.2.1	Derivative of the solution with respect to a thickness increment	124
4.2.2	Adjoint state and derivative of the impedance measurements	124
4.2.3	Thickness reconstruction by minimizing a least square cost functional	125
4.3	Thickness reconstruction via asymptotic model using $\mathcal{Z}_{1,1}$	126
4.3.1	Derivative of solution with respect to a thickness increment	126
4.3.2	Adjoint state and derivative of the impedance measurements	127
4.3.3	Thickness reconstruction by minimizing a least square functional	128
4.4	Numerical tests	129
4.4.1	Parameterized thin layers	129
4.4.2	Reconstruction of arbitrary thin layers	130

In the previous chapter, we studied several asymptotic models using interface transmission conditions to replace highly conductive deposit thin layers. From the numerical results in a simplified case where deposit layers are of constant thickness, we concluded that the transmission conditions $\mathcal{Z}_{1,n}$ with $n = 0, 1$ give sufficient precision of modeling and facilitate the design of inverse methods. In this chapter, we will at first build and numerically validate the asymptotic models with these transmission conditions for general configurations where the layer thickness is variable (Section 4.1). Then we formulate the inverse problems for thickness reconstruction as the minimization of a least square cost functional on layer thickness (Sections 4.2 and 4.3). Finally, some numerical examples of thickness reconstructions are given in Section (4.4). For the use of asymptotic models in inverse problems we may cite the works of Guzina – Bonnet [41], Ozdemir – Haddar – Yaka [66] and Park [69].

4.1 Asymptotic models for deposits with variable layer thickness

In this section, by following the procedure described in Section 3.1.4, we compute the transmission conditions $\mathcal{Z}_{1,n}$ for $n = 0, 1$ between u_{\pm} on Γ_{t_2} to build the 2-D model in the variational formulation with some deposit layer of variable thickness (see Figure 4.1).

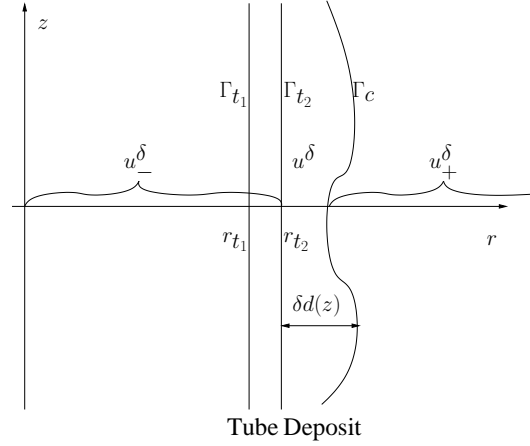


Figure 4.1: Representation of a thin layer deposit.

One remarks that with a slight modification, the formal derivation of asymptotic models described in Section 3.2.3 for deposits with constant thickness works also for cases with variable thickness. Taking $m = 1$, we only have to change the domain $\rho \in [0, 1]$ to $\rho \in [0, d(z)]$ and consider the transmission conditions (3.12) rather than (3.17) on Γ_c .

To simplify the computation, especially the complexities introduced by the transmission conditions (3.12) on the curved boundary Γ_c , we assume that the magnetic permeability of the deposits equals to that of vacuum, that is

$$\mu_c = \mu_v. \quad (4.1)$$

This assumption matches the real case where the deposit is in copper.

4.1.1 Formal derivation of approximate transmission conditions $\mathcal{Z}_{1,0}$

For $(m, n) = (1, 0)$, we apply the procedure of Section 3.2.3 with slight modifications due to the change of deposit domain from a layer with constant thickness to a layer with variable thickness and a curved boundary Γ_c . With the asymptotic development (3.14) and the transmission conditions (3.8) for u^0 on Γ_{t_2} , we have the Cauchy problem for u^0

$$\begin{cases} \partial_{\rho}^2 u^0 = 0 & \rho \in [0, 1], \\ u^0|_{\rho=0} = u_{-}^0|_{r_{t_2}}, \\ \partial_{\rho} u^0|_{\rho=0} = 0. \end{cases}$$

The solution has exactly the same expression (3.42) as in the case for layers with constant thickness. Taking $\rho = d(z)$ in (3.42) and considering the transmission condition (3.12a) for u^0

on Γ_c , we get

$$u_-^0|_{r_{t_2}} = u_+^0|_{r_{t_2}}. \quad (4.2)$$

Then we consider the Cauchy problem for u^1 with initial values given by (3.8) for u^1

$$\begin{cases} \partial_\rho^2 u^1 = -\mathcal{B}_1^1 u^0 = -k_1^2 u^0|_{r_{t_2}} & \rho \in [0, d(z)], \\ u^1|_{\rho=0} = u_-^1|_{r_{t_2}}, \\ \partial_\rho u^1|_{\rho=0} = -\frac{1}{r_{t_2}} u_-^0|_{r_{t_2}} + \frac{1}{r_{t_2}} \frac{\mu_c}{\mu_t} \partial_r(r u_-^0)|_{r_{t_2}}, \end{cases}$$

which implies (3.44) and (3.44) as in the case for layers with constant thickness. The transmission conditions (3.12b) for u^1 on Γ_c imply

$$\partial_\rho u^1|_{\rho=d(z)} = -\frac{1}{r_{t_2}} \left(u_+^0|_{r_{t_2}} - \frac{\mu_c}{\mu_v} \partial_r(r u_+^0)|_{r_{t_2}} \right). \quad (4.3)$$

Equation (3.44) with $\rho = d(z)$ and (4.3) give

$$\frac{1}{r_{t_2}} \frac{\mu_c}{\mu_t} \partial_r(r u_-^0)|_{r_{t_2}} - k_1^2 d(z) u_-^0|_{r_{t_2}} = \frac{1}{r_{t_2}} \frac{\mu_c}{\mu_v} \partial_r(r u_+^0)|_{r_{t_2}}. \quad (4.4)$$

Equations (4.2) and (4.4) and the fact that $k_1^2 = i\omega\sigma_1\mu_c$ imply that

$$\begin{cases} u_+^0 = u_-^0, & (4.5a) \\ \frac{1}{\mu_v} \partial_r(r u_+^0) = \frac{1}{\mu_t} \partial_r(r u_-^0) - i\omega\sigma_1 d(z) r_{t_2} u_-^0. & (4.5b) \end{cases}$$

4.1.2 The asymptotic model of order 0

We denote the solution of the asymptotic problem by

$$u^\delta := \begin{cases} u_-^\delta & \text{in } \Omega_-, \\ u_+^\delta & \text{in } \Omega_+. \end{cases}$$

From (4.5), the approximate transmission conditions at order 0 between $u_\pm^\delta = u_\pm^0$ on Γ_{t_2} write

$$\mathcal{Z}_{1,0} \begin{cases} u_+^\delta = u_-^\delta, & (4.6a) \\ \frac{1}{\mu_v} \partial_r(r u_+^\delta) = \frac{1}{\mu_t} \partial_r(r u_-^\delta) - i\omega\sigma_1 d(z) r_{t_2} u_-^\delta. & (4.6b) \end{cases}$$

The first condition (4.6a) implies the continuity of u^δ through Γ_{t_2} . The strong formulation of the asymptotic model using $\mathcal{Z}_{1,0}$ for u^δ writes

$$\begin{cases} -\operatorname{div} \left(\frac{1}{\mu r} \nabla(r u^\delta) \right) - i\omega\sigma u^\delta = i\omega J & \text{in } \Omega_-, \\ -\operatorname{div} \left(\frac{1}{\mu_v r} \nabla(r u^\delta) \right) = 0 & \text{in } \Omega_+, \\ \text{transmission conditions } \mathcal{Z}_{1,0} & \text{on } \Gamma_{t_2}. \end{cases}$$

We use a generic notation for the variational space $H(\Omega)$ with $\Omega = \Omega_- \cup \Omega_+$ denoting either \mathbb{R}_+^2 or its cut-off $B_{r_*} = \{(r, z) \in \mathbb{R}_+^2 : r < r_*\}$. That is $H(\Omega) = H_{1/2, \lambda}^1(\mathbb{R}_+^2)$ or $H(\Omega) = H_{1/2}^1(B_{r_*})$. We also recall that the variational formulation with $\Omega = B_{r_*}$ can be reduced to a variational formulation posed on $B_{r_*, z_*} = \{(r, z) \in \mathbb{R}^2 : 0 \leq r \leq r_*, |z| < z_*\}$ by introducing appropriate Dirichlet-to-Neumann operators on $z = \pm z_*$ to accelerate the numerical evaluation (see Chapter 1). Then by integration by parts one gets the variational formulation

$$a_{1,0}(u^\delta, v) = \int_{\Omega} i\omega J \bar{v} r \, dr \, dz \quad \forall v \in H(\Omega), \quad (4.7)$$

$$\begin{aligned} \text{where} \quad a_{1,0}(u^\delta, v) := & \int_{\Omega_-} \left(\frac{1}{\mu r} \nabla(ru^\delta) \cdot \nabla(r\bar{v}) - i\omega\sigma u^\delta \bar{v} r \right) dr \, dz \\ & + \int_{\Omega_+} \frac{1}{\mu_v r} \nabla(ru^\delta) \cdot \nabla(r\bar{v}) \, dr \, dz - \int_{\Gamma_{t_2}} i\omega\sigma_1 d(s) u^\delta \bar{v} r \, ds. \end{aligned}$$

Proposition 4.1.1. *Assume that the source $J \in L_{1/2}^2(\Omega)$ has compact support, that the permeability $\mu > 0$ and the conductivity $\sigma \geq 0$ are piecewise constant and bounded in Ω . Assume in addition that there exist $0 < \mu_{\inf} < \mu_{\sup} < +\infty$ such that μ satisfies $\mu_{\inf} < \mu < \mu_{\sup}$. Then variational asymptotic problem (4.7) has a unique solution u^δ in $H(\Omega)$.*

Proof. One verifies that $a_{1,0}$ is a continuous sesquilinear form. It is sufficient to show that $a_{1,0}$ is coercive

$$\begin{aligned} \Re(a_{1,0}(u^\delta, u^\delta)) & \geq \int_{\Omega_-} \frac{1}{\mu r} \left| \nabla(ru^\delta) \right|^2 dr \, dz + \int_{\Omega_+} \frac{1}{\mu_v r} \left| \nabla(ru^\delta) \right|^2 dr \, dz \\ & \geq \frac{1}{\mu_{\sup}} |u^\delta|_{H_{1/2}^1(\Omega)}^2 \geq \frac{C}{\mu_{\sup}} \|u^\delta\|_{H(\Omega)}^2. \end{aligned} \quad (4.8)$$

The last inequality is due to the Poincaré-type inequality (1.5). Therefore, we conclude from the Lax-Milgram Theorem the existence and uniqueness of the solution u^δ . \square

4.1.3 Formal derivation of approximate transmission conditions $\mathcal{Z}_{1,1}$

We pick up the formal derivation in Section 4.1.1 and continue it in higher order to get the approximate transmission conditions $\mathcal{Z}_{1,1}$.

The transmission condition (3.12a) for u^1 writes explicitly

$$u^1|_{\rho=d(z)} = u_+^1|_{r_{t_2}} + \frac{d(z)}{r_{t_2}} (-u_+^0 + \partial_r(ru_+^0))|_{r_{t_2}}. \quad (4.9)$$

From (3.45) with $\rho = d(z)$ and (4.9) we get

$$u_+^1|_{r_{t_2}} = u_-^1|_{r_{t_2}} + \frac{i\omega\sigma_1\mu_c d^2}{2} u_-^0|_{r_{t_2}}. \quad (4.10)$$

To get the second transmission condition for u_\pm^1 , one should consider the Cauchy problem for u^2 . From the asymptotic development (3.14) and the transmission conditions (3.8) for u^2 on

Γ_{t_2} as initial values, we have

$$\left\{ \begin{array}{l} \partial_\rho^2 u^2 = -\mathcal{B}_1^1 u^1 - \mathcal{B}_1^2 u^0 \\ \quad = -k_1^2 u^1|_{r_{t_2}} + \left(\frac{2}{r_{t_2}^2} - \partial_z^2 \right) u_-^0|_{r_{t_2}} - \frac{1}{r_{t_2}^2} \frac{\mu_c}{\mu_t} \partial_r(ru_-^0)|_{r_{t_2}} \\ \quad + \rho k_1^2 \left(\frac{2}{r_{t_2}} u_-^0|_{r_{t_2}} - \frac{1}{r_{t_2}} \frac{\mu_c}{\mu_t} \partial_r(ru_-^0)|_{r_{t_2}} \right) + \rho^2 \frac{k_1^4}{2} u_-^0|_{r_{t_2}} \quad \rho \in [0, d(z)], \\ u^2|_{\rho=0} = u_-^2|_{r_{t_2}}, \\ \partial_\rho u^2|_{\rho=0} = -\frac{1}{r_{t_2}} u_-^1|_{r_{t_2}} + \frac{1}{r_{t_2}} \frac{\mu_c}{\mu_t} \partial_r(ru_-^1)|_{r_{t_2}}. \end{array} \right.$$

The expressions of the solution and its derivative are given in (3.44) and (3.44) respectively. Since $\mu_c = \mu_v$, the transmission condition (3.12b) for u^2 on Γ_c writes

$$\partial_\rho u^2|_{\rho=d(z)} = -\frac{1}{r_{t_2}} (u_+^1 - \partial_r(ru_+^1))|_{r_{t_2}} + d(z) \left(\left(\frac{2}{r_{t_2}^2} - \partial_z^2 \right) u_+^0 - \frac{1}{r_{t_2}^2} \partial_r(ru_+^0) \right) \Big|_{r_{t_2}} \quad (4.11)$$

Comparing (3.44) with $\rho = d(z)$ and (4.11) yields

$$\begin{aligned} \frac{1}{\mu_v} \partial_r(ru_+^1)|_{r_{t_2}} &= \frac{1}{\mu_t} \partial_r(ru_-^1)|_{r_{t_2}} - i\omega\sigma_1 r_{t_2} d(z) u_-^1|_{r_{t_2}} \\ &+ \left(\frac{1}{2} i\omega\sigma_1 d(z)^2 - \frac{1}{6} \omega^2 \sigma_1^2 \mu_c d(z)^3 \right) u_-^0|_{r_{t_2}} - \frac{1}{2} i\omega\sigma_1 \mu_c d(z)^2 \frac{1}{\mu_t} \partial_r(ru_-^0)|_{r_{t_2}}. \end{aligned} \quad (4.12)$$

We introduce the notations of difference $[\cdot]$ and mean $\langle \cdot \rangle$

$$\begin{aligned} [v] &:= v_+|_{r_{t_2}} - v_-|_{r_{t_2}}, & [\mu^{-1} \partial_r(rv)] &= \mu_v^{-1} \partial_r(rv_+)|_{r_{t_2}} - \mu_t^{-1} \partial_r(rv_-)|_{r_{t_2}}, \\ \langle v \rangle &:= \frac{1}{2} (v_+|_{r_{t_2}} + v_-|_{r_{t_2}}) & \langle \mu^{-1} \partial_r(rv) \rangle &= \frac{1}{2} \left(\mu_v^{-1} \partial_r(rv_+)|_{r_{t_2}} - \mu_t^{-1} \partial_r(rv_-)|_{r_{t_2}} \right). \end{aligned}$$

In (4.10) and (4.12), we write the jumps $[u^1]$ and $[\mu^{-1} \partial_r(ru^1)]$ on behave of u_-^j and its derivative on Γ_{t_2} , $j = 0, 1$. A symmetric formulation would write the jumps on bahave of the mean values. From (4.2), (4.4), (4.10) and (4.12), one gets

$$\left\{ \begin{array}{l} [u^1] = \frac{i\omega\sigma_1 \mu_c d(z)^2}{2} \langle u^0 \rangle, \\ [\mu^{-1} \partial_r(ru^1)] = -i\omega\sigma_1 r_{t_2} d(z) \langle u^1 \rangle \\ \quad + \left(\frac{i\omega\sigma_1 d(z)^2}{2} - \frac{\omega^2 \sigma_1^2 \mu_c r_{t_2} d(z)^3}{6} \right) \langle u^0 \rangle - \frac{i\omega\sigma_1 \mu_c d(z)^2}{2} \langle \mu^{-1} \partial_r(ru^0) \rangle. \end{array} \right. \quad (4.13a)$$

$$\left\{ \begin{array}{l} [u^1] = \frac{i\omega\sigma_1 \mu_c d(z)^2}{2} \langle u^0 \rangle, \\ [\mu^{-1} \partial_r(ru^1)] = -i\omega\sigma_1 r_{t_2} d(z) \langle u^1 \rangle \\ \quad + \left(\frac{i\omega\sigma_1 d(z)^2}{2} - \frac{\omega^2 \sigma_1^2 \mu_c r_{t_2} d(z)^3}{6} \right) \langle u^0 \rangle - \frac{i\omega\sigma_1 \mu_c d(z)^2}{2} \langle \mu^{-1} \partial_r(ru^0) \rangle. \end{array} \right. \quad (4.13b)$$

Thus, the approximate transmission conditions $\mathcal{Z}_{1,0}$ at $r = r_{t_2}$ writes

$$\mathcal{Z}_{1,1} \left\{ \begin{array}{l} [u^\delta] = \frac{i\omega\sigma_1 \mu_c d(z)^2}{2} \delta \langle u^\delta \rangle, \\ [\mu^{-1} \partial_r(ru^\delta)] = -i\omega\sigma_1 r_{t_2} d(z) \langle u^\delta \rangle \\ \quad + \left(\frac{i\omega\sigma_1 d(z)^2}{2} - \frac{\omega^2 \sigma_1^2 \mu_c r_{t_2} d(z)^3}{6} \right) \delta \langle u^\delta \rangle - \frac{i\omega\sigma_1 \mu_c d(z)^2}{2} \delta \langle \mu^{-1} \partial_r(ru^\delta) \rangle. \end{array} \right. \quad (4.14a)$$

$$\left\{ \begin{array}{l} [u^\delta] = \frac{i\omega\sigma_1 \mu_c d(z)^2}{2} \delta \langle u^\delta \rangle, \\ [\mu^{-1} \partial_r(ru^\delta)] = -i\omega\sigma_1 r_{t_2} d(z) \langle u^\delta \rangle \\ \quad + \left(\frac{i\omega\sigma_1 d(z)^2}{2} - \frac{\omega^2 \sigma_1^2 \mu_c r_{t_2} d(z)^3}{6} \right) \delta \langle u^\delta \rangle - \frac{i\omega\sigma_1 \mu_c d(z)^2}{2} \delta \langle \mu^{-1} \partial_r(ru^\delta) \rangle. \end{array} \right. \quad (4.14b)$$

One observes easily that the transmission conditions (4.14) contain terms on order $\mathcal{O}(1)$ – which give $\mathcal{Z}_{1,0}$ – and on order $\mathcal{O}(\delta)$. However, one cannot ensure that the asymptotic model using $\mathcal{Z}_{1,1}$ given by (4.14) has coercive sesquilinear form in its variational formulation. To have the coercivity, we add a stabilizer of order $\mathcal{O}(\delta^2)$ to the first transmission condition (4.14a)

$$\alpha i \omega \sigma_1 \mu_c^2 d(z)^3 \delta^2 \langle \mu^{-1} \partial_r(r u^\delta) \rangle,$$

where $\alpha > 0$ is a dimensionless parameter to be determined. We denote still by $\mathcal{Z}_{1,1}$ the modified approximate transmission conditions

$$\mathcal{Z}_{1,1} \begin{cases} [u^\delta] = \frac{i \omega \sigma_1 \mu_c d(z)^2}{2} \delta \langle u^\delta \rangle + \alpha i \omega \sigma_1 \mu_c^2 d(z)^3 \delta^2 \langle \mu^{-1} \partial_r(r u^\delta) \rangle, & (4.15a) \\ [\mu^{-1} \partial_r(r u^\delta)] = -i \omega \sigma_1 r_{t_2} d(z) \langle u^\delta \rangle \\ + \left(\frac{i \omega \sigma_1 d(z)^2}{2} - \frac{\omega^2 \sigma_1^2 \mu_c r_{t_2} d(z)^3}{6} \right) \delta \langle u^\delta \rangle - \frac{i \omega \sigma_1 \mu_c d(z)^2}{2} \delta \langle \mu^{-1} \partial_r(r u^\delta) \rangle. & (4.15b) \end{cases}$$

4.1.4 Mixed formulation for the asymptotic model using $\mathcal{Z}_{1,1}$

From the first transmission condition (4.15a), u^δ is no longer continuous through Γ_{t_2} . Therefore, we consider the function space

$$H(\Omega_- \cup \Omega_+) := \{v : v|_{\Omega_\pm} = v_\pm \in H(\Omega_\pm)\}.$$

The strong formulation of the asymptotic model using $\mathcal{Z}_{1,1}$ for u^δ writes

$$\begin{cases} -\operatorname{div} \left(\frac{1}{\mu r} \nabla(r u^\delta) \right) - i \omega \sigma u^\delta = i \omega J & \text{in } \Omega_-, \\ -\operatorname{div} \left(\frac{1}{\mu_v r} \nabla(r u^\delta) \right) = 0 & \text{in } \Omega_+, \\ \text{transmission conditions } \mathcal{Z}_{1,1} & \text{on } \Gamma_{t_2}, \end{cases}$$

By integration by parts, the first two partial differential equations and the second transmission condition (4.14b) of $\mathcal{Z}_{1,1}$ yields

$$\begin{aligned} & \int_{\Omega_-} \left(\frac{1}{\mu r} \nabla(r u^\delta) \cdot \nabla(r \bar{v}) - i \omega \sigma u^\delta \bar{v} r \right) dr dz + \int_{\Omega_+} \frac{1}{\mu_v r} \nabla(r u^\delta) \cdot \nabla(r \bar{v}) dr dz + c_{1,1} \\ & = \int_{\Omega} i \omega J \bar{v} r dr dz \quad \forall v \in H(\Omega_- \cup \Omega_+), \end{aligned} \quad (4.16)$$

where the term $c_{1,1}$ depicts the transmission condition (4.15b)

$$\begin{aligned} c_{1,1} & := \int_{\Gamma_{t_2}} \left(\frac{1}{\mu_v} \partial_r(r u_+^\delta) \bar{v}_+ - \frac{1}{\mu_t} \partial_r(r u_-^\delta) \bar{v}_- \right) ds \\ & = \int_{\Gamma_{t_2}} \left\{ -i \omega \sigma_1 r_{t_2} d(s) \left(1 - \frac{d(s)}{2 r_{t_2}} \delta - \frac{1}{6} i \omega \sigma_1 \mu_c d(s)^2 \delta \right) \langle u^\delta \rangle \langle \bar{v} \rangle \right. \\ & \quad \left. + \langle \mu^{-1} \partial_r(r u^\delta) \rangle [\bar{v}] - \frac{i \omega \sigma_1 \mu_c d(s)^2}{2} \delta \langle \mu^{-1} \partial_r(r u^\delta) \rangle \langle \bar{v} \rangle \right\} ds. \end{aligned} \quad (4.17)$$

We define a Lagrange multiplier

$$\lambda := \langle \mu^{-1} \partial_r (r u^\delta) \rangle \in L^2(\Gamma_{t_2}) \quad (4.18)$$

and we set

$$\beta(z) := 1 - \frac{d(z)}{2r_{t_2}} \delta = 1 - \frac{f_\delta(z)}{2r_{t_2}}, \quad (4.19)$$

where $f_\delta(z) = d(z)\delta$ is the deposit layer thickness. Since $f_\delta(z)$ is very small compared to the diameter of the tube $2r_{t_2}$, the dimensionless quantity $\beta \in (0, 1)$ is close to 1. From (4.17), (4.18) and (4.19) we re-define

$$\begin{aligned} c_{1,1}(u^\delta, \lambda; v) &:= \int_{\Gamma_{t_2}} \left\{ -i\omega\sigma_1 r_{t_2} d(s) \left(\beta - \frac{i\omega\sigma_1 \mu_c d(s)^2}{6} \delta \right) \langle u^\delta \rangle \langle \bar{v} \rangle + \lambda[\bar{v}] - \frac{i\omega\sigma_1 \mu_c d(s)^2}{2} \delta \lambda \langle \bar{v} \rangle \right\} ds \\ &= \int_{\Gamma_{t_2}} \left\{ -i\omega\sigma_c r_{t_2} f_\delta(s) \left(\beta - \frac{i\omega\sigma_c \mu_c f_\delta(s)^2}{6} \right) \langle u^\delta \rangle \langle \bar{v} \rangle + \lambda[\bar{v}] - \frac{i\omega\sigma_c \mu_c f_\delta(s)^2}{2} \lambda \langle \bar{v} \rangle \right\} ds. \end{aligned} \quad (4.20)$$

Using the Lagrange multiplier (4.18), the first transmission condition (4.15a) yields the weak formulation

$$\begin{aligned} b_{1,1}(u^\delta, \lambda; \zeta) &:= \int_{\Gamma_{t_2}} \left([u^\delta] \bar{\zeta} - \frac{i\omega\sigma_1 \mu_c d(s)^2}{2} \delta \langle u^\delta \rangle \bar{\zeta} - \alpha \frac{i\omega\sigma_1 \mu_c^2 d(s)^3}{r_{t_2}} \delta^2 \lambda \bar{\zeta} \right) ds \\ &= \int_{\Gamma_{t_2}} \left([u^\delta] \bar{\zeta} - \frac{i\omega\sigma_c \mu_c f_\delta(s)^2}{2} \langle u^\delta \rangle \bar{\zeta} - \alpha \frac{i\omega\sigma_c \mu_c^2 f_\delta(s)^3}{r_{t_2}} \lambda \bar{\zeta} \right) ds = 0 \quad \forall \zeta \in L^2(\Gamma_{t_2}). \end{aligned} \quad (4.21)$$

We define the sesquilinear form

$$\begin{aligned} a_{1,1}(u^\delta, \lambda; v, \psi) &:= \int_{\Omega_-} \left(\frac{1}{\mu r} \nabla(r u^\delta) \cdot \nabla(r \bar{v}) - i\omega\sigma u^\delta \bar{v} r \right) dr dz \\ &\quad + \int_{\Omega_+} \frac{1}{\mu v r} \nabla(r u^\delta) \cdot \nabla(r \bar{v}) dr dz + \mathcal{I}_{\Gamma_{t_2}}(u^\delta, \lambda; v, \psi), \end{aligned} \quad (4.22)$$

where

$$\begin{aligned} \mathcal{I}_{\Gamma_{t_2}}(u^\delta, \lambda; v, \psi) &:= c_{1,1}(u^\delta, \lambda; v) - \overline{b_{1,1}(v, \psi; \lambda)} \\ &= \int_{\Gamma_{t_2}} \left\{ -i\omega\sigma_c r_{t_2} f_\delta(s) \left(\beta - \frac{i\omega\sigma_c \mu_c f_\delta(s)^2}{6} \right) \langle u^\delta \rangle \langle \bar{v} \rangle - i\omega\sigma_c \mu_c f_\delta(s)^2 \lambda \langle \bar{v} \rangle - \alpha \frac{i\omega\sigma_c \mu_c^2 f_\delta(s)^3}{r_{t_2}} \lambda \bar{\psi} \right\} ds. \end{aligned} \quad (4.23)$$

Finally, if we denote the function space

$$X := H(\Omega_- \cup \Omega_+) \times L^2(\Gamma_{t_2}), \quad (4.24)$$

then from (4.16), the mixed formulation of the asymptotic problem using transmission conditions $\mathcal{Z}_{1,1}$ writes

$$a_{1,1}(u^\delta, \lambda; v, \psi) + \overline{b_{1,1}(v, \psi; \lambda)} = \int_{\Omega} i\omega J \bar{v} r dr dz \quad \forall (v, \psi) \in X, \quad (4.25a)$$

$$b_{1,1}(u^\delta, \lambda; \zeta) = 0 \quad \forall \zeta \in L^2(\Gamma_{t_2}), \quad (4.25b)$$

with $a_{1,1}$ given by (4.22) and $b_{1,1}$ by (4.21).

We set a dimensionless quantity

$$\xi(z) := 1 - \frac{\omega\sigma_1\mu_c d(z)^2}{6\beta(z)}\delta = 1 - \frac{\omega\sigma_c\mu_c f_\delta(z)^2}{6\beta(z)}. \quad (4.26)$$

For δ (or the layer thickness $f_\delta(z) = d(z)\delta$) small enough, $\xi \in (0, 1)$ is close to 1.

Proposition 4.1.2. *Supposing $f_\delta(z) = d(z)\delta$ is small enough such that the quantities $\beta(z)$, $\xi(z)$ given by (4.19) and (4.26) respectively are bounded in $(0, 1)$. If the coefficient α of the stabilizing term in (4.15) satisfies*

$$\alpha - \frac{1}{4\beta\xi} > 0,$$

then under the same assumptions for J , μ and σ as in Proposition 4.1.1, the mixed formulation (4.25) has a unique solution $(u^\delta, \lambda) \in X$.

Proof. The proof is similar to the proof of [19, Chapter II, Proposition 1.1]. We define a function space

$$X^b := \{(v, \psi) \in X : b_{1,1}(v, \psi; \zeta) = 0 \quad \forall \zeta \in L^2(\Gamma_{t_2})\}.$$

One remarks that if $(u^\delta, \lambda) \in X^b$, then it satisfies the second weak formulation (4.25b). We will show the sesquilinear form $a_{1,1}$ is coercive on X^b . For any (v, ψ) in X^b , one has

$$\begin{aligned} a_{1,1}(v, \psi; v, \psi) &= \int_{\Omega_-} \left(\frac{1}{\mu r} |\nabla(rv)|^2 - i\omega\sigma|v|^2 r \right) dr dz + \int_{\Omega_+} \frac{1}{\mu_v r} |\nabla(rv)|^2 dr dz \\ &\quad + \mathcal{I}_{\Gamma_{t_2}}(v, \psi; v, \psi). \end{aligned}$$

From (4.23)

$$\begin{aligned} \mathcal{I}_{\Gamma_{t_2}}(v, \psi; v, \psi) &= - \int_{\Gamma_{t_2}} \left\{ i\omega\sigma_1 r_{t_2} d(s) \left(\beta - \frac{i\omega\sigma_1\mu_c d(s)^2}{6} \delta \right) |\langle v \rangle|^2 \right. \\ &\quad \left. + i\omega\sigma_1\mu_c d(s)^2 \delta \psi \langle \bar{v} \rangle + \alpha \frac{i\omega\sigma_1\mu_c^2 d(s)^3}{r_{t_2}} \delta^2 |\psi|^2 \right\} ds \\ &= - \int_{\Gamma_{t_2}} i\omega\sigma_1 r_{t_2} d(s) \left\{ \beta \left| \langle v \rangle + \frac{\mu_c d(s)}{2\beta r_{t_2}} \delta \psi \right|^2 + \left(\alpha - \frac{1}{4\beta} \right) \frac{\mu_c^2 d(s)^2}{r_{t_2}^2} \delta^2 |\psi|^2 \right. \\ &\quad \left. - \frac{i\omega\sigma_1\mu_c d(s)^2}{6} \delta |\langle v \rangle|^2 + \frac{i\mu_c d(s)}{r_{t_2}} \delta \Im(\psi \langle \bar{v} \rangle) \right\} ds. \end{aligned}$$

One computes

$$\begin{aligned} \Re(\mathcal{I}_{\Gamma_{t_2}}(v, \psi; v, \psi)) &= \int_{\Gamma_{t_2}} \left\{ -\frac{\omega^2\sigma_1^2\mu_c r_{t_2} d(s)^3}{6} \delta |\langle v \rangle|^2 + \omega\sigma_1\mu_c d(s)^2 \delta \Im(\psi \langle \bar{v} \rangle) \right\} ds, \\ \Im(\mathcal{I}_{\Gamma_{t_2}}(v, \psi; v, \psi)) &= - \int_{\Gamma_{t_2}} \omega\sigma_1 r_{t_2} d(s) \left\{ \beta \left| \langle v \rangle + \frac{\mu_c d(s)}{2\beta r_{t_2}} \delta \psi \right|^2 + \left(\alpha - \frac{1}{4\beta} \right) \frac{\mu_c^2 d(s)^2}{r_{t_2}^2} \delta^2 |\psi|^2 \right\} ds. \end{aligned}$$

Then we have

$$\begin{aligned} \Re(a_{1,1}(v, \psi; v, \psi)) &\geq \int_{\Omega_-} \frac{1}{\mu r} |\nabla(rv)|^2 dr dz + \int_{\Omega_+} \frac{1}{\mu_v r} |\nabla(rv)|^2 dr dz \\ &\quad + \int_{\Gamma_{t_2}} \left\{ -\frac{\omega^2 \sigma_1^2 \mu_c r_{t_2} d(s)^3}{6} \delta |\langle v \rangle|^2 + \omega \sigma_1 \mu_c d(s)^2 \delta \Im(\psi \langle \bar{v} \rangle) \right\} ds, \\ \Im(a_{1,1}(v, \psi; v, \psi)) &\leq - \int_{\Omega_-} \omega \sigma |v|^2 r dr dz \\ &\quad - \int_{\Gamma_{t_2}} \omega \sigma_1 r_{t_2} d(s) \left\{ \beta \left| \langle v \rangle + \frac{\mu_c d(s)}{2\beta r_{t_2}} \delta \psi \right|^2 + \left(\alpha - \frac{1}{4\beta} \right) \frac{\mu_c^2 d(s)^2}{r_{t_2}^2} \delta^2 |\psi|^2 \right\} ds. \end{aligned}$$

Therefore

$$\begin{aligned} |a_{1,1}(v, \psi; v, \psi)| &\geq \Re(a_{1,1}(v, \psi; v, \psi)) + \Im(a_{1,1}(v, \psi; v, \psi)) \\ &\geq \int_{\Omega_-} \frac{1}{\mu r} |\nabla(rv)|^2 dr dz + \int_{\Omega_+} \frac{1}{\mu_v r} |\nabla(rv)|^2 dr dz + \int_{\Omega_-} \omega \sigma |v|^2 r dr dz \\ &\quad + \int_{\Gamma_{t_2}} \left\{ \omega \sigma_1 r_{t_2} d(s) \beta \left| \langle v \rangle + \frac{\mu_c d(s)}{2\beta r_{t_2}} \delta \psi \right|^2 + \omega \sigma_1 r_{t_2} d(s) \left(\alpha - \frac{1}{4\beta} \right) \frac{\mu_c^2 d(s)^2}{r_{t_2}^2} \delta^2 |\psi|^2 \right. \\ &\quad \left. + \omega \sigma_1 \mu_c d(s)^2 \delta \Im(\psi \langle \bar{v} \rangle) - \frac{\omega^2 \sigma_1^2 \mu_c r_{t_2} d(s)^3}{6} \delta |\langle v \rangle|^2 \right\} ds. \end{aligned}$$

As

$$\begin{aligned} &\omega \sigma_1 r_{t_2} d(s) \beta \left| \langle v \rangle + \frac{\mu_c d(s)}{2\beta r_{t_2}} \delta \psi \right|^2 + \omega \sigma_1 \mu_c d(s)^2 \delta \Im(\psi \langle \bar{v} \rangle) - \frac{\omega^2 \sigma_1^2 \mu_c r_{t_2} d(s)^3}{6} \delta |\langle v \rangle|^2 \\ &= \omega \sigma_1 r_{t_2} d(s) \beta \left(\xi |\langle v \rangle|^2 + \left| \frac{\mu_c d(s)}{2\beta r_{t_2}} \delta \psi \right|^2 + \frac{\mu_c d(s)}{\beta r_{t_2}} (\Re(\psi \langle \bar{v} \rangle) + \Im(\psi \langle \bar{v} \rangle)) \right) \\ &\geq \omega \sigma_1 r_{t_2} d(s) \beta \left(\xi |\langle v \rangle|^2 + \left| \frac{\mu_c d(s)}{2\beta r_{t_2}} \delta \psi \right|^2 - \frac{\mu_c d(s)}{\beta r_{t_2}} |\psi| |\langle \bar{v} \rangle| \right) \\ &= \omega \sigma_1 r_{t_2} d(s) \beta \xi \left(|\langle v \rangle| - \left| \frac{\mu_c d(s)}{2\beta \xi r_{t_2}} \delta \psi \right| \right)^2 - \omega \sigma_1 r_{t_2} d(s) \left(\frac{1}{\xi} - 1 \right) \frac{\mu_c^2 d(s)^2}{4\beta r_{t_2}^2} \delta^2 |\psi|^2, \end{aligned}$$

together with $\sigma_c = \frac{\sigma_1}{\delta}$ and $f_\delta(z) = d(z)\delta$, we obtain

$$\begin{aligned} |a_{1,1}(v, \psi; v, \psi)| &\geq \int_{\Omega_-} \frac{1}{\mu r} |\nabla(rv)|^2 dr dz + \int_{\Omega_+} \frac{1}{\mu_v r} |\nabla(rv)|^2 dr dz \\ &\quad + \int_{\Gamma_{t_2}} \left(\alpha - \frac{1}{4\beta \xi} \right) \frac{\omega \sigma_c \mu_c^2 f_\delta(s)^3}{r_{t_2}} |\psi|^2 ds \\ &\geq \frac{C_1}{\mu_{\text{sup}}} \|v\|_{H(\Omega_- \cup \Omega_+)}^2 + C_2 \|\psi\|_{L^2(\Gamma_{t_2})}^2, \end{aligned}$$

where $C_1 > 0$ comes from the Poincaré-type inequality (1.5) and C_2 is a positive constant depending only on the physical coefficients μ_c , σ_c as well as the geometrical parameters $f_\delta(z)$ and r_{t_2} . Thus $a_{1,1}$ is coercive on X^b . One observes easily that $a_{1,1}$ is also continuous. Therefore, the first weak formulation (4.25a) of the mixed formulation has a unique solution (u^δ, λ) in X^b by the Lax-Milgram theorem. \square

4.1.5 Numerical validation of the 2-D asymptotic models

We test the asymptotic models in their variational formulations using $\mathcal{Z}_{1,n}$ ($n = 0, 1$) transmission conditions given by the previous sections. We consider a thin layer of deposit (copper, with permeability $\mu_c = \mu_v$ and conductivity $\sigma_c = 5.8 \times 10^6 S/m$) which covers the shell side of the tube axisymmetrically with $10mm$ in height. The permeability of tube is $\mu_t = 1.01\mu_v$, and the conductivity of tube is $\sigma_t = 9.7 \times 10^5 S/m$. The thickness of the thin layer $f_\delta(z)$ is constant and takes value in the range from $10\mu m$ to $200\mu m$. Hence, in the 2-D representation of the model in the Orz plan (see for example Figure 3.1), the thin layer is in fact a $f_\delta \times 10mm$ rectangle. The other geometrical configurations (positions of the eddy current probe and the tube) are the same as in Section 1.3.

First of all, we build a full model which will serve as reference. The computation of the solution uses a mesh that is adaptively refined with respect to this solution with a maximum edge size $h_{\max} = 1.25mm$ as well as P1 finite elements on the mesh. To have a good simulation of the thin deposit layer, at least 4 layers of mesh elements are used in the thickness direction. The degrees of freedom of the finite element space are about 11000 for the full model on B_{r_*, z_*} with $r_* = 30mm$ and $z_* = 41mm$. To ensure that this full model is close enough to the reality so that one can use it as the reference model, we refine again the mesh and observe that there is no significant difference compared to the previous full model.

Then we build the asymptotic models using either $\mathcal{Z}_{1,0}$ (see (4.6)) or $\mathcal{Z}_{1,1}$ (see (4.15)) transmission conditions on Γ_{t_2} . The mesh is adaptively refined with respect to the solutions with a maximum edge size $h_{\max} = 2.5mm$ – which is two times larger than the edge size used in the full model – and P1 finite elements. The degrees of freedom of the finite element space are about 4000 on B_{r_*, z_*} .

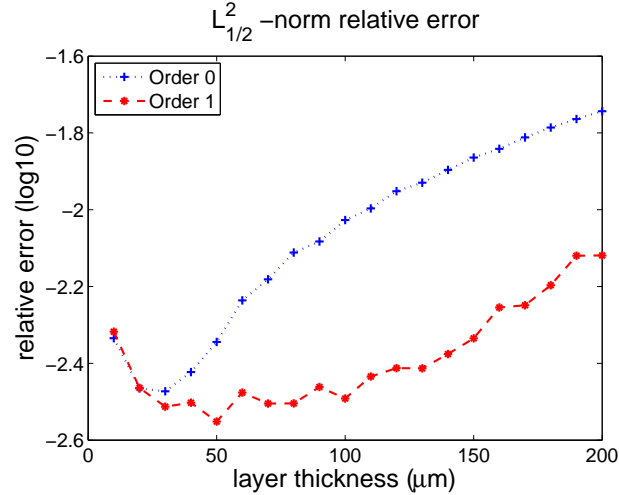


Figure 4.2: Relative error of the asymptotic models using $\mathcal{Z}_{1,n}$ transmission conditions, $n = 0, 1$.

Since the thickness $f_\delta(z)$ is at most $200\mu m$ in our examples, we compute the dimensionless quantity $4\beta\xi < 4$ is at least 2.743. To ensure

$$\alpha - \frac{1}{4\beta\xi} > 0$$

we take $\alpha = 0.4$ as the coefficient of the sablizing term in (4.15a).

Finally, we compare in Figure 4.2 the relative errors of the asymptotic models with regard to the full model in $L^2_{1/2}(B_{r_*, z_*})$ -norm. One observes that the asymptotic model using $\mathcal{Z}_{1,0}$ gives already a good approximation of the full model with a relative error less than 1% for $f_\delta(z) < 100\mu m$. But if $f_\delta(z)$ increases over $100\mu m$, its precision deteriorates. The asymptotic model using $\mathcal{Z}_{1,1}$ conditions is always a good approximation of the full model for the layer thickness $f_\delta(z)$ under $200\mu m$.

4.1.6 Approximation of the impedance measurements

In the cylindrical coordinates for the axisymmetric case, we recall the formula (2.5) of the impedance measurement in the coil k when the electromagnetic field is induced by the coil l

$$\Delta Z_{kl} = \frac{2\pi}{i\omega I^2} \int_{\Omega_d} \left(\left(\frac{1}{\mu} - \frac{1}{\mu^0} \right) \frac{1}{r} \nabla(ru_k) \cdot \nabla(ru_l^0) - i\omega(\sigma - \sigma^0)u_k u_l^0 r \right) dr dz,$$

where $\Omega_d = \Omega_c$, $\mu|_{\Omega_c} = \mu_c$, $\sigma|_{\Omega_c} = \sigma_c$, $\mu^0|_{\Omega_c} = \mu_v$ and $\sigma^0|_{\Omega_c} = 0$ in our case. For the thin layers of deposit in copper, its permeability μ_c is the same as the background permeability for vacuum μ_v (see Table 3.1). Thus the impedance measurement writes

$$\Delta Z_{kl} = -\frac{2\pi}{I^2} \int_{\Omega_c} \sigma_c u_k u_l^0 r dr dz. \quad (4.27)$$

Approximation at order 0

From Section 4.1.1 and the expression of the transmission conditions $\mathcal{Z}_{1,0}$ (4.6), the electric field in the thin layer Ω_c writes

$$u(r, z) = u^\delta(r_{t_2}, z) + \mathcal{O}(\delta) \quad r_{t_2} < r < r_{t_2} + f_\delta(z).$$

Then one has

$$\begin{aligned} \Delta Z_{kl} &= -\frac{2\pi}{I^2} \int_{\Gamma_{t_2}} \int_{r_{t_2}}^{r_{t_2} + f_\delta(s)} \sigma_c u_k(r, s) u_l^0(r, s) r dr ds \\ &= -\frac{2\pi}{I^2} \int_{\Gamma_{t_2}} \int_{r_{t_2}}^{r_{t_2} + f_\delta(s)} \sigma_c u_k^\delta(r_{t_2}, s) u_l^0(r_{t_2}, s) r dr ds + \mathcal{O}(\delta) \\ &= -\frac{2\pi}{I^2} \int_{\Gamma_{t_2}} \sigma_c f_\delta(s) u_k^\delta(r_{t_2}, s) u_l^0(r_{t_2}, s) r_{t_2} ds + \mathcal{O}(\delta). \end{aligned} \quad (4.28)$$

Approximation at order 1

From Section 4.1.3 and the transmission conditions $\mathcal{Z}_{1,1}$ (4.14) without the stabilizer at order $\mathcal{O}(\delta^2)$, we have in the thin layer Ω_c

$$\begin{aligned}
u^1\left(\frac{r-r_{t_2}}{\delta}, z\right) &= u_-^1|_{r_{t_2}} + \frac{1}{r_{t_2}} \left(\frac{\mu_c}{\mu_t} \partial_r(ru_-^0) - u_-^0 \right) \Big|_{r_{t_2}} \frac{r-r_{t_2}}{\delta} - \frac{i\omega\sigma_1\mu_c}{2} u_-^0|_{r_{t_2}} \frac{(r-r_{t_2})^2}{\delta^2} \\
&= \langle u^1 \rangle - \frac{1}{2} [u^1] + \frac{1}{r_{t_2}} \left(\mu_c \langle \mu^{-1} \partial_r(ru^0) \rangle - \frac{\mu_c}{2} [\mu^{-1} \partial_r(ru^0)] - \langle u^0 \rangle \right) \frac{r-r_{t_2}}{\delta} \\
&\quad - \frac{i\omega\sigma_1\mu_c}{2} \langle u^0 \rangle \frac{(r-r_{t_2})^2}{\delta^2} \\
&= \langle u^1 \rangle - \frac{i\omega\sigma_1\mu_c d(z)^2}{4} \langle u^0 \rangle + \left(\frac{\mu_c}{r_{t_2}} \langle \mu^{-1} \partial_r(ru^0) \rangle + \left(\frac{i\omega\sigma_1\mu_c d(z)}{2} - \frac{1}{r_{t_2}} \right) \langle u^0 \rangle \right) \frac{r-r_{t_2}}{\delta} \\
&\quad - \frac{i\omega\sigma_1\mu_c}{2} \langle u^0 \rangle \frac{(r-r_{t_2})^2}{\delta^2}.
\end{aligned}$$

Thus for $r_{t_2} < r < r_{t_2} + f_\delta(z)$

$$\begin{aligned}
u(r, z) &= u^0\left(\frac{r-r_{t_2}}{\delta}, z\right) + \delta u^1\left(\frac{r-r_{t_2}}{\delta}, z\right) + \mathcal{O}(\delta^2) \\
&= \left(1 - \frac{i\omega\sigma_1\mu_c d(z)^2}{4} \delta \right) \langle u^\delta \rangle + \left(\frac{\mu_c}{r_{t_2}} \lambda + \left(\frac{i\omega\sigma_1\mu_c d(z)}{2} - \frac{1}{r_{t_2}} \right) \langle u^\delta \rangle \right) (r-r_{t_2}) \\
&\quad - \frac{i\omega\sigma_1\mu_c}{2\delta} \langle u^\delta \rangle (r-r_{t_2})^2 + \mathcal{O}(\delta^2) \\
&= \left(1 - \frac{i\omega\sigma_c\mu_c f_\delta(z)^2}{4} \right) \langle u^\delta \rangle + \left(\frac{\mu_c}{r_{t_2}} \lambda + \left(\frac{i\omega\sigma_c\mu_c f_\delta(z)}{2} - \frac{1}{r_{t_2}} \right) \langle u^\delta \rangle \right) (r-r_{t_2}) \\
&\quad - \frac{i\omega\sigma_c\mu_c}{2} \langle u^\delta \rangle (r-r_{t_2})^2 + \mathcal{O}(\delta^2).
\end{aligned}$$

Otherwise, the electric field u_l^0 in the deposit-free configuration satisfies the following transmission conditions on Γ_{t_2}

$$\begin{cases} [u_l^0] = 0, \\ [\mu^{-1} \partial_r(ru_l^0)] = 0. \end{cases}$$

Thus one gets the Taylor development

$$u_l^0 r = u_l^0 r_{t_2} + \mu_v \lambda_l^0 (r - r_{t_2}) + \mathcal{O}((r - r_{t_2})^2) \quad r_{t_2} < r < r_{t_2} + f_\delta(z),$$

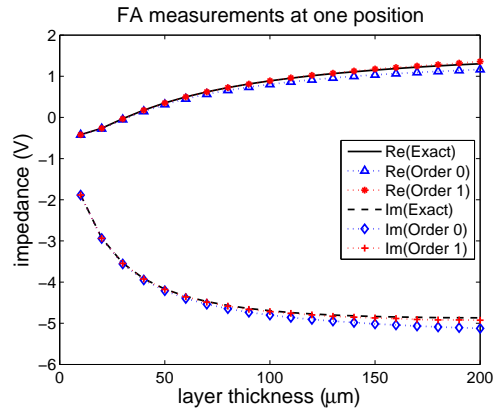
where

$$\lambda_l^0 := \langle \mu^{-1} \partial_r(ru_l^0) \rangle \quad \text{on } \Gamma_{t_2}.$$

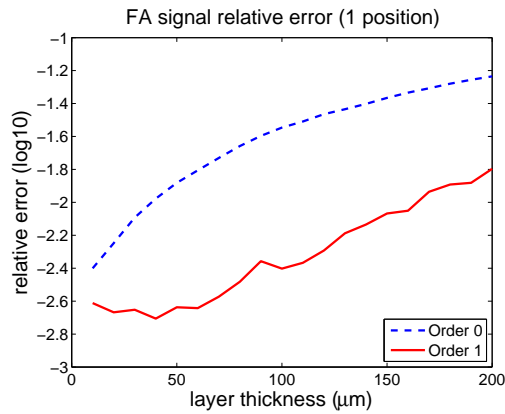
Finally we obtain the approximation at order 1

$$\begin{aligned}
\Delta Z_{kl} &= -\frac{2\pi}{I^2} \int_{\Gamma_{t_2}} \int_{r_{t_2}}^{r_{t_2}+f_\delta(s)} \sigma_c \left\{ \left(1 - \frac{i\omega\sigma_c\mu_c f_\delta(s)^2}{4}\right) \langle u_k^\delta \rangle u_l^0 r_{t_2} \right. \\
&\quad + \left(\mu_c \lambda_k u_l^0 + \left(\frac{i\omega\mu_c r_{t_2} f_\delta(s)}{2} - 1\right) \langle u_k^\delta \rangle u_l^0 + \left(1 - \frac{i\omega\sigma_c\mu_c f_\delta(s)^2}{4}\right) \langle u_k^\delta \rangle \mu_v \lambda_l^0 \right) (r - r_{t_2}) \\
&\quad \left. - \frac{i\omega\sigma_c\mu_c}{2} \langle u_k^\delta \rangle u_l^0 r_{t_2} (r - r_{t_2})^2 \right\} dr ds + \mathcal{O}(\delta^2) \\
&= -\frac{2\pi}{I^2} \int_{\Gamma_{t_2}} \sigma_c \left\{ \left(f_\delta(s) - \frac{f_\delta(s)^2}{2r_{t_2}} - \frac{i\omega\sigma_c\mu_c f_\delta(s)^3}{6}\right) \langle u_k^\delta \rangle u_l^0 r_{t_2} \right. \\
&\quad \left. + \frac{f_\delta(s)^2}{2} \mu_c \lambda_k u_l^0 + \left(\frac{f_\delta(s)^2}{2} - \frac{i\omega\sigma_c\mu_c f_\delta(s)^4}{8}\right) \mu_v \langle u_k^\delta \rangle \lambda_l^0 \right\} ds + \mathcal{O}(\delta^2). \tag{4.29}
\end{aligned}$$

4.1.7 Numerical tests on impedance measurements



(a) one position FA measurements



(b) relative errors

Figure 4.3: Approximation of impedance measurements using asymptotic models with $\mathcal{Z}_{1,n}$, $n = 0, 1$.

We consider the same examples as in Section 4.1.5 for the full model (reference) and for the asymptotic models using $\mathcal{Z}_{1,0}$ and $\mathcal{Z}_{1,1}$ transmission conditions. The eddy current probe is located at the center position in the vertical direction with regard to the thin layer of deposit in copper. We compare the impedance measurement signals in FA mode (see (2.8)) at this position between the full model and the asymptotic models.

Figure 4.3a shows the impedance measurements in their real and imaginary part. One observes that the signals given by the asymptotic model using $\mathcal{Z}_{1,1}$ transmission conditions are closer to those from the full model than the signals obtained from the asymptotic model using $\mathcal{Z}_{1,0}$ conditions. We confirm this observation by Figure 4.3b which illustrates the relative error of the signals in FA mode. The asymptotic model using $\mathcal{Z}_{1,0}$ transmission conditions gives a good approximation only for small layer thickness (under $40\mu\text{m}$), while the asymptotic model using $\mathcal{Z}_{1,1}$ yields an accurate simulation for a large range of layer thickness interested – for instance, the relative error in impedance measurements is under 1% if the thickness is less than $150\mu\text{m}$.

4.2 Thickness reconstruction via asymptotic model using $\mathcal{Z}_{1,0}$

4.2.1 Derivative of the solution with respect to a thickness increment

We assume that $h \in L^2(\Gamma_{t_2})$ is a small thickness increment of the thin layer, i.e.

$$f_\delta(z) \rightarrow f_\delta(z) + h(z).$$

In a configuration with a thin layer of thickness $f_\delta(z)$, we denote the solution to the asymptotic model using $\mathcal{Z}_{1,0}$ (4.7) by $u^\delta(f_\delta)$. Then the derivative of $u^\delta(f_\delta)$ due to the increment h , denoted by $u'(h)$, is defined by

$$u^\delta(f_\delta + h) = u^\delta(f_\delta) + u'(h) + o(h), \quad \lim_{h \rightarrow 0} \frac{\|o(h)\|_H}{\|h\|_{L^2(\Gamma_{t_2})}} = 0.$$

We develop the variational formulation of the asymptotic model using $\mathcal{Z}_{1,0}$ transmission conditions (4.7) with the thin layer thickness $f_\delta + h$ at $h = 0$ with respect to h . The terms of order zero is exactly the variational formulation with the original layer thickness f_δ . The terms of the first order with respect to h yields

$$a_{1,0}(u', v) = \int_{\Gamma_{t_2}} i\omega\sigma_c h(s) u^\delta \bar{v} r \, ds \quad \forall v \in H(\Omega). \quad (4.30)$$

Using the same argument as in Proposition 4.1.1 one has

Corollary 4.2.1. *Under the same assumption as in Proposition 4.1.1, the variational formulation (4.30) has a unique solution u' in $H(\Omega)$.*

4.2.2 Adjoint state and derivative of the impedance measurements

We compute the derivative of the impedance measurement due to a small change in layer thickness ($f_\delta \rightarrow f_\delta + h$). We denote by $\Delta Z_{kl}(f_\delta)$ the impedance measurement for a thin layer with

$f_\delta(z)$ in thickness, and by $\Delta Z'_{kl}$ its derivative with regard to h

$$\Delta Z_{kl}(f_\delta + h) = \Delta Z_{kl}(f_\delta) + \Delta Z'_{kl} + o(h).$$

From (4.28), we have

$$\Delta Z'_{kl} = -\frac{2\pi}{I^2} \int_{\Gamma_{t_2}} \sigma_c \left(h(s) u_k^\delta u_l^0 r_{t_2} + f_\delta(s) u'_k u_l^0 r_{t_2} \right) ds. \quad (4.31)$$

To write $\Delta Z'_{kl}$ explicitly on the thickness increment h (independent of u'_k), we introduce the adjoint state p_l satisfying

$$a_{1,0}^*(p_l, v) = - \int_{\Gamma_{t_2}} i\omega \sigma_c f_\delta(s) \overline{u_l^0} v r_{t_2} ds \quad \forall v \in H(\Omega), \quad (4.32)$$

where

$$a_{1,0}^*(p, v) := \overline{a_{1,0}(v, p)} \quad \forall (p, v) \in H(\Omega)^2. \quad (4.33)$$

One obtains with the same argument as in Proposition 4.1.1

Corollary 4.2.2. *Under the same assumptions as in Proposition 4.1.1, the variational formulation (4.32) has a unique solution p_l in $H(\Omega)$.*

Then we have

Proposition 4.2.3. *Considering u_k^δ the solution to the asymptotic model using $\mathcal{Z}_{1,0}$ (4.7) and p_l the adjoint state satisfying the variational formulation (4.32), the derivative of the impedance measurement ΔZ_{kl} due to a thickness increment $h(z)$ writes*

$$\Delta Z'_{kl} = -\frac{2\pi}{I^2} \int_{\Gamma_{t_2}} \sigma_c h(s) u_k^\delta (u_l^0 + \overline{p_l}) r_{t_2} ds. \quad (4.34)$$

Proof. From (4.32) and (4.30), we have

$$\int_{\Gamma_{t_2}} i\omega \sigma_c f_\delta(s) u'_k u_l^0 r_{t_2} ds = \overline{a_{1,1}^*(p_l, u'_k)} = a_{1,0}(u'_k, p_l) = \int_{\Gamma_{t_2}} i\omega \sigma_c h(s) u_k^\delta \overline{p_l} r_{t_2} ds,$$

which, together with (4.31), implies (4.34). \square

4.2.3 Thickness reconstruction by minimizing a least square cost functional

Similar to the least square cost functional 2.33, we define here another least square cost functional of the layer thickness $f_\delta(z)$

$$\mathcal{J}(f_\delta) = \int_{z_{\min}}^{z_{\max}} |Z(f_\delta; \zeta) - Z_{meas}(\zeta)|^2 d\zeta. \quad (4.35)$$

Z is the impedance measurement either in FA mode or in F3 mode (see (2.8)). Hence, the derivative of the cost functional due to a small increment h of the layer thickness f_δ writes

$$\mathcal{J}'(h) = \int_{z_{\min}}^{z_{\max}} 2\Re(Z'(h; \zeta) \overline{(Z(f_\delta; \zeta) - Z_{meas}(\zeta))}) d\zeta, \quad (4.36)$$

where

$$Z'(h) = \begin{cases} Z'_{FA} = \frac{i}{2}(\Delta Z'_{11} + \Delta Z'_{21}) & \text{FA mode,} \\ Z'_{F3} = \frac{i}{2}(\Delta Z'_{11} - \Delta Z'_{22}) & \text{F3 mode.} \end{cases}$$

From (4.34), one has

$$\mathcal{J}'(h) = -\frac{\pi}{I^2} \int_{\Gamma_{t_2}} g(s)h(s) ds, \quad (4.37)$$

where

$$g = \begin{cases} g_{11} + g_{21} & \text{FA mode,} \\ g_{11} - g_{22} & \text{F3 mode.} \end{cases}$$

and

$$g_{kl} = \int_{z_{\min}}^{z_{\max}} \Re \left(i\sigma_c u_k^\delta (u_l^0 + \bar{p}_l) r_{t_2} \overline{(Z(f_\delta; \zeta) - Z_{meas}(\zeta))} \right) d\zeta. \quad (4.38)$$

One observes that $h = g$ is a descent direction which minimize the cost functional

$$\mathcal{J}'(g) = -\frac{\pi}{I^2} \int_{\Gamma_{t_2}} |g(s)|^2 ds \leq 0.$$

4.3 Thickness reconstruction via asymptotic model using $\mathcal{Z}_{1,1}$

4.3.1 Derivative of solution with respect to a thickness increment

We recall that $h(z)$ is a small increment of the layer thickness $f_\delta(z)$. We denote by $(u^\delta(f_\delta), \lambda(f_\delta))$ the solution to the mixed formulation (4.25) with a layer thickness $f_\delta(z)$. We denote by $(u'(h), \lambda'(h))$ the derivatives of $(u^\delta(f_\delta), \lambda(f_\delta))$ due to the increment h

$$(u^\delta(f_\delta + h), \lambda(f_\delta + h)) = (u^\delta(f_\delta), \lambda(f_\delta)) + (u'(h), \lambda'(h)) + o(h), \quad \lim_{h \rightarrow 0} \frac{\|o(h)\|_X}{\|h\|_{L^2(\Gamma_{t_2})}} = 0.$$

By developing the mixed formulation of the asymptotic model using $\mathcal{Z}_{1,1}$ transmission conditions (4.25) with the thin layer thickness $f_\delta + h$ at $h = 0$ with regard to the order of h , the terms of the first order on h yields

$$a_{1,1}(u', \lambda'; v, \psi) + \overline{b_{1,1}(v, \psi; \lambda')} = L^a(v, \psi) \quad \forall (v, \psi) \in X, \quad (4.39a)$$

$$b_{1,1}(u', \lambda'; \zeta) = L^b(\zeta) \quad \forall \zeta \in L^2(\Gamma_{t_2}), \quad (4.39b)$$

where

$$L^a(v, \psi) := \int_{\Gamma_{t_2}} i\omega\sigma_c h(s) \left\{ r_{t_2} \left(1 - \frac{f_\delta(s)}{r_{t_2}} - \frac{i\omega\sigma_c \mu_c f_\delta(s)^2}{2} \right) \langle u^\delta \rangle \langle \bar{v} \rangle + \mu_c f_\delta(s) \lambda \langle \bar{v} \rangle \right\} ds, \quad (4.40a)$$

$$L^b(\zeta) := \int_{\Gamma_{t_2}} i\omega\sigma_c h(s) \left(\mu_c f_\delta(s) \langle u^\delta \rangle \bar{\zeta} + 3\alpha \frac{\mu_c^2 f_\delta(s)^2}{r_{t_2}} \lambda \bar{\zeta} \right) ds. \quad (4.40b)$$

With the same arguments as in the proof of Proposition 4.1.2, one gets

Corollary 4.3.1. *Under the same assumptions as in Proposition 4.1.2, the mixed formulation (4.39) has a unique solution $(u', \lambda') \in X$.*

4.3.2 Adjoint state and derivative of the impedance measurements

We recall that $\Delta Z'_{kl}$ is the derivative of the impedance measurement $\Delta Z_{kl}(f_\delta)$ due to a small increment in layer thickness ($f \rightarrow f_\delta + h$). From (4.29), one has

$$\begin{aligned} \Delta Z'_{kl} = & -\frac{2\pi}{I^2} \int_{\Gamma_{t_2}} \sigma_c h(s) \left\{ \left(1 - \frac{f_\delta(s)}{r_{t_2}} - \frac{i\omega\sigma_c\mu_c f_\delta(s)^2}{2}\right) \langle u_k^\delta \rangle u_l^0 r_{t_2} + f_\delta(s) \mu_c \lambda_k u_l^0 \right. \\ & \left. + \left(f_\delta(s) - \frac{i\omega\sigma_c\mu_c f_\delta(s)^3}{2}\right) \mu_v \langle u_k^\delta \rangle \lambda_l^0 \right\} ds \\ & - \frac{2\pi}{I^2} \int_{\Gamma_{t_2}} \sigma_c \left\{ \left(f_\delta(s) - \frac{f_\delta(s)^2}{2r_{t_2}} - \frac{i\omega\sigma_c\mu_c f_\delta(s)^3}{6}\right) \langle u'_k \rangle u_l^0 r_{t_2} + \frac{f_\delta(s)^2}{2} \mu_c \lambda'_k u_l^0 \right. \\ & \left. + \left(\frac{f_\delta(s)^2}{2} - \frac{i\omega\sigma_c\mu_c f_\delta(s)^4}{8}\right) \mu_v \langle u'_k \rangle \lambda_l^0 \right\} ds. \end{aligned} \quad (4.41)$$

We build an adjoint state such that the derivative of the impedance measurement $\Delta Z'_{kl}$ has an explicit expression on the thickness increment $h(z)$ independant of the derivatives (u'_k, λ'_k) of the solution. The adjoint state (p_l, η_l) in X is the unique solution of the following mixed formulation

$$a_{1,1}^*(p_l, \eta_l; v, \psi) + \overline{c_{1,1}(v, \psi; p_l)} = M(v, \psi) \quad \forall (v, \psi) \in X, \quad (4.42a)$$

$$c_{1,1}(p_l, \eta_l; w) = 0 \quad \forall w \in H(\Omega_- \cup \Omega_+), \quad (4.42b)$$

where

$$a_{1,1}^*(p, \eta; v, \psi) := \overline{a_{1,1}(v, \psi; p, \eta)} + b_{1,1}(p, \eta; \psi) - \overline{c_{1,1}(v, \psi; p_l)} \quad \forall ((p, \eta), (v, \psi)) \in X^2 \quad (4.43)$$

$$\begin{aligned} M(v, \psi) := & - \int_{\Gamma_{t_2}} i\omega\sigma_c \left\{ \left(f_\delta(s) - \frac{f_\delta(s)^2}{2r_{t_2}} + \frac{i\omega\sigma_c\mu_c f_\delta(s)^3}{6}\right) \overline{u_l^0} \langle \bar{v} \rangle r_{t_2} + \frac{f_\delta(s)^2}{2} \mu_c \overline{u_l^0} \bar{\psi} \right. \\ & \left. + \left(\frac{f_\delta(s)^2}{2} + \frac{i\omega\sigma_c\mu_c f_\delta(s)^4}{8}\right) \mu_v \overline{\lambda_l^0} \langle \bar{v} \rangle \right\} ds \quad \forall (v, \psi) \in X, \end{aligned} \quad (4.44)$$

and $c_{1,1}$ is defined in (4.20).

Corollary 4.3.2. *Under the same assumptions as in Proposition 4.1.2, the mixed formulation (4.42) has a unique solution $(p_l, \eta_l) \in X$.*

Proof. We set the function space

$$X^c := \{(v, \psi) \in X : c_{1,1}(v, \psi; w) = 0 \quad \forall w \in H(\Omega_- \cup \Omega_+)\}.$$

Then one finds easily that the coercivity of $a_{1,1}^*$ on X^c is equivalent to the coercivity of $a_{1,1}$ on X^b . Hence Proposition 4.1.2 implies the existence and uniqueness of solution to the mixed formulation (4.42). \square

Proposition 4.3.3. *With u_k^δ the solution to the asymptotic model using $Z_{1,1}$ (4.25) and (p_l, η_l) the adjoint state satisfying the mixed formulation (4.42), the derivative of the impedance measurement ΔZ_{kl} due to a thickness increment $h(z)$ writes*

$$\begin{aligned} \Delta Z'_{kl} = & -\frac{2\pi}{I^2} \int_{\Gamma_{t_2}} \sigma_c h(s) \left\{ \left(1 - \frac{f_\delta(s)}{r_{t_2}} - \frac{i\omega\sigma_c\mu_c f_\delta(s)^2}{2}\right) \langle u_k^\delta \rangle (u_l^0 + \langle \bar{p}_l \rangle) r_{t_2} \right. \\ & \left. + f_\delta(s) \mu_c \lambda_k (u_l^0 + \langle \bar{p}_l \rangle) + \left(f_\delta(s) - \frac{i\omega\sigma_c\mu_c f_\delta(s)^3}{2}\right) \mu_v \langle u_k^\delta \rangle \lambda_l^0 \right\} ds. \end{aligned} \quad (4.45)$$

Proof. From the mixed formulation (4.42) for the adjoint state, we have

$$\begin{aligned} \overline{M(u'_k, \lambda'_k)} &= \overline{a_{1,1}^*(p_l, \eta_l; u'_k, \lambda'_k)} + c_{1,1}(u'_k, \lambda'_k; p_l) \\ &= a_{1,1}(u'_k, \lambda'_k; p_l, \eta_l) + \overline{b_{1,1}(p_l, \eta_l; \lambda'_k)} = L^a(p_l, \eta_l) \\ &= \int_{\Gamma_{t_2}} i\omega\sigma_c h(s) \left\{ r_{t_2} \left(1 - \frac{f_\delta(s)}{r_{t_2}} - \frac{i\omega\sigma_c\mu_c f_\delta(s)^2}{2}\right) \langle u_k^\delta \rangle \langle \bar{p}_l \rangle + \mu_c f_\delta(s) \lambda_k \langle \bar{p}_l \rangle \right\} ds. \end{aligned}$$

From (4.41) and the definition of M (4.44) we have

$$\begin{aligned} \Delta Z'_{kl} = & -\frac{2\pi}{I^2} \int_{\Gamma_{t_2}} \sigma_c h(s) \left\{ \left(1 - \frac{f_\delta(s)}{r_{t_2}} - \frac{i\omega\sigma_c\mu_c f_\delta(s)^2}{2}\right) \langle u_k^\delta \rangle u_l^0 r_{t_2} + f_\delta(s) \mu_c \lambda_k u_l^0 \right. \\ & \left. + \left(f_\delta(s) - \frac{i\omega\sigma_c\mu_c f_\delta(s)^3}{2}\right) \mu_v \langle u_k^\delta \rangle \lambda_l^0 \right\} ds - \frac{2\pi}{I^2} \frac{1}{i\omega} \overline{M(u'_k, \lambda'_k)}. \end{aligned}$$

Therefore, the above two equalities yield (4.45). \square

4.3.3 Thickness reconstruction by minimizing a least square functional

We use the same inversion method for thickness reconstruction as in Section 4.2.3 by minimizing the cost functional (4.35). Considering the derivative of the impedance measurements (4.45), we get similarly the expression of the derivative of the cost functional as in (4.37)

$$\mathcal{J}'(h) = -\frac{\pi}{I^2} \int_{\Gamma_{t_2}} g(s) h(s) ds, \quad (4.46)$$

where

$$g = \begin{cases} g_{11} + g_{21} & \text{FA mode,} \\ g_{11} - g_{22} & \text{F3 mode.} \end{cases}$$

but with

$$\begin{aligned} g_{kl} = & \int_{z_{\min}}^{z_{\max}} \Re \left\{ i\sigma_c \left(\left(1 - \frac{f_\delta(s)}{r_{t_2}} - \frac{i\omega\sigma_c\mu_c f_\delta(s)^2}{2}\right) \langle u_k^\delta \rangle (u_l^0 + \langle \bar{p}_l \rangle) r_{t_2} \right. \right. \\ & \left. \left. + f_\delta(s) \mu_c \lambda_k (u_l^0 + \langle \bar{p}_l \rangle) + \left(f_\delta(s) - \frac{i\omega\sigma_c\mu_c f_\delta(s)^3}{2}\right) \mu_v \langle u_k^\delta \rangle \lambda_l^0 \right) \overline{(Z(f_\delta; \zeta) - Z_{meas}(\zeta))} \right\} d\zeta. \end{aligned} \quad (4.47)$$

We verify that $h = g$ minimize the cost functional

$$\mathcal{J}'(g) = -\frac{\pi}{I^2} \int_{\Gamma_{t_2}} |g(s)|^2 ds < 0.$$

4.4 Numerical tests

In this section, we consider some numerical examples of thickness reconstruction for highly conductive deposits (copper). Its conductivity is $\sigma_c = 58 \times 10^6 S/m$ and its permeability is $\mu_c = \mu_v$.

The signals of impedance measurements used for inversion are obtained from a full model. Its numerical settings are the same for the reference full model in Section 4.1.5. On a bounded computational domain $B_{r_*, z_*} = \{(r, z) : 0 \leq r \leq r_*, -z_* \leq z \leq z_*\}$ with $r_* = 30mm$ and $z_* = 41mm$, we consider an adaptively refined mesh with respect to the solution with a maximum edge size $h_{\max} = 1.25mm$ and P1 finite elements. The degrees of freedom are about 11000.

In the inversion algorithm, we use asymptotic models to resolve forward problems. The mesh on B_{r_*, z_*} is also adaptively refined with respect to the solution to the asymptotic problem using $\mathcal{Z}_{1,n}$ ($n = 0, 1$) transmission conditions, with a maximum edge size $h_{\max} = 2.5mm$. We remark that this size is two times larger than the maximum edge size used in the full model. With P1 finite elements, the degrees of freedom are about 4000. We set the stopping rule as

$$\mathcal{J}(f_\delta) \leq \epsilon \int_{z_{\min}}^{z_{\max}} |Z_{meas}(\zeta)|^2 d\zeta,$$

where ϵ is a chosen threshold. We take $\epsilon = 10^{-4}$ such that the relative error of the impedance measurements obtained with the reconstructed thin layer is under 1% of the real measurements.

4.4.1 Parameterized thin layers

We consider an axisymmetric thin layer covering vertically 10mm of the tube's shell side. We assume that the layer thickness $f_\delta(z)$ is constant. Thus in the 2-D representation with (r, z) coordinates, the thin layer is a rectangle with f_δ in r -direction and 10mm in z -direction. Since there is only one parameter to reconstruct, we need only the impedance signal in FA mode at one measuring position.

target thickness (μm)	10	20	30	50	75
reconstruction $\mathcal{Z}_{1,0}$	9.86	19.61	29.34	N.A.	N.A.
reconstruction $\mathcal{Z}_{1,1}$	9.89	19.69	29.41	48.30	71.03

Table 4.1: Reconstruction layer thickness using FA signals.

Table 4.1 gives the reconstruction results with the asymptotic models using either $\mathcal{Z}_{1,0}$ or $\mathcal{Z}_{1,1}$ transmission conditions. We observe that for a small target thickness (say, less than $30\mu m$), both models yield satisfying reconstruction results. However, when the target thickness gets larger, the inversion algorithm with the asymptotic model using $\mathcal{Z}_{1,0}$ conditions does not converge. In fact, due to the modeling error, the minimum of the cost functional is bounded away from 0. For instance, for a target thickness $50\mu m$, Figure 4.4 shows the relative cost functional obtained with the asymptotic model using $\mathcal{Z}_{1,0}$ transmission conditions. Its minimum is about $10^{-2.5}$, still far away from 10^{-4} which is our chosen stopping threshold for the inversion algorithm.

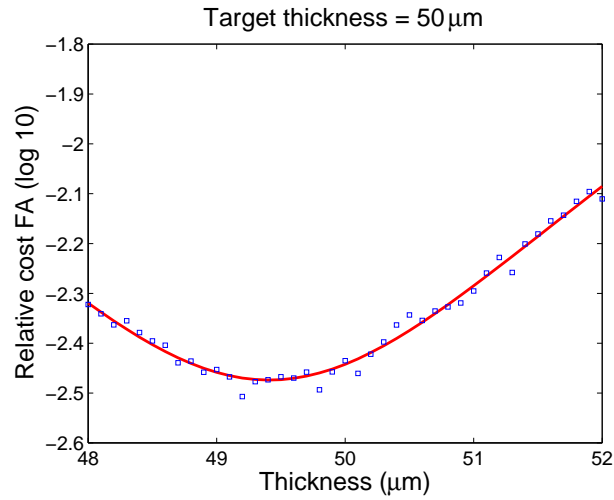
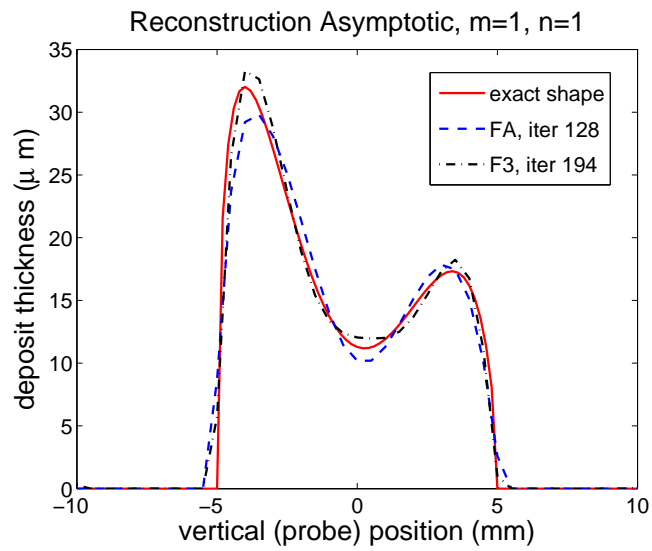


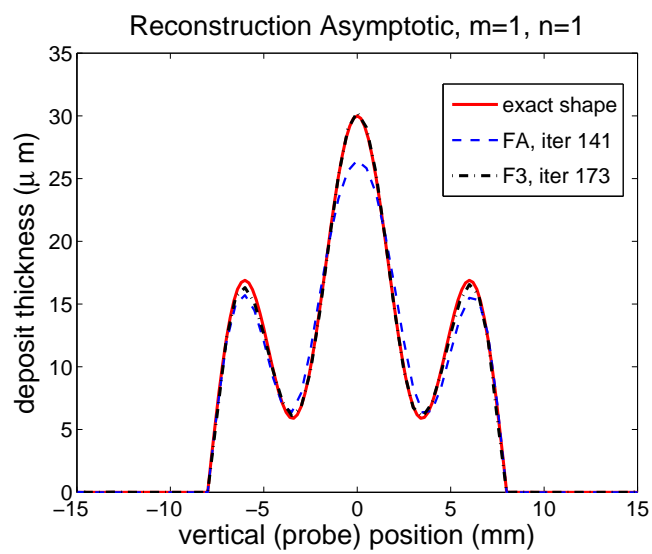
Figure 4.4: Cost functional for asymptotic model using $\mathcal{Z}_{1,0}$ around the target thickness.

4.4.2 Reconstruction of arbitrary thin layers

We consider some arbitrary thin layers of copper with variable thickness. In the inversion algorithm, we use the asymptotic model with $\mathcal{Z}_{1,1}$ transmission conditions. Figures 4.5 show some reconstruction results using either FA signals or F3 signals. In the first example (Figure 4.5a), we take the signals from 41 probe positions with 0.5mm between each two neighboring positions. In the second example (Figure 4.5b), signals from 61 probe positions are used for reconstruction. Both examples show satisfying reconstruction of the thin layers.



(a)



(b)

Figure 4.5: Reconstruction of some arbitrary thin layers.

Part III

Extension to the 3-D case

Eddy current tomography using shape optimization

Contents

5.1 Formulation via vector potentials	136
5.1.1 Problem for vector potential with Coulomb gauge condition	136
5.1.2 Variational formulation of the eddy current problem via vector potentials	138
5.2 Deposit reconstruction via shape optimization	139
5.2.1 Shape and material derivatives of the solution	139
5.2.2 Shape derivative of the impedance measurements	145
5.2.3 Expression of the impedance shape derivative using the adjoint state	148
5.2.4 Shape derivative for a least square cost functional	151
5.2.5 Validation for axisymmetric configurations	152
5.3 Appendices	152
5.3.1 Differential identities	152
5.3.2 Proof of Lemma 5.2.6	152

In the previous chapters, we discussed the eddy current model and different inversion methods for axisymmetric configurations. However, the presence of broached quatrefoil support plates (Figure 5.1) and non-axisymmetric deposits in real industry context motivate us to consider a 3-D eddy current model though the axial eddy current probe is not sensible to angular variations.

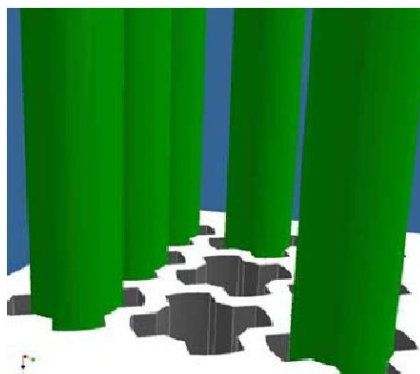


Figure 5.1: SG tubes maintained by a broached quatrefoil support plate.

The 3-D eddy current model is derived from Maxwell's equations under the assumptions of low frequency and high conductivity. In Chapter 1, the formulation of the eddy current model

is based on the electric field \mathbf{E} by eliminating the magnetic field \mathbf{H} . But due to complicated geometrical configurations of different components (tube, support plate, deposits), one should assume some topological restrictions to ensure the existence and uniqueness for the same approach in the 3-D case. For instance, Bossavit [17, Chapter 5] discussed the configuration where the insulator domain $\Omega_{\mathcal{I}}$ is simply connected, which is not our case.

Alonso – Fernandes – Valli [3] built the eddy current model for the magnetic field \mathbf{H} based on the elimination of the electric field \mathbf{E} , which leads to an existence and uniqueness result without preliminary topological assumptions. This approach establishes the weak formulation on a vectorial function space with conditions on the insulator domain

$$V := \{\mathbf{v} \in H_0(\text{curl}; \Omega) : \text{curl } \mathbf{v}_{\mathcal{I}} = 0 \quad \text{in } \Omega_{\mathcal{I}}\},$$

With this formulation, we encounter a numerical difficulty since classical finite elements do not ensure the above condition on $\Omega_{\mathcal{I}}$.

To overcome this difficulty, we consider a formulation for a vector magnetic potential \mathbf{A} and a scalar electric potential V in the conducting domain $\Omega_{\mathcal{C}}$. This formulation reported by Bíró [14] furnishes a magnetic field \mathbf{H} satisfying the formulation by Alonso – Fernandes – Valli and does not provoke essential numerical difficulties.

This chapter is organized as follows. In Section 5.1 we build the 3-D eddy current model for vector potentials with Coulomb gauge condition. Section 5.2 then derives the inversion scheme by evaluating the material derivative of the solution to the forward model and by using a classical least square minimization method.

5.1 Formulation via vector potentials

5.1.1 Problem for vector potential with Coulomb gauge condition

This part is largely inspired from Alonso – Valli [4, Chapter 6]. We set the problem in a bounded domain $\Omega \subset \mathbb{R}^3$. We assume that the conductor domain $\Omega_{\mathcal{C}}$ is strictly contained in Ω , i.e. $\overline{\Omega_{\mathcal{C}}} \subset \Omega$. In our configuration, $\Omega_{\mathcal{C}} = \Omega_t \cup \Omega_d \cup \Omega_p$, where t stands for the tube, d for the deposit and p for the supporting plates. The insulator writes $\Omega_{\mathcal{I}} = \Omega \setminus \Omega_{\mathcal{C}} = \Omega_s \cup \Omega_v$, where Ω_s stands for the region inside the tube where the probe (thus the source \mathbf{J}) is located, and Ω_v for the vacuum outside the tube. $\Gamma_* = \partial\Omega_{\mathcal{C}} \cap \partial\Omega_{\mathcal{I}}$ is the interface between the conductor and the insulator.

We recall the time-harmonic Maxwell equations:

$$\begin{cases} \text{curl } \mathbf{H} + (i\omega\epsilon - \sigma)\mathbf{E} = \mathbf{J} & \text{in } \Omega, \\ \text{curl } \mathbf{E} - i\omega\mu\mathbf{H} = 0 & \text{in } \Omega, \end{cases} \quad (5.1a)$$

$$(5.1b)$$

with boundary conditions

$$\mathbf{H} \times \mathbf{n} = 0 \quad \text{on } \partial\Omega. \quad (5.2)$$

We assume that the current density $\mathbf{J}_{\mathcal{I}} = \mathbf{J}|_{\Omega_{\mathcal{I}}}$ satisfies:

$$\text{div } \mathbf{J}_{\mathcal{I}} = 0 \quad \text{in } \Omega_{\mathcal{I}}, \quad \mathbf{J}_{\mathcal{I}} \cdot \mathbf{n} = 0 \quad \text{on } \partial\Omega. \quad (5.3)$$

As $\omega\epsilon \ll \sigma$ in the conductor, with the assumption (5.3), the Maxwell equations (5.1) yield the eddy current equations:

$$\begin{cases} \operatorname{curl} \mathbf{H} - \sigma \mathbf{E} = \mathbf{J} & \text{in } \Omega, \\ \operatorname{curl} \mathbf{E} - i\omega\mu\mathbf{H} = 0 & \text{in } \Omega. \end{cases} \quad (5.4a)$$

$$(5.4b)$$

Since the permittivity ϵ is neglected in the eddy current model, we lose the information contained in the first Maxwell's equation (5.1a). In fact, applying the divergence operator to (5.1a) considering the assumption (5.3) yields

$$\begin{cases} \operatorname{div}(\epsilon\mathbf{E}) = 0 & \text{in } \Omega_{\mathcal{I}}, \\ \epsilon\mathbf{E} \cdot \mathbf{n} = 0 & \text{on } \partial\Omega. \end{cases} \quad (5.5)$$

Therefore, it is necessary to add the condition (5.5) to complete the eddy current model (5.4).

Inspired by the divergence-free property of the magnetic induction $\mu\mathbf{H}$, we consider the formulation via a vector magnetic potential \mathbf{A} and a scalar electric potential V such that

$$\begin{cases} \mu\mathbf{H} = \operatorname{curl} \mathbf{A} & \text{in } \Omega, \\ \mathbf{E} = i\omega\mathbf{A} + \nabla V & \text{in } \Omega_{\mathcal{C}}. \end{cases} \quad (5.6)$$

Therefore, in the distribution sense, (5.4) implies

$$\operatorname{curl}(\mu^{-1} \operatorname{curl} \mathbf{A}) - \sigma(i\omega\mathbf{A} + \nabla V) = \mathbf{J} \quad \text{in } \Omega.$$

As a new unknown V is added to the system, some additional condition is necessary to obtain a unique \mathbf{A} . Considering the divergence of the equation (5.4a) and the complementary condition (5.5), we introduce the Coulomb gauge condition to complete the system.

$$\begin{cases} \operatorname{div} \mathbf{A} = 0 & \text{in } \Omega, \\ \mathbf{A} \cdot \mathbf{n} = 0 & \text{on } \partial\Omega. \end{cases} \quad (5.7)$$

Finally we get the complete eddy current problem

$$\begin{cases} \operatorname{curl}(\mu^{-1} \operatorname{curl} \mathbf{A}) - \sigma(i\omega\mathbf{A} + \nabla V) = \mathbf{J} & \text{in } \Omega, & (5.8a) \\ \operatorname{div} \mathbf{A} = 0 & \text{in } \Omega, & (5.8b) \\ \mathbf{A} \cdot \mathbf{n} = 0 & \text{on } \partial\Omega, & (5.8c) \\ (\mu^{-1} \operatorname{curl} \mathbf{A}) \times \mathbf{n} = 0 & \text{on } \partial\Omega, & (5.8d) \end{cases}$$

where the last boundary condition (5.8d) comes from (5.2).

It is difficult to deal with the Coulomb gauge condition (5.8b), since classical finite elements do not keep the divergence-free property. [4, Chapter 6] proposes the addition of a penalization term: by introducing a constant $\mu_* > 0$ representing a suitable average of μ in Ω , the Coulomb gauge condition is incorporated in (5.8a):

$$\operatorname{curl}(\mu^{-1} \operatorname{curl} \mathbf{A}) - \mu_*^{-1} \nabla \operatorname{div} \mathbf{A} - \sigma(i\omega\mathbf{A} + \nabla V) = \mathbf{J} \quad \text{in } \Omega.$$

To ensure

$$\begin{cases} \operatorname{div}(\sigma \mathbf{E}) = -\operatorname{div} \mathbf{J} = 0 & \text{in } \Omega_{\mathcal{C}}, \\ \sigma \mathbf{E} \cdot \mathbf{n} = [\mathbf{J}]_{\Gamma_*} \cdot \mathbf{n} = 0 & \text{on } \Gamma_*, \end{cases}$$

where $[\cdot]_{\Gamma_*}$ is the jump through the interface Γ_* : $[a]_{\Gamma_*} = a_{\mathcal{I}} - a_{\mathcal{C}}$, we also add the following conditions

$$\begin{cases} \operatorname{div}(\sigma(i\omega \mathbf{A} + \nabla V)) = -\operatorname{div} \mathbf{J} = 0 & \text{in } \Omega_{\mathcal{C}}, \\ \sigma(i\omega \mathbf{A} + \nabla V) \cdot \mathbf{n} = [\mathbf{J}]_{\Gamma_*} \cdot \mathbf{n} = 0 & \text{on } \Gamma_*. \end{cases}$$

Therefore, we get the problem

$$\begin{cases} \operatorname{curl}(\mu^{-1} \operatorname{curl} \mathbf{A}) - \mu_*^{-1} \nabla \operatorname{div} \mathbf{A} - \sigma(i\omega \mathbf{A} + \nabla V) = \mathbf{J} & \text{in } \Omega, & (5.9a) \\ \operatorname{div}(\sigma(i\omega \mathbf{A} + \nabla V)) = -\operatorname{div} \mathbf{J} = 0 & \text{in } \Omega_{\mathcal{C}}, & (5.9b) \\ \sigma(i\omega \mathbf{A} + \nabla V) \cdot \mathbf{n} = [\mathbf{J}]_{\Gamma_*} \cdot \mathbf{n} = 0 & \text{on } \Gamma_*, & (5.9c) \\ \mathbf{A} \cdot \mathbf{n} = 0 & \text{on } \partial\Omega, & (5.9d) \\ (\mu^{-1} \operatorname{curl} \mathbf{A}) \times \mathbf{n} = 0 & \text{on } \partial\Omega. & (5.9e) \end{cases}$$

[4, Lemma 6.1] show the equivalence between the problems (5.8) and (5.9).

It is worth noting that in numerical tests, the convergence of nodal finite element approximation is generally not ensured due to the presence of re-entrant corners or edges (see Costabel – Dauge [32]). Nevertheless, [4, Remark 6.6] states that the nodal finite element approximation is convergent for the Coulomb gauged vector potential formulation.

5.1.2 Variational formulation of the eddy current problem via vector potentials

We define the function space

$$X(\Omega) = H(\operatorname{curl}, \Omega) \cap H_0(\operatorname{div}, \Omega). \quad (5.10)$$

We multiply (5.9a) by $\overline{\Psi}$ and (5.9b) by Φ . By integration by parts, one gets the variational formulation of (5.9)

$$a(\mathbf{A}, V; \Psi, \Phi) = \int_{\Omega} \mathbf{J} \cdot \overline{\Psi} \, dx - \frac{1}{i\omega} \int_{\Omega_{\mathcal{C}}} \mathbf{J} \cdot \nabla \overline{\Phi} \, dx \quad \forall (\Psi, \Phi) \in X(\Omega) \times H^1(\Omega_{\mathcal{C}})/\mathbb{C}, \quad (5.11)$$

where

$$\begin{aligned} a(\mathbf{a}, v; \psi, \phi) &:= \int_{\Omega} \left(\frac{1}{\mu} \operatorname{curl} \mathbf{a} \cdot \operatorname{curl} \overline{\psi} + \frac{1}{\mu_*} \operatorname{div} \mathbf{a} \operatorname{div} \overline{\psi} \right) dx \\ &\quad + \frac{1}{i\omega} \int_{\Omega_{\mathcal{C}}} \sigma(i\omega \mathbf{a} + \nabla v) \cdot (\overline{i\omega \psi + \nabla \phi}) \, dx \quad \forall (\mathbf{a}, v), (\psi, \phi) \in X(\Omega) \times H^1(\Omega_{\mathcal{C}})/\mathbb{C}. \end{aligned} \quad (5.12)$$

We may refer to [4, Theorem 6.3] to see the equivalence between the variational formulation (5.11) and the strong problem (5.9). We conclude from [4, Section 6.1.2] that

Proposition 5.1.1. *Let $\mu > 0$, $\sigma \geq 0$ belong to $L^\infty(\Omega)$. $\mathbf{J} \in L^2(\Omega)^3$ has compact support in $\Omega_s \subset \Omega_{\mathcal{I}}$ and satisfies $\operatorname{div} \mathbf{J} = 0$ in Ω_s . Then the variational problem (5.11) has a unique solution (\mathbf{A}, V) in $X(\Omega) \times H^1(\Omega_{\mathcal{C}})/\mathbb{C}$.*

5.2 Deposit reconstruction via shape optimization

5.2.1 Shape and material derivatives of the solution

For any regular open set $\mathcal{Q} \subset \mathbb{R}^3$, we consider a domain deformation as a perturbation of the identity

$$\begin{aligned} \text{Id} + \boldsymbol{\theta} : \mathcal{Q} &\rightarrow \mathcal{Q}_\theta \\ x &\mapsto y, \end{aligned} \quad (5.13)$$

where $\boldsymbol{\theta} \in W^{1,\infty}(\mathcal{Q}, \mathcal{Q})^3$ is a small perturbation. To make a difference between the differential operators before and after the variable substitution, we denote by $\text{curl}_x, \text{div}_x, \nabla_x$ the curl, divergence and gradient operators on \mathcal{Q} with x -coordinates and by $\text{curl}_y, \text{div}_y, \nabla_y$ those on \mathcal{Q}_θ with y -coordinates. For any $(\mathbf{a}(\mathcal{Q}_\theta), v(\mathcal{Q}_\theta))$ defined on \mathcal{Q}_θ , we set

$$\mathbf{a}_\nabla(\boldsymbol{\theta}) = \mathbf{a}(\mathcal{Q}_\theta) \circ (\text{Id} + \boldsymbol{\theta}), \quad (5.14a)$$

$$\mathbf{a}_{\text{curl}}(\boldsymbol{\theta}) = (I + \nabla\boldsymbol{\theta})^t \mathbf{a}_\nabla, \quad (5.14b)$$

$$\mathbf{a}_{\text{div}}(\boldsymbol{\theta}) = \det(I + \nabla\boldsymbol{\theta})(I + \nabla\boldsymbol{\theta})^{-1} \mathbf{a}_\nabla, \quad (5.14c)$$

$$v_\nabla(\boldsymbol{\theta}) = v(\mathcal{Q}_\theta) \circ (\text{Id} + \boldsymbol{\theta}). \quad (5.14d)$$

which conserve the corresponding differential operators (see for example [62, (3.75), Corollary 3.58, Lemma 3.59])

$$(I + \nabla\boldsymbol{\theta})^{-t} \nabla_x \mathbf{a}_\nabla(\boldsymbol{\theta}) = (\nabla_y \mathbf{a}(\Omega_\theta)) \circ (\text{Id} + \boldsymbol{\theta}), \quad (5.15a)$$

$$\frac{I + \nabla\boldsymbol{\theta}}{\det(I + \nabla\boldsymbol{\theta})} \text{curl}_x \mathbf{a}_{\text{curl}}(\boldsymbol{\theta}) = (\text{curl}_y \mathbf{a}(\Omega_\theta)) \circ (\text{Id} + \boldsymbol{\theta}), \quad (5.15b)$$

$$\frac{1}{\det(I + \nabla\boldsymbol{\theta})} \text{div}_x \mathbf{a}_{\text{div}}(\boldsymbol{\theta}) = (\text{div}_y \mathbf{a}(\Omega_\theta)) \circ (\text{Id} + \boldsymbol{\theta}), \quad (5.15c)$$

$$(I + \nabla\boldsymbol{\theta})^{-t} \nabla_x v_\nabla(\boldsymbol{\theta}) = (\nabla_y v(\Omega_\theta)) \circ (\text{Id} + \boldsymbol{\theta}), \quad (5.15d)$$

where $\nabla\boldsymbol{\theta} := (\frac{\partial\theta_i}{\partial x_j})_{i,j}$ is the Jacobian matrix. In the sequel, we write curl, div and ∇ for $\text{curl}_x, \text{div}_x$ and ∇_x respectively.

Definition 5.2.1. *Let $(\mathbf{a}(\mathcal{Q}), v(\mathcal{Q}))$ some shape-dependent functions that belong to some Banach space $B(\mathcal{Q})$, and $\boldsymbol{\theta} \in W^{1,\infty}(\mathcal{Q}, \mathcal{Q})^3$ a shape perturbation. The material derivatives $(\mathbf{b}(\boldsymbol{\theta}), u(\boldsymbol{\theta}))$ of (\mathbf{a}, v) are defined by*

$$\mathbf{a}_{\text{curl}}(\boldsymbol{\theta}) = \mathbf{a}_{\text{curl}}(0) + \mathbf{b}(\boldsymbol{\theta}) + o(\boldsymbol{\theta}) = \mathbf{a}(\mathcal{Q}) + \mathbf{b}(\boldsymbol{\theta}) + o(\boldsymbol{\theta}), \quad (5.16)$$

$$v_\nabla(\boldsymbol{\theta}) = v_\nabla(0) + u(\boldsymbol{\theta}) + o(\boldsymbol{\theta}) = v(\mathcal{Q}) + u(\boldsymbol{\theta}) + o(\boldsymbol{\theta}), \quad (5.17)$$

where $\lim_{\boldsymbol{\theta} \rightarrow 0} \frac{\|o(\boldsymbol{\theta})\|_{B(\mathcal{Q})}}{\|\boldsymbol{\theta}\|_{1,\infty}} = 0$. We also define the shape derivatives $(\mathbf{a}'(\boldsymbol{\theta}), v'(\boldsymbol{\theta}))$ of (\mathbf{a}, v) by

$$\mathbf{a}'(\boldsymbol{\theta}) = \mathbf{b}(\boldsymbol{\theta}) - (\boldsymbol{\theta} \cdot \nabla) \mathbf{a}(\mathcal{Q}) - (\nabla\boldsymbol{\theta})^t \mathbf{a}(\mathcal{Q}), \quad (5.18)$$

$$v'(\boldsymbol{\theta}) = u(\boldsymbol{\theta}) - \boldsymbol{\theta} \cdot \nabla v(\mathcal{Q}). \quad (5.19)$$

The derivatives $\mathbf{b}_{\text{div}}(\boldsymbol{\theta})$ and $\mathbf{b}_{\nabla}(\boldsymbol{\theta})$ of \mathbf{a} which conserve the divergence operator and the gradient operator respectively are given by

$$\mathbf{b}_{\text{div}}(\boldsymbol{\theta}) = \mathbf{b}(\boldsymbol{\theta}) + (\text{div } \boldsymbol{\theta} I - \nabla \boldsymbol{\theta} - (\nabla \boldsymbol{\theta})^t) \mathbf{a}(\mathcal{Q}), \quad (5.20)$$

$$\mathbf{b}_{\nabla}(\boldsymbol{\theta}) = \mathbf{b}(\boldsymbol{\theta}) - (\nabla \boldsymbol{\theta})^t \mathbf{a}(\mathcal{Q}). \quad (5.21)$$

Remark 5.2.2. Using the chain rule, we have from Definition 5.2.1 that formally, in $\omega \subset \mathcal{Q} \cap \mathcal{Q}_\theta$,

$$\mathbf{a}(\mathcal{Q}_\theta) = \mathbf{a}(\mathcal{Q}) + \mathbf{a}'(\boldsymbol{\theta}) + o(\boldsymbol{\theta}), \quad (5.22)$$

$$\mathbf{a}_{\text{div}}(\boldsymbol{\theta}) = \mathbf{a}_{\text{div}}(0) + \mathbf{b}_{\text{div}}(\boldsymbol{\theta}) + o(\boldsymbol{\theta}) = \mathbf{a}(\mathcal{Q}) + \mathbf{b}_{\text{div}}(\boldsymbol{\theta}) + o(\boldsymbol{\theta}), \quad (5.23)$$

$$\mathbf{a}_{\nabla}(\boldsymbol{\theta}) = \mathbf{a}_{\nabla}(0) + \mathbf{b}_{\nabla}(\boldsymbol{\theta}) + o(\boldsymbol{\theta}) = \mathbf{a}(\mathcal{Q}) + \mathbf{b}_{\nabla}(\boldsymbol{\theta}) + o(\boldsymbol{\theta}), \quad (5.24)$$

$$v(\mathcal{Q}_\theta) = v(\mathcal{Q}) + v'(\boldsymbol{\theta}) + o(\boldsymbol{\theta}). \quad (5.25)$$

Remark 5.2.3. The definition of the material derivative $\mathbf{b}(\boldsymbol{\theta})$ of \mathbf{a} here is slightly different from that in the axisymmetric 2-D case, which is similar to the definition of the derivative $\mathbf{b}_{\nabla}(\boldsymbol{\theta})$ which conserves the gradient operator. In fact, the material derivative is defined so as to keep the boundary or transmission conditions. In the axisymmetric 2-D case, we apply the gradient operator on the weighted azimuthal electric field w and its material derivative defined with respect to the gradient operator keeps the same transmission conditions at the interface with jumps of coefficients. In the 3-D case, however, it is the curl operator that one applies on the vector potential. Thus its material derivative is defined with respect to the curl operator to conserve the transmission conditions.

Precisely speaking, if we denote by $[\cdot]$ the jump through the interface Γ , i.e. for any $f(x)$ defined in a vicinity of Γ and any $x_0 \in \Gamma$

$$[f](x_0) := f_+(x_0) - f_-(x_0),$$

$$\text{with } f_+(x_0) = \lim_{\Omega_v \ni x \rightarrow x_0} f(x) \quad \text{and} \quad f_-(x_0) = \lim_{\Omega_d \ni x \rightarrow x_0} f(x).$$

then the transmission conditions satisfied by $\mathbf{A} \in X(\Omega)$

$$[\mathbf{n} \cdot \text{curl } \mathbf{A}] = [\mu^{-1} \mathbf{n} \times \text{curl } \mathbf{A}] = 0 \quad \text{on } \Gamma, \quad (5.26)$$

are also satisfied by its material derivative $\mathbf{B}(\boldsymbol{\theta}) \in X(\Omega)$

$$[\mathbf{n} \cdot \text{curl } \mathbf{B}] = [\mu^{-1} \mathbf{n} \times \text{curl } \mathbf{B}] = 0 \quad \text{on } \Gamma. \quad (5.27)$$

We rewrite the variational formulation (5.11) on Ω_θ

$$\begin{aligned} & \int_{\Omega_\theta} \left(\frac{1}{\mu} \text{curl}_y \mathbf{A} \cdot \text{curl}_y \overline{\boldsymbol{\Psi}} + \frac{1}{\mu_*} \text{div}_y \mathbf{A} \text{div}_y \overline{\boldsymbol{\Psi}} \right) dy + \frac{1}{i\omega} \int_{\Omega_{C\theta}} \sigma(i\omega \mathbf{A} + \nabla V) \cdot (i\omega \boldsymbol{\Psi} + \nabla \Phi) dy \\ &= \int_{\Omega_\theta} \mathbf{J} \cdot \overline{\boldsymbol{\Psi}} dy - \frac{1}{i\omega} \int_{\Omega_{C\theta}} \mathbf{J} \cdot \nabla \overline{\Phi} dy \quad \forall (\boldsymbol{\Psi}, \Phi) \in X(\Omega_\theta) \times H^1(\Omega_{C\theta})/\mathbb{C}. \end{aligned} \quad (5.28)$$

We set

$$\begin{aligned} \mathbf{A}_{\nabla}(\boldsymbol{\theta}) &= \mathbf{A}(\Omega_\theta) \circ (\text{Id} + \boldsymbol{\theta}), \\ \mathbf{A}_{\text{curl}}(\boldsymbol{\theta}) &= (I + \nabla \boldsymbol{\theta})^t \mathbf{A}_{\nabla}, \\ \mathbf{A}_{\text{div}}(\boldsymbol{\theta}) &= \det(I + \nabla \boldsymbol{\theta}) (I + \nabla \boldsymbol{\theta})^{-1} \mathbf{A}_{\nabla}, \\ V_{\nabla}(\boldsymbol{\theta}) &= V(\Omega_\theta) \circ (\text{Id} + \boldsymbol{\theta}), \end{aligned}$$

and we choose the test functions such that

$$\boldsymbol{\Psi} = (I + \nabla\boldsymbol{\theta})^t \boldsymbol{\Psi}(\Omega_\theta) \circ (\text{Id} + \boldsymbol{\theta}), \quad \bar{\Phi} = \bar{\Phi}(\Omega_\theta) \circ (\text{Id} + \boldsymbol{\theta}). \quad (5.29)$$

We set also

$$\boldsymbol{\Psi}_{\text{div}}(\boldsymbol{\theta}) = \det(I + \nabla\boldsymbol{\theta})(I + \nabla\boldsymbol{\theta})^{-1}(I + \nabla\boldsymbol{\theta})^{-t} \boldsymbol{\Psi} = \det(I + \nabla\boldsymbol{\theta})(I + \nabla\boldsymbol{\theta})^{-1} \boldsymbol{\Psi}(\Omega_\theta) \circ (\text{Id} + \boldsymbol{\theta})$$

which conserves the divergence operator

$$\frac{1}{\det(I + \nabla\boldsymbol{\theta})} \text{div} \boldsymbol{\Psi}_{\text{div}}(\boldsymbol{\theta}) = (\text{div}_y \boldsymbol{\Psi}(\Omega_\theta)) \circ (\text{Id} + \boldsymbol{\theta}).$$

By variable substitution $y = (\text{Id} + \boldsymbol{\theta})x$, the left-hand-side of (5.28) writes

$$\begin{aligned} & \int_{\Omega} \left(\frac{1}{\mu} \frac{(I + \nabla\boldsymbol{\theta})^t (I + \nabla\boldsymbol{\theta})}{|\det(I + \nabla\boldsymbol{\theta})|} \text{curl} \mathbf{A}_{\text{curl}} \cdot \text{curl} \bar{\boldsymbol{\Psi}} + \frac{1}{\mu_*} \frac{1}{|\det(I + \nabla\boldsymbol{\theta})|} \text{div} \mathbf{A}_{\text{div}} \text{div} \bar{\boldsymbol{\Psi}}_{\text{div}} \right) dx \\ & + \frac{1}{i\omega} \int_{\Omega_c} \sigma |\det(I + \nabla\boldsymbol{\theta})| (I + \nabla\boldsymbol{\theta})^{-1} (I + \nabla\boldsymbol{\theta})^{-t} (i\omega \mathbf{A}_{\text{curl}} + \nabla V_{\nabla}) \cdot (\overline{i\omega \boldsymbol{\Psi}} + \nabla \bar{\Phi}) dx. \end{aligned} \quad (5.30)$$

Since $\text{supp} \mathbf{J} \cap \text{supp} \boldsymbol{\theta} = \emptyset$, the right-hand side of the weak formulation (5.28) writes simply:

$$\int_{\Omega} \mathbf{J} \cdot \bar{\boldsymbol{\Psi}} dx - \frac{1}{i\omega} \int_{\Omega_c} \mathbf{J} \cdot \nabla \bar{\Phi} dx. \quad (5.31)$$

Like in Definition 5.2.1, we denote by $(\mathbf{B}(\boldsymbol{\theta}), U(\boldsymbol{\theta}))$ the material derivatives of (\mathbf{A}, V) , and by $\mathbf{b}_{\text{div}}(\boldsymbol{\theta})$ and $\mathbf{b}_{\nabla}(\boldsymbol{\theta})$ the derivatives of \mathbf{A} which keep the divergence and the gradient operator respectively. Considering the developments

$$\begin{aligned} |\det(I + \nabla\boldsymbol{\theta})| &= 1 + \text{div} \boldsymbol{\theta} + o(\boldsymbol{\theta}), \\ (I + \nabla\boldsymbol{\theta})^{-1} &= I - \nabla\boldsymbol{\theta} + o(\boldsymbol{\theta}), \end{aligned}$$

we develop the left-hand-side (5.30) and the right-hand-side (5.31) with respect to $\boldsymbol{\theta}$. The terms of order zero with respect to $\boldsymbol{\theta}$ give exactly the variational formulation (5.11) on Ω and therefore vanish. Using the Coulombe gauge condition $\text{div} \mathbf{A} = 0$, the first order terms with respect to $\boldsymbol{\theta}$ yield

$$\begin{aligned} & \int_{\Omega} \left(\frac{1}{\mu} \text{curl} \mathbf{B}(\boldsymbol{\theta}) \cdot \text{curl} \bar{\boldsymbol{\Psi}} + \frac{1}{\mu_*} \text{div} \mathbf{B}_{\text{div}}(\boldsymbol{\theta}) \text{div} \bar{\boldsymbol{\Psi}} \right) dx \\ & + \frac{1}{i\omega} \int_{\Omega_c} \sigma (i\omega \mathbf{B}(\boldsymbol{\theta}) + \nabla U(\boldsymbol{\theta})) \cdot (\overline{i\omega \boldsymbol{\Psi}} + \nabla \bar{\Phi}) dx \\ & = \int_{\Omega} \frac{1}{\mu} (\text{div} \boldsymbol{\theta} I - \nabla\boldsymbol{\theta} - (\nabla\boldsymbol{\theta})^t) \text{curl} \mathbf{A} \cdot \text{curl} \bar{\boldsymbol{\Psi}} dx \\ & + \frac{1}{i\omega} \int_{\Omega_c} \sigma (-\text{div} \boldsymbol{\theta} I + \nabla\boldsymbol{\theta} + (\nabla\boldsymbol{\theta})^t) (i\omega \mathbf{A} + \nabla V) \cdot (\overline{i\omega \boldsymbol{\Psi}} + \nabla \bar{\Phi}) dx. \end{aligned} \quad (5.32)$$

We substitute \mathbf{B}_{div} by (5.20) in (5.32), and get the weak formulation for the material derivatives $(\mathbf{B}(\boldsymbol{\theta}), U(\boldsymbol{\theta}))$

$$a(\mathbf{B}(\boldsymbol{\theta}), U(\boldsymbol{\theta}); \boldsymbol{\Psi}, \bar{\Phi}) = L(\boldsymbol{\Psi}, \bar{\Phi}) \quad \forall (\boldsymbol{\Psi}, \bar{\Phi}) \in X(\Omega) \times H^1(\Omega_c)/\mathbb{C}, \quad (5.33)$$

where

$$\begin{aligned}
L(\boldsymbol{\Psi}, \Phi) &:= \int_{\Omega} \frac{1}{\mu} (\operatorname{div} \boldsymbol{\theta} I - \nabla \boldsymbol{\theta} - (\nabla \boldsymbol{\theta})^t) \operatorname{curl} \bar{\mathbf{A}} \cdot \operatorname{curl} \bar{\boldsymbol{\Psi}} \, dx \\
&\quad - \int_{\Omega_d + \Omega_d^c} \frac{1}{\mu_*} \operatorname{div} \left((\operatorname{div} \boldsymbol{\theta} I - \nabla \boldsymbol{\theta} - (\nabla \boldsymbol{\theta})^t) \mathbf{A} \right) \cdot \operatorname{div} \bar{\boldsymbol{\Psi}} \, dx \\
&\quad + \frac{1}{i\omega} \int_{\Omega_C} \sigma (-\operatorname{div} \boldsymbol{\theta} I + \nabla \boldsymbol{\theta} + (\nabla \boldsymbol{\theta})^t) (i\omega \mathbf{A} + \nabla V) \cdot \overline{(i\omega \boldsymbol{\Psi} + \nabla \Phi)} \, dy. \tag{5.34}
\end{aligned}$$

Remark 5.2.4. In the above expression of $L(\boldsymbol{\Psi}, \Phi)$ we used the notation $\int_{\Omega_d + \Omega_d^c}$ which means the integrals on Ω_d and on Ω_d^c separately. That is because the term $\operatorname{div}((\operatorname{div} \boldsymbol{\theta} I - \nabla \boldsymbol{\theta} - (\nabla \boldsymbol{\theta})^t) \mathbf{A})$ is not defined on the whole domain $\Omega = \Omega_d \cup \Omega_d^c$ for lack of regularity on Γ , but only on the subdomains Ω_d and Ω_d^c .

Using the same argument as for Proposition 5.1.1, we obtain

Proposition 5.2.5. Let $\boldsymbol{\theta} \in W^{1,\infty}(\Omega, \Omega)^3$ a domain perturbation. Under the same assumptions as in Proposition 5.1.1, the variational formulation for the material derivatives (5.11) has a unique solution $(\mathbf{B}(\boldsymbol{\theta}), U(\boldsymbol{\theta}))$ in $X(\Omega) \times H^1(\Omega_C)/\mathcal{C}$.

To simplify the expression of the variational formulation (5.33), we introduce a computational result. We assume that on $\mathcal{Q} \subset \Omega$, the coefficients μ and σ are constant. We define a shape-dependent form

$$\alpha_{\mu,\sigma}(\mathcal{Q})(\mathbf{a}, v; \boldsymbol{\psi}, \phi) := \int_{\mathcal{Q}} \frac{1}{\mu} \operatorname{curl} \mathbf{a} \cdot \operatorname{curl} \bar{\boldsymbol{\psi}} \, dx + \frac{1}{i\omega} \int_{\mathcal{Q}} \sigma (i\omega \mathbf{a} + \nabla v) \cdot \overline{(i\omega \boldsymbol{\psi} + \nabla \phi)} \, dx. \tag{5.35}$$

We denote the tangential component a vector and the tangential gradient operator on some boundary or interface by

$$\begin{aligned}
\mathbf{a}_\tau &:= \mathbf{a} - (\mathbf{a} \cdot \mathbf{n}) \mathbf{n}, \\
\nabla_\tau v &:= \nabla v - \partial_n v \mathbf{n}.
\end{aligned}$$

Lemma 5.2.6. Let \mathcal{Q} a regular open set, $\mu > 0$ and $\sigma \geq 0$ constant on \mathcal{Q} and $\operatorname{Id} + \boldsymbol{\theta} : \mathcal{Q} \rightarrow \mathcal{Q}_\theta$ a deformation. Let $(\mathbf{a}, v) = (\mathbf{a}(\mathcal{Q}), v(\mathcal{Q}))$ and $(\boldsymbol{\psi}, \phi) = (\boldsymbol{\psi}(\mathcal{Q}), \phi(\mathcal{Q}))$ some shape-dependent functions with sufficient regularity. We assume that the material derivatives $(\mathbf{b}(\boldsymbol{\theta}), u(\boldsymbol{\theta}))$ of (\mathbf{a}, v) , the shape derivatives $(\mathbf{a}'(\boldsymbol{\theta}), v'(\boldsymbol{\theta}))$ of (\mathbf{a}, v) and the material derivatives $(\boldsymbol{\eta}(\boldsymbol{\theta}), \chi(\boldsymbol{\theta}))$ of $(\boldsymbol{\psi}, \phi)$ defined as in Definition 5.2.1 exist. If $(\mathbf{a}(\mathcal{Q}), v(\mathcal{Q}))$ satisfy in the weak sense

$$\begin{cases} \operatorname{curl}(\mu^{-1} \operatorname{curl} \mathbf{a}) - \sigma (i\omega \mathbf{a} + \nabla v) = 0 & \text{in } \mathcal{Q}, & (5.36a) \\ \operatorname{div} \mathbf{a} = 0 & \text{in } \mathcal{Q}, & (5.36b) \\ \sigma (i\omega \mathbf{a} + \nabla v) \cdot \mathbf{n} = 0 & \text{on } \partial \mathcal{Q}, & (5.36c) \end{cases}$$

then the shape derivative of $\alpha_{\mu,\sigma}(\mathcal{Q})(\mathbf{a}, v; \boldsymbol{\psi}, \phi)$ that we denote by $\alpha'_{\mu,\sigma}(\mathcal{Q})(\boldsymbol{\theta})(\mathbf{a}, v; \boldsymbol{\psi}, \phi)$, i.e.

$$\begin{aligned}
&\alpha_{\mu,\sigma}(\mathcal{Q}_\theta)(\mathbf{a}(\mathcal{Q}_\theta), v(\mathcal{Q}_\theta); \boldsymbol{\psi}(\mathcal{Q}_\theta), \phi(\mathcal{Q}_\theta)) \\
&= \alpha_{\mu,\sigma}(\mathcal{Q})(\mathbf{a}(\mathcal{Q}), v(\mathcal{Q}); \boldsymbol{\psi}(\mathcal{Q}), \phi(\mathcal{Q})) + \alpha'_{\mu,\sigma}(\mathcal{Q})(\boldsymbol{\theta})(\mathbf{a}(\mathcal{Q}), v(\mathcal{Q}); \boldsymbol{\psi}(\mathcal{Q}), \phi(\mathcal{Q})) + o(\boldsymbol{\theta}),
\end{aligned}$$

satisfies

$$\begin{aligned}
& \alpha'_{\mu,\sigma}(\mathcal{Q})(\theta)(\mathbf{a}, v; \boldsymbol{\psi}, \phi) \\
&= \alpha_{\mu,\sigma}(\mathcal{Q})(\mathbf{a}'(\theta), v'(\theta); \boldsymbol{\psi}, \phi) + \alpha_{\mu,\sigma}(\mathcal{Q})(\mathbf{a}, v; \boldsymbol{\eta}(\theta), \chi(\theta)) \\
&+ \int_{\partial\mathcal{Q}} \frac{1}{\mu} (\boldsymbol{\theta} \cdot \operatorname{curl} \mathbf{a})(\mathbf{n} \cdot \operatorname{curl} \bar{\boldsymbol{\psi}}) \, ds + \frac{1}{i\omega} \int_{\partial\mathcal{Q}} \sigma (\mathbf{n} \cdot \boldsymbol{\theta})(i\omega \mathbf{a}_\tau + \nabla_\tau v) \cdot (\overline{i\omega \boldsymbol{\psi}_\tau + \nabla_\tau \phi}) \, ds. \quad (5.37)
\end{aligned}$$

The proof, which involves some exhaustive computations, is given in Section 5.3.2.

Proposition 5.2.7. *Under the same assumptions as in Proposition 5.2.5, we assume in addition that μ, σ are piecewise constant and constant in each subdomain ($\Omega_s, \Omega_t, \Omega_d, \Omega_v$ or Ω_p). If the domain perturbation $\boldsymbol{\theta}$ has support only on a vicinity of the interface Γ between the deposit domain Ω_d and the vacuum Ω_v ($\Gamma = \partial\Omega_d \cap \partial\Omega_v$) and vanishes in Ω_s , then the material derivatives $(\mathbf{B}(\boldsymbol{\theta}), U(\boldsymbol{\theta}))$ of (\mathbf{A}, V) satisfies*

$$a(\mathbf{B}(\boldsymbol{\theta}), U(\boldsymbol{\theta}); \boldsymbol{\Psi}, \Phi) = \mathcal{L}(\boldsymbol{\Psi}, \Phi) \quad \forall (\boldsymbol{\Psi}, \Phi) \in X(\Omega) \times H^1(\Omega_C)/\mathbb{C}, \quad (5.38)$$

where

$$\begin{aligned}
& \mathcal{L}(\boldsymbol{\Psi}, \Phi) \\
&:= \int_{\Omega_d + \Omega_d^e} \left(\frac{1}{\mu} \operatorname{curl}((\boldsymbol{\theta} \cdot \nabla) \mathbf{A} + (\nabla \boldsymbol{\theta})^t \mathbf{A}) \cdot \operatorname{curl} \bar{\boldsymbol{\Psi}} + \frac{1}{\mu_*} \operatorname{div}((\boldsymbol{\theta} \cdot \nabla) \mathbf{A} + (\nabla \boldsymbol{\theta})^t \mathbf{A}) \operatorname{div} \bar{\boldsymbol{\Psi}} \right) \, dx \\
&+ \frac{1}{i\omega} \int_{\Omega_C} \sigma \left(i\omega((\boldsymbol{\theta} \cdot \nabla) \mathbf{A} + (\nabla \boldsymbol{\theta})^t \mathbf{A}) + \nabla(\boldsymbol{\theta} \cdot \nabla V) \right) \cdot (\overline{i\omega \boldsymbol{\Psi} + \nabla \Phi}) \, dx \\
&+ \int_{\Gamma} \left[\frac{1}{\mu} \right] (\boldsymbol{\theta} \cdot \mathbf{n})(\mathbf{n} \cdot \operatorname{curl} \mathbf{A})(\mathbf{n} \cdot \operatorname{curl} \bar{\boldsymbol{\Psi}}) \, ds \\
&+ \frac{1}{i\omega} \int_{\Gamma} (\boldsymbol{\theta} \cdot \mathbf{n}) [\sigma] (i\omega \mathbf{A}_\tau + \nabla_\tau V) \cdot (\overline{i\omega \boldsymbol{\Psi}_\tau + \nabla_\tau \Phi}) \, ds \quad \forall (\boldsymbol{\Psi}, \Phi) \in X(\Omega) \times H^1(\Omega_C)/\mathbb{C}. \quad (5.39)
\end{aligned}$$

Proof. Let $\Lambda = \{s, t, d, v, p\}$ a set of indices with its elements designating the different subdomains as well as the corresponding permeabilities and conductivities. We rewrite left-hand-side of the variational formulation (5.28) for $(\mathbf{A}(\Omega_\theta), V(\Omega_\theta))$ as

$$\underbrace{\sum_{i \in \Lambda} \alpha_{\mu_i, \sigma_i}(\Omega_{i\theta})(\mathbf{A}(\Omega_\theta), V(\Omega_\theta); \boldsymbol{\Psi}(\Omega_\theta), \Phi(\Omega_\theta))}_{\mathcal{A}(\Omega_\theta)} + \underbrace{\int_{\Omega_\theta} \frac{1}{\mu_*} \operatorname{div}_y \mathbf{A}(\Omega_\theta) \cdot \operatorname{div}_y \bar{\boldsymbol{\Psi}}(\Omega_\theta) \, dy}_{\mathcal{P}(\Omega_\theta)}.$$

If we choose the test functions $(\boldsymbol{\Psi}, \Phi)$ as in (5.29), their material derivatives vanish. Since $(\mathbf{A}(\Omega_\theta), V(\Omega_\theta))$ satisfy both (5.8) and (5.9), we can apply Lemma 5.2.6 to the terms $\alpha_{\mu_i, \sigma_i}(\Omega_{i\theta})$,

which yields the shape derivative of \mathcal{A}

$$\begin{aligned}
\mathcal{A}'(\Omega)(\boldsymbol{\theta}) &= \sum_{i \in \Lambda} \alpha'_{\mu_i, \sigma_i}(\Omega_i)(\boldsymbol{\theta})(\mathbf{A}, V; \boldsymbol{\Psi}, \Phi) \\
&= \sum_{i \in \Lambda} \alpha_{\mu_i, \sigma_i}(\Omega_i)(\mathbf{A}'(\boldsymbol{\theta}), V'(\boldsymbol{\theta}); \boldsymbol{\Psi}, \Phi) \\
&\quad - \int_{\Gamma} \left[\frac{1}{\mu} (\boldsymbol{\theta} \cdot \operatorname{curl} \mathbf{A})(\mathbf{n} \cdot \operatorname{curl} \bar{\boldsymbol{\Psi}}) \right] ds - \frac{1}{i\omega} \int_{\Gamma} (\boldsymbol{\theta} \cdot \mathbf{n}) [\sigma] (i\omega \mathbf{A}_{\tau} + \nabla_{\tau} V) \cdot (\overline{i\omega \boldsymbol{\Psi}_{\tau} + \nabla_{\tau} \Phi}) ds \\
&= \sum_{i \in \Lambda} \left(\alpha_{\mu_i, \sigma_i}(\Omega_i)(\mathbf{B}(\boldsymbol{\theta}), U(\boldsymbol{\theta}); \boldsymbol{\Psi}, \Phi) + \alpha_{\mu_i, \sigma_i}(\Omega_i)(-\boldsymbol{\theta} \cdot \nabla) \mathbf{A} - (\nabla \boldsymbol{\theta})^t \mathbf{A}, -(\boldsymbol{\theta} \cdot \nabla V); \boldsymbol{\Psi}, \Phi \right) \\
&\quad - \int_{\Gamma} \left[\frac{1}{\mu} \left((\boldsymbol{\theta} \cdot \mathbf{n})(\mathbf{n} \cdot \operatorname{curl} \mathbf{A}) + \boldsymbol{\theta} \cdot (\mathbf{n} \times (\operatorname{curl} \mathbf{A} \times \mathbf{n})) \right) (\mathbf{n} \cdot \operatorname{curl} \bar{\boldsymbol{\Psi}}) \right] ds \\
&\quad - \frac{1}{i\omega} \int_{\Gamma} (\boldsymbol{\theta} \cdot \mathbf{n}) [\sigma] (i\omega \mathbf{A}_{\tau} + \nabla_{\tau} V) \cdot (\overline{i\omega \boldsymbol{\Psi}_{\tau} + \nabla_{\tau} \Phi}) ds \\
&= a(\mathbf{B}(\boldsymbol{\theta}), U(\boldsymbol{\theta}); \boldsymbol{\Psi}, \Phi) - \int_{\Omega} \frac{1}{\mu_*} \operatorname{div} \mathbf{B}(\boldsymbol{\theta}) \operatorname{div} \bar{\boldsymbol{\Psi}} dx \\
&\quad - \int_{\Omega_d + \Omega_d^c} \frac{1}{\mu} \operatorname{curl}((\boldsymbol{\theta} \cdot \nabla) \mathbf{A} + (\nabla \boldsymbol{\theta})^t \mathbf{A}) \cdot \operatorname{curl} \bar{\boldsymbol{\Psi}} dx \\
&\quad - \frac{1}{i\omega} \int_{\Omega_c} \sigma \left(i\omega((\boldsymbol{\theta} \cdot \nabla) \mathbf{A} + (\nabla \boldsymbol{\theta})^t \mathbf{A}) + \nabla(\boldsymbol{\theta} \cdot \nabla V) \right) \cdot (\overline{i\omega \boldsymbol{\Psi} + \nabla \Phi}) dx \\
&\quad - \int_{\Gamma} \left[\frac{1}{\mu} \right] (\boldsymbol{\theta} \cdot \mathbf{n})(\mathbf{n} \cdot \operatorname{curl} \mathbf{A})(\mathbf{n} \cdot \operatorname{curl} \bar{\boldsymbol{\Psi}}) ds \\
&\quad - \frac{1}{i\omega} \int_{\Gamma} (\boldsymbol{\theta} \cdot \mathbf{n}) [\sigma] (i\omega \mathbf{A}_{\tau} + \nabla_{\tau} V) \cdot (\overline{i\omega \boldsymbol{\Psi}_{\tau} + \nabla_{\tau} \Phi}) ds. \tag{5.40}
\end{aligned}$$

In the last equality we have used the transmission conditions

$$[\mathbf{n} \cdot \operatorname{curl} \mathbf{A}] = [\mathbf{n} \times (\mu^{-1} \operatorname{curl} \mathbf{A} \times \mathbf{n})] = 0 \quad \text{on } \Gamma.$$

From the derivation of $L(\boldsymbol{\Psi}, \Phi)$ (5.34), one deduces easily that the shape derivative of the penalization term \mathcal{P} is

$$\mathcal{P}'(\Omega)(\boldsymbol{\theta}) = \int_{\Omega} \frac{1}{\mu_*} \operatorname{div} \mathbf{B}(\boldsymbol{\theta}) \operatorname{div} \bar{\boldsymbol{\Psi}} dx + \int_{\Omega_d + \Omega_d^c} \frac{1}{\mu_*} \operatorname{div} \left((\operatorname{div} \boldsymbol{\theta} I - \nabla \boldsymbol{\theta} - (\nabla \boldsymbol{\theta})^t) \mathbf{A} \right) \operatorname{div} \bar{\boldsymbol{\Psi}} dx.$$

Using the identities (5.57) and the Coulombe gauge condition $\operatorname{div} \mathbf{A} = 0$, one verifies that on each subdomain Ω_i ($i \in \Lambda$) of Ω

$$\begin{aligned}
\operatorname{div}((\operatorname{div} \boldsymbol{\theta} I - \nabla \boldsymbol{\theta} - (\nabla \boldsymbol{\theta})^t) \mathbf{A}) &= \operatorname{div}((\operatorname{div} \boldsymbol{\theta} I - \nabla \boldsymbol{\theta} - (\nabla \boldsymbol{\theta})^t) \mathbf{A} - \operatorname{curl}(\mathbf{A} \times \boldsymbol{\theta})) \\
&= \operatorname{div}(\operatorname{div} \boldsymbol{\theta} \mathbf{A} - (\mathbf{A} \cdot \nabla) \boldsymbol{\theta} - (\nabla \boldsymbol{\theta})^t \mathbf{A} - \mathbf{A} \operatorname{div} \boldsymbol{\theta} + \boldsymbol{\theta} \operatorname{div} \mathbf{A} - (\boldsymbol{\theta} \cdot \nabla) \mathbf{A} + (\mathbf{A} \cdot \nabla) \boldsymbol{\theta}) \\
&= -\operatorname{div}((\boldsymbol{\theta} \cdot \nabla) \mathbf{A} + (\nabla \boldsymbol{\theta})^t \mathbf{A}).
\end{aligned}$$

Thus

$$\mathcal{P}'(\Omega)(\boldsymbol{\theta}) = \int_{\Omega} \frac{1}{\mu_*} \operatorname{div} \mathbf{B}(\boldsymbol{\theta}) \operatorname{div} \bar{\boldsymbol{\Psi}} dx - \int_{\Omega_d + \Omega_d^c} \frac{1}{\mu_*} \operatorname{div}((\boldsymbol{\theta} \cdot \nabla) \mathbf{A} + (\nabla \boldsymbol{\theta})^t \mathbf{A}) \operatorname{div} \bar{\boldsymbol{\Psi}} dx. \tag{5.41}$$

We derive easily from (5.40) and (5.41) the variational formulation (5.38) with $\mathcal{L}(\Psi, \Phi)$ given by (5.39). \square

Remark 5.2.8. *The shape derivatives $(\mathbf{A}'(\boldsymbol{\theta}), V'(\boldsymbol{\theta}))$ are less regular than the material derivatives $(\mathbf{B}(\boldsymbol{\theta}), U(\boldsymbol{\theta}))$. With local regularity of \mathbf{A} in Ω_d and in $\Omega_d^{\mathbb{C}}$, we have from the definition (5.18)*

$$\operatorname{curl} \mathbf{A}'(\boldsymbol{\theta}) = \operatorname{curl} \mathbf{B}(\boldsymbol{\theta}) - \operatorname{curl}((\boldsymbol{\theta} \cdot \nabla) \mathbf{A} + (\nabla \boldsymbol{\theta})^t \mathbf{A}) = \operatorname{curl} \mathbf{B}(\boldsymbol{\theta}) + \operatorname{curl}(\boldsymbol{\theta} \times \operatorname{curl} \mathbf{A}).$$

One observes that in a vicinity of Γ the term $\operatorname{curl} \mathbf{A}$ is only in $L^2(\Omega)^3$, thus one can only write $\operatorname{curl}(\operatorname{curl} \mathbf{A} \times \boldsymbol{\theta})$ in the weak sense. In fact, in the distribution sense, a simple layer potential should be added to describe the discontinuity (see for example [39, Chapter 3]). Thus \mathbf{A} is in the function space

$$X(\Omega_d \cup \Omega_d^{\mathbb{C}}) := \{\mathbf{a} : \mathbf{a}|_{\Omega_d} \in X(\Omega_d), \mathbf{a}|_{\Omega_d^{\mathbb{C}}} \in X(\Omega_d^{\mathbb{C}})\}.$$

We can define a form similar to $a(\cdot, \cdot; \cdot, \cdot)$

$$\begin{aligned} \check{a}(\mathbf{a}, v; \boldsymbol{\psi}, \phi) &:= \int_{\Omega_d + \Omega_d^{\mathbb{C}}} \left(\frac{1}{\mu} \operatorname{curl} \mathbf{a} \cdot \operatorname{curl} \bar{\boldsymbol{\psi}} + \frac{1}{\mu_*} \operatorname{div} \mathbf{a} \operatorname{div} \bar{\boldsymbol{\psi}} \right) dx \\ &+ \frac{1}{i\omega} \int_{\Omega_C} \sigma(i\omega \mathbf{a} + \nabla v) \cdot \overline{(i\omega \boldsymbol{\psi} + \nabla \phi)} dx \quad \forall (\mathbf{a}, v), (\boldsymbol{\psi}, \phi) \in X(\Omega_d \cup \Omega_d^{\mathbb{C}}) \times H^1(\Omega_C)/\mathbb{C}. \end{aligned}$$

From (5.38) and the relations (5.18) – (5.19) we have

$$\begin{aligned} \check{a}(\mathbf{A}'(\boldsymbol{\theta}), V'(\boldsymbol{\theta}); \Psi, \Phi) &= \int_{\Gamma} \left[\frac{1}{\mu} \right] (\boldsymbol{\theta} \cdot \mathbf{n})(\mathbf{n} \cdot \operatorname{curl} \mathbf{A})(\mathbf{n} \cdot \operatorname{curl} \bar{\Psi}) ds \\ &+ \frac{1}{i\omega} \int_{\Gamma} (\boldsymbol{\theta} \cdot \mathbf{n})[\sigma](i\omega \mathbf{A}_{\tau} + \nabla_{\tau} V) \cdot \overline{(i\omega \Psi_{\tau} + \nabla_{\tau} \Phi)} ds \quad \forall (\Psi, \Phi) \in X(\Omega_d \cup \Omega_d^{\mathbb{C}}) \times H^1(\Omega_C)/\mathbb{C}. \end{aligned} \quad (5.42)$$

To complete the system, we should consider a mixed formulation based on (5.42) and an additional formulation describing the discontinuity of $(\mathbf{n} \cdot \operatorname{curl} \mathbf{A}'(\boldsymbol{\theta}))$ and $(\mu^{-1} \operatorname{curl} \mathbf{A}'(\boldsymbol{\theta}) \times \mathbf{n})$ on the interface Γ

$$\begin{aligned} [\mathbf{n} \cdot \operatorname{curl} \mathbf{A}'(\boldsymbol{\theta})] &= [\mathbf{n} \cdot \operatorname{curl}(\boldsymbol{\theta} \times \operatorname{curl} \mathbf{A})], \\ [\mu^{-1} \operatorname{curl} \mathbf{A}'(\boldsymbol{\theta}) \times \mathbf{n}] &= [\mu^{-1} \operatorname{curl}(\boldsymbol{\theta} \times \operatorname{curl} \mathbf{A}) \times \mathbf{n}]. \end{aligned}$$

5.2.2 Shape derivative of the impedance measurements

We recall the expression of the impedance measurement in 3-D

$$\Delta Z_{kl} = \frac{1}{i\omega I^2} \int_{\Omega_d} \left(\left(\frac{1}{\mu} - \frac{1}{\mu^0} \right) \operatorname{curl} \mathbf{E}_k \cdot \operatorname{curl} \mathbf{E}_l^0 - i\omega(\sigma - \sigma^0) \mathbf{E}_k \cdot \mathbf{E}_l^0 \right) dx$$

By substituting the electric field by the vector potentials (see (5.6)) one gets the impedance measurement as a shape-dependent functional

$$\begin{aligned} \Delta Z_{kl}(\Omega_d) &= \frac{i\omega}{I^2} \int_{\Omega_d} \left(\left(\frac{1}{\mu} - \frac{1}{\mu^0} \right) \operatorname{curl} \mathbf{A}_k \cdot \operatorname{curl} \mathbf{A}_l^0 \right. \\ &\quad \left. - \frac{1}{i\omega} (\sigma - \sigma^0) (i\omega \mathbf{A}_k + \nabla V_k) \cdot (i\omega \mathbf{A}_l^0 + \nabla V_l^0) \right) dx. \end{aligned} \quad (5.43)$$

Proposition 5.2.9. *Let (\mathbf{A}_k, V_k) the solution to the variational formulation (5.11) with coefficients μ, σ , and (\mathbf{A}_l^0, V_l^0) the solution to (5.11) with coefficients μ^0, σ^0 which do not depend on the deposit domain Ω_d . Let (\mathbf{A}'_k, V'_k) the shape derivatives of (\mathbf{A}, V) . Under the same assumptions as in Proposition 5.2.7, the shape derivative of the impedance measurement $\Delta Z_{kl}(\Omega_d)$ writes*

$$\begin{aligned} & \Delta Z'_{kl}(\Omega_d)(\boldsymbol{\theta}) \\ &= \frac{i\omega}{I^2} \int_{\Omega_d} \left(\left(\frac{1}{\mu} - \frac{1}{\mu^0} \right) \operatorname{curl} \mathbf{A}'_k \cdot \operatorname{curl} \mathbf{A}_l^0 - \frac{1}{i\omega} (\sigma - \sigma^0) (i\omega \mathbf{A}'_k + \nabla V'_k) \cdot (i\omega \mathbf{A}_l^0 + \nabla V_l^0) \right) dx \\ &+ \frac{i\omega}{I^2} \int_{\Gamma} (\boldsymbol{\theta} \cdot \mathbf{n}) \left(\left(\frac{1}{\mu} - \frac{1}{\mu^0} \right) \operatorname{curl} \mathbf{A}_k \cdot \operatorname{curl} \mathbf{A}_l^0 \right. \\ &\quad \left. - \frac{1}{i\omega} (\sigma - \sigma^0) (i\omega \mathbf{A}_{k\tau} + \nabla_{\tau} V_k) \cdot (i\omega \mathbf{A}_{l\tau}^0 + \nabla_{\tau} V_l^0) \right) ds. \end{aligned} \quad (5.44)$$

Proof. From (5.43) one has

$$\frac{I^2}{i\omega} \Delta Z_{kl}(\Omega_d) = \alpha_{\mu, \sigma}(\Omega_d)(\mathbf{A}_k, V_k; \overline{\mathbf{A}_l^0}, -\overline{V_l^0}) - \alpha_{\mu^0, \sigma^0}(\Omega_d)(\mathbf{A}_l^0, V_l^0; \overline{\mathbf{A}_k}, -\overline{V_k}).$$

As (\mathbf{A}_k, V_k) satisfy (5.36) with constant μ, σ in Ω_d , and \mathbf{A}^0, V_k^0 verify (5.36) with constant μ^0, σ^0 in Ω_d , Lemma 5.2.6 implies

$$\begin{aligned} & \frac{I^2}{i\omega} \Delta Z'_{kl}(\Omega_d)(\boldsymbol{\theta}) = \alpha'_{\mu, \sigma}(\Omega_d)(\boldsymbol{\theta})(\mathbf{A}_k, V_k; \overline{\mathbf{A}_l^0}, -\overline{V_l^0}) - \alpha'_{\mu^0, \sigma^0}(\Omega_d)(\boldsymbol{\theta})(\mathbf{A}_l^0, V_l^0; \overline{\mathbf{A}_k}, -\overline{V_k}) \\ &= \alpha_{\mu, \sigma}(\Omega_d)(\mathbf{A}'_k(\boldsymbol{\theta}), V'_k(\boldsymbol{\theta}); \overline{\mathbf{A}_l^0}, -\overline{V_l^0}) + \alpha_{\mu, \sigma}(\Omega_d)(\mathbf{A}_k, V_k; \overline{\mathbf{B}_l^0(\boldsymbol{\theta})}, -\overline{U_l^0(\boldsymbol{\theta})}) \\ &\quad - \alpha_{\mu^0, \sigma^0}(\Omega_d)(\mathbf{A}_l^{0'}(\boldsymbol{\theta}), V_l^{0'}(\boldsymbol{\theta}); \overline{\mathbf{A}_k}, -\overline{V_k}) - \alpha_{\mu^0, \sigma^0}(\Omega_d)(\mathbf{A}_l^0, V_l^0; \overline{\mathbf{B}_k(\boldsymbol{\theta})}, -\overline{V_k(\boldsymbol{\theta})}) \\ &\quad + \int_{\partial\Omega_d} \left(\frac{1}{\mu} (\boldsymbol{\theta} \cdot \operatorname{curl} \mathbf{A}_k) (\mathbf{n} \cdot \operatorname{curl} \mathbf{A}_l^0) - \frac{1}{\mu^0} (\boldsymbol{\theta} \cdot \operatorname{curl} \mathbf{A}_l^0) (\mathbf{n} \cdot \operatorname{curl} \mathbf{A}_k) \right) ds \\ &\quad - \frac{1}{i\omega} \int_{\partial\Omega_d} (\sigma - \sigma^0) (\boldsymbol{\theta} \cdot \mathbf{n}) (i\omega \mathbf{A}_{k\tau} + \nabla_{\tau} V_k) \cdot (i\omega \mathbf{A}_{l\tau}^0 + \nabla_{\tau} V_l^0) ds, \end{aligned} \quad (5.45)$$

where $(\mathbf{B}_k(\boldsymbol{\theta}), U_k(\boldsymbol{\theta}))$, $(\mathbf{B}_l^0(\boldsymbol{\theta}), U_l^0(\boldsymbol{\theta}))$ are the material derivatives of (\mathbf{A}_k, V_k) and (\mathbf{A}_l^0, V_l^0) respectively. Now we will compute term by term (5.45). Remark at first that

$$\alpha_{\mu^0, \sigma^0}(\Omega_d)(\mathbf{A}_l^{0'}(\boldsymbol{\theta}), V_l^{0'}(\boldsymbol{\theta}); \overline{\mathbf{A}_k}, -\overline{V_k}) = 0$$

because the shape derivatives $(\mathbf{A}_l^{0'}(\boldsymbol{\theta}), V_l^{0'}(\boldsymbol{\theta}))$ vanish as the potentials (\mathbf{A}_l^0, V_l^0) in the deposit-free configuration do not depend on Ω_d . This, together with (5.18) and (5.19), also implies

$$\mathbf{B}_l^0(\boldsymbol{\theta}) = (\boldsymbol{\theta} \cdot \nabla) \mathbf{A}_l^0 + (\nabla \boldsymbol{\theta})^t \mathbf{A}_l^0, \quad U_l^0(\boldsymbol{\theta}) = \boldsymbol{\theta} \cdot \nabla V_l^0.$$

Hence, by substituting $(\mathbf{B}_l^0(\boldsymbol{\theta}), U_l^0(\boldsymbol{\theta}))$ with the above expressions in the expression of

$\alpha_{\mu,\sigma}(\Omega_d)(\mathbf{A}_k, V_k; \overline{\mathbf{B}}_l^0(\boldsymbol{\theta}), -\overline{U}_l^0(\boldsymbol{\theta}))$, one gets

$$\begin{aligned} \alpha_{\mu,\sigma}(\Omega_d)(\mathbf{A}_k, V_k; \overline{\mathbf{B}}_l^0(\boldsymbol{\theta}), -\overline{U}_l^0(\boldsymbol{\theta})) &= \alpha_{\mu,\sigma}(\Omega_d) \left(\mathbf{A}_k, V_k; \overline{(\boldsymbol{\theta} \cdot \nabla) \mathbf{A}_l^0 + (\nabla \boldsymbol{\theta})^t \mathbf{A}_l^0}, -\overline{\boldsymbol{\theta} \cdot \nabla V_l^0} \right) \\ &= \underbrace{\int_{\Omega_d} \frac{1}{\mu} \operatorname{curl} \mathbf{A}_k \cdot \operatorname{curl} \left((\boldsymbol{\theta} \cdot \nabla) \mathbf{A}_l^0 + (\nabla \boldsymbol{\theta})^t \mathbf{A}_l^0 \right) dx}_{\mathcal{S}_1} \\ &\quad - \underbrace{\frac{1}{i\omega} \int_{\Omega_d} \sigma(i\omega \mathbf{A}_k + \nabla V_k) \cdot \left(i\omega \left((\boldsymbol{\theta} \cdot \nabla) + (\nabla \boldsymbol{\theta})^t \right) \mathbf{A}_l^0 + \nabla(\boldsymbol{\theta} \cdot \nabla V_l^0) \right) dx}_{\mathcal{S}_2}. \end{aligned}$$

We compute \mathcal{S}_1 and \mathcal{S}_2

$$\begin{aligned} \mathcal{S}_1 &= \int_{\Omega_d} \frac{1}{\mu} \operatorname{curl} \mathbf{A}_k \cdot \operatorname{curl}(\operatorname{curl} \mathbf{A}_l^0 \times \boldsymbol{\theta}) dx \\ &= \int_{\Omega_d} \operatorname{curl} \left(\frac{1}{\mu} \operatorname{curl} \mathbf{A}_k \right) \cdot (\operatorname{curl} \mathbf{A}_l^0 \times \boldsymbol{\theta}) dx + \int_{\partial\Omega_d} \frac{1}{\mu} (\operatorname{curl} \mathbf{A}_k \times \mathbf{n}) \cdot (\operatorname{curl} \mathbf{A}_l^0 \times \boldsymbol{\theta}) ds \\ &= \int_{\Omega_d} \sigma(i\omega \mathbf{A}_k + \nabla V_k) \cdot (\operatorname{curl} \mathbf{A}_l^0 \times \boldsymbol{\theta}) dx + \int_{\partial\Omega_d} \frac{1}{\mu} (\operatorname{curl} \mathbf{A}_k \times \mathbf{n}) \cdot (\operatorname{curl} \mathbf{A}_l^0 \times \boldsymbol{\theta}) ds, \end{aligned}$$

and

$$\begin{aligned} \mathcal{S}_2 &= \frac{1}{i\omega} \int_{\Omega_d} \sigma(i\omega \mathbf{A}_k + \nabla V_k) \cdot \left(i\omega (\nabla(\boldsymbol{\theta} \cdot \mathbf{A}_l^0) + \operatorname{curl} \mathbf{A}_l^0 \times \boldsymbol{\theta}) + \nabla(\boldsymbol{\theta} \cdot \nabla V_l^0) \right) dx \\ &= \frac{1}{i\omega} \int_{\Omega_d} \sigma(i\omega \mathbf{A}_k + \nabla V_k) \cdot \left((i\omega \operatorname{curl} \mathbf{A}_l^0 \times \boldsymbol{\theta}) + \nabla(\boldsymbol{\theta} \cdot (i\omega \mathbf{A}_l^0 + \nabla V_k)) \right) dx \\ &= \frac{1}{i\omega} \int_{\Omega_d} \sigma(i\omega \mathbf{A}_k + \nabla V_k) \cdot (i\omega \operatorname{curl} \mathbf{A}_l^0 \times \boldsymbol{\theta}) dx. \end{aligned}$$

The last equality is obtained by integration by parts and by the fact that $\operatorname{div}(\sigma(i\omega \mathbf{A}_k + \nabla V_k)) = 0$ in Ω_d and that $\sigma(i\omega \mathbf{A}_k + \nabla V_k) \cdot \mathbf{n} = 0$ on $\partial\Omega_d$. Therefore

$$\begin{aligned} \alpha_{\mu,\sigma}(\Omega_d)(\mathbf{A}_k, V_k; \overline{\mathbf{B}}_l^0(\boldsymbol{\theta}), -\overline{U}_l^0(\boldsymbol{\theta})) &= \mathcal{S}_1 - \mathcal{S}_2 \\ &= \int_{\partial\Omega_d} \frac{1}{\mu} (\operatorname{curl} \mathbf{A}_k \times \mathbf{n}) \cdot (\operatorname{curl} \mathbf{A}_l^0 \times \boldsymbol{\theta}) ds \\ &= \int_{\partial\Omega_d} \frac{1}{\mu} \left((\boldsymbol{\theta} \cdot \mathbf{n})(\operatorname{curl} \mathbf{A}_k \cdot \operatorname{curl} \mathbf{A}_l^0) - (\boldsymbol{\theta} \cdot \operatorname{curl} \mathbf{A}_k)(\mathbf{n} \cdot \operatorname{curl} \mathbf{A}_l^0) \right) ds. \end{aligned} \quad (5.46)$$

Similarly, we have

$$\begin{aligned} \alpha_{\mu^0,\sigma^0}(\Omega_d)(\mathbf{A}_l^0, V_l^0; \overline{\mathbf{B}}_k^0(\boldsymbol{\theta}), -\overline{U}_k^0(\boldsymbol{\theta})) &= \alpha_{\mu^0,\sigma^0}(\Omega_d)(\mathbf{A}_l^0, V_l^0; \overline{\mathbf{A}}_k'(\boldsymbol{\theta}), -\overline{V}_k'(\boldsymbol{\theta})) \\ &\quad + \alpha_{\mu^0,\sigma^0}(\Omega_d) \left(\mathbf{A}_l^0, V_l^0; \overline{(\boldsymbol{\theta} \cdot \nabla) \mathbf{A}_k + (\nabla \boldsymbol{\theta})^t \mathbf{A}_k}, -\overline{\boldsymbol{\theta} \cdot \nabla V_k} \right) \\ &= \alpha_{\mu^0,\sigma^0}(\Omega_d)(\mathbf{A}_k'(\boldsymbol{\theta}), V_k'(\boldsymbol{\theta}); \overline{\mathbf{A}}_l^0, -\overline{V}_l^0) \\ &\quad + \int_{\partial\Omega_d} \frac{1}{\mu^0} \left((\boldsymbol{\theta} \cdot \mathbf{n})(\operatorname{curl} \mathbf{A}_k \cdot \operatorname{curl} \mathbf{A}_l^0) - (\mathbf{n} \cdot \operatorname{curl} \mathbf{A}_k)(\boldsymbol{\theta} \cdot \operatorname{curl} \mathbf{A}_l^0) \right) ds. \end{aligned} \quad (5.47)$$

From (5.45), (5.46) and (5.47), and considering the fact that the support of $\boldsymbol{\theta}$ is on a vicinity of Γ , we get (5.44). \square

On Γ , we have

$$\begin{aligned} \operatorname{curl} \mathbf{A}_k \cdot \operatorname{curl} \mathbf{A}_l^0 &= ((\mathbf{n} \cdot \operatorname{curl} \mathbf{A}_k) \mathbf{n} + \mathbf{n} \times (\operatorname{curl} \mathbf{A}_k \times \mathbf{n})) \cdot ((\mathbf{n} \cdot \operatorname{curl} \mathbf{A}_l^0) \mathbf{n} + \mathbf{n} \times (\operatorname{curl} \mathbf{A}_l^0 \times \mathbf{n})) \\ &= (\mathbf{n} \cdot \operatorname{curl} \mathbf{A}_k)(\mathbf{n} \cdot \operatorname{curl} \mathbf{A}_l^0) + (\operatorname{curl} \mathbf{A}_k \times \mathbf{n}) \cdot (\operatorname{curl} \mathbf{A}_l^0 \times \mathbf{n}). \end{aligned}$$

With the above equality and the relations (5.18) – (5.19), it follows that

$$\begin{aligned} &\Delta Z'_{kl}(\Omega_d)(\boldsymbol{\theta}) \\ &= \frac{i\omega}{I^2} \int_{\Omega_d} \left\{ \left(\frac{1}{\mu} - \frac{1}{\mu^0} \right) \operatorname{curl} \mathbf{B}_k \cdot \operatorname{curl} \mathbf{A}_l^0 - \frac{1}{i\omega} (\sigma - \sigma^0) (i\omega \mathbf{B}_k + \nabla U_k) \cdot (i\omega \mathbf{A}_l^0 + \nabla V_l^0) \right\} dx \\ &\quad - \frac{i\omega}{I^2} \int_{\Omega_d} \left\{ \left(\frac{1}{\mu} - \frac{1}{\mu^0} \right) \operatorname{curl}((\boldsymbol{\theta} \cdot \nabla) \mathbf{A}_k + (\nabla \boldsymbol{\theta})^t \mathbf{A}_k) \cdot \operatorname{curl} \mathbf{A}_l^0 \right. \\ &\quad \quad \left. - \frac{1}{i\omega} (\sigma - \sigma^0) \left(i\omega ((\boldsymbol{\theta} \cdot \nabla) \mathbf{A}_k + (\nabla \boldsymbol{\theta})^t \mathbf{A}_k) + \nabla(\boldsymbol{\theta} \cdot \nabla U_k) \right) \cdot (i\omega \mathbf{A}_l^0 + \nabla V_l^0) \right\} dx \\ &\quad + \frac{i\omega}{I^2} \int_{\Gamma} (\boldsymbol{\theta} \cdot \mathbf{n}) \left\{ \left(\frac{1}{\mu} - \frac{1}{\mu^0} \right) (\mathbf{n} \cdot \operatorname{curl} \mathbf{A}_k)(\mathbf{n} \cdot \operatorname{curl} \mathbf{A}_l^0) \right. \\ &\quad \quad - (\mu - \mu^0) \left(\frac{1}{\mu} \operatorname{curl} \mathbf{A}_k \times \mathbf{n} \right) \cdot \left(\frac{1}{\mu^0} \operatorname{curl} \mathbf{A}_l^0 \times \mathbf{n} \right) \\ &\quad \quad \left. - \frac{1}{i\omega} (\sigma - \sigma^0) (i\omega \mathbf{A}_{k\tau} + \nabla_{\tau} V_k) \cdot (i\omega \mathbf{A}_{l\tau}^0 + \nabla_{\tau} V_l^0) \right\} ds. \end{aligned} \quad (5.48)$$

5.2.3 Expression of the impedance shape derivative using the adjoint state

We follow the method of Hadamard representation to give an expression of $Z'_{kl}(\Omega_d)(\boldsymbol{\theta})$ independent of the shape or material derivatives ($(\mathbf{A}'(\boldsymbol{\theta}), V'(\boldsymbol{\theta}))$ or $(\mathbf{B}(\boldsymbol{\theta}), U(\boldsymbol{\theta}))$) of the solution (\mathbf{A}, V) by introducing the adjoint state $(\mathbf{P}_l, W_l) \in X(\Omega) \times H^1(\Omega_C)/\mathbb{C}$ related to the solution (\mathbf{A}_l^0, V_l^0) in the deposit-free case. The adjoint problem writes

$$a^*(\mathbf{P}_l, W_l; \boldsymbol{\Psi}, \Phi) = L^*(\boldsymbol{\Psi}, \Phi) \quad \forall (\boldsymbol{\Psi}, \Phi) \in X(\Omega) \times H^1(\Omega_C)/\mathbb{C} \quad (5.49)$$

where for any (\mathbf{a}, v) , $(\boldsymbol{\psi}, \phi)$ in $X(\Omega) \times H^1(\Omega_C)/\mathbb{C}$

$$\begin{aligned} a^*(\mathbf{a}, v; \boldsymbol{\psi}, \phi) &:= \overline{a(\boldsymbol{\psi}, \phi; \mathbf{a}, v)} \\ &= \int_{\Omega} \left(\frac{1}{\mu} \operatorname{curl} \mathbf{a} \cdot \operatorname{curl} \overline{\boldsymbol{\psi}} + \frac{1}{\mu^*} \operatorname{div} \mathbf{a} \operatorname{div} \overline{\boldsymbol{\psi}} \right) dx - \frac{1}{i\omega} \int_{\Omega_C} \sigma (i\omega \mathbf{a} + \nabla v) \cdot (\overline{i\omega \boldsymbol{\psi} + \nabla \phi}) dx, \\ L^*(\boldsymbol{\psi}, \phi) &:= \int_{\Omega_d} \left(\left(\frac{1}{\mu} - \frac{1}{\mu^0} \right) \operatorname{curl} \overline{\mathbf{A}_l^0} \cdot \operatorname{curl} \overline{\boldsymbol{\psi}} + \frac{1}{i\omega} (\sigma - \sigma^0) \overline{(i\omega \mathbf{A}_l^0 + \nabla V_l^0)} \cdot (\overline{i\omega \boldsymbol{\psi} + \nabla \phi}) \right) dx. \end{aligned}$$

Proposition 5.2.10. *Let (\mathbf{P}_l, W_l) the solution to the adjoint problem (5.49). Under the same assumptions as in Proposition 5.1.1 for μ and σ , one verifies*

$$\operatorname{div} \mathbf{P}_l = 0 \quad \text{in } \Omega.$$

Proof. By integration by parts, one verifies that the variational formulation for the adjoint problem (5.49) is equivalent to the following strong formulation of the problem with penalization

$$\left\{ \begin{array}{ll} \text{curl}(\mu^{-1} \text{curl } \mathbf{P}_l) - \mu_*^{-1} \nabla \text{div } \mathbf{P}_l + \sigma(i\omega \mathbf{P}_l + \nabla W_l) \\ \quad = \left(\frac{1}{\mu} - \frac{1}{\mu^0}\right) \text{curl}(\text{curl } \overline{\mathbf{A}}_l^0) - (\sigma - \sigma^0)(i\omega \mathbf{A}_l^0 + \nabla V_l^0) & \text{in } \Omega_d, \quad (5.50a) \\ \text{curl}(\mu^{-1} \text{curl } \mathbf{P}_l) - \mu_*^{-1} \nabla \text{div } \mathbf{P}_l + \sigma(i\omega \mathbf{P}_l + \nabla W_l) = 0 & \text{in } \Omega_d^c, \quad (5.50b) \\ [\mathbf{n} \cdot \text{curl } \mathbf{P}_l] = 0 & \text{on } \Gamma, \quad (5.50c) \\ [\mu^{-1} \text{curl } \mathbf{P}_l \times \mathbf{n}] = -\left(\frac{1}{\mu} - \frac{1}{\mu^0}\right) \text{curl } \overline{\mathbf{A}}_l^0 \times \mathbf{n} & \text{on } \Gamma, \quad (5.50d) \\ \text{div}(\sigma(i\omega \mathbf{P}_l + \nabla W_l)) = 0 & \text{in } \Omega_C, \quad (5.50e) \\ \sigma(i\omega \mathbf{P}_l + \nabla W_l) \cdot \mathbf{n} = 0 & \text{on } \Gamma_*, \quad (5.50f) \\ \mathbf{P}_l \cdot \mathbf{n} = 0 & \text{on } \partial\Omega, \quad (5.50g) \\ (\mu^{-1} \text{curl } \mathbf{P}_l) \times \mathbf{n} = 0 & \text{on } \partial\Omega. \quad (5.50h) \end{array} \right.$$

Using the same arguments as in the proof of [4, Lemma 6.1], we verify that $\text{div } \mathbf{P}_l = 0$ on Ω . \square

Proposition 5.2.11. *Let (\mathbf{A}_k, V_k) the potentials induced by the coil k of the eddy current problem with deposit domain Ω_d , (\mathbf{A}_l^0, V_k^0) the potentials induced by the coil l for the deposit free case, and (\mathbf{P}_l, W_l) the adjoint states related to (\mathbf{A}_l^0, V_k^0) which satisfy the adjoint problem (5.49). Then under the same assumptions as in Proposition 5.1.1 for μ and σ , the impedance shape derivative (5.48) writes also*

$$\begin{aligned} \Delta Z'_{kl}(\Omega_d)(\boldsymbol{\theta}) &= \frac{i\omega}{I^2} \int_{\Gamma} (\mathbf{n} \cdot \boldsymbol{\theta}) \left\{ \left[\frac{1}{\mu} \right] (\mathbf{n} \cdot \text{curl } \mathbf{A}_k)(\mathbf{n} \cdot \overline{\mathbf{P}}_l - \mathbf{n} \cdot \text{curl } \mathbf{A}_l^0) \right. \\ &\quad - [\mu] \left(\frac{1}{\mu} \text{curl } \mathbf{A}_k \times \mathbf{n} \right) \cdot \left(\frac{1}{\mu^0} (\text{curl } \overline{\mathbf{P}}_l)_+ \times \mathbf{n} - \frac{1}{\mu^0} \text{curl } \mathbf{A}_l^0 \times \mathbf{n} \right) \\ &\quad \left. + \frac{1}{i\omega} [\sigma] (i\omega \mathbf{A}_{k\tau} + \nabla_{\tau} V_k) \cdot (i\omega \overline{\mathbf{P}}_{l\tau} + \nabla_{\tau} \overline{W}_l + i\omega \mathbf{A}_{l\tau}^0 + \nabla_{\tau} V_l^0) \right\} ds. \quad (5.51) \end{aligned}$$

Proof. Taking $(\boldsymbol{\Psi}, \Phi) = (\mathbf{B}_k(\boldsymbol{\theta}), U_k(\boldsymbol{\theta})) \in X(\Omega) \times H^1(\Omega_C)/\mathbb{C}$ in the adjoint problem (5.49) yields

$$a^*(\mathbf{P}_l, W_l; \mathbf{B}_k(\boldsymbol{\theta}), U_k(\boldsymbol{\theta})) = L^*(\mathbf{B}_k(\boldsymbol{\theta}), U_k(\boldsymbol{\theta})).$$

On the other hand, taking $(\boldsymbol{\Psi}, \Phi) = (\mathbf{P}_l, W_l)$ in the variational formulation (5.38) for the material derivatives $(\mathbf{B}_k(\boldsymbol{\theta}), U_k(\boldsymbol{\theta}))$ implies

$$a(\mathbf{B}_k(\boldsymbol{\theta}), U_k(\boldsymbol{\theta}); \mathbf{P}_l, W_l) = \mathcal{L}(\mathbf{P}_l, W_l).$$

Since

$$\overline{a^*(\mathbf{P}_l, W_l; \mathbf{B}_k(\boldsymbol{\theta}), U_k(\boldsymbol{\theta}))} = a(\mathbf{B}_k(\boldsymbol{\theta}), U_k(\boldsymbol{\theta}); \mathbf{P}_l, W_l)$$

and $\operatorname{div} \mathbf{P}_l = 0$ (see Proposition 5.2.10), one obtains

$$\begin{aligned}
\overline{L^*(\mathbf{B}_k(\boldsymbol{\theta}), U_k(\boldsymbol{\theta}))} &= \mathcal{L}(\mathbf{P}_l, W_l). \\
&= \int_{\Omega_d + \Omega_d^c} \frac{1}{\mu} \operatorname{curl} \left((\boldsymbol{\theta} \cdot \nabla) \mathbf{A}_k + (\nabla \boldsymbol{\theta})^t \mathbf{A}_k \right) \cdot \operatorname{curl} \overline{\mathbf{P}_l} \, dx \\
&\quad + \frac{1}{i\omega} \int_{\Omega_C} \sigma \left(i\omega \left((\boldsymbol{\theta} \cdot \nabla) \mathbf{A}_k + (\nabla \boldsymbol{\theta})^t \mathbf{A}_k \right) + \nabla(\boldsymbol{\theta} \cdot \nabla V_k) \right) \cdot (\overline{i\omega \mathbf{P}_l + \nabla W_l}) \, dx \\
&\quad + \int_{\Gamma} \left[\frac{1}{\mu} \right] (\boldsymbol{\theta} \cdot \mathbf{n})(\mathbf{n} \cdot \operatorname{curl} \mathbf{A}_k)(\mathbf{n} \cdot \operatorname{curl} \overline{\mathbf{P}_l}) \, ds \\
&\quad + \frac{1}{i\omega} \int_{\Gamma} (\boldsymbol{\theta} \cdot \mathbf{n})[\sigma](i\omega \mathbf{A}_{k\tau} + \nabla_{\tau} V_k) \cdot (\overline{i\omega \mathbf{P}_{l\tau} + \nabla_{\tau} W_l}) \, ds.
\end{aligned}$$

In Ω_d or in Ω_d^c one verifies

$$\begin{aligned}
(\boldsymbol{\theta} \cdot \nabla) \mathbf{A}_k + (\nabla \boldsymbol{\theta})^t \mathbf{A}_k &= \operatorname{curl} \mathbf{A}_k \times \boldsymbol{\theta} + \nabla(\boldsymbol{\theta} \cdot \mathbf{A}_k), \\
\operatorname{curl} \left((\boldsymbol{\theta} \cdot \nabla) \mathbf{A}_k + (\nabla \boldsymbol{\theta})^t \mathbf{A}_k \right) &= \operatorname{curl} (\operatorname{curl} \mathbf{A}_k \times \boldsymbol{\theta}).
\end{aligned}$$

Thus, considering (5.50e) and (5.50f), we compute

$$\begin{aligned}
\overline{L^*(\mathbf{B}_k(\boldsymbol{\theta}), U_k(\boldsymbol{\theta}))} &= \mathcal{L}(\mathbf{P}_l, W_l) \\
&= \underbrace{\int_{\Omega_d + \Omega_d^c} \frac{1}{\mu} \operatorname{curl} (\operatorname{curl} \mathbf{A}_k \times \boldsymbol{\theta}) \cdot \operatorname{curl} \overline{\mathbf{P}_l} \, dx + \frac{1}{i\omega} \int_{\Omega_C} \sigma i\omega (\operatorname{curl} \mathbf{A}_k \times \boldsymbol{\theta}) \cdot (\overline{i\omega \mathbf{P}_l + \nabla W_l}) \, dx}_{\mathcal{I}} \\
&\quad + \int_{\Gamma} \left[\frac{1}{\mu} \right] (\boldsymbol{\theta} \cdot \mathbf{n})(\mathbf{n} \cdot \operatorname{curl} \mathbf{A}_k)(\mathbf{n} \cdot \operatorname{curl} \overline{\mathbf{P}_l}) \, ds \\
&\quad + \frac{1}{i\omega} \int_{\Gamma} (\boldsymbol{\theta} \cdot \mathbf{n})[\sigma](i\omega \mathbf{A}_{k\tau} + \nabla_{\tau} V_k) \cdot (\overline{i\omega \mathbf{P}_{l\tau} + \nabla_{\tau} W_l}) \, ds. \tag{5.52}
\end{aligned}$$

We remind that $(\operatorname{curl} \mathbf{A}_k \times \boldsymbol{\theta})$ belongs to $X(\Omega_d \cup \Omega_{d,0}^c)$. We multiply (5.50a), (5.50b) by $(\overline{\operatorname{curl} \mathbf{A}_k \times \boldsymbol{\theta}})$, integrate by parts and then take the complex conjugate, which implies

$$\begin{aligned}
\mathcal{I} &= \int_{\Omega_d} \left(\frac{1}{\mu} - \frac{1}{\mu^0} \right) \operatorname{curl} \mathbf{A}_l^0 \cdot \operatorname{curl}(\operatorname{curl} \mathbf{A}_k \times \boldsymbol{\theta}) \, dx \\
&\quad - \frac{1}{i\omega} \int_{\Omega_d} (\sigma - \sigma^0)(i\omega \mathbf{A}_l^0 + \nabla V_l^0) \cdot (i\omega(\operatorname{curl} \mathbf{A}_k \times \boldsymbol{\theta})) \, dx \\
&\quad + \int_{\Gamma} \left[\frac{1}{\mu} \operatorname{curl} \overline{\mathbf{P}_l} \cdot ((\operatorname{curl} \mathbf{A}_k \times \boldsymbol{\theta}) \times \mathbf{n}) \right] \, ds + \int_{\Gamma} \left(\frac{1}{\mu} - \frac{1}{\mu^0} \right) \operatorname{curl} \overline{\mathbf{A}_l^0} \cdot ((\operatorname{curl} \mathbf{A}_k \times \boldsymbol{\theta}) \times \mathbf{n}) \, ds \\
&= \int_{\Omega_d} \left(\frac{1}{\mu} - \frac{1}{\mu^0} \right) \operatorname{curl} \mathbf{A}_l^0 \cdot \operatorname{curl} \left((\boldsymbol{\theta} \cdot \nabla) \mathbf{A}_k + (\nabla \boldsymbol{\theta})^t \mathbf{A}_k \right) \, dx \\
&\quad - \frac{1}{i\omega} \int_{\Omega_d} (\sigma - \sigma^0)(i\omega \mathbf{A}_l^0 + \nabla V_l^0) \cdot \left(i\omega \left((\boldsymbol{\theta} \cdot \nabla) \mathbf{A}_k + (\nabla \boldsymbol{\theta})^t \mathbf{A}_k \right) + \nabla(\boldsymbol{\theta} \cdot \nabla V_k) \right) \, dx \\
&\quad - \int_{\Gamma} (\boldsymbol{\theta} \cdot \mathbf{n})[\mu] \left(\frac{1}{\mu} \operatorname{curl} \mathbf{A}_k \times \mathbf{n} \right) \cdot \left(\frac{1}{\mu^0} (\operatorname{curl} \overline{\mathbf{P}_l})_+ \times \mathbf{n} \right) \, ds \tag{5.53}
\end{aligned}$$

The last equality is due to the transmission conditions (5.50c) – (5.50d) for \mathbf{P}_l and those for \mathbf{A}_k (5.26) on Γ . (5.52) and (5.53) imply

$$\begin{aligned} & \overline{L^*(\mathbf{B}_k(\boldsymbol{\theta}), U_k(\boldsymbol{\theta}))} - \int_{\Omega_d} \left(\frac{1}{\mu} - \frac{1}{\mu^0} \right) \operatorname{curl} \mathbf{A}_l^0 \cdot \operatorname{curl} \left((\boldsymbol{\theta} \cdot \nabla) \mathbf{A}_k + (\nabla \boldsymbol{\theta})^t \mathbf{A}_k \right) dx \\ & + \frac{1}{i\omega} \int_{\Omega_d} (\sigma - \sigma^0) (i\omega \mathbf{A}_l^0 + \nabla V_l^0) \cdot \left(i\omega \left((\boldsymbol{\theta} \cdot \nabla) \mathbf{A}_k + (\nabla \boldsymbol{\theta})^t \mathbf{A}_k \right) + \nabla (\boldsymbol{\theta} \cdot \nabla V_k) \right) dx \\ & = \int_{\Gamma} (\boldsymbol{\theta} \cdot \mathbf{n}) \left\{ \left[\frac{1}{\mu} \right] (\mathbf{n} \cdot \operatorname{curl} \mathbf{A}_k) (\mathbf{n} \cdot \operatorname{curl} \overline{\mathbf{P}}_l) - [\mu] \left(\frac{1}{\mu} \operatorname{curl} \mathbf{A}_k \times \mathbf{n} \right) \cdot \left(\frac{1}{\mu^0} (\operatorname{curl} \overline{\mathbf{P}}_l)_+ \times \mathbf{n} \right) \right. \\ & \quad \left. + \frac{1}{i\omega} [\sigma] (i\omega \mathbf{A}_{k\tau} + \nabla_{\tau} V_k) \cdot (\overline{i\omega \mathbf{P}_{l\tau} + \nabla_{\tau} W_l}) \right\} ds. \end{aligned} \quad (5.54)$$

We remark that on Γ one has

$$\left[\frac{1}{\mu} \right] = \frac{1}{\mu^0} - \frac{1}{\mu}, \quad [\mu] = \mu^0 - \mu, \quad [\sigma] = \sigma^0 - \sigma.$$

Considering the definition of $L^*(\cdot, \cdot)$, we substitute the above integral (5.54) in the expression of shape derivative of ΔZ_{kl} (5.48) and finally obtain (5.51). \square

5.2.4 Shape derivative for a least square cost functional

We recall the least square cost functional

$$\mathcal{J}(\Omega_d) = \int_{z_{\min}}^{z_{\max}} |Z(\Omega_d; \zeta) - Z_{meas}(\zeta)|^2 d\zeta,$$

where Z is either Z_{FA} or Z_{F3} according to the measurement mode. Since

$$\begin{aligned} Z_{FA}(\Omega_d) &= \frac{i}{2} (\Delta Z_{11}(\Omega_d) + \Delta Z_{21}(\Omega_d)), & Z_{F3}(\Omega_d) &= \frac{i}{2} (\Delta Z_{11}(\Omega_d) - \Delta Z_{22}(\Omega_d)), \\ Z'_{FA}(\boldsymbol{\theta}) &= \frac{i}{2} (\Delta Z'_{11}(\boldsymbol{\theta}) + \Delta Z'_{21}(\boldsymbol{\theta})), & Z'_{F3}(\boldsymbol{\theta}) &= \frac{i}{2} (\Delta Z'_{11}(\boldsymbol{\theta}) - \Delta Z'_{22}(\boldsymbol{\theta})), \end{aligned}$$

the shape derivative of $\mathcal{J}(\Omega_d)$ is in the form

$$\mathcal{J}'(\Omega_d)(\boldsymbol{\theta}) = -\frac{\omega}{I^2} \int_{\Gamma_0} (\mathbf{n} \cdot \boldsymbol{\theta}) g ds, \quad (5.55)$$

where the shape-dependent functional g depends on the solutions to the forward problem (\mathbf{A}_k, V_k) , (\mathbf{A}_l^0, V_l^0) and the adjoint state (\mathbf{P}_l, W_l) . Precisely,

$$g = \begin{cases} g_{11} + g_{21} & \text{absolute mode,} \\ g_{11} - g_{22} & \text{differential mode,} \end{cases}$$

with

$$\begin{aligned} g_{kl} &= \int_{z_{\min}}^{z_{\max}} \Re \left(\overline{(Z(\Omega_d; \zeta) - Z_{meas}(\zeta))} \left\{ \left[\frac{1}{\mu} \right] (\mathbf{n} \cdot \operatorname{curl} \mathbf{A}_k) (\mathbf{n} \cdot \operatorname{curl} \overline{\mathbf{P}}_l - \mathbf{n} \cdot \operatorname{curl} \mathbf{A}_l^0) \right. \right. \\ & \quad \left. \left. - [\mu] \left(\frac{1}{\mu} \operatorname{curl} \mathbf{A}_k \times \mathbf{n} \right) \cdot \left(\frac{1}{\mu^0} \operatorname{curl} \overline{\mathbf{P}}_l|_{\Omega_d^c} \times \mathbf{n} - \frac{1}{\mu^0} \operatorname{curl} \mathbf{A}_l^0 \times \mathbf{n} \right) \right. \right. \\ & \quad \left. \left. + \frac{1}{i\omega} [\sigma] (i\omega \mathbf{A}_{k\tau} + \nabla_{\tau} V_k) \cdot (\overline{i\omega \mathbf{P}_{l\tau} + \nabla_{\tau} W_l} + i\omega \mathbf{A}_{l\tau}^0 + \nabla_{\tau} V_l^0) \right\} \right) d\zeta. \end{aligned} \quad (5.56)$$

We choose the shape perturbation $\boldsymbol{\theta}$ such that

$$\boldsymbol{\theta} = g\mathbf{n} \quad \text{on } \Gamma,$$

which is a minimizing direction since

$$\mathcal{J}'(\Omega_d)(\boldsymbol{\theta}) = -\frac{\omega}{I^2} \int_{\Gamma_0} |g|^2 ds \leq 0.$$

5.2.5 Validation for axisymmetric configurations

We consider an axisymmetric case and reduce the above 3-D eddy current model to 2-D in cylindrical coordinates $O - rz$. From (5.6) we have

$$\begin{cases} \operatorname{curl} \mathbf{E} = i\omega\mu\mathbf{H} = \operatorname{curl}(i\omega\mathbf{A}) & \text{in } \Omega, \\ \mathbf{E} = i\omega\mathbf{A} + \nabla V & \text{in } \Omega_C. \end{cases}$$

We already know that in the axisymmetric case, only the azimuthal component E_θ of \mathbf{E} is non-trivial. We denote by $w = rE_\theta$ the weighted electric field. Similarly, for the adjoint state we set \mathbf{Q} such that

$$\begin{cases} \operatorname{curl} \mathbf{Q} = \operatorname{curl}(i\omega\mathbf{P}) & \text{in } \Omega, \\ \mathbf{Q} = i\omega\mathbf{P} + \nabla W & \text{in } \Omega_C, \end{cases}$$

and we denote by $p = rQ_\theta$ the weighted azimuthal component of \mathbf{Q} . Then with the expressions of operator curl in the cylindrical coordinates, one verifies easily that the functional g_{kl} given by (5.56) has exactly the 2-D expression (2.34) for axisymmetric configurations.

5.3 Appendices

5.3.1 Differential identities

$$\operatorname{curl}(\nabla f) = 0, \tag{5.57a}$$

$$\operatorname{div}(\operatorname{curl} \mathbf{v}) = 0, \tag{5.57b}$$

$$(\mathbf{u} \cdot \nabla)\mathbf{v} = (\nabla\mathbf{v})\mathbf{u}, \tag{5.57c}$$

$$\operatorname{curl} \mathbf{u} \times \mathbf{v} = (\nabla\mathbf{u} - (\nabla\mathbf{u})^t)\mathbf{v}, \tag{5.57d}$$

$$\nabla(\mathbf{u} \cdot \mathbf{v}) = \mathbf{u} \times \operatorname{curl} \mathbf{v} + \mathbf{v} \times \operatorname{curl} \mathbf{u} + (\mathbf{u} \cdot \nabla)\mathbf{v} + (\mathbf{v} \cdot \nabla)\mathbf{u}, \tag{5.57e}$$

$$\operatorname{curl}(\mathbf{u} \times \mathbf{v}) = \mathbf{u} \operatorname{div} \mathbf{v} - \mathbf{v} \operatorname{div} \mathbf{u} + (\mathbf{v} \cdot \nabla)\mathbf{u} - (\mathbf{u} \cdot \nabla)\mathbf{v}. \tag{5.57f}$$

5.3.2 Proof of Lemma 5.2.6

Proof. By definition, one has

$$\begin{aligned} \alpha_{\mu,\sigma}(\mathcal{Q}_\theta)(\mathbf{a}(\mathcal{Q}_\theta), v(\mathcal{Q}_\theta); \boldsymbol{\psi}(\mathcal{Q}_\theta), \phi(\mathcal{Q}_\theta)) &= \int_{\mathcal{Q}_\theta} \frac{1}{\mu} \operatorname{curl}_y \mathbf{a}(\mathcal{Q}_\theta) \cdot \operatorname{curl}_y \overline{\boldsymbol{\psi}(\mathcal{Q}_\theta)} dy \\ &+ \frac{1}{i\omega} \int_{\mathcal{Q}_\theta} \sigma(i\omega\mathbf{a}(\mathcal{Q}_\theta) + \nabla_y v(\mathcal{Q}_\theta)) \cdot \overline{(i\omega\boldsymbol{\psi}(\mathcal{Q}_\theta) + \nabla_y \phi(\mathcal{Q}_\theta))} dy. \end{aligned}$$

Considering the variable substitution $(\text{Id} + \boldsymbol{\theta})^{-1} : y \mapsto x$ with the notations introduced in (5.14) and the differential identities (5.15), we rewrite the above form on $\mathcal{Q} = (\text{Id} + \boldsymbol{\theta})^{-1}\mathcal{Q}_\theta$

$$\begin{aligned} \alpha_{\mu,\sigma}(\mathcal{Q}_\theta)(\mathbf{a}(\mathcal{Q}_\theta), v(\mathcal{Q}_\theta); \boldsymbol{\psi}(\mathcal{Q}_\theta), \phi(\mathcal{Q}_\theta)) &= \int_{\mathcal{Q}} \frac{1}{\mu} \frac{(I + \nabla\boldsymbol{\theta})^t(I + \nabla\boldsymbol{\theta})}{|\det(I + \nabla\boldsymbol{\theta})|} \text{curl } \mathbf{a}_{\text{curl}} \cdot \text{curl } \overline{\boldsymbol{\psi}_{\text{curl}}} dx \\ &+ \frac{1}{i\omega} \int_{\mathcal{Q}} \sigma |\det(I + \nabla\boldsymbol{\theta})| (I + \nabla\boldsymbol{\theta})^{-1} (I + \nabla\boldsymbol{\theta})^{-t} (i\omega \mathbf{a}_{\text{curl}} + \nabla v) \cdot (\overline{i\omega \boldsymbol{\psi}_{\text{curl}} + \nabla \phi}) dx. \end{aligned}$$

If $(\mathbf{b}(\boldsymbol{\theta}), u(\boldsymbol{\theta}))$, $(\boldsymbol{\eta}(\boldsymbol{\theta}), \chi(\boldsymbol{\theta}))$ are respectively the material derivatives of (\mathbf{a}, v) and $(\boldsymbol{\psi}, \phi)$, then one can develop the above form with respect to $\boldsymbol{\theta}$. Since $(\mathbf{a}_{\text{curl}}(0), v_\nabla(0)) = (\mathbf{a}(\mathcal{Q}), v(\mathcal{Q}))$, $(\boldsymbol{\psi}_{\text{curl}}(0), \phi_\nabla(0)) = (\boldsymbol{\psi}(\mathcal{Q}), \phi(\mathcal{Q}))$, the terms of order zero with respect to $\boldsymbol{\theta}$ give exactly

$$\alpha_{\mu,\sigma}(\mathcal{Q})(\mathbf{a}(\mathcal{Q}), v(\mathcal{Q}); \boldsymbol{\psi}(\mathcal{Q}), \phi(\mathcal{Q})),$$

and the first order terms with respect to $\boldsymbol{\theta}$ are

$$\begin{aligned} &\alpha_{\mu,\sigma}(\mathcal{Q})(\mathbf{b}(\boldsymbol{\theta}), u(\boldsymbol{\theta}); \boldsymbol{\psi}(\mathcal{Q}), \phi(\mathcal{Q})) + \alpha_{\mu,\sigma}(\mathcal{Q})(\mathbf{a}(\mathcal{Q}), v(\mathcal{Q}); \boldsymbol{\eta}(\boldsymbol{\theta}), \chi(\boldsymbol{\theta})) \\ &+ \underbrace{\int_{\mathcal{Q}} \frac{1}{\mu} (-\text{div } \boldsymbol{\theta} + \nabla\boldsymbol{\theta} + (\nabla\boldsymbol{\theta})^t) \text{curl } \mathbf{a} \cdot \text{curl } \overline{\boldsymbol{\psi}} dx}_{\mathcal{I}_1} \\ &+ \underbrace{\frac{1}{i\omega} \int_{\mathcal{Q}} \sigma (\text{div } \boldsymbol{\theta} I - \nabla\boldsymbol{\theta} - (\nabla\boldsymbol{\theta})^t) (i\omega \mathbf{a} + \nabla v) \cdot (\overline{i\omega \boldsymbol{\psi} + \nabla \phi}) dx}_{\mathcal{I}_2}. \end{aligned} \quad (5.58)$$

We compute term by term. Using the differential identities (5.57) and the fact that (\mathbf{a}, v) satisfy the conditions (5.36), one verifies

$$\begin{aligned} &(-\text{div } \boldsymbol{\theta} I + \nabla\boldsymbol{\theta} + (\nabla\boldsymbol{\theta})^t) \text{curl } \mathbf{a} \\ &= -\text{curl}(\text{curl } \mathbf{a} \times \boldsymbol{\theta} + \nabla(\boldsymbol{\theta} \cdot \mathbf{a})) + \nabla(\boldsymbol{\theta} \cdot \text{curl } \mathbf{a}) + \text{curl}(\text{curl } \mathbf{a}) \times \boldsymbol{\theta} \\ &= -\text{curl}((\boldsymbol{\theta} \cdot \nabla) \mathbf{a} + (\nabla\boldsymbol{\theta})^t \mathbf{a}) + \nabla(\boldsymbol{\theta} \cdot \text{curl } \mathbf{a}) + \text{curl}(\text{curl } \mathbf{a}) \times \boldsymbol{\theta} \\ &= -\text{curl}((\boldsymbol{\theta} \cdot \nabla) \mathbf{a} + (\nabla\boldsymbol{\theta})^t \mathbf{a}) + \nabla(\boldsymbol{\theta} \cdot \text{curl } \mathbf{a}) + \mu\sigma(i\omega \mathbf{a} + \nabla v) \times \boldsymbol{\theta}. \end{aligned}$$

Hence

$$\begin{aligned} \mathcal{I}_1 &= - \int_{\mathcal{Q}} \frac{1}{\mu} \text{curl}((\boldsymbol{\theta} \cdot \nabla) \mathbf{a} + (\nabla\boldsymbol{\theta})^t \mathbf{a}) \cdot \text{curl } \overline{\boldsymbol{\psi}} dx \\ &+ \underbrace{\int_{\mathcal{Q}} \frac{1}{\mu} \nabla(\boldsymbol{\theta} \cdot \text{curl } \mathbf{a}) \cdot \text{curl } \overline{\boldsymbol{\psi}} dx}_{\mathcal{I}_{11}} + \underbrace{\int_{\mathcal{Q}} \sigma ((i\omega \mathbf{a} + \nabla v) \times \boldsymbol{\theta}) \cdot \text{curl } \overline{\boldsymbol{\psi}} dx}_{\mathcal{I}_{12}}. \end{aligned}$$

By Stoke's theorem, one has

$$\mathcal{I}_{11} = \int_{\mathcal{Q}} \frac{1}{\mu} \text{div}((\boldsymbol{\theta} \cdot \text{curl } \mathbf{a}) \text{curl } \overline{\boldsymbol{\psi}}) dx = \int_{\partial\mathcal{Q}} \frac{1}{\mu} (\boldsymbol{\theta} \cdot \text{curl } \mathbf{a})(\mathbf{n} \cdot \text{curl } \overline{\boldsymbol{\psi}}) ds.$$

By integration by parts, we compute

$$\begin{aligned}
\mathcal{I}_{12} &= \int_{\mathcal{Q}} \sigma \operatorname{curl}((i\omega \mathbf{a} + \nabla v) \times \boldsymbol{\theta}) \cdot \bar{\boldsymbol{\psi}} \, dx + \int_{\partial \mathcal{Q}} \sigma \{((i\omega \mathbf{a} + \nabla v) \times \boldsymbol{\theta}) \times \mathbf{n}\} \cdot \bar{\boldsymbol{\psi}} \, ds \\
&= \int_{\mathcal{Q}} \sigma \{ \operatorname{div} \boldsymbol{\theta} (i\omega \mathbf{a} + \nabla v) - \operatorname{div} (i\omega \mathbf{a} + \nabla v) \boldsymbol{\theta} + (\boldsymbol{\theta} \cdot \nabla) (i\omega \mathbf{a} + \nabla v) - \nabla \boldsymbol{\theta} (i\omega \mathbf{a} + \nabla v) \} \cdot \bar{\boldsymbol{\psi}} \, dx \\
&\quad + \int_{\partial \mathcal{Q}} \sigma \{ ((i\omega \mathbf{a} + \nabla v) \cdot \mathbf{n}) \cdot \boldsymbol{\theta} - (\boldsymbol{\theta} \cdot \mathbf{n}) (i\omega \mathbf{a} + \nabla v) \} \cdot \bar{\boldsymbol{\psi}} \, ds \\
&= -\frac{1}{i\omega} \int_{\mathcal{Q}} \sigma \{ (\operatorname{div} \boldsymbol{\theta} I - \nabla \boldsymbol{\theta}) (i\omega \mathbf{a} + \nabla v) + (\boldsymbol{\theta} \cdot \nabla) (i\omega \mathbf{a} + \nabla v) \} \cdot (\overline{i\omega \boldsymbol{\psi}}) \, dx \\
&\quad + \frac{1}{i\omega} \int_{\partial \mathcal{Q}} \sigma (\boldsymbol{\theta} \cdot \mathbf{n}) (i\omega \mathbf{a} + \nabla v) \cdot (\overline{i\omega \boldsymbol{\psi}}) \, ds.
\end{aligned}$$

Therefore

$$\begin{aligned}
\mathcal{I}_1 &= - \int_{\mathcal{Q}} \frac{1}{\mu} \operatorname{curl}((\boldsymbol{\theta} \cdot \nabla) \mathbf{a} + (\nabla \boldsymbol{\theta})^t \mathbf{a}) \cdot \operatorname{curl} \bar{\boldsymbol{\psi}} \, dx + \mathcal{I}_{11} + \mathcal{I}_{12} \\
&= - \int_{\mathcal{Q}} \frac{1}{\mu} \operatorname{curl}((\boldsymbol{\theta} \cdot \nabla) \mathbf{a} + (\nabla \boldsymbol{\theta})^t \mathbf{a}) \cdot \operatorname{curl} \bar{\boldsymbol{\psi}} \, dx \\
&\quad - \frac{1}{i\omega} \int_{\mathcal{Q}} \sigma \{ (\operatorname{div} \boldsymbol{\theta} I - \nabla \boldsymbol{\theta}) (i\omega \mathbf{a} + \nabla v) + (\boldsymbol{\theta} \cdot \nabla) (i\omega \mathbf{a} + \nabla v) \} \cdot (\overline{i\omega \boldsymbol{\psi}}) \, dx \\
&\quad + \int_{\partial \mathcal{Q}} \frac{1}{\mu} (\boldsymbol{\theta} \cdot \operatorname{curl} \mathbf{a}) (\mathbf{n} \cdot \operatorname{curl} \bar{\boldsymbol{\psi}}) \, ds + \frac{1}{i\omega} \int_{\partial \mathcal{Q}} \sigma (\boldsymbol{\theta} \cdot \mathbf{n}) (i\omega \mathbf{a} + \nabla v) \cdot (\overline{i\omega \boldsymbol{\psi}}) \, ds. \tag{5.59}
\end{aligned}$$

Now we compute the term \mathcal{I}_2

$$\begin{aligned}
\mathcal{I}_2 &= \frac{1}{i\omega} \int_{\mathcal{Q}} \sigma (\operatorname{div} \boldsymbol{\theta} I - \nabla \boldsymbol{\theta} - (\nabla \boldsymbol{\theta})^t) (i\omega \mathbf{a} + \nabla v) \cdot (\overline{i\omega \boldsymbol{\psi}}) \, dx \\
&\quad + \underbrace{\frac{1}{i\omega} \int_{\mathcal{Q}} \sigma \operatorname{div} \boldsymbol{\theta} (i\omega \mathbf{a} + \nabla v) \cdot \nabla \bar{\phi} \, dx}_{\mathcal{I}_{21}} + \underbrace{\frac{1}{i\omega} \int_{\mathcal{Q}} \sigma (-\nabla \boldsymbol{\theta} - (\nabla \boldsymbol{\theta})^t) (i\omega \mathbf{a} + \nabla v) \cdot \nabla \bar{\phi} \, dx}_{\mathcal{I}_{22}}.
\end{aligned}$$

One computes

$$\begin{aligned}
\mathcal{I}_{21} &= \frac{1}{i\omega} \int_{\partial \mathcal{Q}} \sigma (\boldsymbol{\theta} \cdot \mathbf{n}) (i\omega \mathbf{a} + \nabla v) \cdot \nabla \bar{\phi} \, ds - \frac{1}{i\omega} \int_{\mathcal{Q}} \sigma \boldsymbol{\theta} \cdot \nabla ((i\omega \mathbf{a} + \nabla v) \cdot \nabla \bar{\phi}) \, dx \\
&= \frac{1}{i\omega} \int_{\partial \mathcal{Q}} \sigma (\boldsymbol{\theta} \cdot \mathbf{n}) (i\omega \mathbf{a} + \nabla v) \cdot \nabla \bar{\phi} \, ds \\
&\quad - \frac{1}{i\omega} \int_{\mathcal{Q}} \sigma \boldsymbol{\theta} \cdot \left(\nabla \bar{\phi} \times \operatorname{curl} (i\omega \mathbf{a}) + D^2 \bar{\phi} (i\omega \mathbf{a} + \nabla v) + (\nabla \bar{\phi} \cdot \nabla) (i\omega \mathbf{a} + \nabla v) \right) \, dx \\
&= \frac{1}{i\omega} \int_{\partial \mathcal{Q}} \sigma (\boldsymbol{\theta} \cdot \mathbf{n}) (i\omega \mathbf{a} + \nabla v) \cdot \nabla \bar{\phi} \, ds - \frac{1}{i\omega} \int_{\mathcal{Q}} i\omega \sigma (\operatorname{curl} \mathbf{a} \times \boldsymbol{\theta}) \cdot \nabla \bar{\phi} \, dx \\
&\quad - \frac{1}{i\omega} \int_{\mathcal{Q}} \sigma D^2 \bar{\phi} (i\omega \mathbf{a} + \nabla v) \cdot \boldsymbol{\theta} \, dx - \frac{1}{i\omega} \int_{\mathcal{Q}} \sigma \left(i\omega (\nabla \mathbf{a})^t \boldsymbol{\theta} + D^2 v \boldsymbol{\theta} \right) \cdot \nabla \bar{\phi} \, dx \\
&= \frac{1}{i\omega} \int_{\partial \mathcal{Q}} \sigma (\boldsymbol{\theta} \cdot \mathbf{n}) (i\omega \mathbf{a} + \nabla v) \cdot \nabla \bar{\phi} \, ds - \frac{1}{i\omega} \int_{\mathcal{Q}} i\omega \sigma (\boldsymbol{\theta} \cdot \nabla) \mathbf{a} \cdot \nabla \bar{\phi} \, dx \\
&\quad - \frac{1}{i\omega} \int_{\mathcal{Q}} \sigma D^2 \bar{\phi} (i\omega \mathbf{a} + \nabla v) \cdot \boldsymbol{\theta} \, dx - \frac{1}{i\omega} \int_{\mathcal{Q}} \sigma D^2 v \boldsymbol{\theta} \cdot \nabla \bar{\phi} \, dx,
\end{aligned}$$

and

$$\begin{aligned}
\mathcal{I}_{22} &= -\frac{1}{i\omega} \int_{\mathcal{Q}} \sigma(\nabla\boldsymbol{\theta})^t(i\omega\mathbf{a} + \nabla v) \cdot \nabla\bar{\phi} \, dx - \frac{1}{i\omega} \int_{\mathcal{Q}} \sigma\nabla\boldsymbol{\theta}(i\omega\mathbf{a} + \nabla v) \cdot \nabla\bar{\phi} \, dx \\
&= -\frac{1}{i\omega} \int_{\mathcal{Q}} \sigma(\nabla\boldsymbol{\theta})^t(i\omega\mathbf{a} + \nabla v) \cdot \nabla\bar{\phi} \, dx - \frac{1}{i\omega} \int_{\partial\mathcal{Q}} (\sigma(i\omega\mathbf{a} + \nabla v) \cdot \mathbf{n})(\boldsymbol{\theta} \cdot \bar{\phi}) \, ds \\
&\quad + \frac{1}{i\omega} \int_{\mathcal{Q}} \sigma \left\{ \operatorname{div}(i\omega\mathbf{a} + \nabla v)(\boldsymbol{\theta} \cdot \bar{\phi}) + D^2\bar{\phi}(i\omega\mathbf{a} + \nabla v) \cdot \boldsymbol{\theta} \right\} \, dx \\
&= -\frac{1}{i\omega} \int_{\mathcal{Q}} \sigma(\nabla\boldsymbol{\theta})^t(i\omega\mathbf{a} + \nabla v) \cdot \nabla\bar{\phi} \, dx + \frac{1}{i\omega} \int_{\mathcal{Q}} D^2\bar{\phi}(i\omega\mathbf{a} + \nabla v) \cdot \boldsymbol{\theta} \, dx.
\end{aligned}$$

The last equality is due to the fact that $\operatorname{div}(\sigma(i\omega\mathbf{a} + \nabla v)) = 0$ obtained by applying the divergence operator to (5.36a). With the differential identities (5.57), one verifies also that

$$D^2v\boldsymbol{\theta} + (\nabla\boldsymbol{\theta})^t\nabla v = (\boldsymbol{\theta} \cdot \nabla)\nabla v + (\nabla\boldsymbol{\theta})^t\nabla v = \nabla(\boldsymbol{\theta} \cdot \nabla v).$$

Hence

$$\begin{aligned}
\mathcal{I}_2 &= \frac{1}{i\omega} \int_{\mathcal{Q}} \sigma(\operatorname{div}\boldsymbol{\theta}I - \nabla\boldsymbol{\theta} - (\nabla\boldsymbol{\theta})^t)(i\omega\mathbf{a} + \nabla v) \cdot (\overline{i\omega\boldsymbol{\psi}}) \, dx + \mathcal{I}_{21} + \mathcal{I}_{22} \\
&= \frac{1}{i\omega} \int_{\mathcal{Q}} \sigma(\operatorname{div}\boldsymbol{\theta}I - \nabla\boldsymbol{\theta} - (\nabla\boldsymbol{\theta})^t)(i\omega\mathbf{a} + \nabla v) \cdot (\overline{i\omega\boldsymbol{\psi}}) \, dx \\
&\quad + \frac{1}{i\omega} \int_{\partial\mathcal{Q}} \sigma(\boldsymbol{\theta} \cdot \mathbf{n})(i\omega\mathbf{a} + \nabla v) \cdot \nabla\bar{\phi} \, ds - \frac{1}{i\omega} \int_{\mathcal{Q}} \sigma i\omega((\boldsymbol{\theta} \cdot \nabla)\mathbf{a} + (\nabla\boldsymbol{\theta})^t\mathbf{a}) \cdot \nabla\bar{\phi} \, dx \\
&\quad - \frac{1}{i\omega} \int_{\mathcal{Q}} \sigma\nabla(\boldsymbol{\theta} \cdot \nabla v) \cdot \nabla\bar{\phi} \, dx. \tag{5.60}
\end{aligned}$$

(5.59), (5.60) and the fact that $\sigma(i\omega\mathbf{a} + \nabla v) \cdot \mathbf{n} = 0$ on $\partial\mathcal{Q}$ imply

$$\begin{aligned}
\mathcal{I}_1 + \mathcal{I}_2 &= -\int_{\mathcal{Q}} \frac{1}{\mu} \operatorname{curl}((\boldsymbol{\theta} \cdot \nabla)\mathbf{a} + (\nabla\boldsymbol{\theta})^t\mathbf{a}) \cdot \operatorname{curl}\bar{\boldsymbol{\psi}} \, dx \\
&\quad - \frac{1}{i\omega} \int_{\mathcal{Q}} \sigma \left(i\omega((\boldsymbol{\theta} \cdot \nabla)\mathbf{a} + (\nabla\boldsymbol{\theta})^t\mathbf{a}) + \nabla(\boldsymbol{\theta} \cdot \nabla v) \right) \cdot (\overline{i\omega\boldsymbol{\psi} + \nabla\bar{\phi}}) \, dx \\
&\quad + \int_{\partial\mathcal{Q}} \frac{1}{\mu} (\boldsymbol{\theta} \cdot \operatorname{curl}\mathbf{a})(\mathbf{n} \cdot \operatorname{curl}\bar{\boldsymbol{\psi}}) \, ds + \frac{1}{i\omega} \int_{\partial\mathcal{Q}} \sigma(\boldsymbol{\theta} \cdot \mathbf{n})(i\omega\mathbf{a} + \nabla v) \cdot (\overline{i\omega\boldsymbol{\psi} + \nabla\bar{\phi}}) \, ds \\
&= \alpha_{\mu,\sigma}(\mathcal{Q})(-(\boldsymbol{\theta} \cdot \nabla)\mathbf{a} - (\nabla\boldsymbol{\theta})^t\mathbf{a}, -(\boldsymbol{\theta} \cdot \nabla v); \boldsymbol{\psi}, \phi) \\
&\quad + \int_{\partial\mathcal{Q}} \frac{1}{\mu} (\boldsymbol{\theta} \cdot \operatorname{curl}\mathbf{a})(\mathbf{n} \cdot \operatorname{curl}\bar{\boldsymbol{\psi}}) \, ds + \frac{1}{i\omega} \int_{\partial\mathcal{Q}} \sigma(\boldsymbol{\theta} \cdot \mathbf{n})(i\omega\mathbf{a}_\tau + \nabla_\tau v) \cdot (\overline{i\omega\boldsymbol{\psi}_\tau + \nabla\bar{\phi}_\tau}) \, ds. \tag{5.61}
\end{aligned}$$

From (5.58), (5.61) and the definition of shape derivatives (5.18) – (5.19), one concludes the result (5.37). \square

Conclusion and perspectives

The problems studied in the present thesis provide a rich spectrum of further research issues, and we would like to mention a few among them with a brief recall of the mains results.

In Chapter 1 we built a 2-D forward model of eddy current testing under the assumption of axial symmetry for a simplified case (no supporting plates, no nearby tubes). We in particular studied several domain cut-off strategies using different artificial boundary conditions in radial and axial directions and gave the cut-off error with semi-analytical calculates. A first perspective is to investigate similar domain cut-off methods in the 3-D case which is critical in reducing the numerical cost of modeling.

Chapter 2 furnishes a framework of deposit shape reconstruction using shape optimization applied to a least-square cost functional. We focused on the theoretical feasibility of the reconstruction via a relationship between an arbitrary shape perturbation and the resulting derivative of the cost functional, which allows to determinate a descent gradient in aid of a properly defined adjoint state. Then we illustrated the reconstruction performance with several numerical examples. It would be interesting to discuss on the pertinence of these methods with regard to different configurations (length scale, physical parameters, etc.). Other improvements could be made in numerical aspects to have a more efficient inversion algorithm.

We then concentrated on the problem of reconstructing thin deposits of high conductivity for which the previous methods become numerically inefficient. To overcome this difficulty, we first carried out a survey of several asymptotic models in Chapter 3 which substitute the thin layer of deposits by the effective transmission conditions. According to the results of some 1-D numerical examples, we chose the most pertinent asymptotic model which is both precise and easy to inverse. Then in Chapter 4 we discussed the consequent modeling and inversion techniques for arbitrary thin deposits, always under 2-D axisymmetry assumption. Further work may deal with the general 3-D thin layer of highly conducting deposits.

In Chapter 5 we studied the 3-D eddy current testing problem via a formulation of vector potentials and discussed the deposit shape reconstruction methods only on the theoretical level. A joint work with Kamel Riahi on simulation is in progress and, as mentioned above, further studies on efficient numerical methods are indispensable to exploit the reconstruction framework in real case.

Bibliography

- [1] Milton Abramowitz and Irene A. Stegun. *Handbook of mathematical functions with formulas, graphs, and mathematical tables*, volume 55 of *National Bureau of Standards Applied Mathematics Series*. For sale by the Superintendent of Documents, U.S. Government Printing Office, Washington, D.C., 1964. (Cited on page 18.)
- [2] Grégoire Allaire. *Conception optimale de structures*, volume 58 of *Mathématiques & Applications (Berlin) [Mathematics & Applications]*. Springer-Verlag, Berlin, 2007. With the collaboration of Marc Schoenauer (INRIA) in the writing of Chapter 8. (Cited on pages 4, 49 and 54.)
- [3] A. Alonso Rodríguez, P. FERNANDES, and A. VALLI. Weak and strong formulations for the time-harmonic eddy-current problem in general multi-connected domains. *European Journal of Applied Mathematics*, null:387–406, 8 2003. (Cited on page 136.)
- [4] Ana Alonso Rodríguez and Alberto Valli. *Eddy current approximation of Maxwell equations*, volume 4 of *MS&A. Modeling, Simulation and Applications*. Springer-Verlag Italia, Milan, 2010. Theory, algorithms and applications. (Cited on pages 3, 10, 136, 137, 138 and 149.)
- [5] Luigi Ambrosio and Giuseppe Buttazzo. An optimal design problem with perimeter penalization. *Calc. Var. Partial Differential Equations*, 1(1):55–69, 1993. (Cited on page 4.)
- [6] Habib Ammari, Annalisa Buffa, and Jean-Claude Nédélec. A justification of eddy currents model for the Maxwell equations. *SIAM J. Appl. Math.*, 60(5):1805–1823, 2000. (Cited on page 3.)
- [7] Franck Assous, Patrick Ciarlet Jr., and Simon Labrunie. Theoretical tools to solve the axisymmetric Maxwell equations. *Math. Methods Appl. Sci.*, 25(1):49–78, 2002. (Cited on pages 10 and 11.)
- [8] B. A. Auld and J. C. Moulder. Review of advances in quantitative eddy current nondestructive evaluation. *Journal of Nondestructive Evaluation*, 18:3–36, 1999. 10.1023/A:1021898520626. (Cited on page 51.)
- [9] B.A. Auld, S.R. Jefferies, and J.C. Moulder. Eddy-current signal analysis and inversion for semielliptical surface cracks. *Journal of Nondestructive Evaluation*, 7(1-2):79–94, 1988. (Cited on page 1.)
- [10] Árpád Baricz. Bounds for Turánians of modified Bessel functions. *Preprint*, 2013, arXiv:1202.4853 [math.CA]. (Cited on page 39.)
- [11] R. Beissner. Approximate model of eddy-current probe impedance for surface-breaking flaws. *Journal of Nondestructive Evaluation*, 7:25–34, 1988. (Cited on page 1.)
- [12] M.P. Bendsoe and O. Sigmund. *Topology Optimization: Theory, Methods and Applications*. Engineering online library. Springer, 2003. (Cited on page 4.)

-
- [13] Alfredo Bermúdez, Carlos Reales, Rodolfo Rodríguez, and Pilar Salgado. Numerical analysis of a finite-element method for the axisymmetric eddy current model of an induction furnace. *IMA J. Numer. Anal.*, 30(3):654–676, 2010. (Cited on pages 9 and 10.)
- [14] Oszkár Bíró. Edge element formulations of eddy current problems. *Comput. Methods Appl. Mech. Engrg.*, 169(3-4):391–405, 1999. (Cited on page 136.)
- [15] Jack Blitz. *Electrical and Magnetic Methods of Non-Destructive Testing*. Non-destructive evaluation series. Chapman & Hall, 1997. (Cited on page 1.)
- [16] Marc Bonnet and Bojan B. Guzina. Sounding of finite solid bodies by way of topological derivative. *Internat. J. Numer. Methods Engrg.*, 61(13):2344–2373, 2004. (Cited on pages 4 and 49.)
- [17] Alain Bossavit. *Électromagnétisme, en vue de la modélisation*, volume 14 of *Mathématiques & Applications (Berlin) [Mathematics & Applications]*. Springer-Verlag, Paris, 1993. (Cited on page 136.)
- [18] Haïm Brezis. *Analyse fonctionnelle*. Collection Mathématiques Appliquées pour la Maîtrise. [Collection of Applied Mathematics for the Master’s Degree]. Masson, Paris, 1983. Théorie et applications. [Theory and applications]. (Cited on pages 17, 37 and 39.)
- [19] Franco Brezzi and Michel Fortin. *Mixed and hybrid finite element methods*, volume 15 of *Springer Series in Computational Mathematics*. Springer-Verlag, New York, 1991. (Cited on page 118.)
- [20] Dorin Bucur and Giuseppe Buttazzo. *Variational methods in shape optimization problems*. Progress in Nonlinear Differential Equations and their Applications, 65. Birkhäuser Boston Inc., Boston, MA, 2005. (Cited on page 4.)
- [21] Dorin Bucur and Jean-Paul Zolésio. N -dimensional shape optimization under capacity constraint. *J. Differential Equations*, 123(2):504–522, 1995. (Cited on page 4.)
- [22] Giuseppe Buttazzo and Gianni Dal Maso. Shape optimization for Dirichlet problems: relaxed formulation and optimality conditions. *Appl. Math. Optim.*, 23(1):17–49, 1991. (Cited on page 4.)
- [23] Giuseppe Buttazzo and Gianni Dal Maso. An existence result for a class of shape optimization problems. *Arch. Rational Mech. Anal.*, 122(2):183–195, 1993. (Cited on page 4.)
- [24] R. Glandon D. Mari J. Rappaz C. Chaboudez, S. Clain and M. Swierkosz. Numerical modeling in induction heating for axisymmetric geometries. *IEEE Transactions on Magnetics*, 33:739 – 745, 1997. (Cited on page 10.)
- [25] John Cagnol and Matthias Eller. Shape optimization for the maxwell equations under weaker regularity of the data. *Comptes Rendus Mathématique*, 348(21 - 22):1225 – 1230, 2010. (Cited on page 4.)

- [26] Antonin Chambolle. A density result in two-dimensional linearized elasticity, and applications. *Arch. Ration. Mech. Anal.*, 167(3):211–233, 2003. (Cited on page 4.)
- [27] L. Chatellier, S. Dubost, F. Peisey, Y. Goussard, and R. Guichard. Characterization of small depth surface breaking defects with eddy current sensor measurements. In *Proc. ECNDT 2006*, 2006. (Cited on page 1.)
- [28] Nicolas Chaulet. *Modèles d'impédance généralisée en diffraction inverse*. PhD thesis, École Polytechnique. (Cited on pages 5 and 50.)
- [29] Denise Chenais. On the existence of a solution in a domain identification problem. *J. Math. Anal. Appl.*, 52(2):189–219, 1975. (Cited on page 4.)
- [30] Xavier Claeys. *Analyse asymptotique et numérique de la diffraction d'ondes par des fils minces*. PhD thesis, Université de Versailles-Saint Quentin en Yvelines, 12 2008. (Cited on pages 5 and 82.)
- [31] David Colton and Rainer Kress. *Inverse acoustic and electromagnetic scattering theory*, volume 93 of *Applied Mathematical Sciences*. Springer, New York, third edition, 2013. (Cited on page 5.)
- [32] Martin Costabel and Monique Dauge. Singularities of electromagnetic fields in polyhedral domains. *Arch. Ration. Mech. Anal.*, 151(3):221–276, 2000. (Cited on page 138.)
- [33] Martin Costabel, Monique Dauge, and Serge Nicaise. Singularities of eddy current problems. *M2AN Math. Model. Numer. Anal.*, 37(5):807–831, 2003. (Cited on page 3.)
- [34] Martin Costabel and Frédérique Le Louër. Shape derivatives of boundary integral operators in electromagnetic scattering. Part I: Shape differentiability of pseudo-homogeneous boundary integral operators. *Integral Equations Operator Theory*, 72(4):509–535, 2012. (Cited on page 4.)
- [35] Robert Dautray and Jacques-Louis Lions. *Mathematical analysis and numerical methods for science and technology. Vol. 3*. Springer-Verlag, Berlin, 1990. Spectral theory and applications, With the collaboration of Michel Artola and Michel Cessenat, Translated from the French by John C. Amson. (Cited on page 18.)
- [36] Bérandère Delourme. *Modèles et asymptotiques des interfaces fines et périodiques*. PhD thesis, Université Pierre et Marie Curie. (Cited on pages 5 and 82.)
- [37] Oliver Dorn and Dominique Lesselier. Level set methods for inverse scattering—some recent developments. *Inverse Problems*, 25(12):125001, 11, 2009. (Cited on pages 4 and 49.)
- [38] H. Eschenauer, N. Olhoff, and W. Schnell. *Applied Structural Mechanics: Fundamentals of Elasticity, Load-Bearing Structures, Structural Optimization : Including Exercises*. U.S. Government Printing Office, 1997. (Cited on page 4.)
- [39] Gerald B. Folland. *Introduction to partial differential equations*. Princeton University Press, Princeton, NJ, second edition, 1995. (Cited on page 145.)

- [40] B. B. Guzina and M. Bonnet. Topological derivative for the inverse scattering of elastic waves. *Quart. J. Mech. Appl. Math.*, 57(2):161–179, 2004. (Cited on pages 4 and 49.)
- [41] Bojan B. Guzina and Marc Bonnet. Small-inclusion asymptotic of misfit functionals for inverse problems in acoustics. *Inverse Problems*, 22(5):1761–1785, 2006. (Cited on page 111.)
- [42] J. Hadamard. *Lectures on Cauchy’s Problem in Linear Partial Differential Equations*. Yale University Press, New Haven, 1923. (Cited on page 5.)
- [43] Jacques Salomon Hadamard. *Mémoire sur le problème d’analyse relatif à l’équilibre des plaques élastiques encastrées*. Mémoires présentés par divers savants à l’Académie des sciences de l’Institut de France: Extrait. Imprimerie nationale, 1908. (Cited on page 4.)
- [44] Housseem Haddar, Patrick Joly, and Hoai-Minh Nguyen. Generalized impedance boundary conditions for scattering problems from strongly absorbing obstacles: the case of Maxwell’s equations. *Math. Models Methods Appl. Sci.*, 18(10):1787–1827, 2008. (Cited on page 5.)
- [45] Antoine Henrot and Michel Pierre. *Variation et optimisation de formes*, volume 48 of *Mathématiques & Applications (Berlin) [Mathematics & Applications]*. Springer, Berlin, 2005. Une analyse géométrique. [A geometric analysis]. (Cited on page 4.)
- [46] Frank Hettlich. The domain derivative of time-harmonic electromagnetic waves at interfaces. *Math. Methods Appl. Sci.*, 35(14):1681–1689, 2012. (Cited on page 4.)
- [47] S.R.H. Hoole, S. Subramaniam, R. Saldanha, J. L Coulomb, and J.-C. Sabonnadiere. Inverse problem methodology and finite elements in the identification of cracks, sources, materials, and their geometry in inaccessible locations. *Magnetics, IEEE Transactions on*, 27(3):3433–3443, 1991. (Cited on page 4.)
- [48] Mourad E. H. Ismail. Complete monotonicity of modified Bessel functions. *Proc. Amer. Math. Soc.*, 108(2):353–361, 1990. (Cited on page 13.)
- [49] John David Jackson. *Classical electrodynamics*. Wiley, New York, NY, 3rd ed. edition, 1999. (Cited on page 3.)
- [50] Tosio Kato. *Perturbation theory for linear operators*. Classics in Mathematics. Springer-Verlag, Berlin, 1995. Reprint of the 1980 edition. (Cited on page 19.)
- [51] Andreas Kirsch. *An introduction to the mathematical theory of inverse problems*, volume 120 of *Applied Mathematical Sciences*. Springer, New York, second edition, 2011. (Cited on page 5.)
- [52] M. A. Leontovich. On approximate boundary conditions for electromagnetic fields on the surface of highly conducting bodies. *Research in the propagation of radio waves*, pages 5 – 12, 1948. (Cited on page 5.)
- [53] Jacques-Louis Lions and Enrico Magenes. *Problèmes aux limites non homogènes et applications. Vol. 1*. Travaux et Recherches Mathématiques, No. 17. Dunod, Paris, 1968. (Cited on pages 20 and 58.)

- [54] Bruno Luong and Fadil Santosa. Quantitative imaging of corrosion in plates by eddy current methods. *SIAM J. Appl. Math.*, 58(5):1509–1531, 1998. (Cited on page 1.)
- [55] M. Masmoudi, J. Pommier, and B. Samet. Application of the topological asymptotic expansion to inverse scattering problems. In *Numerical methods for scientific computing. Variational problems and applications*, pages 108–127. Internat. Center Numer. Methods Eng. (CIMNE), Barcelona, 2003. (Cited on page 4.)
- [56] Mohamed Masmoudi, Julien Pommier, and Bessem Samet. The topological asymptotic expansion for the Maxwell equations and some applications. *Inverse Problems*, 21(2):547–564, 2005. (Cited on page 4.)
- [57] James Clerks Maxwell. *On Physical Lines of Force*. 1861. (Cited on page 3.)
- [58] James Clerks Maxwell. *A Dynamical Theory of the Electromagnetic Field*. 1865. (Cited on page 3.)
- [59] James Clerks Maxwell. *A Treatise on Electricity and Magnetism*. 1873. (Cited on page 3.)
- [60] I.D. Mayergoyz. *Nonlinear Diffusion of Electromagnetic Fields: With Applications to Eddy Currents and Superconductivity*. Electromagnetism Series. Academic Press, 1998. (Cited on page 3.)
- [61] B. Mohammadi and O. Pironneau. *Applied shape optimization for fluids*. Numerical Mathematics and Scientific Computation. The Clarendon Press Oxford University Press, New York, 2001. Oxford Science Publications. (Cited on page 4.)
- [62] Peter Monk. *Finite element methods for Maxwell's equations*. Numerical Mathematics and Scientific Computation. Oxford University Press, New York, 2003. (Cited on page 139.)
- [63] François Murat and Jacques Simon. Etude de problèmes d'optimal design. In Jean Cea, editor, *Optimization Techniques Modeling and Optimization in the Service of Man Part 2*, volume 41 of *Lecture Notes in Computer Science*, pages 54–62. Springer Berlin Heidelberg, 1976. (Cited on pages 4 and 49.)
- [64] François Murat and Jacques Simon. Sur le contrôle par un domaine géométrique. Technical Report LAN-76015, Université Pierre et Marie Curie (Paris), 1976. (Cited on pages 4 and 49.)
- [65] Dimitri Nicolas. *Couplage de méthodes d'échantillonnage et de méthodes d'optimisation de formes pour des problèmes de diffraction inverse*. PhD thesis, École Polytechnique. (Cited on pages 5 and 49.)
- [66] O. Ozdemir, H. Haddar, and A. Yaka. Reconstruction of the electromagnetic field in layered media using the concept of approximate transmission conditions. *Antennas and Propagation, IEEE Transactions on*, 59(8):2964–2972, 2011. (Cited on page 111.)
- [67] Olivier Pantz. Sensibilité de l'équation de la chaleur aux sauts de conductivité. *C. R. Math. Acad. Sci. Paris*, 341(5):333–337, 2005. (Cited on page 49.)

- [68] Il-Han Park, Lee Beam-taek, and Song-Yop Hahn. Sensitivity analysis based on analytic approach for shape optimization of electromagnetic devices: interface problem of iron and air. *Magnetics, IEEE Transactions on*, 27(5):4142–4145, 1991. (Cited on page 4.)
- [69] Won-Kwang Park. *Inverse Scattering from Two-Dimensional Thin Inclusions and Cracks*. PhD thesis, École Polytechnique. (Cited on page 111.)
- [70] G. Pichenot, D. Prémel, T. Sollier, and V. Maillot. Development of a 3d electromagnetic model for eddy current tubing inspection: Application to steam generator tubing. In *AIP Conference Proceedings*, volume 700, pages 321–328, 2003. 10.1063/1.1711640. (Cited on page 52.)
- [71] Clair Poinard. Approximate transmission conditions through a weakly oscillating thin layer. *Mathematical Methods in the Applied Sciences*, 32(4):435–453, 2009. (Cited on pages 5 and 82.)
- [72] Roland Potthast. Domain derivatives in electromagnetic scattering. *Math. Methods Appl. Sci.*, 19(15):1157–1175, 1996. (Cited on page 4.)
- [73] William Prager. *Introduction to structural optimization*. Springer-Verlag, Vienna, 1974. Course held at the Department of Mechanics of Solids, International Centre for Mechanical Sciences, Udine, October, 1974, International Centre for Mechanical Sciences, Courses and Lectures, No. 212. (Cited on page 4.)
- [74] J.A. Ramirez and E.M. Freeman. Shape optimization of electromagnetic devices including eddy-currents. *Magnetics, IEEE Transactions on*, 31(3):1948–1951, 1995. (Cited on page 4.)
- [75] Fadil Santosa. A level-set approach for inverse problems involving obstacles. *ESAIM Contrôle Optim. Calc. Var.*, 1:17–33, 1995/96. (Cited on pages 4 and 49.)
- [76] K. Schmidt. *High-order numerical modelling of highly conductive thin sheets*. PhD thesis, ETH Zurich, 2008. (Cited on page 5.)
- [77] K. Schmidt, O. Sterz, and R. Hiptmair. Estimating the eddy-current modeling error. *Magnetics, IEEE Transactions on*, 44(6):686–689, 2008. (Cited on page 3.)
- [78] T.B.A. Senior and J.L. Volakis. *Approximate Boundary Conditions in Electromagnetics*. IEE Publication Series. Institution of Electrical Engineers, 1995. (Cited on page 5.)
- [79] V. Šverák. On optimal shape design. *J. Math. Pures Appl. (9)*, 72(6):537–551, 1993. (Cited on page 4.)
- [80] J.A. Tegopoulos and E.E. Kriezis. *Eddy currents in linear conducting media*. Studies in electrical and electronic engineering. Elsevier, 1985. (Cited on page 3.)
- [81] A. N. Tikhonov. On the solution of incorrectly put problems and the regularisation method. In *Outlines Joint Sympos. Partial Differential Equations (Novosibirsk, 1963)*, pages 261–265. Acad. Sci. USSR Siberian Branch, Moscow, 1963. (Cited on page 5.)

-
- [82] Sébastien Tordeux. *Méthodes Asymptotiques pour la Propagation des Ondes dans les Milieux comportant des Fentes*. PhD thesis, Université de Versailles-Saint Quentin en Yvelines, 2004. (Cited on pages 5 and 82.)
- [83] Adrien Trillon. *Reconstruction de défauts à partir de données issues de capteurs à courants de Foucault avec modèle direct différentiel*. PhD thesis, École Centrale de Nantes, 2010. (Cited on page 1.)
- [84] Adrien Trillon, Frédéric Sirois, Jérôme Idier, Yves Goussard, Nicolas Paul, and Alexandre Girard. Eddy current tomography based on a finite element forward model with additive regularization. In *AIP Conference Proceedings*, volume 1211, pages 782–789, 2009. 10.1063/1.3362478. (Cited on page 49.)
- [85] J.-P. Zolésio. Introduction to shape optimization problems and free boundary problems. In *Shape optimization and free boundaries (Montreal, PQ, 1990)*, volume 380 of *NATO Adv. Sci. Inst. Ser. C Math. Phys. Sci.*, pages 397–457. Kluwer Acad. Publ., Dordrecht, 1992. (Cited on pages 4 and 49.)
- [86] R. Zorgati, B. Duchene, D. Lesselier, and F. Pons. Eddy current testing of anomalies in conductive materials. i. qualitative imaging via diffraction tomography techniques. *Magnetics, IEEE Transactions on*, 27(6):4416–4437, 1991. (Cited on page 1.)
- [87] R. Zorgati, D. Lesselier, B. Duchene, and F. Pons. Eddy current testing of anomalies in conductive materials. ii. quantitative imaging via deterministic and stochastic inversion techniques. *Magnetics, IEEE Transactions on*, 28(3):1850–1862, 1992. (Cited on page 1.)

Some inversion methods applied to non-destructive testings of steam generator via eddy current probe

Abstract: The main objective of this thesis is to propose and test some shape optimization techniques to identify and reconstruct deposits at the shell side of conductive tubes in steam generators using signals from eddy current coils. This problem is motivated by non-destructive testing applications in the nuclear power industry where the deposit clogging the cooling circuit may affect power productivity and structural safety. We consider in a first part an axisymmetric case for which we set the model by establishing a 2-D differential equation describing the eddy current phenomenon, which enable us to simulate the impedance measurements as the observed signals to be used in the inversion. To speed up numerical simulations, we discuss the behavior of the solution of the eddy current problem and build artificial boundary conditions, in particular by explicitly constructing DtN operators, to truncate the domain of the problem. In the deposit reconstruction, we adapt two different methods according to two distinct kinds of deposits. The first kind of deposit has relatively low conductivity (about $1 \times 10^4 S/m$). We apply the shape optimization method which consists in expliciting the signal derivative due to a shape perturbation of the deposit domain and to build the gradient by using the adjoint state with respect to the derivative and the cost functional. While for the second kind of deposit with high conductivity ($5.8 \times 10^7 S/m$) but in the form of thin layer (in micrometers), the previous method encounter a high numerical cost due to the tiny size of the mesh used to model the layer. To overcome this difficulty, we build an adapted asymptotic model by appropriately selecting the family of effective transmissions conditions on the interface between the deposit and the tube. The name of the asymptotic model is due to the fact that the effective transmissions conditions are derived from the asymptotic expansion of the solution with respect to a small parameter δ characterizing the thickness of the thin layer and the conductivity behavior. Then the inverse problem consists in reconstructing the parameters representing the layer thickness of the deposit. For both of the two approaches, we validate numerically the direct and inverse problems. In a second part we complement this work by extending the above methods to the 3-D case for a non-axisymmetric configuration. This is motivated by either non axisymmetric deposits or the existence of non axisymmetric components like support plates of steam generator tubes.

Keywords: Inverse problems, electromagnetism, eddy current equations, DtN operators, shape optimization, asymptotic models.

Contrôle non-destructif de générateurs de vapeur via des sondes courants de Foucault : nouvelles approches

Résumé : L'objectif principal de cette thèse est de proposer et de tester quelques méthodes de l'optimisation de forme afin d'identifier et de reconstruire des dépôts qui couvrent la paroi extérieure d'un tube conducteur dans un générateur de vapeur en utilisant des signaux courant de Foucault. Ce problème est motivé par des applications industrielles en contrôle non-destructif dans le secteur de l'énergie nucléaire. En fait, des dépôts peuvent obstruer le passage de circuit de refroidissement entre les tubes et les plaques entretoises qui les soutiennent, ce qui entraînerait une baisse de productivité et mettrait la structure en danger. On considère dans un premier temps un cas axisymétrique dans le cadre duquel on construit un modèle 2-D par des équations aux dérivées partielles pour le courant de Foucault, ce qui nous permet ensuite de reproduire des mesures d'impédances qui correspondent en réalité les signaux courants de Foucault. Pour réduire le coût de calculs de la simulation numérique, on tronque le domaine du problème en posant des conditions aux bords artificielles basées sur des études sur le comportement de la solution, notamment sur un calcul semi-analytique de l'opérateur D-t-N dans la direction axiale. Pour la partie identification et reconstruction, on distingue deux sortes de dépôts et établit pour chacun une méthode d'inversion spécifique. Le premier cas concernent des dépôts dont la conductivité est relativement faible (d'environ $1.e4 S/m$). On utilise la méthode d'optimisation de forme qui consiste à exprimer explicitement la dérivée des mesures d'impédance par rapport au domaine du dépôt en fonction d'une déformation et à représenter le gradient d'un fonctionnel de coût à minimiser par l'intermédiaire d'un état adjoint proprement défini. Motivé par la présence des dépôts et des plaques de maintien non-axisymétriques, on fait aussi une extension en 3-D des méthodes précédentes. Pour le deuxième cas, des dépôts sont fortement conducteurs et sous forme de couche mince d'une épaisseur de l'ordre de micron. La méthode adaptée à la première sorte de dépôts devient ici trop coûteuse à cause du degré de liberté très élevé des éléments finis sur un maillage extrêmement raffiné à l'échelle de la couche mince. Pour relever cette difficulté, les études sont portées sur plusieurs modèles asymptotiques qui remplacent la couche mince par des conditions d'interface sur la surface du tube portante du dépôt. Le nom de modèle asymptotique vient du fait que les conditions d'interface effectives sont obtenues par le développement asymptotique de la solution en fonction d'un paramètre caractérisant la conductivité et l'épaisseur de la couche mince. La validation numérique a permis de retenir un modèle asymptotique qui est à la fois suffisamment précis et simple à inverser. L'inversion (recherche de l'épaisseur du dépôt) consiste alors à rechercher des paramètres dans les conditions d'interface (non standard). Pour les deux cas, la validation et des exemples numériques sont proposés pour le modèle direct et l'inversion.

Mots-clés : Problèmes inverses, électromagnétisme, équations de courant de Foucault, opérateur DtN, optimisation de forme, modèles asymptotiques.
